



HAL
open science

**Transport des matières en suspension et du carbone
organique à l'échelle d'un bassin versant agricole :
analyse de la dynamique et modélisation
agro-hydrologique (SWAT)**

Chantha Oeurng

► **To cite this version:**

Chantha Oeurng. Transport des matières en suspension et du carbone organique à l'échelle d'un bassin versant agricole : analyse de la dynamique et modélisation agro-hydrologique (SWAT). Hydrologie. Université Paul Sabatier - Toulouse III, 2010. Français. NNT : . tel-00741915

HAL Id: tel-00741915

<https://theses.hal.science/tel-00741915v1>

Submitted on 15 Oct 2012

HAL is a multi-disciplinary open access archive for the deposit and dissemination of scientific research documents, whether they are published or not. The documents may come from teaching and research institutions in France or abroad, or from public or private research centers.

L'archive ouverte pluridisciplinaire **HAL**, est destinée au dépôt et à la diffusion de documents scientifiques de niveau recherche, publiés ou non, émanant des établissements d'enseignement et de recherche français ou étrangers, des laboratoires publics ou privés.



THÈSE

N° d'ordre :

En vue de l'obtention du

DOCTORAT DE L'UNIVERSITÉ DE TOULOUSE

Délivré par Université Toulouse 3 Paul Sabatier (UT3 Paul Sabatier)

Discipline ou spécialité : Hydrologie et Ressources en eau

**Présentée et soutenue par OEURNG Chantha
Le 27 Septembre 2010**

Transport des matières en suspension et du carbone organique à l'échelle
d'un bassin versant agricole : analyse de la dynamique et
modélisation agro-hydrologique (SWAT)

JURY

M. Francesc GALLART GALLEGRO, Profesor de Investigación au CSIC, Barcelone

M. Pierre ANSCHUTZ, Professeur à l'Université Bordeaux 1

M. Sovannarath LEK, Professeur à l'Université Paul Sabatier, Toulouse

M. Ramiro NEVES, Professeur associé à l'Institut Scientifique et Technique de Lisbonne

M. José Miguel SANCHEZ-PEREZ, Directeur de Recherche au CNRS, Toulouse

Mme Sabine SAUVAGE, Ingénieur de Recherche au CNRS, Toulouse

Rapporteur

Rapporteur

Président

Examineur

Directeur de thèse

Co-directrice de thèse

Ecole doctorale : *Sciences de l'univers, de l'environnement et de l'espace (SDU2E)*

Unité de recherche : ECOLAB, UMR 5245, CNRS-UPS-INP

Directeur(s) de Thèse :

M. José Miguel SANCHEZ-PEREZ (Directeur de thèse)

Mme Sabine SAUVAGE (Co-directrice de thèse)

REMERCIEMENTS

Ces travaux de thèse ont été réalisés dans le cadre de la bourse de Coopération entre le Gouvernement Français et Cambodgien. Cette thèse est réalisée au Laboratoire d'Ecologie Fonctionnelle, Toulouse.

Tout d'abord, je tiens à remercier énormément mes directeurs de thèse : **José Miguel Sánchez Pérez** et **Sabine Sauvage** pour m'avoir accepté dans le laboratoire EcoLab et pour m'avoir soutenu durant toutes ces années. Sans eux, il est certain que ce travail n'aurait jamais vu le jour.

J'exprime également tous mes remerciements sincères au Professeur émérite **Puy Lim**, pour m'avoir mis en contact avec mes directeurs. Mr Puy Lim m'a aidé beaucoup lors de mon arrivée à Toulouse. Je n'oublierai jamais sa générosité et ses conseils. Merci à Professeur **Sovann Lek** et sa femme pour leurs conseils et leurs invitations au repas chez eux.

Je dois également remercier l'équipe, les personnels, les doctorants, et les post-doctorants du laboratoire : Gaël Durbe, David Baque, Frédéric Julien, Francis, François Oehler, Sophie Durandea, Anaïs Abraham, Marixu Guiresse, Huges Alexandre, Jean Luc Probst, **Annick Correge**, Catherine Monier, Christiane Terre, Lobat Taghavi, Thierry Polard, Sylvain Ferrant, Laurie Boithias et David Bailly. Je m'excuse pour les personnes que j'ai oubliées. Je remercie aussi Cécile Théodore et Mattieu Mouclier pour l'aide à la correction du français dans ce mémoire de thèse.

Je remercie également la CACG, Météo-France et le Cemagref de Bordeaux pour les données qui m'ont été nécessaires dans le cadre des travaux présentés ici sur le bassin versant de la SAVE.

Je tiens également à remercier Alexandra Coynel, Henri Etcheber et Eric Maneux du laboratoire EPOC de Bordeaux pour leur accueil, collaboration et discussions sur une partie de ce travail.

Je tiens à remercier tous les membres de mon jury.

Mes remerciements s'adressent également au Crous Toulouse, notamment à Pierre Dedieu pour son aide sur les affaires administratives liées à la bourse.

J'adresse aussi mes remerciements à mes anciens enseignants, mon chef de département de Génie Rural, Mme MEN Nareth, mes collègues, et mes amis de mon établissement d'origine - Institut de Technologie du Cambodge.

Merci enfin énormément à toute ma famille pour son soutien permanent. Et surtout merci à **Chea Phallika (my beloved person)**, qui m'a supporté et donné le courage de continuer et d'achever ce travail. Je n'oublie pas de remercier toutes les familles cambodgiennes que je connais à Toulouse et merci à tous mes amis cambodgiens pour les souvenirs inoubliables de ces trois ans ensemble : Chhun Labo, Khov Makara, Sam Sopheak, Bang Pisey et les autres.

SOMMAIRES

Introduction générale	1
Chapter 1: Introduction	5
1.1. Context and problematic	6
1.2. Objectives	9
1.3. Thesis structure	9
Chapter 2: Suspended sediment, organic carbon transport and modelling	11
2.1. Origins of suspended sediment	12
2.2. Anthropogenic activities	13
2.3. Processes and mechanics of soil erosion	14
2.4. Detachment of soil particles by flow	15
2.5. Factors influencing soil erosion	16
2.5.1. <i>Rainfall erosivity</i>	15
2.5.2. <i>Soil erodibility</i>	15
2.5.3. <i>Soil occupation</i>	16
2.5.4. <i>Topography</i>	17
2.6. Channel erosion	17
2.7. Sediment delivery and transport processes in river	18
2.7.1. <i>Concept of sediment delivery ratio</i>	18
2.7.2. <i>Mechanisms of suspended sediment transport</i>	20
2.7.3. <i>Movement and particle deposition</i>	21
2.7.4. <i>Empirical relationship between suspended sediment and discharge</i>	23
2.7.5. <i>Sediment dynamics linked to particle availability</i>	26
2.8. Measurement of suspended sediment concentrations in rivers	26
2.8.1. <i>Water sampling</i>	26
2.8.2. <i>Turbidity measurement</i>	27
2.8.3. <i>Acoustic method</i>	27
2.8.4. <i>Acoustic Doppler Current Profiler (ADCP) method</i>	27
2.8.5. <i>Nuclear Method</i>	28
2.8.6. <i>Optical measurement</i>	28
2.8.7. <i>Laser measurement</i>	28

2.9. Organic carbon transport	29
2.9.1. <i>Global carbon and water cycle</i>	29
2.9.2. <i>Significance of organic carbon in rivers</i>	29
2.9.3. <i>The link between hydrological flow and organic carbon fluxes</i>	31
2.9.4. <i>Sources and origins of organic carbon</i>	31
2.10. Overview of soil erosion and sediment transport models.....	33
2.10.1. <i>Statistical models</i>	33
2.10.2. <i>Empirical models</i>	35
2.10.3. <i>Conceptual models</i>	37
2.10.4. <i>Physically- based catchment erosion models</i>	37
2.11. Uncertainties of catchment model simulation	40
2.12. Synthesis of literature review	41
Chapter 3: Materials and methods	43
3.1. Study area.....	44
3.1.1. <i>General description and location</i>	44
3.1.2. <i>Soil and geomorphology</i>	45
3.1.3. <i>Landuse and management practices</i>	46
3.1.4. <i>Climate and hydrology</i>	47
3.2. Instrumentation and water quality monitoring	48
3.2.1. <i>Sonde YSI and Ecotech preleveur</i>	48
3.2.2. <i>Calibration processes of Sonde</i>	49
3.2.3. <i>Physico-chemical parameters in situ and water sampling</i>	50
3.3. Technical problems	51
3.4. Determination of suspended sediment and organic carbon.....	52
3.4.1. <i>Filtration and determination of suspended sediment concentration</i>	52
3.4.2. <i>Organic carbon analysis</i>	52
3.5. SWAT model selection and description.....	54
3.5.1. <i>SWAT water balance</i>	55
3.5.2. <i>Surface runoff</i>	56
3.5.3. <i>Evapotranspiration</i>	57
3.5.4. <i>Groundwater</i>	58
3.5.5. <i>Erosion and Sediment component</i>	59
3.5.6. <i>SWAT model input</i>	62

Chapter 4: Dynamics of suspended sediment transport and yield in a large agricultural catchment, southwest France 65

Chapter 5: Fluvial transport of suspended sediment and organic carbon in a large agricultural catchment during flood events in southwest France 79

5.1. Introduction	82
5.2. Materials and methods	84
5.2.1. Study area.....	84
5.2.2. Instrumentation and sampling method.....	85
5.2.3. Data sources and treatment	86
5.2.4. SS concentration data and calculation of fluxes	87
5.2.5. Statistical analyses	87
5.3. Results	89
5.3.1. Hydrometeorology during the study period	89
5.3.2. SS, POC and DOC concentrations and relationship with discharge.....	91
5.3.3. SS, POC and DOC fluxes	94
5.3.4. Relationship among POC, DOC and hydro-climatological variables.....	95
5.4. Discussion	98
5.4.1. Temporal variability in SS, POC and DOC transport and yield	98
5.4.2. Discharge, SS, POC and DOC relationships and probable origins	100
5.5. Conclusion.....	101
5.6. Acknowledgements	102
5.7. References	103

Chapter 6: Assessment of hydrology, sediment and particulate organic carbon yield in a large agricultural catchment using the SWAT model 109

6.1. Introduction	112
6.2. Materials and methods	113
6.2.1. Study area.....	113
6.2.2. Catchment water quality monitoring.....	116
6.2.3. Determination of suspended sediment and POC concentrations.....	116
6.3. Modelling approach.....	117
6.3.1. The SWAT model.....	117

6.3.2. Hydrological modelling component in SWAT.....	117
6.3.3. Suspended sediment modelling component in SWAT.....	118
6.3.4. Particulate organic carbon modelling	120
6.3.5. SWAT data input.....	121
6.3.6. Model evaluation.....	122
6.3.7. Calibration process.....	123
6.4. Results and Discussion.....	124
6.4.1. Discharge simulation and hydrological assessment	124
6.4.2. Suspended sediment simulation and yield.....	126
6.4.3. POC simulation and yield	130
6.4.4. Identification of critical areas of soil erosion.....	130
6.5. Conclusions	131
6.6. Acknowledgement.....	132
6.7. References	133
Chapter 7: General Discussion	139
7.1. SS, POC and DOC transport dynamics and modelling.....	140
7.2. Agro hydrological modelling using the SWAT model	142
7.2.1. Input data and sub-catchment delineation.....	142
7.2.2. Challenges in model calibration and evaluation	143
Chapter 8: Conclusion and perspectives	147
8.1. Conclusion.....	148
8.2. Perspectives	149
Conclusion générale	151
References	153
Annexe 1.....	172
Annexe 2.....	183
Annexe 3.....	185

LISTE DES FIGURES

▪ Figure 2-1: Different types of soil erosion: (A) gully erosion, (B) rill erosion, (C) channel erosion.....	13
▪ Figure 2-2: Shear stress of soil and water through the impact of raindrop or splash effect	14
▪ Figure 2-3: Relation between Sediment Delivery Ratio and the catchment sizes (From Lu et al. (2006), modified from Ferro and Minacapilli (1995) and Walling (1983).	18
▪ Figure 2-4: Suspended sediment motion by convection and diffusion processes (Huber Chanson, 2004).....	21
▪ Figure 2-5: Diagram of Shields – Yalin (1977)	22
▪ Figure 2-6: Diagram de Hjulstrom (1935): relationship between the water velocity and particle size to determine the context of erosion and sedimentation.....	22
▪ Figure 2-7: Typology of relationship between suspended sediment concentration (SSC) and discharge (Q) (From Lefrançois et al. (2007), modified from Williams (1989))	25
▪ Figure 2-8: The carbon compartments of a terrestrial ecosystem (carbon dynamics) source: WBGU, 1998	32
▪ Figure 2-9: Catchment seasonal rating curves showing long discharge (Q) and log suspended sediment concentrations (SSC) with 95% confidence intervals for (a) summer-autumn and (b) winter-spring period (From Smith 2008).....	34
▪ Figure 3-1: Location and topography of study area (Source: Cemagref de Bordeaux (UR ADBX))	44
▪ Figure 3-2: Major soils in the Save catchment (source: Cemagref de Bordeaux (UR ADBX))	45
▪ Figure 3-3: Landuse in the Save catchment with major agricultural land	47
▪ Figure 3-4: Summary of mean monthly discharge ($m^3 s^{-1}$), specific discharge ($l s^{-1} km^2$) and runoff (mm) in the Save catchment at Larra gauging station (1965-2006)	48
▪ Figure 3-5: Sonde YSI 6920 and Ecotech Preleveur with 24 of 1 litter bottles	49
▪ Figure 3-6: Schema of installing water quality monitoring system at Larra station: A) pump inlet and Sonde pipe, B) Automatic Water Sampler EcoTech, C) Sampling site at Larra bridge	51
▪ Figure 3-7: Photo of filtration for obtaining suspended sediment concentration.....	52
▪ Figure 3-8: Photo of Shimadzu TOC-5000 analyzer (ECOLAB Analytical Laboratory, Toulouse).....	53
▪ Figure 3-9: Photo of LECO CS200 analyzer (EPOC Analytical Laboratory, Bordeaux)..	54
▪ Figure 3-10: Schema of HRUs definition	55
▪ Figure 3-11: Schematic representation of the hydrological cycle (From SWAT model theory).....	56
▪ Figure 3-12: (A) Digital Elevation Model of the study area, (B) Major soils of study area, (C) Major landuse of the study area.....	64

- Figure 5-1: Location, landuse and topographical maps of the Save catchment..... 84
- Figure 5-2: Hourly discharge in the 15 flood events observed during the study period (January 2008 to June 2009) at Larra sampling station..... 89
- Figure 5-3: Temporal variability in particulate (POC) and dissolved (DOC) organic carbon during the study period (January 2008, June 2009). 91
- Figure 5-4: Relationship between POC contents (% of dry weight) and suspended sediment concentrations (mg l^{-1}) from the Save catchment at Larra sampling station..... 92
- Figure 5-5: Relationship between discharge and DOC (a) and POC (b). 92
- Figure 5-6: Relationship between discharge and suspended sediment (SS), particulate organic carbon (POC) and dissolved organic carbon (DOC), showing different hysteresis patterns..... 94
- Figure 6-1: (A) Location of study area; (B) Topographical map; (C) Major agricultural landuses (D) Major soil types in the Save catchment..... 114
- Figure 6-2: Relationship between instantaneous suspended sediment concentration (SSC) and particulate organic carbon (POC) at Larra sampling station..... 120
- Figure 6-3: Map showing 91 sub-basins in the Save catchment. 122
- Figure 6-4: Observed and simulated daily discharge at Larra station (January 1999 to March 2009). 126
- Figure 6-5: Observed and simulated daily discharge (A) and observed and simulated suspended sediment concentration (B) at Larra sampling station (January 2007 to March 2009). 127
- Figure 6-6: (A) Simulated daily suspended sediment concentration (SSC) and particulate organic carbon (POC) (January 1999-March 2009), (B) simulated annual sediment yield (1999-2008) and observed annual sediment yield (2007-2008) and (C) simulated annual particulate organic carbon yield (POC) (1999-2008) and observed annual POC yield (2008)..... 128
- Figure 6-7: Empirical correlation between annual water yield and annual sediment yield with 95% confidence interval for the Save catchment..... 129
- Figure 6-8: Simulated soil erosion within the 91 sub-basins, based on average sediment yield (199-2008)..... 131

LISTE DES TABLEAUX

- Table 2-1: Examples of proposed relationships between sediment delivery ration and catchment characteristics 19
- Table 5-1: Names, abbreviations and units for the variables used to characterise flood events and to perform Pearson correlation matrix and factorial analysis 88
- Table 5-2: Summary of the main flood characteristics recorded during the study period in Save catchment 90
- Table 5-3: TSS, DOC, POC concentrations and transport rates during 15 studied flood events 95
- Table 5-4: Pearson correlation matrix among all variables (n=13)..... 96

- Table 5-5: Summary of varimax rotated factor for all variables presented in Table 5-1 (Eigen-values <0.50 were excluded) 99
- Table 6-1: Parameters used to calibrate flow and sediment at Larra gauging station..... 125

Introduction générale

Les matières particulaires transférées entre le continent et l'océan sont pour l'essentiel le résultat du transport par les fleuves et reflètent les processus d'érosion « naturelle modifiés » par la pression anthropique à l'échelle des bassins versants (Meybeck, 1988). En effet, la quantité et la qualité des matières arrachées au continent et véhiculées par les fleuves réduisent le potentiel des terres agricoles, génèrent des pertes de surfaces productives et ont un impact sur les processus biogéochimiques se déroulant en milieu aqueux (Meybeck, 1988). Il est donc essentiel de comprendre les cycles des apports aux rivières et les processus qui affectent les matières qui y sont transportées si l'on veut maintenir une bonne qualité physico-chimique des eaux de rivières.

Les processus d'érosion, et de transport des matières en suspension (MES) sont des composants clés pour la compréhension des phénomènes et des mesures du fonctionnement du système Terre. L'érosion et les processus de redistribution de MES conditionnent les principaux événements de développement du paysage et jouent un rôle important dans le développement de sol. Le transport des MES dans une rivière fournit également, une mesure importante de son morpho-dynamisme, de l'hydrologie de son bassin de drainage, et de l'érosion ainsi que des processus de transport des MES dans ce bassin. Les changements de transfert des MES (terre-océan) aboutiront aux changements des cycles biogéochimiques globaux, particulièrement du cycle du carbone, puisque les MES jouent un rôle important dans le flux d'éléments et de nutriments clés, y compris le carbone organique. Le transport des MES dans la rivière peut aboutir à des taux accélérés de sédimentation dans des réservoirs, des problèmes pour le développement de la ressource en eau, des impacts défavorables sur des habitats aquatiques et des écosystèmes, provenant notamment de substances toxiques tels que les métaux lourds et les pesticides associés aux MES. Des nombreuses études ont déjà montré que le carbone organique particulaire fixé sur les MES et que les transferts entre les surfaces continentales et les océans doivent être intégrés dans le cycle global du carbone (Meybeck et Vörösmarty 1999 ; Ludwig et al. 1996 ; Coynel et al. 2005 ; Etcheber et al. 2007). La quantification des flux des MES peut donner des informations sur la quantité de sols érodés dans le bassin et alerter les gestionnaires de ce bassin pour chercher des stratégies afin de lutter contre ces problèmes. De plus, la quantification du flux de carbone associé aux MES est importante pour bien comprendre le cycle du carbone des

continents vers l'océan (Meybeck, 1993). Le carbone organique total (carbone organique particulaire et dissous) est un indicateur important pour la qualité de l'eau mais aussi un indice de la contamination organique.

Plusieurs études ont été faites sur des petits bassins versants agricoles inférieurs de 100 km² (Gao et al., 2007; Lefrançois et al., 2007; Estrany et al., 2009; Deasy et al., 2009) afin de bien étudier la dynamique de transport de MES. D'ailleurs, les études de cas pour le transport du carbone organique sont nombreuses pour les bassins versants composés de tourbières (Hope et al., 1997; Dawson et al., 2002; Worrall et al., 2003; Pawson et al., 2008) et de forêts (Meybeck, 1993; Molot and Dillon, 1996; Kao and Liu, 1997; Meybeck and Vörösmarty, 1999; Shibata et al., 2001). Par contre, les bassins versants agricoles sont très peu étudiés en termes de dynamique de transport avec une forte résolution des données lors des périodes de crue. Actuellement, très peu d'études ont été réalisées pour comprendre la dynamique des MES et du carbone (particulaire et dissous) pour de grands bassins versants agricoles intensifs dans différents contextes climatiques influencés par la région montagneuse des Pyrénées, l'océan Atlantique et la mer Méditerranée car il y a de fortes variabilités spatio-temporelles du climat, de l'occupation des sols et de la texture des sols. Les mesures sur le terrain et les échantillonnages sont généralement des tâches difficiles, rarement achevées sur le long terme dans de grands bassins versants. De part ces contraintes de terrain, les modèles jouent un rôle essentiel pour caractériser sur le long terme les flux de MES et le transport du carbone organique, sur les bassins versants. Beaucoup de modèles ont été développés tels que les modèles statistiques, empiriques, conceptuels et déterministes, afin de résoudre ces problèmes.

Le travail de thèse présenté dans ce mémoire traite des données acquises sur un bassin versant agricole dans la région de Coteaux de Gascogne (Sud-ouest de la France) dans un contexte d'agriculture intensive (bassin de la Save, affluent de la Garonne) de Janvier 2007 à Juin 2009. L'objet de cette étude est la dynamique du transport des MES et du carbone organique, parallèlement à une approche de modélisation. Les questions de recherche sont les suivantes:

- Quelles sont les dynamiques de transport et les facteurs influençant le transport des MES et du carbone organique (particulaire et dissous) à l'échelle du bassin versant dans un contexte d'agriculture intensive ?
- Quelle part de MES et de carbone organique sont transportées lors des crues ?

- Les particules mises en jeu proviennent-elles préférentiellement des versants (loin où proche par rapport à la station de la mesure), des bas-fonds des cours d'eau et aussi quelles sont les origines de ces matières ?
- Quel sont les flux de MES et de carbone organique à long terme ?

Les objectifs de la recherche sont, d'une part, de décrire et analyser la dynamique des MES et du carbone organique, particulaire (COP) et dissous (COD), lors des périodes de crue ainsi que d'évaluer la contribution des événements de crue sur les flux annuels et, d'autre part, de quantifier ces flux sur le long-terme par l'approche de modélisation agro-hydrologique.

La thèse comprend 3 publications (2 acceptée, 1 under review).

Le **chapitre 2** présente un état de l'art sur le transport des MES et du carbone organique et la modélisation à l'échelle du bassin versant. Il présente les différents processus et les équations qui gouvernent la dynamique. Les différentes méthodes pour mesurer la concentration de MES dans la rivière sont présentées. Il décrit le cycle du carbone, la relation entre l'hydrologie et le flux du carbone et leurs origines. La synthèse des différents modèles existantes utilisées pour reproduire le flux de MES est aussi présentée.

Le **chapitre 3** s'attache aux matériels et méthodes utilisés afin d'accomplir les objectifs. Les matériels concernent la description du bassin versant étudié (localisation, pédologie, occupation du sol et régime hydro-climatique), l'installation et le type de préleveur pour l'échantillonnage et les appareils pour déterminer les concentrations de MES et de carbone organique (particulaire et dissous). Le choix et la détail du modèle sont aussi présentés.

Le **chapitre 4** concerne l'analyse de la dynamique du transport des MES à l'échelle d'un bassin versant agricole, notamment pendant les crues pour différentes saisons, avec la contribution des flux des MES par rapport au flux annuel. Les facteurs hydro-climatiques conditionnant le transport de MES vers l'exutoire du bassin versant étudié pendant les périodes de crue sont identifiés par analyse des statistiques de corrélations et analyse en composante principale (ACP). Cette partie aborde également l'analyse des hystérésis et indentifie les sources de MES afin de déterminer ces origines. Cette partie présente la publication acceptée à *Journal of Earth Surface Processes and Landforms* (ESPL).

Le **chapitre 5** s'attache à décrire le transport fluvial et la relation entre les MES, le carbone organique particulaire et dissous dans le contexte d'un bassin versant agricole intensif. Le flux est quantifié pour chaque crue étudiée. Leurs relations avec le débit, les variables hydro-climatiques, et l'origine de ces matières sont étudiés afin de comprendre les facteurs qui contrôlent le transport des flux et les sources d'origine de ces matières. L'analyse des hystérésis pour différents événements de crue étudiés est aussi discutée. Cette partie était écrite sous la forme de publication qui a été acceptée à *Hydrological Processes*.

Le **chapitre 6** montre l'approche de modélisation pour caractériser le transport de MES et le carbone organique particulaire en utilisant le model agro-hydrologique SWAT (Soil and Water Assessment Tool). La simulation de MES est comparée avec les MES observés pour les deux années de suivis. Les résultats du modèle en calage sont présentés ainsi que la reconstitution de chroniques de flux de MES et COP (simulé par la relation entre le MES et COP) non mesurés. Le bilan d'eau du bassin est évalué. Les flux long-terme de MES et de COP sont estimés à partir des résultats de la simulation de concentration des MES et carbone organique particulaire. La relation empirique entre le flux annuel de sédiment et le flux d'eau est établie. De plus, les zones potentielles d'érosion sont identifiées. Cette partie était écrite sous la forme de publication qui a été soumise à *Journal of Hydrology* (Under Review)

Le **chapitre 7** constitue la discussion générale de ce travail de thèse. Il est ainsi discuté successivement les résultats scientifiques des chapitres 4, 5 et 6 et le modèle utilisé.

Enfin, le dernier chapitre se termine par une conclusion qui rappelle les principaux résultats de ce travail, et les perspectives qu'ils permettent d'envisager.

1. Introduction

This chapter addresses the general context of the research, research problematic and questions, the objectives of the thesis and follows by chapter descriptions containing in thesis.

1.1. Context and problematic

The processes of erosion, sediment delivery and sediment transport are key components and measures of the functioning of the earth system. Erosion and sediment redistribution processes are the primary drivers of landscape development and play an important role in soil development. Equally, the sediment load of a river provides an important measure of its morpho dynamics, the hydrology of its drainage basin, and the erosion and sediment delivery processes operating within that basin. The magnitudes of the sediment loads transported by rivers have important implications for the functioning of the system; for example through their influence on material fluxes, geochemical cycling, water quality, channel morphology, delta development, and the aquatic ecosystems and habitats supported by the river. In addition to their key role in the functioning of the natural earth system, erosion and sediment dynamics have important implications for human exploitation of that system and the sustainable use of natural resources. They must therefore be seen as having a highly significant socio-economic dimension. Soil erosion is integrally linked to land degradation, and excessive soil loss resulting from poor land management has important implications for crop productivity and food security and thus for the sustainable use of the global soil resource (Montgomery, 2007).

Similarly, the sediment loads of rivers can exert an important control on the use of a river for water supply, transport and related purposes. High sediment loads can, in particular, result in major problems for water resource development, through reservoir sedimentation and the siltation of water diversion and irrigation schemes, as well as increasing the cost of treating water abstracted from a river. High sediment inputs into lakes and coastal seas can result in sedimentation and changes in nutrient cycling. Furthermore, high sediment loads can result in pollution and habitat degradation in river systems. Against this background, changes in erosion rates and in sediment transport by the world's rivers can have important repercussions at a range of levels. From a global perspective, changes in erosion rates have important implications for the global soil resource and its sustainable use for food production. Changes in land-ocean sediment transfer will result in changes in global biogeochemical cycles, particularly in the carbon cycle, since sediment plays an important role in the flux of many key elements and nutrients, including organic carbon. At the regional and local levels, changes in erosion rates can have important implications for the sustainability of agricultural production and for food security. Equally, changes in the sediment load of a river can give rise to numerous problems. For example, increased sediment loads can result in accelerated

rates of sedimentation in reservoirs, river channels and water conveyance systems, causing problems for water resource development, and adverse impacts on aquatic habitats and ecosystems resulting from toxic substances such as heavy metals and pesticides associated with the sediments. Conversely, reduced sediment loads can result in the scouring of river channels and the erosion of delta shorelines as well as causing reduced nutrient inputs into aquatic and riparian ecosystems – particularly lakes, deltas and coastal seas. Because of their close links to land cover, land use and the hydrology of a river basin, erosion and sediment transport processes are sensitive to changes in climate and land cover and to a wide range of human activities. These include forest cutting and land-clearance, the expansion of agriculture, land use practices, mineral extraction, urbanization and infrastructural development, sand mining, dam and reservoir construction, and programmes for soil conservation and sediment control (Walling, 2005). Although recent concern about the impact of global change on the earth system has emphasized the impact of climate change resulting from the increased emission of greenhouse gases and associated global warming, it is important to consider other measures of the functioning of the system. Soil erosion rates and the sediment loads transported by the world's rivers provide an important and sensitive indicator of changes in the operation of the earth system and, as indicated above, widespread changes in erosion rates and sediment flux can have important repercussions and give rise to significant socio-economic and environmental problems.

Organic carbon fluxes and transfer through rivers have been found to have increased in relation to both sources and sinks due to large-scale human activities including landuse and landcover changes (Tate et al., 2000; Smith et al., 2001). Therefore, accelerated amounts of this flux into marine sediments and aquatic ecosystems maybe an important and significant net sink for anthropogenic CO₂ (Sarin et al., 2002). Some research has recently focused on the functional and dynamic nature of terrestrial ecosystems in connection with their role in the global carbon, nutrient and hydrological cycles (Kucharik et al., 2000). The export of organic carbon from the land's surface and terrestrial ecosystems to rivers through surface runoff and streamflow is an important gap in the modelling of the global biogeochemical carbon cycle. This gap can be addressed by the application of relevant hydrological modelling and organic load estimation approaches. The study of the organic carbon transport through World Rivers provides information on the rates of erosion of continents, the cycling of carbon on earth and the contribution of terrestrial carbon the aquatic systems and oceans (Meybeck, 1982; Meybeck, 1983; Sarin et al., 2002; Peel et al., 2003). The transport of organic carbon from

terrestrial ecosystems by rivers and hydrological fluxes to the oceans plays important role in regional budget of organic carbon entering the continent-ocean interface (Sarin et al., 2002). The fluxes of hydrological organic carbon have been found to correlate with environmental variables such as edaphic, climatic, topographic, ecologic and hydrological processes (Meybeck, 1993; Meybeck and Vorosmarty, 1999; Sarin et al., 2002).

So far, many studies have been conducted in small-scale agricultural catchments of less than 100 km² (Gao et al., 2007; Lefrançois et al., 2007; Estrany et al., 2009; Deasy et al., 2009) in order to understand the suspended sediment transport dynamics. Moreover, there is a wide range of literature investigating fluvial transport of organic carbon from peatland environments (Hope et al., 1997; Dawson et al., 2002; Worrall et al., 2003; Pawson et al., 2008). Such large investigations have been also conducted in forest environment (Meybeck, 1993; Molot and Dillon, 1996; Kao and Liu, 1997; Meybeck and Vörösmarty, 1999; Shibata et al., 2001). However, very few works have been investigated to study transport dynamics of suspended sediment and organic carbon with high resolution of extensive dataset within large agricultural catchments where intensive agriculture has been adopted and the climate is influenced by different conditions (the mountain regions of Pyrenees, Atlantic Ocean and Mediterranean regions). This lack was due to many difficulties such as spatiotemporal variability in climatic conditions, landuse and soil texture. Furthermore, field measurements and data collection are generally difficult tasks, rarely achieved over long timescales in large catchments. Due to these constraints, the application of models plays a vital role to characterize long-term sediment and organic carbon transport from the catchments. Lots of models have been developed such as statistical, empirical, conceptual and deterministic models to solve these problems.

The research was based on the data collection from January 2007 through June 2009 in the Save agricultural catchment, tributary of the Garonne River, located in Coteau Gascogne Region in Southwest France where intensive agriculture has been practiced. This work focuses on transport dynamics of suspended sediment and organic carbon together with modelling approach. The research questions are as following:

- How are their transport dynamics and what factors influencing the transport at catchment scale within the context of intensive agriculture?
- How are their loads transported during floods?

- Where are they come from? The distant sources such as hill slope erosion, river deposited sediment etc. and what are their origins?
- What are their long-term fluxes?

1.2. Objectives

The objectives of the research are, on the one hand, to describe and analyse the transport dynamics of suspended sediment (SS), and dissolved and particulate organic carbon (DOC and POC) during flood events with assessment of flood load contribution and, on the other hand, to quantify the long term fluxes by agro-hydrological modelling approach.

1.3. Thesis structure

The thesis consists of 3 publications (2 accepted and 1 under review).

Chapter 2 starts with the state-of-the art on suspended sediment, organic carbon transport and modelling at catchment scale. This also presents different processes and equations that govern its dynamics. Different methods of suspended sediment measurement in river were presented. The carbon cycle, relationship with hydrological processes and their origins were described. At the end of the chapter, a review of existing sediment transport models was raised.

Chapter 3 describes the materials and methods used to accomplish the objectives. The materials concern with the description of the study area (localisation, soil, landuse and hydro-climatic regime), installation of automatic water sampler and Sonde, and instruments to determine suspended sediment, dissolved and particulate organic carbon. The model selection and description were also attributed.

Chapter 4 involves the analysis of suspended sediment transport dynamics in the studied agricultural catchment with the assessment of flood load contribution. The hydro-climatic factors influencing the mobilisation of sediment load from the catchment outlet during flood events were identified by means of statistical analysis of correlations and Principle Component Analysis (PCA). This part details hysteresis patterns of each flood and identifies their suspended sediment sources in order to determine their origins. This chapter presented the publication accepted in *Journal of Earth Surfaces Processes and Landforms* (ESPL).

Chapter 5 describes the fluvial transport and relationship between suspended sediment and organic carbon (DOC and POC) within the agricultural catchment context. The fluxes were estimated during each flood events. Their relationship with discharge and hydro-climatic variables, and their origins were studied in order to comprehend the hydrological processes controlling the transport and their sources of origins. The analysis of each hysteresis pattern during different seasonal floods was discussed. This chapter was written in the form of publication accepted in *Journal of Hydrological Processes*.

Chapter 6 is concerned with modelling approach to characterise the transport of suspended sediment and particulate organic carbon using agro-hydrological model, the SWAT model (Soil and Water Assessment Tool). The simulation of suspended sediment was compared with observed sediment data from the two year observation. The catchment water balance was also evaluated. The fluxes of sediment and POC were estimated via long-term simulation of suspended sediment and POC concentrations. An empirical correlation between annual water yield and annual sediment yield was established and potential source areas of erosion were also identified for the studied catchment. This chapter was written in the form of publication which has been under review in *Journal of Hydrology*.

Chapter 7 provides the general discussion of the whole results and the model.

The last chapter is ended by the conclusion that reviewed the main researching findings of the study and perspectives from this research.

Chapter 2

Suspended sediment, organic carbon transport and modelling

The chapter starts with the state-of-the art on suspended sediment, organic carbon transport and modelling at catchment scale. This also presents different processes and equations that govern its dynamics. Different methods of suspended sediment measurement in river were presented. The carbon cycle, relationship with hydrological processes and their origins were described. At the end of the chapter, a review of existing sediment transport models was introduced.

2.1. Origins of suspended sediment

Suspended Sediment can be described as the motion of sediment particles during which the particles are surrounded by fluid (Chanson, 2004). The grains are maintained within the mass of fluid by turbulent agitation without (frequent) bed contact. Sediment suspension takes place when the flow turbulence is strong enough to balance the particle weight. The suspended sediment that we observed at the catchment outlet could originate from the contribution of three main processes: hillslope erosion, gully erosion, and channel bank erosion (Figure 2-1).



(A)



(B)



(C)

Figure 2-1 : Different types of soil erosion: (A) gully erosion, (B) rill erosion, (C) channel erosion

In our study, we focus on agricultural catchment; therefore, urban waste water and industrial emission were dismissed. The factor influencing erosion taken into account to study the erosion phenomenon can be grouped: soil erodibility, rainfall erosivity, soil occupation, topography and climate.

2.2. Anthropogenic activities

The erosion within the catchment can be the natural processes and anthropogenic activities. The modification of soil practices and intensification of agriculture, urbanization, could increase the soil erosion within the catchment. Walling (1999) showed that through geographical surface, the soil erosion rates under cultivation are 16 to 900 times higher than soil under natural conditions. Many authors have studied the impacts of agriculture on sediment to the river networks (Svoray & Ben-Said., 2009; Abaci et al., 2009; Outeiro et al., 2010). The changes of landuse resulted in soil loss when agricultural practices are not properly undertaken. Regarding the urbanization, the increasing of impermeable surface area (road, parking, and building) has decreased the infiltration surface and led the augmentation of surface runoff which drives up streamflow in the river, by affecting the bank erosion from the rapid velocity. Moreover, the barrage construction also has major impact on the sediment stocking at upstream part where it is located; for instance, the Assouan barrage on Nil River which decreased sediment flux of $100. 10^6 \text{ t year}^{-1}$ to zero and the barrage on Mississippi River in 1950s reducing nearly 70% of sediment load, while soil erosion from surface runoff remained constant (Walling and Fang, 2003).

2.3. Processes and mechanics of soil erosion

Soil erosion is a two-phase process consisting of the detachment of individual soil particles from the soil mass and their transport by erosive agents such as running water and wind (Morgan, 2005). When sufficient energy is no longer available to transport the particles, a third phase, deposition, occurs. Rainsplash is the most important detaching agent. As a result of raindrops striking a bare soil surface, soil particles may be thrown through the air over distances of several centimetres (Figure 2-2). Continuous exposure to intense rainstorms considerably weakens the soil. The soil is also broken up by weathering processes, both mechanical, by alternate wetting and drying, freezing and thawing and frost action, and biochemical. Soil is disturbed by tillage operations and by the trampling of people and livestock. Running water and wind are further contributors to the detachment of soil particles. All these processes loosen the soil so that it is easily removed by the agents of transport. The transporting agents comprise those that act areally and contribute to the removal of a relatively uniform thickness of soil, and those that concentrate their action in channels. The first group consists of rainsplash, surface runoff in the form of shallow flows of infinite width, sometimes termed sheet flow but more correctly called overland flow, and wind. The second group covers water in small channels, known as rills, which can be obliterated by weathering and ploughing, or in the larger more permanent features of gullies and rivers. A distinction is commonly made for water erosion between rill erosion and erosion on the land between the rills by the combined action of raindrop impact and overland flow, so called interrill erosion.

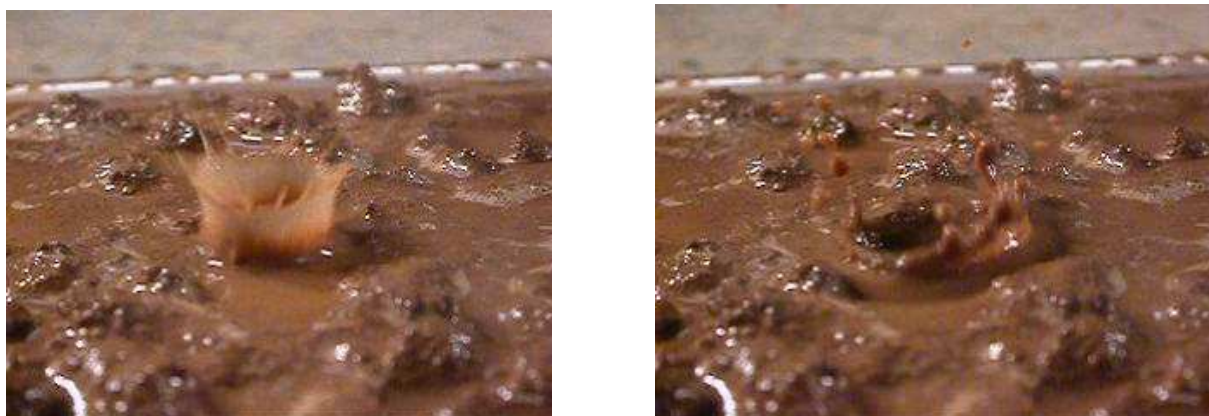


Figure 2-2 : Shear stress of soil and water through the impact of raindrop or splash effect

2.4. Detachment of soil particles by flow

The important factor in the hydraulic relationships is the flow velocity. Because of an inherent resistance of the soil, velocity must attain a threshold value before erosion commences. Basically, the detachment of an individual soil particle from the soil mass occurs when the forces exerted by the flow exceed the forces keeping the particle at rest. Shields (1936) made a fundamental analysis of the processes involved and the forces at work to determine the critical conditions for initiating particle movement over relatively gentle slopes in rivers in terms of the dimensionless shear stress (θ) of the flow and the particle roughness Reynolds number (Re^*), defined respectively by:

$$\theta = \frac{\rho_w u_*^2}{g (\rho_s - \rho_w) D} \quad (2-1)$$

Where,

- θ is known as the Shields number,
- ρ_w is the density of water,
- U_* is the shear velocity of the flow
- g is the acceleration of gravity,
- ρ_s is the density of the sediment,
- D is the diameter of the particle and u^* is the shear velocity of the flow.

2.5. Factors influencing soil erosion

2.5.1. Rainfall erosivity

Soil loss is closely related to rainfall partly through the detaching power of raindrops striking the soil surface and partly through the contribution of rain to runoff. This applies particularly to erosion by overland flow and rills, for which intensity is generally considered to be the most important characteristic.

2.5.2. Soil erodibility

Erodibility defines the resistance of the soil the forces of detachment, entrapment and transport resulting from raindrop impact and shear of surface flow. Although a soil resistance to erosion depends in part on topographic position, slope steepness and the amount of disturbance, such as during tillage, the properties of the soil are the most important

determinants. Erodibility varies with soil texture, aggregate stability, shear strength, infiltration capacity and organic chemical content. The large soil particles are resistant to transport because of the greater force required to entrain them and that fine particles are resistant to detachment because of their cohesiveness. The least resistant particles are silts and fine sands.

The shear strength of the soil is a measure of its cohesiveness and resistance to shearing forces exerted by gravity, moving fluids and mechanical loads. Its strength is derived from the frictional resistance met by its constituent particles when they are forced to slide over one another or to move out of interlocking positions, the extent to which stresses or forces are absorbed by solid-to-solid contact among the particles, cohesive forces related to chemical bonding of the clay minerals and surface tension forces within the moisture films in unsaturated soils. These controls over shear strength are only understood qualitatively, so that, for practical purposes, shear strength is expressed by an empirical equation:

$$\tau = c + \sigma \tan \phi \quad (2-2)$$

Where,

- τ is the shear stress required for failure to take place,
- c is a measure of cohesion,
- σ is the stress normal to the shear plane (all in units of force per unit area),
- ϕ is the angle of internal friction.

Both c and ϕ are best regarded as empirical parameters rather than as physical properties of the soil.

2.5.3. Soil occupation

Vegetation acts as a protective layer or buffer between the atmosphere and the soil. It serves as the obstacle to runoff which influences particle transport. The effectiveness of plant cover in reducing erosion by raindrop impact depends upon the height and continuity of the canopy and the density of ground cover. A plant cover dissipates the energy of running water by imparting roughness to the flow, thereby reducing its velocity.

2.5.4. Topography

Erosion would normally be expected to increase with increases in slope steepness and slope length as a result of respective increases in velocity and volume of surface runoff. Slope is the main factor in determine flow velocity, which transport the soil particles from the catchment. The catchment with steepness slope always produces more erosion and sediment transport to the stream networks. Further, while on a flat surface raindrops splash soil particles randomly in all directions, on sloping ground more soil is splashed downslope than upslope, the proportion increasing as the slope steepens

2.6. Channel erosion

Stream bank erosion occurs under natural conditions, particularly during peak storm flows and is part of an on-going cycle of sediment erosion and deposition within the stream system. The factors controlling river and stream formation are complex and interrelated. These factors include the amount and rate of supply of water and sediment into stream systems, catchment geology, and the type and extent of vegetation in the catchment. As these factors change over time, river systems respond by altering their shape, form and/or location. In stable streams, the rate of these changes is generally slow and imperceptible.

Some significant events which we always observe like flooding can trigger dramatic and sudden changes in rivers and streams. However, land use and stream management can also trigger erosion responses. The responses can be complex, often resulting in accelerated rates of erosion and sometimes affecting stability for decades. Over-clearing of catchment and stream bank vegetation, poorly managed sand and gravel extraction, and stream straightening works are examples of management practices which result in accelerated rates of bank erosion. Bank erosion can also be accelerated by factors such as:

- Stream bed lowering or infill,
- Inundation of bank soils followed by rapid drops in flow after flooding,
- Saturation of banks from off-stream sources,
- Redirection and acceleration of flow around infrastructure, obstructions, debris or vegetation within the stream channel,
- Removal or disturbance of protective vegetation from stream banks as a result of trees falling from banks or through poorly managed stock grazing, clearing or fire,

- Bank soil characteristics such as poor drainage or seams of readily erodible material within the bank profile,
- Wave action generated by wind or boat wash,
- Excessive or inappropriate sand and gravel extraction,
- Intense rainfall events.

2.7. Sediment delivery and transport processes in river

2.7.1. Concept of sediment delivery ratio

The Sediment Delivery Ratio (SDR) is the ratio between the rate of the sediment export from a tributary catchment and the rate of sediment production to channels within that catchment (Kasai et al., 2001). The SDR of a drainage catchment consists of two parts. The percentage of the material that reaches the stream is called the hillslope SDR (HSDR). The second part of the SDR of a drainage catchment is determined by the percentage of the sediment that is supplied to the stream and that reaches the catchment outlet. This is called the Channel SDR (CSDR). SDR is very different from a catchment to another (Figure 2-3)

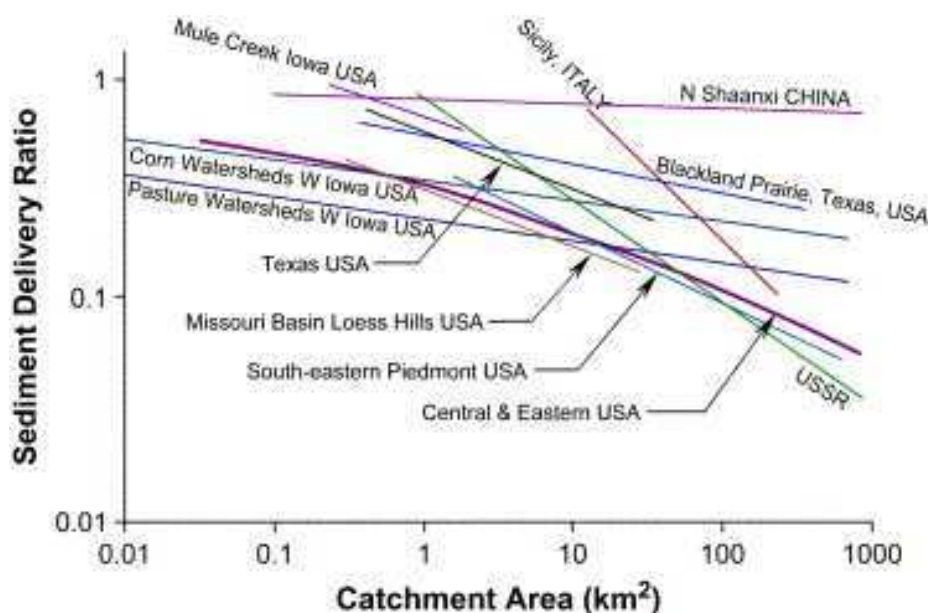


Figure 2-3: Relation between Sediment Delivery Ratio and the catchment sizes (From Lu et al. (2006), modified from Ferro and Minacapilli (1995) and Walling (1983).

Analysis of the SDR for a tributary catchment would provide information needed to understand the linkage between the three stages of sediment production to main-stem channels. Calculation of SDRs is particularly important when sediment budget are being

constructed to explore relationships between hillslope and channel processes (Kasai et al., 2001). A procedure for calculating SDR would thus be very useful for constructing sediment budgets. However, a generally applicable prediction equation for this ratio seems difficult to obtain for several reasons (Walling, 1983). Firstly, Walling points out that this is because ‘assessments that have been undertaken are themselves primarily based on a comparison of measured sediment yield with an estimate of gross erosion’. As catchment sizes increases, direct measurement of sediment produced from sources within catchment becomes increasingly difficult and the use of erosion equations become more unreliable. Valid estimates must account for the highly episodic nature of mass movement erosion, which often dominates sediment production in steepland catchments, and this generally requires field assessment or locally calibrated predictive equations for each erosion type (e.g. gully, landslide, and earth flow). Secondly, SDRs often vary widely between individual events (Trustrum et al., 1999). Marutani et al. (1999) have reported SDRs less than 1 for individual events within catchments where net channel degradation ($SDR > 1$) dominated in the longer term. In a review of SDRs, Richards (1993) concluded that the direct comparison between results of different studies is impossible because different degrees of temporal averaging were used. Despite the above analysis problems, Walling (1983) outlined some studies (Table 2-1) which have shown that SDRs can be influenced by morphological variables.

Table 2-1: Examples of proposed relationships between sediment delivery ration and catchment characteristics

Reference	Equation
Maner (1958)	$\log SDR = 2.962 + 0.869 \log R - 0.854 \log L$
Roehl (1962)	$\log SDR = 4.5 - 0.23 \log 10A - 0.510 \log R/L - 2.786 \log BR$
Williams and Berndt (1972)	$SDR = 0.627 S_d^{0.403}$
Williams (1977)	$SDR = 1.366 \times 10^{-11} A^{-0.100} R/L^{0.363} CN^{-5.444}$
Mou and Meng (1980)	$SDR = 1.29 + 1.37 \ln R - 0.025 \ln A$

R=catchment relief; L= catchment length; A=catchment area; R/L=relief ratio; BR=bifurcation ratio; S_d = slope of main stem channel (%); CN=SCS curve number (an index number to express the relationship between rainfall and runoff for wet conditions of the catchment, based on the Soil Conservation Service curve number technique (US Department

of Agriculture, Soil Conservation Service, 1972); R_c = gully density (units vary between equations). (After Walling, 1983).

Equations that incorporate geomorphological variables relating the process of sediment movement from source to delivery in the main channel can thus help to improve the prediction of SDRs.

2.7.2. Mechanisms of suspended sediment transport

The transport of suspended sediment occurs by a combination of advective turbulent diffusion and convection. Advective diffusion characterizes the random motion and mixing of particles through the water depth superimposed to the longitudinal flow motion (Chanson, 2004). In a stream with particles heavier than water, the sediment concentration is larger next to the bottom and turbulent diffusion induces an upward migration of the grains to region of lower concentrations. A time-averaged balance between settling and diffusive flux derives from the continuity equation for sediment matter:

$$D_s \frac{dc_s}{dy} = -w_o c_s \quad (2-3)$$

Where,

- c_s : the local sediment concentration at a distance y measured normal to the channel bed (mg l^{-1}),
- D_s : the sediment diffusivity
- w_o : the particle settling velocity (m s^{-1})

Sediment motion by convection occurs when the turbulent mixing length is large compared to the sediment distribution length scale. Convective transport may be described as the entrainment of sediments by very-large scale vortices: e.g. at bed drops, in stilling basins and hydraulic jumps (Figure 2-4).

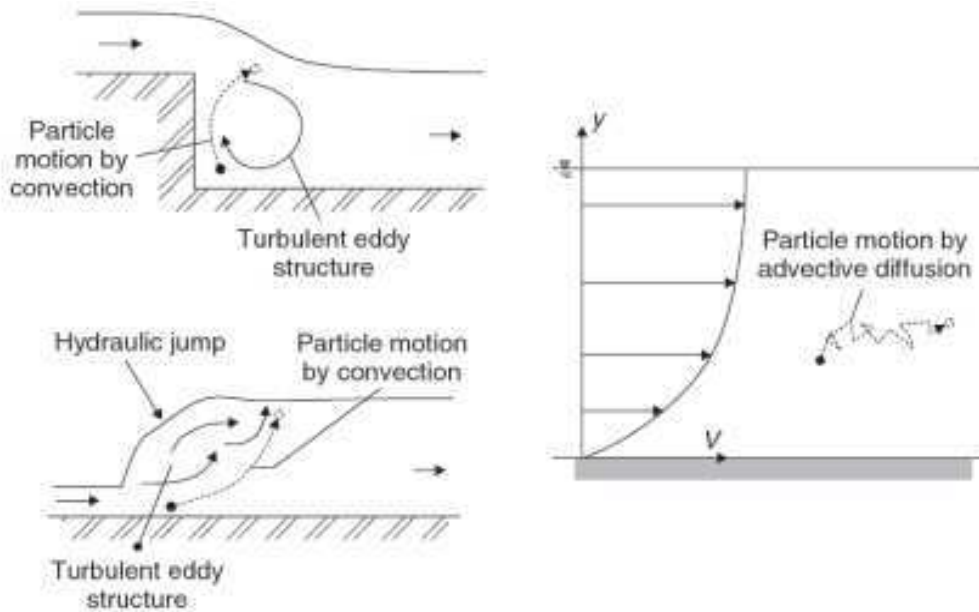


Figure 2-4: Suspended sediment motion by convection and diffusion processes (Huber Chanson, 2004)

2.7.3. Movement and particle deposition

Yalin (1977) indicated that for particle with diameter (d), there is a critical traction force in which the particle is in movement. This force has to be sufficient to compensate a weight and friction force exercised by other sediments in contact with particle. The diagram of Yalin-Shields (Figure 2-5) gives the value of parameter τ^* (quantifying the critical traction force) in function with the value of d^* and allows to distinguish the phase of movement of repos. τ^* and d^* are two dimensionless values defined as following:

$$d^* = d \left(\frac{\rho_s - \rho_e}{\rho_e} \frac{g}{\nu^2} \right)^{\frac{1}{3}} \quad \tau^* = \frac{\rho_e}{\rho_s - \rho_e} \frac{R}{d} i \quad (2-4)$$

Where,

- ρ_s : density of particle (kg m^{-3})
- ρ_e : water density (kg m^{-3})
- g : gravity (m s^{-2})
- ν : viscosity of water ($10^{-6} \text{ m}^2 \text{ s}^{-1}$)
- R : hydraulic radius (m)
- i : slope of water surface (%)
- d : particle diameter (m)

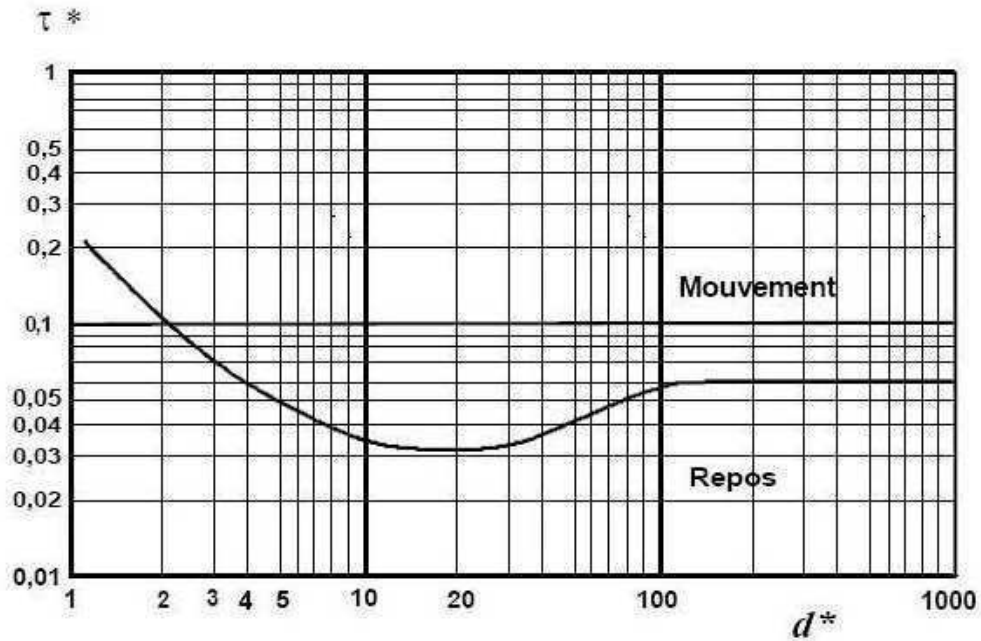


Figure 2-5: Diagram of Shields – Yalin (1977)

The particle alternates between phase of transport and phase of deposition according to their particle size, flow velocity within the environment (Figure 2-6) (Hjulstrom, 1935), shear stress, turbulence, flow movement, density and bed cohesion (Goodwin et al., 2003).

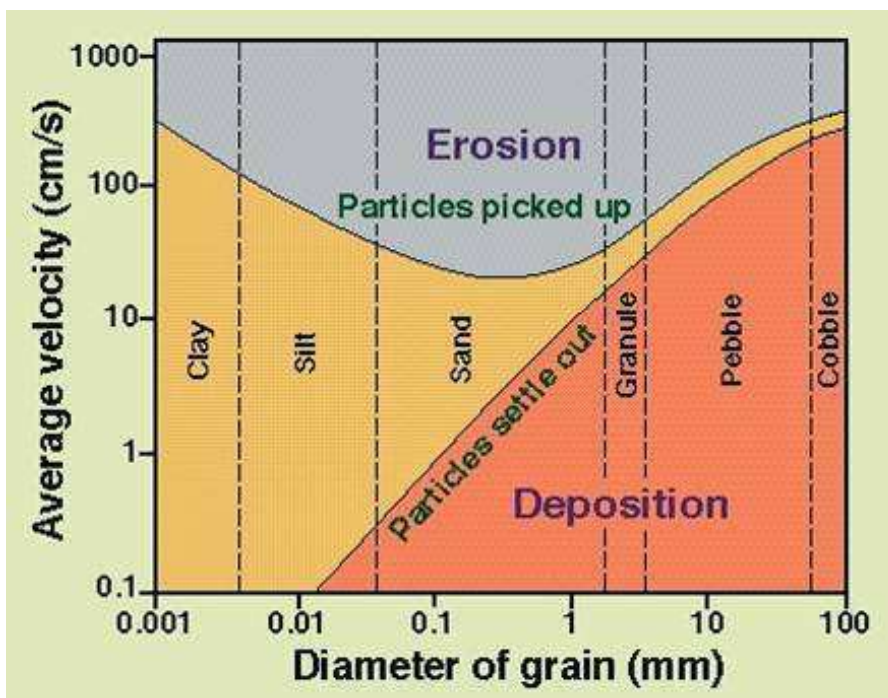


Figure 2-6: Diagram de Hjulstrom (1935): relationship between the water velocity and particle size to determine the context of erosion and sedimentation

Once the particle is in movement, it can have several modes of displacement: bedload transport, siltation and suspension. The transport mode depends on the flow velocity and particle size.

- Bedload transport concerns with gravel materials which displace by rolling or slipping on bed layer. This mode takes place when the flow increases within the flooding period or high topographic gradient.
- Siltation is concerned with the sufficiently light materials to be lifted from bed but too heavy to be suspended.
- Suspension is concerned with the fine materials such as clay, silt, or microorganism which can be in suspension due to the flow turbulence without contacting with river bed.

The particles in suspension can depose and then re-suspend or mobilize in another mode of transport depending on the energetic context.

2.7.4. Empirical relationship between suspended sediment and discharge

Suspended sediment is originated from process of soil erosion and transport, which can vary through hydrological conditions. The flow variability results in the different dynamics. The first consequence is the increase of suspended sediment with discharge. The empirical relation “rating curve” between suspended sediment concentrations and discharge was established by Van Rijn (1984) and used by lots of authors (Fenn et al., 1985; Crawford, 1991; Asselman, 1999; Syviski et al., 2000; Horowitz, 2003). The relation is a power function as below:

$$C = aQ^b \quad (2-5)$$

Where,

- C: suspended sediment concentration (mg l^{-1})
- Q: water discharge $\text{m}^3 \text{s}^{-1}$
- a and b are regression parameters

The precision of this relation is always weak because of strong dispersion. The inaccuracy is that the flux could be underestimated 50% (Ferguson, 1986). Lots of studies have been carried out in order to reduce the data dispersion, to characterize the term of empirical relation, or to

determine the causes of this dispersion. To decrease the dispersion, the authors proposed to modify the time step of integration of measurement. For instance, Haritashaya et al. (2005) reduced the variance of data by using the monthly mean instead of daily data. Morehead et al. (2003) directly integrate the variability of concentrations in dimensionless expression of empirical relation by considering the long-term mean:

$$\left(\frac{Q_s}{Q_{sl}} \right) = \Psi \left(\frac{Q}{Q_1} \right)^C \quad (2-6)$$

Where,

- Q_s : daily sediment discharge (kg s^{-1})
- Q : daily water discharge ($\text{m}^3 \text{s}^{-1}$)
- Q_{sl} : long-term mean of Q_s (kg s^{-1})
- Ψ & C : correlation parameters

The other authors searched for understanding the signification of this empirical relation but their interpretations were different according to explicative factors used. Syvitski et al. (2000) tried to characterize the parameters a & b through the geographical factors from the data of many catchments. Kazama et al. (2005) reached to propose an equation issued from the equation of Itakura-Kishi (1980), in which the sediment flux can be estimated from three factors: particle size, riverbed roughness and slope. However, this kind of equation is valid for only some types of rivers. The behaviour of suspended sediment and changes in suspended sediment concentration (SSC) during flood events are not only a function of energy conditions, i.e. sediment is stored at low flow and transported under high flow conditions, but are also related to variations in sediment supply and sediment depletion. These changes in sediment availability result in so-called hysteresis effects (Asselman, 1999).

A typology with three classes, inspired by Williams (1989) is presented in Figure (2-7). In the first class, peaks of SSC and discharge arrive simultaneously. The SSC-discharge plot is symmetrical between rising and falling limbs, with little or no hysteresis. This class is classically interpreted as the mobilization and transport of particles (Jansson, 2002), whose availability is not restricted during the flood for the concerned range of discharge. At low discharge, particles are coming from fine deposited sediment (Hudson, 2003) or maybe from bank materials. At high discharge, particles are coming from coarser deposited sediment

and/or from bank and channel hydrological erosion. Particles can also come from more remote sources, such as surface soil erosion, when discharge is principally linked to surface runoff. In the second class, the SSC peak arrives before the discharge peak and the relationship between SSC and discharge describes a clockwise hysteretic loop. This class is classically interpreted as the mobilization of particles whose availability is restricted during the event for the concerned range of discharge. Particles are believed to come from the removal of sediment deposited in the channel, with a decreasing availability during the event (Lenzi and Lorenzo, 2000; Steegen et al., 2000; Jansson, 2002; Goodwin et al., 2003). Particle production by erosion cannot resupply the deposited sediment stock decrease. The hypothesis of an important contribution of hillslope soils can be dismissed. In the third class, the SSC peak arrives later than the discharge peak and the SSC-discharge relationship describes an anticlockwise hysteretic loop (Williams, 1989). This class is classically interpreted as the arrival of more distant particles, coming from hillslope soil erosion or the upstream channel (Brasington and Richards, 2000; Lenzi and Lorenzo, 2000; Goodwin *et al.*, 2003; Orwin and Smart, 2004). Particles can also come from processes with slow dynamics (slower than the discharge rise), e.g. bank collapse may happen when bank material is sufficiently saturated. However, when there are multiple peaks of discharges during a flood event, the hysteresis patterns are mixed between clockwise and anti-clockwise with the form of eight shapes.

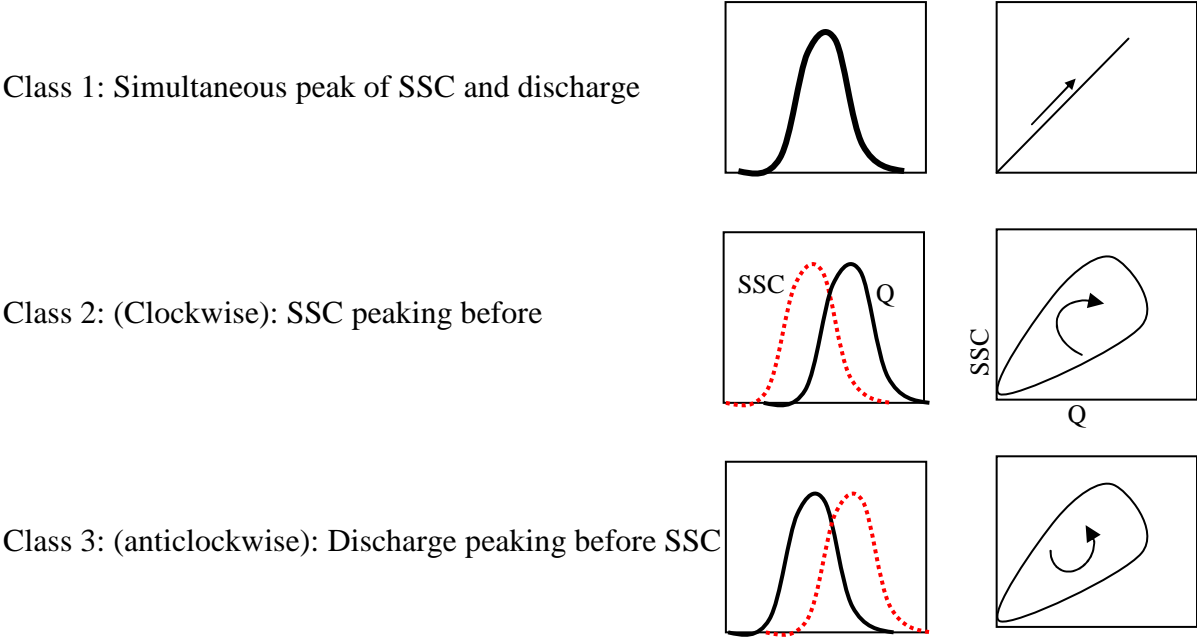


Figure 2-7: Typology of relationship between suspended sediment concentration (SSC) and discharge (Q) (From Lefrançois et al. (2007), modified from Williams (1989))

2.7.5. Sediment dynamics linked to particle availability

The availability of particle is defined as the quantity which can mobilize from sediment sources such as soil erosion from the catchment and channel erosion. The availability is susceptible to vary throughout the year and seasonal floods. The variability in event sediment transport during successive peaks of similar magnitude is influenced by sediment exhaustion effects. An example is the progressive reduction in suspended load at different temporal scales (within floods and within multiple-peak events, during a succession of events, and seasonally) related to the exhaustion of sediment availability. Alexandrov et al. (2003) observed that due to a sediment exhaustion effect, SSC levels during secondary floods in the Nahal Eshtemoa basin (Israel) were lower than those observed during a primary flood. The role of in-channel sediment storage, which controls suspended sediment transport during inter-flood periods of stable flow (Smith and Dragovich, 2008) is taken into account. Therefore, after a period of relatively high sediment transport (supply-rich floods), sediment becomes less and less available from the channel (exhaustion phenomenon) and sediment concentrations recorded during successive floods events are consequently lower (Walling, 1978). Lots of studies used the variability of the relationship between suspended sediment and discharge to identify the particle sources. The form of the curve is function of flow velocity and distance of sediment sources compared with a sampling point (sampling station).

2.8. Measurement of suspended sediment concentrations in rivers

There are many different techniques of suspended sediment concentration presented by Wren et al. (2000) such as acoustic, bottle sampling, pump sampling, focused beam reflectance, laser diffraction, nuclear, optical and remote spectral reflectance methods. Only some methods from existing literature are presented as following:

2.8.1. Water sampling

This method is very simple and direct. We conduct the sampling manually or by automatic sampling then we filter the water through filter paper such as nitrocellulose filter (GF 0.45 μm) or glass microfiber filter paper (Whatman GF/F 0.7 μm). After that, the filter is dried in an oven and then weight in order to determine suspended sediment concentration (SSC). Glass microfiber filter can be burnt to analyse other particulate matters such as particulate organic carbon etc.

2.8.2. Turbidity measurement

This method is mostly preferred to measure continuously the suspended sediment in the streams (Gippel 1995; Sadar 2002; Downing 2005). Continuous records of SSC can be obtained simply and conveniently by monitoring the turbidity of the river water, provided there is a close relationship between fluctuations in sediment concentration and turbidity. Thus, it needs sampling of SSC for a large range of hydrological conditions (high flow and low flow). Turbidity can be defined as an optical property of a water sample, which measures the degree to which a beam of light passing through the water is absorbed or scattered. Turbidity can be measured by turbidimetry or nephelometry (Minella et al., 2008). The former measures the attenuation or absorption of a ray of light as it passes through a liquid medium and the latter measures the degree of scattering that the light undergoes. Scattering refers to the light that is reflected or refracted by the surface of a particle, and absorption refers to light that is transformed into other forms of energy (such as heat) upon collision with a particle.

2.8.3. Acoustic method

Short bursts ($\approx 10\mu\text{s}$) of high frequency sound (1 to 5 MHz) emitted from a transducer are directed toward the measurement volume. Sediment in suspension will direct a portion of this sound back to the transducer (Thorne et al., 1991). When the sediment is of uniform size, the strength of the back scattered signal allows the calculation of sediment concentration. The water column is sampled in discrete increments based on the return time of the echo. The backscattered strength is dependent on particle size as well as concentration. This method is advantageous for good spatial and temporal resolution and measures over wide vertical range and nonintrusive. However, backscattered acoustic signal is difficult to translate and the signal attenuates at high particle concentration.

2.8.4. Acoustic Doppler Current Profiler (ADCP) method

Various authors (Holdaway et al., 1999; Hoitink et Hoekstra, 2005; Dinehart et Bureau 2005; Kostaschuk et al., 2005) have used ADCP method in their studies. This method is based on the same principle as acoustic method but used the profiler Doppler, dedicated initially to flow measurement. Indeed, the signal intensity gives information on suspended sediment concentration in water column by the sonar equation. This method is importantly advantageous to be capable of measuring the complete profile within the river cross-section rapidly. Yet, the calibration through sampling method is necessary to inverse the intensity

signal in concentrations. The measurement can carry out continuously by using a sensor type H-ADCP, installed permanently on the river bank.

2.8.5. Nuclear Method

Nuclear measurement utilizes the attenuation or backscatter of radiation. There are three basic types of nuclear sediment gauges: (1) those that measure backscattered radiation from an artificial source; (2) those that measure transmission of radiation from an artificial source; and (3) those that measure radiation emitted naturally by sediments (McHenry et al., 1967; Welch et Allen., 1973; Tazioli 1981). The first two have the broadest applicability. In backscattered gauges, radiation is directed into the measurement volume with the radioactive source isolated from the detector by lead. A sensor in the same plane as the emitter measures radiation backscattered from the sediment. In transmission gauges, the detector is opposed to the emitter and the attenuation of the radiation caused by the sediment is measured and compared to the attenuation of the rays caused by passage through distilled water. The ratio between these measurements allows calculation of sediment concentration. This method has low power consumption and can measure wide particle size and concentration range but the sensitivity is low.

2.8.6. Optical measurement

In this method, backscatter or transmission of visible or infrared light through water-sediment sample is measured. It is simple with good temporal resolution and allows remote deployment and data logging, relatively inexpensive. However, this method exhibits strong particle-size dependency, flow intrusive, point measurement only and instrument fouling.

2.8.7. Laser measurement

This method is based on the refraction angle of laser incident on sediment particles to be measure. There is no particle dependency but this method is unreliable, expensive, flow intrusive, point measurement only with limited particle-size range. Phillips & Walling (1995) used laser backscatter probe to measure the particle size characteristics of fluvial suspended sediment.

2.9. Organic carbon transport

2.9.1. Global carbon and water cycle

The increase in atmospheric CO₂ concentrations and the associated effects on the global climate have catalyzed the need for improved understanding of the carbon cycle (Robertson et al., 1996; Aumont et al., 2001). The role of hydrology in the carbon budget in terms of carbon fluxes at the catchment scale is focused. Carbon is stored on our planet in several major sinks: (1) as the gas carbon dioxide (CO₂) in the atmosphere; (2) in terrestrial ecosystems (living-dead biomass and soil); (3) fossil fuels and sedimentary rocks in the lithosphere; (4) the ocean carbon stocks and calcium carbonate in the marine organisms (Pidwirny; 2000). Soil carbon is a major component of the global inventory and exerts significant influence on carbon dynamics in connection with changes in climate and landuse (Sheimel et al., 1994). Soil organic carbon comprises approximately two-thirds of terrestrial carbon storage (Schimel et al., 1990; Townsend et al., 1992) or sink (Tans et al., 1990; Harrison et al., 1993) of carbon dynamics in response to climate changes and atmospheric CO₂. Water, organic carbon and other chemical substances in hydrological processes are connected through ecosystem processes and are strongly influenced by climate. Human activities have also significantly affected hydrological processes and nutrient cycling in terrestrial and freshwater aquatic ecosystems (Galloway et al., 1995). Land cover changes affect hydrological processes and these changes interact with organic carbon and nutrients in many significant ways. For example, landuse and land management activities affect the hydrological response of a system and thus nutrient fluxes through changes in land cover, evapotranspiration, and soil characteristics. These changes are followed by feedback mechanisms among water, carbon, and other chemical substances that bring further changes in these linked processes (Alexander and Smith, 1990). Recent studies on river ecosystems have shown that streamflow, primary production and litter pool sizes in catchment and the development of agriculture in catchments are major processes which influence the fluxes of organic carbon in river (Robertson et al., 1996). A review by Robertson et al. (1996) revealed three main categories of factors which govern organic carbon fluxes in catchments: streamflow, land management and quality of carbon.

2.9.2. Significance of organic carbon in rivers

The hydrological flux of organic carbon in rivers is a significant and essential element of river ecosystem (Robertson et al., 1996). Previous studies and findings on river ecosystems have

shown that hydrology, vegetation productivity, litter pool size and soil organic carbon in the catchment are the major agents which affect the fluxes of organic carbon in streams and rivers (Meybeck and Varosmarty, 1999; Neff and Asner, 2001; Raymond and Bauer, 2001; McDowell, 2002). Sarin et al. (2002) suggested that the hydrological flux of organic carbon is a minor but important component of the global carbon cycle. The transfer of organic carbon from terrestrial environments to the oceans and marine ecosystems may present a significant flux of organic carbon at a regional landscape scale (Meybeck and Varosmarty, 1999; Sarin et al. 2002).

The global system of river is increasingly being recognized as a major component of the carbon cycle. This is because of the important role of rivers in the terrestrial water cycle, regulating the mobilization and transfer of components from the land to the oceans. The erosion and transport of riverine organic carbon by rivers through surface runoff and streamflow from terrestrial ecosystems to the oceans provide a fundamental link in the global carbon cycle. This hydrological flux of organic carbon is correlated with the environmental properties of catchments in terms of climate (rainfall, temperature, evaporation, evapotranspiration) and hydrological processes (runoff coefficient, streamflow, unit hydrograph, flow duration curve) (Seitzinger and Kroeze, 1998; Meybeck and Vorosmarty, 1999).

Although anthropogenic activities have been altering these links for a long time, their impacts have accelerated in the past few decades causing significant regional and global changes (Robertson et al., 1996). Human activities including landuse and land cover changes affect hydrological processes and that these processes interact with carbon in many significant ways (Potter, 1991), certainly having major effects on; for example, rates of dissolved and particulate organic carbon (DOC and POC) that are leached or flushed from the land surface to river networks (Shlesinger, 1986). In spite of the considerable number of research activities over the past decades in relation to the global carbon cycle, the hydrological fluxes of organic carbon (DOC and POC) in rivers are still poorly understood (wood et al., 2002). The failure by the modelling to recognize the significance of the hydrological flux of organic carbon is not because water sampling data are inadequate. It is more oversight in the modelling.

Regardless of the role of hydrological and terrestrial organic carbon fluxes in the global carbon cycle, terrestrial organic carbon inputs provide the energy that drives aquatic food webs, particularly in forested rivers with low in-stream productivity. Organic carbon is a

carrier of energy flow through environmental systems (Rosenfeld and Roff, 1992; Galloway et al., 1995). The more reactive constituents of organic carbon make a significant contribution to heterotrophic metabolism in rivers (Kieber et al., 1989). These compounds of organic carbon also interact with other organic components and are absorbed by the surfaces of mineral solids, thus affecting the surface chemistry (pH, Alkalinity) and rate of aggregation (Raymond, 2005). Organic carbon especially DOC is an importance source of food for heterotrophic bacterial production, stimulating the bioavailability of iron to phytoplankton and providing some protection for aquatic organisms (McDowell, 2002). DOC also affects the complexity, solubility and mobility of metals, thus reducing the toxicity of these metals in rivers. Organic carbon input of DOC and POC play a central role in stream chemistry because they affect pH, and alkalinity, and acts as a substrate for microbial production (Dillon and Molot, 1997). As a result, the importance of the role of organic carbon in rivers can be productivity and significant impacts on food webs and bioavailability and toxicity of metals.

2.9.3. The link between hydrological flow and organic carbon fluxes

Variations in hydrological flow through terrestrial ecosystems have significant impacts including on the rates of dissolved and particulate substances. Predicting these changes requires an understanding of the relationship between organic carbon and its hydrological fluxes in terrestrial and riverine systems. Measurement of organic carbon concentrations (DOC and POC) and corresponding hydrological variables such as rainfall, and streamflow at comparable temporal and spatial scales must primarily be obtained. No full estimation is possible of organic carbon transported by rivers if there is no appropriate monitoring data such as climate, hydrological, and organic carbon data (Fuhrer et al., 1999). Variation in streamflow is the major controlling factor in the supply of carbon from catchments to the river networks. It is also a key factor controlling the rates, forms and distribution of primary production in the catchment and river. However, the relationship between discharge variations, and the transport of dissolved organic carbon (DOC) and particulate organic carbon (POC) through the river networks is still lacking.

2.9.4. Sources and origins of organic carbon

A major source of organic carbon (DOC and POC) is the carbon pools of terrestrial biosphere (Esser and Kohlmaire, 1989; Bauer and Druffel, 1998). These pools consist of living biomass (above ground biomass), dead biomass (litter) and soil organic carbon (SOC) largely resulting

from litter (WBGU, 1998). Figure (2-8) shows the carbon compartments of a terrestrial ecosystem (carbon dynamics).

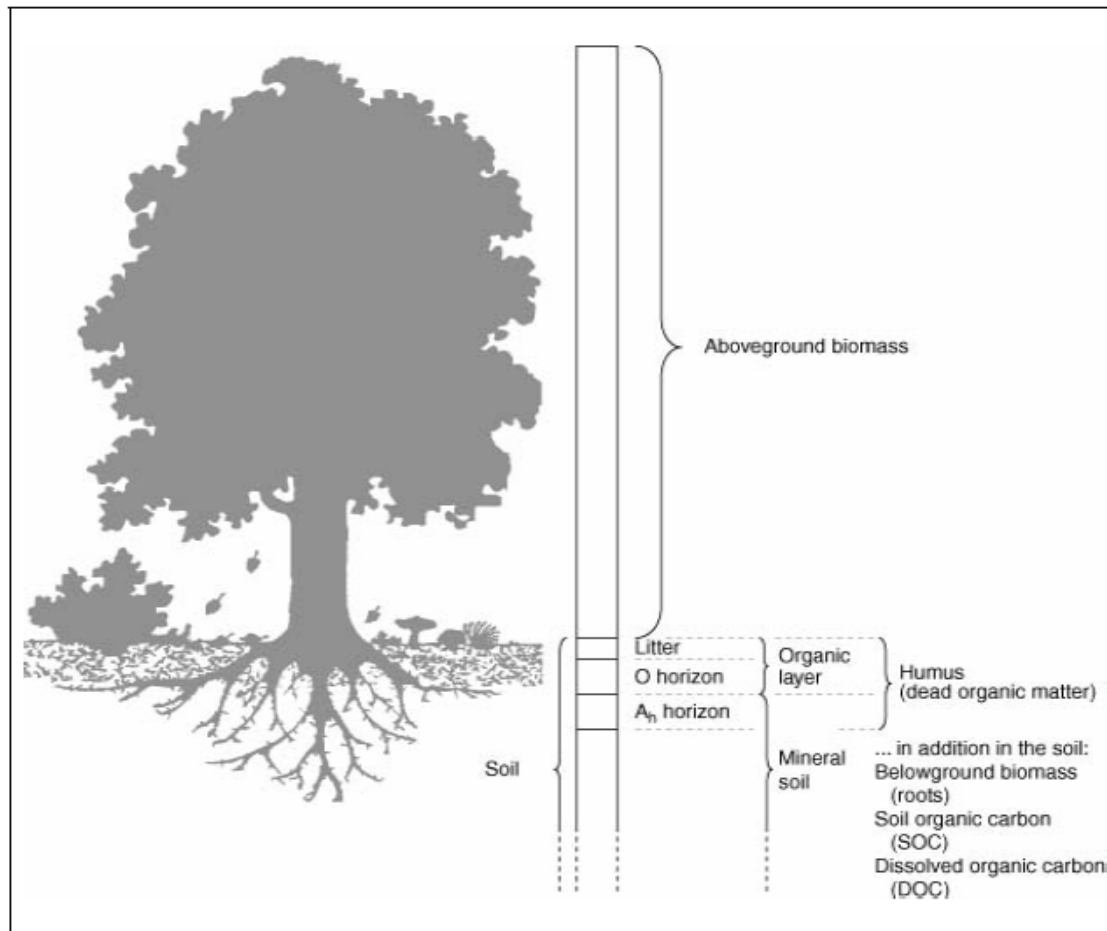


Figure 2-8: The carbon compartments of a terrestrial ecosystem (carbon dynamics) source: WBGU, 1998

Organic carbon in rivers can be classified into three size-classes of particles, in two main categories (Wotton, 1994):

- Particulate organic carbon or POC which includes: coarse particulate organic carbon (CPOC) (diameter >1mm) and fine particulate organic carbon (FPOC) (0.45 μ m to 1 mm)
- Dissolved organic carbon (DOC) (<0.45 μ m)

POC mainly originates from soil and riparian/litter environments. The main sources of coarse particulate organic carbon are fallen leaves, woody debris from the catchment and water plant (Maltby, 1992; Walker et al., 1994; Allan, 1995). FPOC includes the products of CPOC breakdown, and aggregation of DOC, litter and soil material (Meybeck, 1982; Ward et al.,

1994; Robertson et al., 1996). DOC is leached through catchment litter and soil organic carbon, which is imported in groundwater and produced by algae and water plants (Wotton, 1994; Robertson et al., 1996). DOC derives mainly from recent organic matter from topsoils in the catchment (Hélie and Hillaire-Marcel, 2006).

CPOC and FPOC can be consolidated into particulate organic carbon (POC). The total pool of instream organic carbon (TOC) therefore consists POC and DOC. This consolidated pool ($TOC = POC + DOC$) contains organic carbon from autochthonous (in-stream) sources and allochthonous (off-stream) sources (Robertson et al., 1996). An input of carbon through land or allochthonous sources is usually greater in amount than the input of organic carbon generated through aquatic plants within the stream channel (Lovett and Price, 1999).

2.10. Overview of soil erosion and sediment transport models

There are many existing sediment transport models which have been developed in recent decades. These models are based on statistical, empirical, conceptual or distributed approach. Aksoy et Kavvas (2005) have done a review of hillslope and catchment scale erosion and sediment transport models.

2.10.1. Statistical models

The simple relation between discharge and suspended sediment concentration ($C = a.Q^b$) was also frequently used to generate suspended sediment concentrations (Serrat, 1999; Asselman, 2000; Horowitz, 2003; Smith, 2008, Picouet et al. 2009). This type of relation can be defined by different temporal variability (hourly, daily, seasonal or annually). The performance is extremely variable in accordance with many controlling factors such as river discharge, catchment physiographic conditions, deposition/transport phenomenon, management practices within the catchment and seasons. For instance, Smith (2008) presented a sediment-discharge rating curve to estimate sediment load in an upland headwater catchment (53.5 km²) of the Lachlan River in south-eastern Australia based on seasonal rating curve (Figure 2-9).

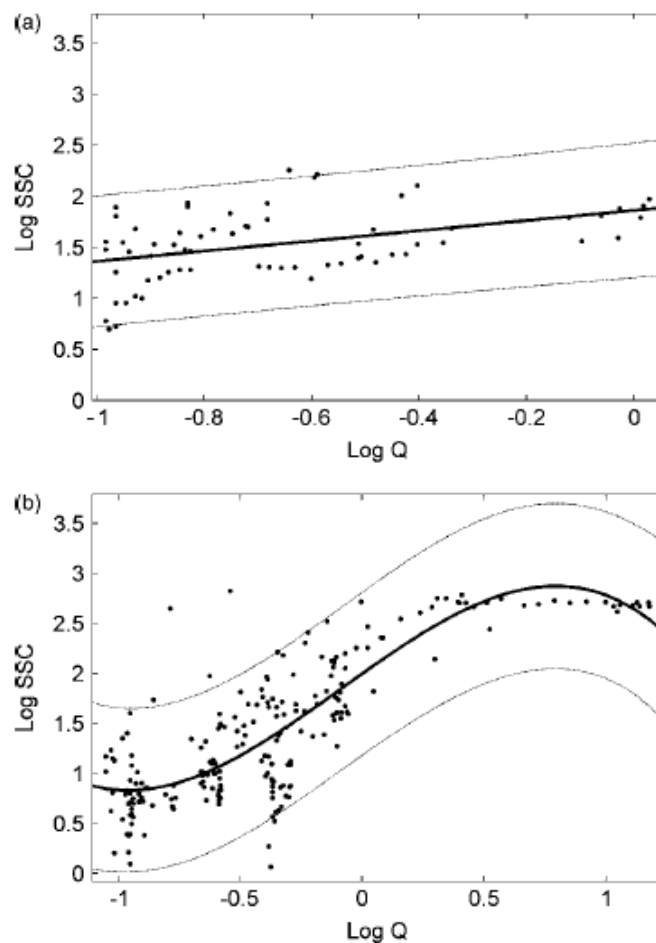


Figure 2-9: Catchment seasonal rating curves showing long discharge (Q) and log suspended sediment concentrations (SSC) with 95% confidence intervals for (a) summer-autumn and (b) winter-spring period (From Smith 2008)

Picouet et al. (2009) established two SSC-discharges relationship based on the rising stage of the flood and the falling stage of the flood to simulate SSC in Upper Niger River Basin. The two statistical equations were presented as following:

- For rising stage, the equation is a power function $C = a_1 Q^{b_1}$
- For falling stage, the equation is a linear function $C = a_2 + b_2 Q$

The variability of the relation could be explained by hysteresis effects during strong sediment transport event and deposition along the river within the catchment. The variability could be linked to the sediment stock which is easily mobilized during flood events reaching the sufficient capacity to transport those sediments.

2.10.2. Empirical models

These models were established from many empirical experiments from lots of catchments or agricultural plots (Universal Soil Loss Equation).

- Universal Soil Loss Equation (USLE)

The Universal Soil Loss Equation (Wischmeier et Smith 1978) is given by:

$$E = R \times K \times C \times L \times S \times P \quad (2-7)$$

Where,

E: average annual soil loss ($t \text{ ha}^{-1} \text{ year}^{-1}$)

R: rainfall erosivity factor ($\text{MJ mm ha}^{-1} \text{ year}^{-1}$)

K: soil erodibility factor ($t \text{ ha h ha}^{-1} \text{ year}^{-1}$)

C: cropping management factor

L: length of the slope

S: slope

P: supporting conservation practice factor

This equation is based on the huge amount of data from the United States. This equation was established originally to estimate the soil loss from agricultural plot and nowadays it is used to assess specific sediment flux at catchment scale by using calibrating parameters in the model. Its modified version (MUSLE) has been an attempt to compute soil loss for a single storm event. The USLE was revised (RUSLE) (Renard et al., 1991) and revisited (Renard et al., 1994) for improvement. A revised version of the USLE (RUSLE, Revised USLE) has been proposed by Renard *et al.* (1997) to replace the empirical model with a more conceptual one. However, the original model is still used in many countries since it represents an appropriate method for combining acceptable accuracy with relative simplicity and the ability to use quite basic data (Risse *et al.*, 1993; Kinnell and Risse, 1998; Hann and Morgan, 2006).

- Modified Universal Soil Loss Equation (MUSLE)

Williams (1995) developed the MUSLE by replacing the rainfall energy factor in the USLE with a runoff energy factor. The equation was developed using individual storm data from 18 basins in Texas and Nebraska and subsequently validated on 102 basins throughout the

United States using runoff data generated by the hydrologic component of the SWRRB model (Williams, 1982). The MUSLE is:

$$E = 11.8(Qq_p) \times K \times C \times L \times S \times P \quad (2-8)$$

Where,

- E: sediment yield (metric tonnes)
- Q: runoff volume (m³)
- Q_p : peak runoff rate (m³ s⁻¹)
- K, C, LS and P are the standard USLE factors for soil erodibility, crop management (cover), slope length-gradient, and erosion control practice.

The main advantages of MUSLE are its simplicity, the direct conceptual and physical relevance of its factors, the large data base upon which the empirical relationship was developed, and the capability to insert management considerations into factor selection. The main disadvantages are that the model is empirical and does not consider all physical factors affecting sediment yield, and generally there are fairly large errors associated with both soil loss (USLE) and runoff estimates.

○ Ludwig and Probst empirical equation

In 1998, Ludwig and Probst proposed an empirical relation to estimate specific sediment fluxes. This empirical equation was established from 58 catchments. The equation was based on the correlation from many explaining variables (hydro-climatic, lithological, pedological, morphological, and biological factors). Only significant parameters which were taken into account in order to avoid parameter multiplication. Thus, the equation is presented as below:

$$y = 0.020 \times Q \times \text{FOUR} \times \text{Slope} \quad (2-9)$$

(n=58; r = 0.91)

Where,

- y: suspended sediment-specific load (t km⁻² year⁻¹)
- Q: mean annual water yield (mm)
- FOUR: sum of the square of the mean monthly precipitations over then mean annual precipitation for all 12 months of the year (mm)

2.10.3. Conceptual models

Many conceptual models were created before and at the same time with the huge development of deterministic models, such as LASCAM (Viney and Sivapalan, 1999), Negev model, Lee and Singh reservoir model (Lee and Singh, 2005), Gafref model (Gafrej, 1993).

❖ LASCAM (Viney and Sivapalan, 1999)

LASCAM is a conceptual model of sediment transport which was developed from an existing conceptual model of water and salt fluxes (LASCAM) coupling with sediment modeling algorithm (Viney and Sivapalan, 1999). In the model, sediment generation is based on a modified version of the universal soil loss equation. However, the developed sediment transport algorithm does not discriminate between sediment size classes. This model was originally developed to predict of the effect of landuse and climate change on the daily trends of water yield and quality in forested catchment in Western Australia.

❖ Lee and Singh reservoir model (Lee and Singh, 2005)

The sediment component of model is based on the hydrological model of reservoir from Tank model (Sugawara, 1995). Three tanks were used in this study. Each tank represents a specific runoff component: the first tank represents the surface runoff component, the second tank represents the intermediate runoff (or interflow), and the third tank represents the groundwater runoff component (or baseflow). Similarly, it is assumed that the sediment yield from the first tank was produced by surface runoff, the second tank by intermediate runoff and the third tank from groundwater runoff. The sediment concentration was determined in each tank based on the sediment production of unit hydrogramme. The detail of the sediment module in tank model was well reported in Lee and Singh (2005).

2.10.4. Physically-based catchment erosion models

A number of physically-based models such as CREAMS (Knisel, 1980), ANSWERS (Beasley et al., 1980), KIREROS (Smith, 1981), WEPP (Nearing et al., 1989), HSPF (Bicknell *et al.*, 1997), EUROSEM (Morgan et al., 1998), SWAT, (Arnold et al., 1998), SHETRAN (Ewen et al., 2000), AnnAGPS (Binger and Theurer, 2003) have been used to study sediment transport at the catchment scale. Some model descriptions were presented as following:

❖ CREAMS (Knisel, 1980)

CREAMS (Chemicals, Runoff, and Erosion from Agricultural Management Systems) have the sediment transport component which analyzes the interrill area and rill separately. Detachment on both rill and interrill area is determined by the modified USLE. The procedure allows parameters to change along the overland flow profile and along waterways to describe spatial variability (Foster et al., 1981).

❖ ANSWERS (Beasley et al., 1980)

The ANSWERS model (Areal Nonpoint Source Watershed Response Simulation) is a catchment scale, distributed parameter, event oriented, physically based model. The ANSWERS was developed to simulate the influence of catchment management practices on runoff and sediment loss. The overall model structure consists of a hydrological model, a sediment detachment and transport model, and several routing components necessary to describe the movement of water in overland, sub surface and channel flow phases. The model operates on cell basis. Soil detachment, transport, and deposition are modelled as a function of the precipitation and the runoff process. The erosion process assumes that sediment can be detached by both rainfall and runoff but can only be transported by runoff.

❖ KIREROS (Smith, 1981)

KINEROS (Kinematic Erosion Simulation) model is composed of elements of a network such as planes, channels or conduits, and ponds or detention storages, connected each other. Channel erosion is taken the same as upland erosion except for the omission of the splash erosion as it is no longer effective on erosion in the channel phase. KINERO is an extension of KINGEN model developed by Rovey et al. (1977), with incorporation of erosion and sediment transport components. The sediment component of model is based upon the one dimensional unsteady state continuity equation. Erosion/deposition rate is the combination of raindrop splash erosion and hydraulic erosion/deposition rates. The model does not explicitly separate rill and interrill erosion.

❖ WEPP (Nearing et al., 1989)

WEPP (Water Erosion Prediction Project) is a continuous simulation model that predicts sediment yield and deposition from overland flow on hill slopes, sediment yield and

deposition from concentrated flow in small channels, and sediment deposition in impoundments. The model divides runoff between rills and interrill areas; thus, it calculates the erosion in the rills and interrills separately. The model computes spatial and temporal distributions of sediment yield and deposition, and provides explicit estimates of when and where in a catchment or on a hill slope that erosion occurs so that conservation measures can be selected to most effectively control soil erosion (Flanagan and Nearing, 1995).

❖ HSPF (Bicknell *et al.*, 1997)

HSPF (Hydrological Simulation Program Fortran) is a deterministic, lumped-parameter continuous time model which can also be used as a distributed parameter model as it reproduces spatial variability by dividing the basin in hydrologically homogeneous land segments and simulating runoff for each land segment independently. HSPF simulates three sediment types (sand, silt, and clay), in addition to single organic chemical and transformation products of that chemical. Re-suspension and settling of silt and clay (cohesive solids) are defined in terms of shear stress at the sediment-water interface. For sand, the capacity of the catchment or channel system to transport sand at a particular flow is calculated and re-suspension or settling is defined by the difference between the sand in suspension and the capacity. Calibration of the model requires data for each of the three solid types.

❖ EUROSEM (Morgan *et al.*, 1998)

The European Soil Erosion Model (EUROSEM) is a dynamic distributed (process-based) model designed to simulate the erosion, transport and deposition of sediment over the land surface by interrill and rill processes (Morgan *et al.*, 1998). The model can be applied to individual storm events and to spatial scales ranging from small fields to small catchments. It is designed particularly to predict soil loss from those storms that contribute most of the annual soil loss since it was thought that erosion was dominated by only a few events per year. EUROSEM has explicit simulation of interrill and rill flow; plant cover effects on interception and rainfall energy; rock fragments or stoniness effects on infiltration, flow velocity and splash erosion; and changes in the shape and size of rill channels as a result of erosion and deposition.

❖ SWAT (Arnold *et al.*, 1998)

SWAT is a physically based, semi distributed parameter, catchment scale model that operates on a continuous daily time step. The model simulates hydrological processes, sediment yield, nutrient loss, and pesticide losses into surface/groundwater and the effects of agricultural management practices on water in large ungauged watersheds (Arnold *et al.*, 1998). SWAT incorporates the effects of weather, surface runoff, evapotranspiration, crop growth, irrigation, groundwater flow, nutrient loading, pesticide loading, and water routing, as well as the long-term effects of varying agricultural management practices (Neitsch *et al.*, 2002, 2005). Sediment yield is estimated from the Modified Universal Soil Loss Equation (MUSLE). SWAT has been applied extensively for streamflow, sediment yield, and nutrient modelling in both small and large agricultural catchment.

❖ AnnAGPS (Binger and Theurer, 2003)

AnnAGPS is a batch-process, continuous simulation, daily time step, pollutant-loading model developed to simulate longterm runoff, sediment, and chemical transport from agricultural catchments (Cronshey and Theurer, 1998; Bingner and Theurer, 2003). It is a direct replacement for the single event model, Agricultural Non-Point Source (AGNPS) (Young *et al.*, 1989), and retains many features of AGNPS (Yuan *et al.*, 2001). Unlike AGNPS, AnnAGNPS divides the catchment into drainage areas with homogenous land use, soils, etc. and integrates these areas by simulated rivers and streams that route runoff and pollutants from each area downstream. AnnAGNPS uses the RUSLE to calculate sediment delivered to a field edge as a result of runoff from any type of precipitation.

2.11. Uncertainties of catchment model simulation

Uncertainties in the simulation are the important issue to consider in the simulation of hydrology, sediment yield. The main sources of uncertainties are:

- Simplifications in the conceptual model. For instance, the simplifications in a hydrological model, or the assumptions in the equations for estimating surface erosion and sediment yield, or the assumptions in calculating flow velocity in a river.
- Processes occurring in the catchment but not included in the model such as wind erosion, soil losses caused by landslides.

- Processes which are included in the model but their occurrences in the catchment are unknown to the modeler or unaccountable; for instance, reservoirs, water diversions, irrigations, or farm management affecting water quality.
- Processes that are not known to the modeler and not include in the model. These include dumping of waste material that may last for a number of years and drastically changes the hydrology or water quality such as construction of roads, bridges, tunnels, and dams.
- Errors in the input variables such as meteorological data (precipitation, temperature, etc.)
- Errors in the observed data such as observed flow, sediment data.

2.12. Synthesis of literature review

In this chapter, we addressed catchment soil erosion, the origins of suspended sediment and transport processes that govern its dynamics in the river. Soil erosion and transport of suspended sediment are complex and involve many factors such as rainfall erosivity, soil erodibility, soil occupation, topography. Hydrological factor is the main agent in mobilizing the sediment to the catchment outlet. The relationship between suspended sediment and discharge known as hysteresis patterns was explained. The location of sediment sources (sediment nearby the sampling station, river deposited sediment, hillslope sediment) is important to characterize the hysteresis class (symmetric line, clockwise, anticlockwise or complex pattern). The analysis of hysteresis through different flood events could be used to interpret sediment sources. To measure suspended sediment in river, different methods were presented. The choice of the method depends on the sediment range of the river which is observed and also the availability of the instruments. Among these methods, turbidity measurement is mostly preferred to measure continuously. The carbon cycle, relationship with hydrological processes and their origins were described in this chapter. This explained the link between hydrological flow and organic carbon fluxes. At the end of the chapter, a review of existing sediment transport models was introduced. Among these models, SWAT will be used in this study. The model is free assessable and user friendly environment.

The next chapter will present the methods used to accomplish the objectives of the research.

Chapter 3 Materials and methods

This chapter describes the materials and methods used to accomplish the objectives. The materials concern with the description of the study area (localisation, soil, landuse and hydro-climatic regime), installation of automatic water sampler and Sonde, and instruments to determine suspended sediment, dissolved and particulate organic carbon. The model selection and description of the model concepts were also described.

3.1. Study area

3.1.1. General description and location

The Save catchment, located in the area of Coteaux de Gascogne, is an agricultural catchment of 1110 km² and has its source in the piedmont zone of the Pyrenees Mountains (south-west France) at an altitude of 600 m, joining the Garonne River after a 140 km course with a linear shape and an average slope of 3.6‰ (Figure 3-1). This catchment lies on detrital sediments from the Pyrenees Mountains. It is bound on the east by the Garonne River, on the south by the Pyrenees and on the west by the Atlantic Ocean. The catchment elevation ranges from 98 to 620 m. There are 5 meteorological stations within the catchment.

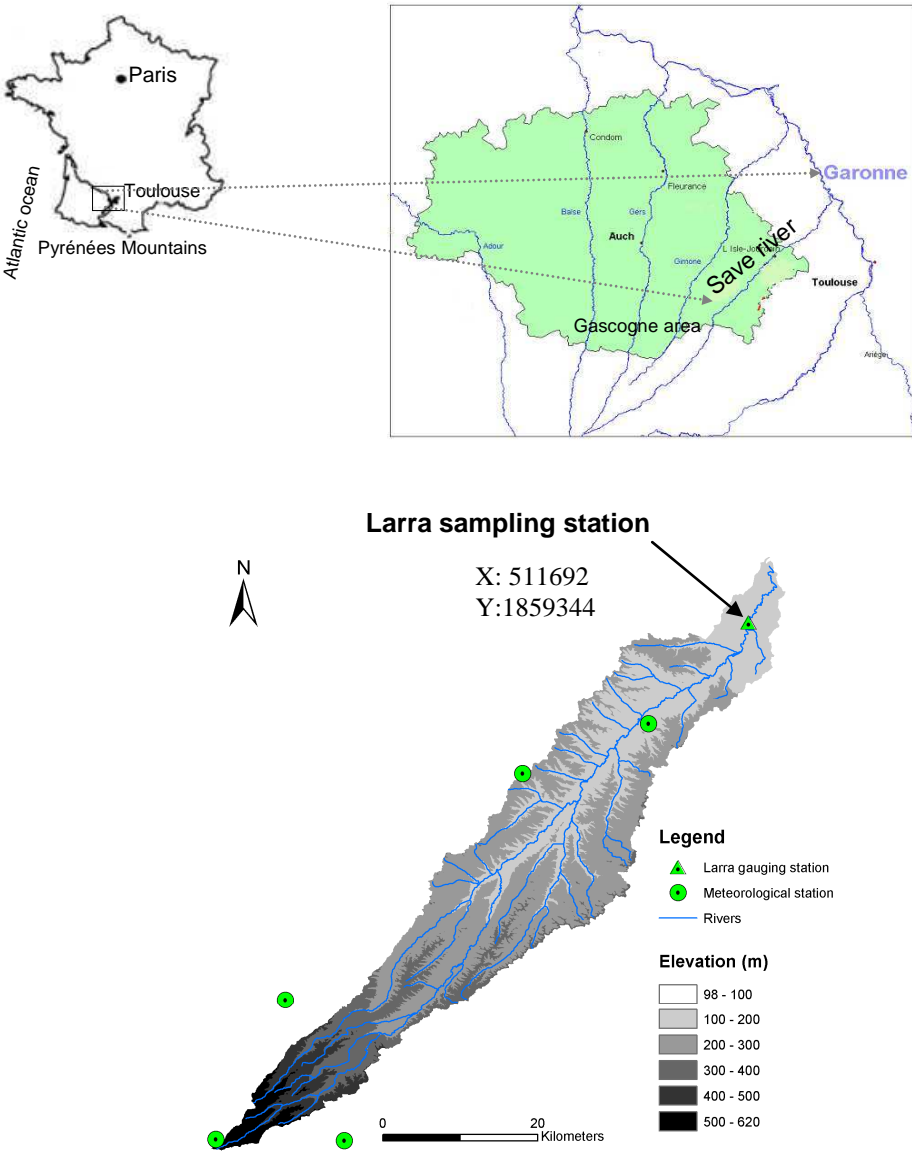


Figure 3-1: Location and topography of study area (Source: Cemagref de Bordeaux (UR ADBX))

3.1.2. Soil and geomorphology

Throughout the Oligocene and Miocene, this catchment served as an emergent zone of subsidence that received sandy, clay and calcareous sediments derived from the erosion of the Pyrenees Mountains, which were in an orogenic phase at that time. The heterogeneous materials were of low energetic value and produced a thick detrital formation of molasse type in the Miocene. From the Pleistocene onwards, the river became channelized, cutting broad valleys in the molasse deposits and leaving terraces of coarse alluvium (Revel and Guiresse 1995). The substratum of the catchment consists of impervious Miocene molassic deposits.

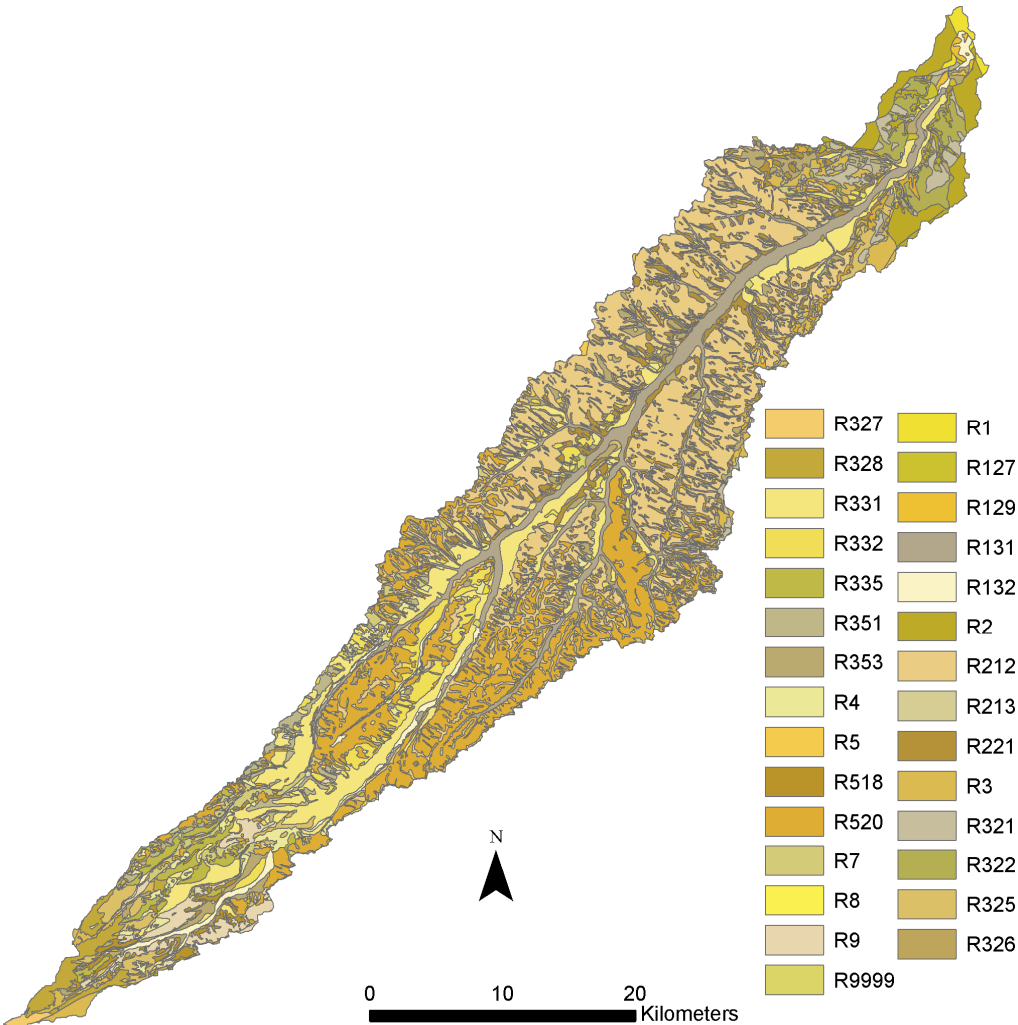


Figure 3-2: Major soils in the Save catchment (source: Cemagref de Bordeaux (UR ADBX))

In this area, which has been cultivated since the Middle Ages, mechanical erosion by ploughing has had a greater impact on downward soil displacement than water erosion, with a major impact on surface relief, mainly on levelling and soil distribution (Guiresse and Revel,

1995). Very weak erosion has led to the development of calcic luvisols (UN FAO soil units) on the tertiary substratum and local rendosols on the hard calcareous sandstone beds. On hillsides with very gentle slope, the calcic cambisols have been subjected to moderate erosion. Non-calcic silty soils, locally named boubènes, represent less than 10% of the soil in this area. Calcic soils are dominated by a clay content ranging from 40% to 50%, while non-calcic soils are silty (50-60%). There are 29 soil classes within the Save catchment presented in Figure 3-2. However there are some soil types which are found dominant in the whole catchment. The Deep calcaric soil (R 212) is dominant at the downstream area while the upstream area is mainly Calcaric Lithosol (R 520). The plane alluvial of the Save is composed of Calcaric Fluvisol (R 131) while the other zones are heterogenous, particularly the ancient terraces at the upstream area.

3.1.3. Landuse and management practices

The upstream part of the catchment is a hilly agricultural area mainly covered with dominant pastures and little forest. The downstream catchment is flat and devoted to intensive agriculture with many crop types such as winter wheat, corn, sunflower, soybean, cabbage etc. (90% of the area used for agricultural purposes) (Figure 3-3). Sunflower and winter wheat in rotation are mainly dominated at the downstream of the Save.

For pastures, there is one rotation of corn during a period of 4 years. Tillage works were practiced during April within this area. For sunflower-winter wheat rotation, the planting date of sunflower is on April 10 then is harvested on July 10. After that, winter wheat begins on October 9 then it is harvested on July 10, following year. The rotation of winter wheat-sunflower follows the same pattern by plant begins of winter wheat on October 9 and it is harvested on July 10. For following year, sunflower is planted on April 10, is harvested on July 10. The soil cover is empty from July through April during this rotation once per two years.

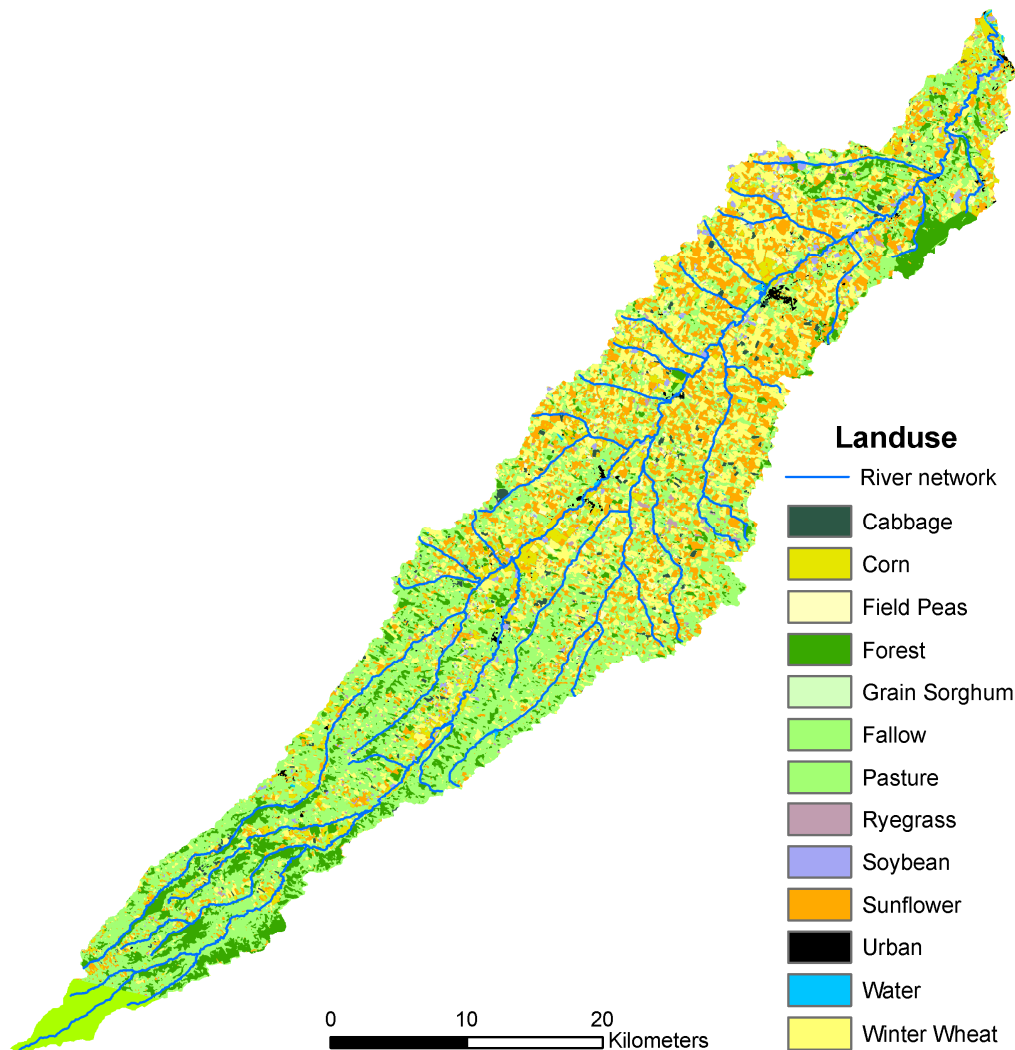


Figure 3-3: Landuse in the Save catchment with major agricultural land (Macary et al. 2006)

3.1.4. Climate and hydrology

The climatic conditions are oceanic, with annual precipitation of 700-900 mm and annual evaporation of 500-600 mm. The dry period runs from July to September (the month with maximum deficit) and the wet period from October to June (Ribeyeix-Claret, 2001). The mean temperature of the catchment is 13 °C with a minimum in January (5°C in average) and a maximum in August (20°C in average).

The hydrology regime of the catchment is mainly pluvial, i.e. regulated by rainfall (Echanchu, 1988), with maximum daily discharge in spring and low flows during summer (July to October). The summary of mean monthly discharge, specific discharge and runoff was presented in Figure 3-4.

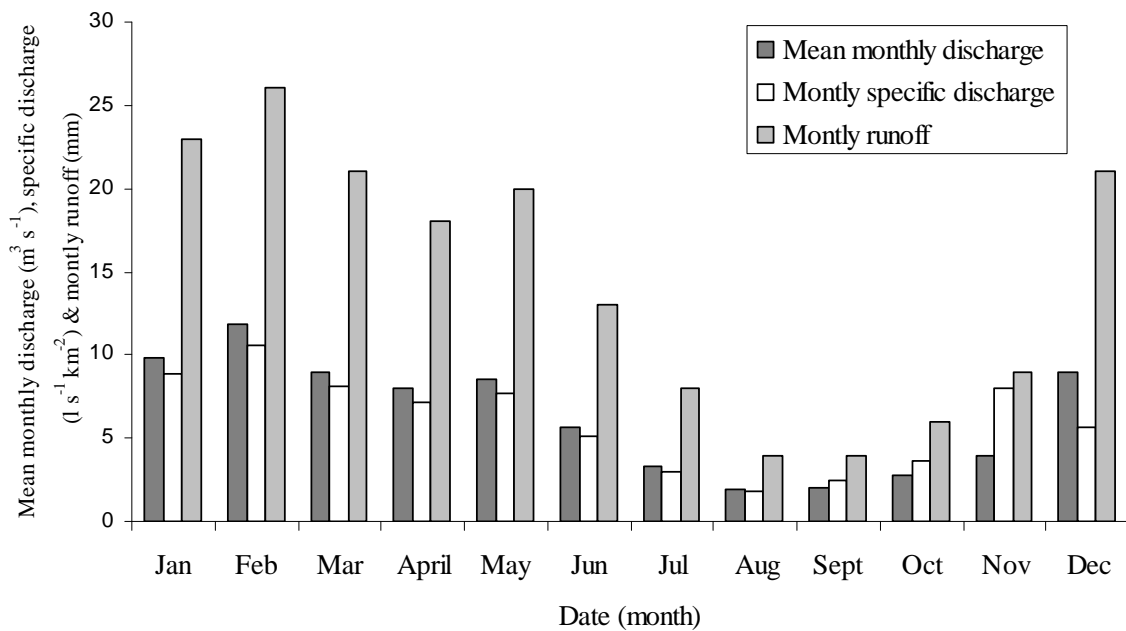


Figure 3-4: Summary of mean monthly discharge ($\text{m}^3 \text{s}^{-1}$), specific discharge ($\text{l s}^{-1} \text{km}^2$) and runoff (mm) in the Save catchment at Larra gauging station (1965-2006) (Data from CAGG) (banque hydro <http://www.hydro.eaufrance.fr/>)

The catchment substratum is relatively impermeable due to its high clay content. Consequently, the river discharge is mainly supplied by surface and subsurface runoff, and groundwater is limited to alluvial and colluvial phreatic aquifers. The maximum instantaneous discharge for the long-term period (1965-2006) is $620 \text{ m}^3 \text{ s}^{-1}$ (1st July 1977) (data from CACG: Compagnie d'Aménagement des Coteaux de Gascogne). During the low flow periods, the Save River was sustained by the Neste canal about $1 \text{ m}^3 \text{ s}^{-1}$.

3.2. Instrumentation and water quality monitoring

3.2.1. Sonde YSI and Ecotech preleveur

Sonde YSI 6920 (YSI incorporated, Ohio, USA) measuring probe and Automatic Water Sampler (EcoTech Umwelt-Meßsysteme GmbH, Bonn, Germany) were used for water quality monitoring in the studied catchment at Larra sampling station (Figure 3-5). The sonde can contain with many sensors such as nitrate, turbidity, pH, oxygen, redox, electrical conductivity. Each sensor has to be calibrated before installing in the river. EcoTech can be programmed to activate the sampling based on water level variations and time intervals. The

automatic water sampler contains 24 bottles of 1 litre, which allows taking many water samples during both small and high magnitude flood.

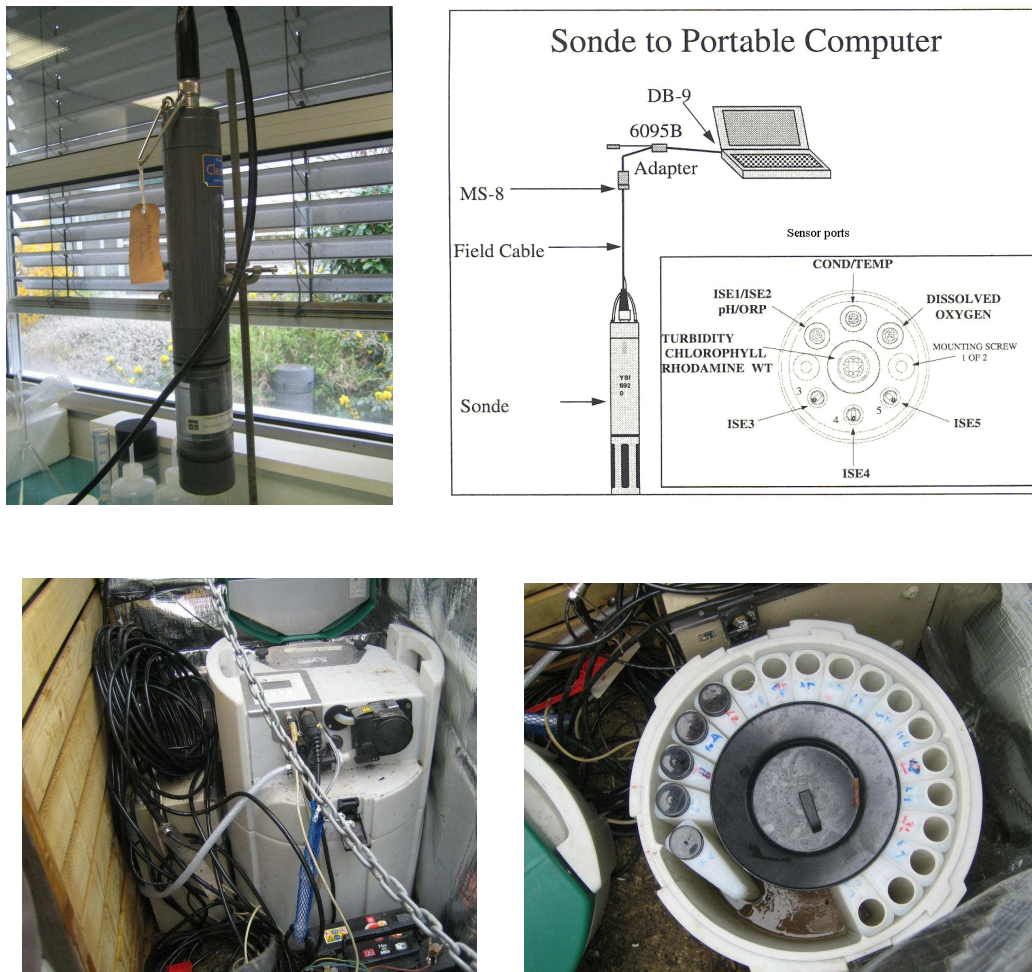


Figure 3-5: Sonde YSI 6920 and Ecotech Preleveur with 24 of 1 litre bottles

3.2.2. Calibration processes of Sonde

The Sonde has been calibrated before installing at Larra gauging station. The sensors of each parameter were calibrated separately as following:

- Depth with one point at zero in atmospheric environment
- Conductivity: 1413 $\mu\text{s}/\text{cm}$ at 25 °C
- pH with three points: 7 (-40mV and 40 mV), 4 (140 et 220 mV); 10 (170 and 180 mV)

- Nitrate with three points: 100 mg l⁻¹, 1 mg l⁻¹, and 1 mg l⁻¹ at cold temperature lower than 10 °C
- Turbidity with two points: 0 and 1000 NTU (Nephelometric Turbidity Units)

3.2.3. Physico-chemical parameters in situ and water sampling

We installed Sonde YSI 6920 (YSI Incorporated, Ohio, USA) measuring probe and Automatic Water Sampler with 24 bottles of 1 litre at the Save catchment outlet (Larra bridge) in January 2007 (Figure 3-6). The Sonde was positioned near the bank of the river under the bridge, where homogeneity of water movement was properly considered for all hydrological conditions. The pump inlet was placed next to the Sonde pipe. The dissolved oxygen content, electrical conductivity, nitrate, pH, turbidity and water level were recorded at 10-min intervals. The values of the different parameters in water were detected by sensors on the Sonde YSI and the data then transferred to the ecoTech memory. We programmed the Sonde to activate the automatic water sampler for pumping water. The automatic water sampler was activated by water level variations $\Delta x(\text{cm})$ ranged from 10 cm to 30 cm, depending on seasonal hydrological conditions for both the rising and falling stage. This sampling method provided high sampling frequency during flood events. Manual sampling was also carried out using a 2 litter bottle lowered from the Larra bridge, near the Sonde position, at weekly intervals when water levels were not remarkably varied. Temperature, pH, and electric conductivity were measured by WTW instrument (pH/Cond 340i/SET) at the field for weekly water samples.



Figure 3-6: Schema of installing water quality monitoring system at Larra station: A) pump inlet and Sonde pipe, B) Automatic Water Sampler EcoTech, C) Sampling site at Larra bridge

3.3. Technical problems

During the study period, several technical problems such as sensor derivation and crushing led to occasional difficulties in measuring continuous water turbidity. Sensors were exhausted after a period of 3 to 5 months; therefore, each sensor had to be recalibrated or possibly replaced by the new one. By so doing, we could avoid from signal errors resulting from

sensor derivation. However, we missed continuous measurements for some flood periods, but we carried out intensive manual sampling, particularly during the flood events.

3.4. Determination of suspended sediment and organic carbon

3.4.1. Filtration and determination of suspended sediment concentration

We filtered the water samples from both manual and automatic sampling in the laboratory using pre-weighed nitrocellulose filter (GF/F 0.45 μm) to separate the suspended sediment fraction. We filtered water volume, ranging from 150 ml to 1000 ml according to the particle load. After filtration, the filters containing suspended particles were dried at 40 $^{\circ}\text{C}$ for 48 hours then weight again to determine suspended sediment concentration (Figure 3-7).



Water samples



Filtration material



Incubator



Filters after filtration

Figure 3-7: Photo of filtration for obtaining suspended sediment concentration

3.4.2. Organic carbon analysis

A-Dissolved organic carbon (DOC)

The water sample had been again filtered through another type of filter-glass microfiber filter (GF/F Whatman 0.7 μm) which was burnt at 450 $^{\circ}\text{C}$ for 5:30 hours before utilizing in order to eliminate organic track. After filtering, each water sample was then acidified with HCL (12N;

pH=2) and store at 4 °C until analyses as soon as possible. The DOC analyses were carried out on Shimadzu TOC-5000 analyzer (Figure 3-8).



Figure 3-8: Photo of Shimadzu TOC-5000 analyzer (ECOLAB Analytical Laboratory, Toulouse)

B-Particulate organic carbon (POC)

The filtered paper containing suspended sediment were then acidified with HCL 2N in order to remove carbonates and dried at 60 °C for 24 h. Particulate organic carbon (POC) analyses were carried out using LECO CS200 analyzer (Etcheber et al, 2007) (Figure 3-9) at EPOC Laboratory, Bordeaux. POC contents are expressed as a percentage of dry weight of sediment, abbreviated to POC% and POC concentrations are expressed in mg l^{-1} .



Figure 3-9: Photo of LECO CS200 analyzer (EPOC Analytical Laboratory, Bordeaux)

3.5. SWAT model selection and description

SWAT 2005 (Soil and Water Assessment Tool) was selected in this study is firstly because of many applications to assess hydrology and sediment transport in both small and large catchments undertaken in different regions. Secondly, the model is free (<http://swatmodel.tamu.edu/>) and user friendliness environment. Thirdly, SWAT project of the Save catchment could be extended afterwards to study other problematic such as nitrate and pesticide transport dynamics.

SWAT is physically based distributed, agro-hydrological model that operates on a daily time step and is designed to predict the impact of management on water, sediment, and agricultural chemical yields in ungauged catchments (Arnold et al., 1998). The model is computationally efficient and capable of continuous simulation in large complex catchments with varying soils, and management conditions over long time periods. SWAT uses readily available inputs and has the capability of routing runoff and chemicals through stream and reservoirs, and allows the addition of flows and the inclusion of measured data from point sources. Major component models include weather, hydrology, soil temperature, plant growth, nutrients, pesticides and land management. SWAT can analyze both small and large catchments by discretizing into sub-basins, which are then further subdivided into hydrological response

units (HRUs), having homogenous land use, soil type and slope (Figure 3-10). The SWAT system embedded within geographical information system (GIS) that can integrate various spatial environmental data including soil, land cover, climate and topographical features.

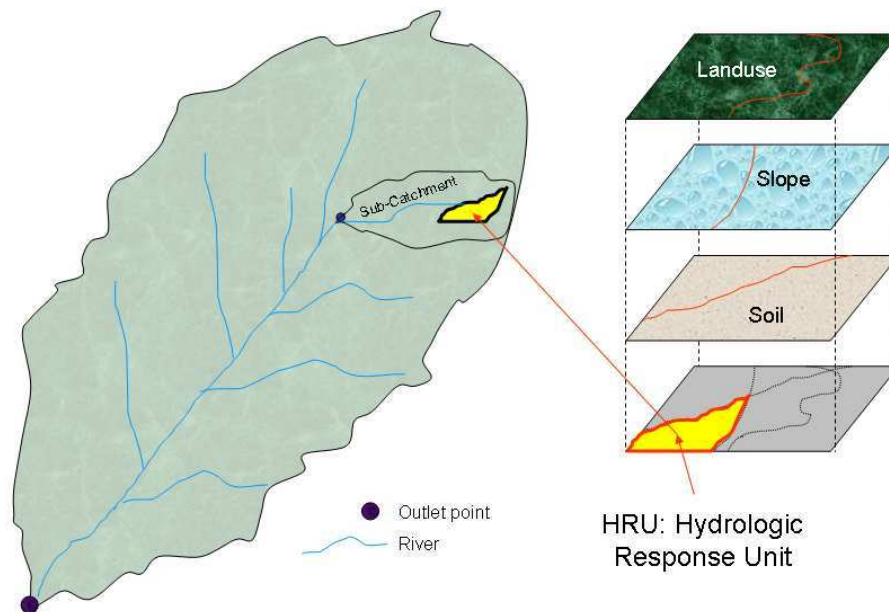


Figure 3-10: Schema of HRUs definition

3.5.1. SWAT water balance

In SWAT, water balance is the driving force behind everything that happens in the catchment. To accurately predict the movement of pesticides, sediments or nutrients, the hydrological cycle as simulated by the model must conform to what is happening in the catchment. Simulation of the hydrology of a catchment can be separated into two major divisions. The first division is the land phase of the hydrological cycle, presented in Figure (3-11). The land phase of the hydrological cycle controls the amount of water, sediment, nutrient and pesticides loadings to the main channel in each sub-basin. The second division is the water or routing phase of the hydrological cycle which can be defined as the movement of water, sediments, etc. through the channel network of the catchment to the outlet. SWAT simulates the hydrological cycle based on the soil and water balance equation as following:

$$SW_t = SW_0 + \sum_{i=1}^t (R_{\text{day}} - Q_{\text{surf}} - E_a - W_{\text{seep}} - Q_{\text{gw}})_i \quad (3-1)$$

Where,

- SW_t : the final soil water content (mm),
- SW_0 : the initial soil water content on day i (mm),
- t : the time (days), R_{day} is the amount of precipitation on day i (mm),
- Q_{surf} : the amount of surface runoff on day i (mm),
- E_a : the amount of evapotranspiration on day i (mm),
- W_{seep} : the amount of water entering the vadose zone from the soil profile on day i (mm),
- Q_{gw} : the amount of return flow into the river on day i (mm).

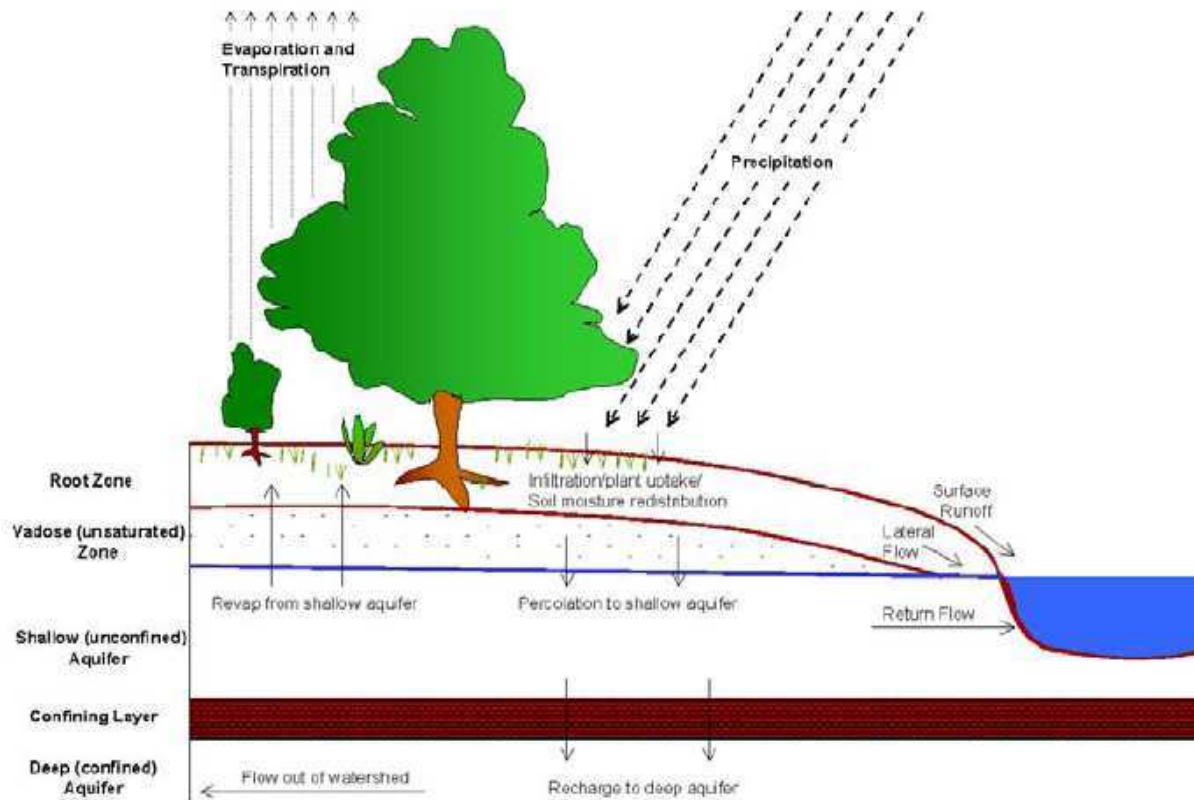


Figure 3-11: Schematic representation of the hydrological cycle (From SWAT model theory)

3.5.2. Surface runoff

Surface runoff occurs whenever the rate of precipitation exceeds the rate of infiltration. SWAT has two methods for estimating surface runoff: the SCS curve number method (USDA-SCS, 1972) and the Green & Ampt method. For sub daily data, it is suitable to use

Green & Ampt method. In this study, the SCS method was used to compute surface runoff volume for each HRU. The SCS curve number equation is:

$$Q_{\text{surf}} = \frac{(R_{\text{day}} - 0.2S)^2}{(R_{\text{day}} + 0.8S)} \quad (3-2)$$

Where,

- Q_{surf} : the accumulated runoff or rainfall excess (mm)
- R_{day} : the rainfall depth for the day (mm)
- S : retention parameter (mm), calculated by $S = 25.4 \left(\frac{100}{\text{CN}} - 10 \right)$

The SCS curve number (CN) is a function of the soil's permeability, landuse and antecedent soil water conditions. CN is a parameter of the model. The detail of CN values is presented in the SWAT theory document.

Peak runoff rate is estimated using a modification of the Rational Method (Chow et al., 1988). Daily rainfall data is used for calculations. Flow is routed through the channel using a variable storage coefficient method (Williams, 1969) or the Muskingum routing method (Cunge, 1969). The modified rational formula used to estimate peak flow is given below:

$$q_{\text{peak}} = \frac{\alpha_{\text{tc}} \times Q_{\text{surf}} \times \text{Area}}{3.6 \times t_{\text{conc}}} \quad (3-3)$$

Where,

- q_{peak} : the peak runoff rate ($\text{m}^3 \text{s}^{-1}$)
- α_{tc} : the fraction of daily rainfall that occurs during the time of concentration
- Q_{surf} : the surface runoff (mm H_2O)
- Area: the subbasin area (km^2)
- t_{conc} : the time of concentration for the subbasin (hr)
- 3.6 : unit conversion factor

3.5.3. Evapotranspiration

There are three methods for estimating potential evapotranspiration (PET) used in SWAT: Prisley Taylor (1972), Penman Monteith (Monteith, 1965) and Hargreaves & Samani (1985).

In this study, Penman method was used to estimate potential evapotranspiration. The three PET methods included in SWAT vary in the amount of required inputs. The Penman method requires solar radiation, air temperature, relative humidity and wind speed. The Priestley-Taylor method requires solar radiation, air temperature and relative humidity but the Hargreaves method requires only temperature. For this study, we used Penman method. The Penman-Monteith equation is:

$$\lambda E = \frac{\Delta \cdot (H_{\text{net}} - G) + \rho_{\text{air}} \cdot c_p [e_z^0 - e_z]}{\Delta + \gamma \cdot (1 + r_c / r_a)} \quad (3-4)$$

Where,

- λE : The latent heat flux density ($\text{MJ m}^{-2} \text{d}^{-1}$)
- E : the depth rate evaporation (mm d^{-1})
- Δ : The slope of the saturation vapor pressure-temperature curve, de/dT ($\text{KPa } ^\circ\text{C}^{-1}$)
- H_{net} : the net radiation ($\text{MJ m}^{-2} \text{d}^{-1}$)
- G : the heat flux density to the ground ($\text{MJ m}^{-2} \text{d}^{-1}$)
- ρ_{air} : the air density (kg m^{-3})
- C_p : the specific heat at constant pressure ($\text{MJ kg}^{-1} \text{ } ^\circ\text{C}^{-1}$)
- e_z^0 : the saturation vapor pressure of air at height z (kPa)
- e_z : the water vapor pressure of air at height z (kPa)
- γ : the psychrometric constant ($\text{kPa } ^\circ\text{C}^{-1}$)
- r_c : the plant canopy resistance (s m^{-1})
- r_a : the diffusion resistance of the air layer (aerodynamic resistance) (s m^{-1})

3.5.4. Groundwater

The groundwater simulation is partitioned into aquifer system i.e an unconfined aquifer (shallow 2 to 20m) and a deep-confined aquifer (>20m) in each sub basin. Percolation from the bottom of the root zone is considered as recharge to the shallow aquifer. Water that enters the deep aquifer is assumed to contribute to streamflow outside the catchment (Arnold et al., 1993). In SWAT 2005, the water balance for a shallow aquifer is calculated with equation below:

$$aq_{\text{sh},i} = aq_{\text{sh},i-1} + w_{\text{rchrg}} - Q_{\text{gw}} - w_{\text{revap}} - w_{\text{deep}} - w_{\text{pump,sh}} \quad (3-5)$$

Where,

- $a_{q_{sh,1}}$: the amount of water stored in the shallow aquifer on day i (mm)
- $a_{q_{sh,i-1}}$: the amount of water stored in the shallow aquifer on day i (mm)
- w_{rchrg} : the amount of recharge entering the aquifer on day i (mm)
- Q_{gw} : the groundwater flow, or base flow into a main channel on day i (mm)
- w_{revap} : the amount of water moving into the soil zone in response to water deficiencies on day i (mm)
- w_{deep} : the amount of water percolating from the shallow aquifer into the deep aquifer on day i (mm)
- $w_{pump, sh}$: the amount of water removed from the shallow aquifer by pumping on day i (mm).

The steady state response of groundwater flow to recharge is estimated by the equation below:

$$Q_{gw} = \frac{800 \times K_{sat}}{L_{gw}} \times h_{wtbl} \quad (3-6)$$

Where,

- Q_{gw} : the groundwater flow, or base flow into a main channel on day i (mm)
- K_{sat} : the hydraulic conductivity of the aquifer (mm/day)
- L_{gw} : the distance from the ridge or sub basin divide for the groundwater system to the main channel (m)
- h_{wtbl} : the water table height (m)

3.5.5. Erosion and Sediment component

The sediment from sheet erosion for each HRU is calculated using the Modified Universal Soil Loss Equation (MUSLE) (Williams, 1975). The USLE uses rainfall as an indicator of erosive energy but MUSLE uses the amount of runoff to simulate erosion and sediment yield. The benefits of the substitution are: the prediction accuracy of the model is increased, the need for a delivery ration is eliminated, and single storm estimates of sediment yields can be calculated.

The equation of MUSLE in SWAT is presented as below:

$$\text{Sed} = 11.8 \times (Q_{\text{surf}} \times q_{\text{peak}} \times A_{\text{hru}})^{0.56} \times K_{\text{USLE}} \times C_{\text{USLE}} \times P_{\text{USLE}} \times LS_{\text{USLE}} \times \text{CFRG} \quad (3-7)$$

Where,

- Sed is the sediment yield (t) on a given day,
- Q_{surf} is the surface runoff volume (mm ha^{-1}),
- q_{peak} is the peak runoff rate ($\text{m}^3 \text{s}^{-1}$), A_{hru} is the area of the HRUs (ha),
- K_{USLE} is the soil erodibility factor,
- C_{USLE} is the cover and management factor,
- P_{USLE} is the support practice factor,
- LS_{USLE} is the USLE topographic factor,
- CFRG is the coarse fragment factor.

The details of the USLE factors can be found in (Neithsch et al., 2005).

The sediment concentration is obtained from the sediment yield which corresponds to flow volume within the channel on a given day. The transport of sediment in the channel is controlled by simultaneous operation of two processes: deposition and degradation. When Channel deposition or channel degradation occurs, it depends the sediment loads from the upland areas and transport capacity of the channel network. If the sediment load in a channel segment is larger than its sediment transport capacity, channel deposition will be the dominant process. Otherwise, channel degradation occurs over the channel segment. SWAT calculates the maximum amount of sediment that can be transported from channel segment as a function of the peak channel velocity:

$$\text{conc}_{\text{sed,ch,mx}} = \text{SPCON} \times v^{\text{spexp}} \quad (3-8)$$

Where,

- $\text{conc}_{\text{sed,ch,mx}}$ (ton m^{-3}) is the maximum concentration of sediment that can be transported by streamflow (i.e., transport capacity),
- SPCON is a coefficient defined by user, spexp is exponent parameter for calculating sediment reentrained in channel sediment routing that is defined by the user ($1 < \text{spexp} < 2$)
- v (m s^{-1}) is the peak channel velocity.

The peak channel velocity in a reach segment at each time step is calculated from:

$$v = \frac{PRF}{n} \times R_{ch}^{2/3} \times S_{ch}^{1/2} \quad (3-9)$$

Where,

- v is the peak channel velocity ($m\ s^{-1}$),
- PRF is the peak rate adjustment factor with a default value of unity,
- n is manning 's roughness coefficient, R_{ch} is the hydraulic radius(m),
- S_{ch} is the channel invert slope ($m\ m^{-1}$).

The maximum concentration in the reach is compared with the concentration of sediment in the reach at the beginning of the time step, $conc_{sed,ch,i}$,

- If $conc_{sed,ch,i} > conc_{sed,ch,mx}$, deposition is the dominant process in the reach segment. The net amount of sediment deposited is calculated by:

$$Sed_{dep} = (conc_{sed,ch,i} - conc_{sed,ch,mx}) \times V_{ch} \quad (3-10)$$

Where,

- sed_{dep} is the amount of sediment deposited in the reach segment (metric tons),
- $conc_{sed,ch,i}$ is the initial sediment that can be transported by water (kg/l or ton/m^3)
- V_{ch} is the volume of water in the reach segment (m^3).

- If $conc_{sed,ch,i} < conc_{sed,ch,mx}$, degradation is the dominant process in the reach segment. The net amount of sediment reentrained is calculated by:

$$Sed_{deg} = (conc_{sed,ch,mx} - conc_{sed,ch,i}) \times V_{ch} \times K_{ch} \times C_{ch} \quad (3-11)$$

Where,

- sed_{deg} is the amount of sediment reentrained in the reach segment (metric tons),
- $conc_{sed,ch,mx}$ is the maximum concentration of sediment that can be transported by water ($kg\ l^{-1}$ or $ton\ m^{-3}$),
- V_{ch} is the volume of water in the reach segment (m^3),
- K_{ch} (CH_EROD) is the channel erodibility factor ($cm\ h^{-1}\ Pa^{-1}$),
- C_{ch} (CH_COV) is the channel cover factor.

The final amount of sediment in the reach is calculated by:

$$\text{sed}_{\text{ch}} = \text{sed}_{\text{ch},i} - \text{sed}_{\text{dep}} + \text{sed}_{\text{deg}} \quad (3-12)$$

Where,

- sed_{ch} is the amount of suspended sediment in the reach (metric tons),
- $\text{sed}_{\text{ch},i}$ is the amount of the suspended sediment in the reach at the beginning of the time period (metric tons),
- sed_{dep} is the amount of sediment reentrained in the reach segment (metric tons).

The total amount of sediment that is transported out of the reach segment is computed as:

$$\text{sed}_{\text{out}} = \text{sed}_{\text{ch}} \times \frac{V_{\text{out}}}{V_{\text{ch}}} \quad (3-13)$$

Where,

- sed_{out} is the total amount of sediment transported out of the reach (metric tons),
- sed_{ch} is the amount of suspended sediment in the reach (metric tons),
- V_{out} is the volume of water leaving the reach segment (m^3) at each time step,
- V_{ch} is the volume of water in the reach segment (m^3) at each time step.

3.5.6. SWAT model input

The spatially distributed data (GIS input) needed for ArcSWAT interface include the Digital Elevation Model (DEM), soil data and landuse data. Meteorological data and river discharge were also used for prediction of streamflow and calibration purposes.

○ Digital Elevation Model

Topography is defined by a DEM that de-scribes the elevation of any point in a given area at a specific spatial resolution. The DEM was used to delineate the watershed and to analyze the drain-age patterns of the land surface terrain. Subbasin parameters such as slope gradient, slope length of the terrain, and the stream network characteristics such as channel slope, length, and width were derived from the DEM. In this study, Digital elevation map (DEM) with a resolution of $25 \text{ m} \times 25 \text{ m}$ was received from BD TOPO R IGN France- Cemagref de Bordeaux (UR ADBX) (Figure 3-12 A)

- Meteorological data

Meteorological data included 5 rainfall stations with daily precipitation from Meteo France (Figure 3-12 A). Some past and missing data was generated for some stations by linear regression equation from the data of the nearest stations with complete measurement. Two stations at the upstream part having a complete measurement of daily minimum and maximum air temperature, wind speed, solar radiation and relative humidity was used to simulate the potential evapotranspiration (PET) in the model by Penman method.

- Soil data

SWAT model requires different soil textural and physico-chemical properties such as soil texture, available water content, hydraulic conductivity, bulk density and organic carbon content for different layers of each soil type. These data were obtained mainly from the following sources: soil map from CACG and digitized by Cemagref de Bordeaux (UR ADBX) (Macary et al. 2006) with the scale of 1:80 000 and soil properties for SWAT soil data base (Lescot et al. 2009). In this study, soil classes were simplified (Figure 3-12 B).

- Landuse and management practices

Land use is one of the most important factors that affect runoff, evapotranspiration and surface erosion in a catchment. In this study, landuse data was obtained from Landsat 2005 (Macary et al. 2006). The management practices were taken into account in the model for simulation. The dominant landuse in the catchment were pasture, sunflower/winter wheat in rotation (Figure 3-12 C). The starting dates of plant beginning, amounts, date of fertilizer and irrigation applications were included. For pastures, there is one rotation of corn during a period of 4 years. Tillage works were practiced during April within this area. For sunflower-winter wheat rotation, the planting date of sunflower is on April 10 then is harvested on July 10. After that, winter wheat begins on October 9 then it is harvested on July 10, following year. The rotation of winter wheat-sunflower follows the same pattern by plant begins of winter wheat on October 9 and it is harvested on July 10. For following year, sunflower is planted on April 10, is harvested on July 10. The soil cover is empty from July through April during this rotation once per two years.

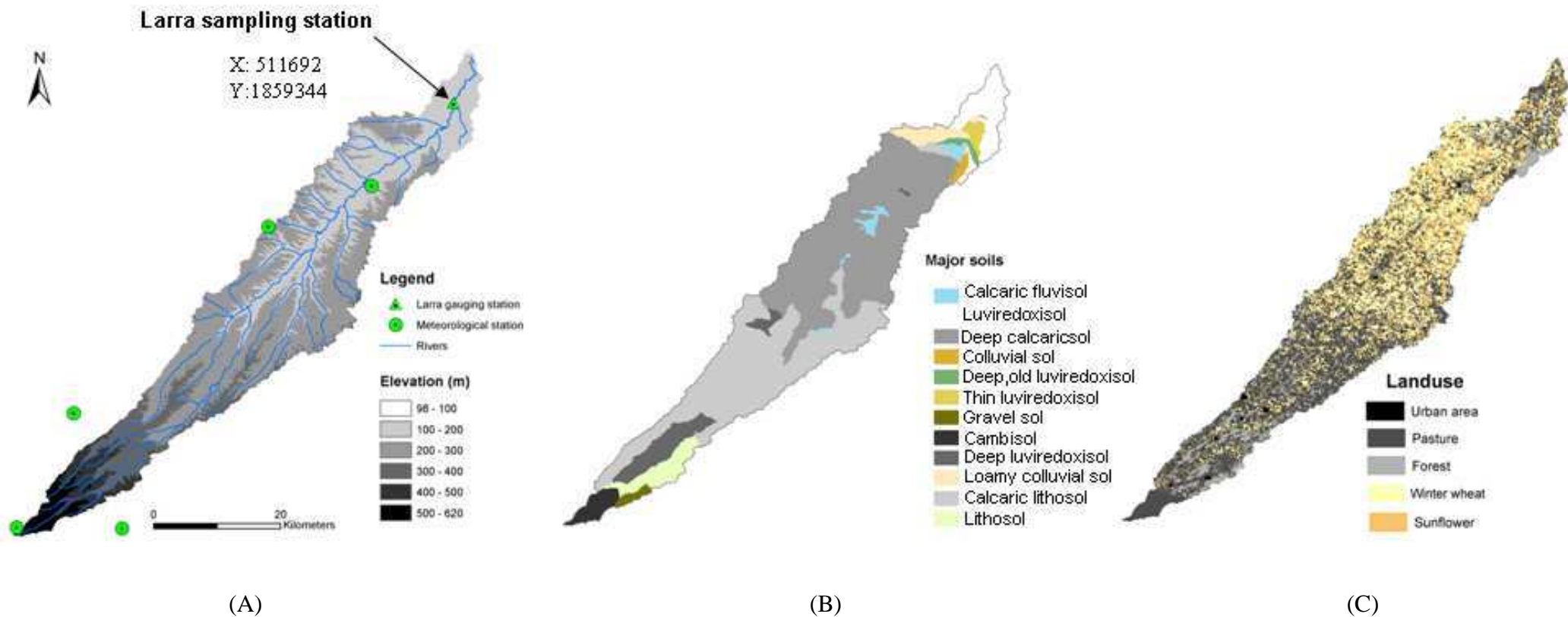


Figure 3-12 (A) Digital Elevation Model of the study area, (B) Major soils of study area, (C) Major landuse of the study area

Chapter 4

Dynamics of suspended sediment transport and yield in a large agricultural catchment, southwest France

*This chapter presents the first result of the analysis of suspended sediment transport dynamics in the studied agricultural catchment with the assessment of flood load contribution. The hydro-climatic factors influencing the mobilisation of sediment load from the catchment outlet during flood events were identified by means of statistical analysis of correlations and Principle Component Analysis (PCA). This part details hysteresis patterns of each flood and identifies their suspended sediment sources in order to determine their origins. This chapter presented the publication accepted in **Journal of Earth Surfaces Processes and Landforms (ESPL)** with the following reference:*

Oeurng C, Sauvage S, Sánchez-Pérez J.-M. 2010. Dynamics of suspended sediment transport and yield in a large agricultural catchment, South-west France. *Earth Surface Processes and Landforms* 35: 1289-1301

EARTH SURFACE PROCESSES AND LANDFORMS
Earth Surf. Process. Landforms 35, 1289–1301 (2010)
Copyright © 2010 John Wiley & Sons, Ltd.
Published online 28 January 2010 in Wiley Online Library
(wileyonlinelibrary.com) DOI: 10.1002/esp.1971

Dynamics of suspended sediment transport and yield in a large agricultural catchment, southwest France

Chantha Oeurng,¹ Sabine Sauvage,^{1,2,*} and José-Miguel Sánchez-Pérez^{1,2}

¹ Université de Toulouse, INPT, UPS, ECOLAB (Laboratoire Ecologie Fonctionnelle), Ecole Nationale Supérieure Agronomique de Toulouse (ENSAT), Castanet Tolosan, France

² CNRS, ECOLAB (Laboratoire Ecologie Fonctionnelle), Castanet Tolosan, France

Received 3 June 2009; Revised 22 October 2009; Accepted 9 November 2009

*Correspondence to: Sabine Sauvage, Université de Toulouse, INPT, UPS, ECOLAB (Laboratoire Ecologie Fonctionnelle), Ecole Nationale Supérieure Agronomique de Toulouse (ENSAT), Avenue de l'Agrobiopole, BP 32607 Auzeville Tolosane 31326 Castanet Tolosan Cedex, France. E-mail: sauvage@cict.fr

ESPL
Earth Surface Processes and Landforms

ABSTRACT: The dynamics of suspended sediment transport were monitored continuously in a large agricultural catchment in southwest France from January 2007 to March 2009. The objective of this paper is to analyse the temporal variability in suspended sediment transport and yield in that catchment. Analyses were also undertaken to assess the relationships between precipitation, discharge and suspended sediment transport, and to interpret sediment delivery processes using suspended sediment–discharge hysteresis patterns. During the study period, we analysed 17 flood events, with high resolution suspended sediment data derived from continuous turbidity and automatic sampling. The results revealed strong seasonal, annual and inter-annual variability in suspended sediment transport. Sediment was strongly transported during spring, when frequent flood events of high magnitude and intensity occurred. Annual sediment transport in 2007 yielded 16 614 tonnes, representing 15 t km⁻² (85% of annual load transport during floods for 16% of annual duration), while the 2008 sediment yield was 77 960 tonnes, representing 70 t km⁻² (95% of annual load transport during floods for 20% of annual duration). Analysis of the relationships between precipitation, discharge and suspended sediment transport showed that there were significant correlations between total precipitation, peak discharge, total water yield, flood intensity and sediment variables during the flood events, but no relationship with antecedent conditions. Flood events were classified in relation to suspended sediment concentration (SSC)–discharge hysteric loops, complemented with temporal dynamics of SSC–discharge ranges during rising and falling flow. The hysteric shapes obtained for all flood events reflected the distribution of probable sediment sources throughout the catchment. Regarding the sediment transport during all flood events, clockwise hysteric loops represented 68% from river deposited sediments and nearby source areas, anticlockwise 29% from distant source areas, and simultaneity of SSC and discharge 3%. Copyright © 2010 John Wiley & Sons, Ltd.

KEYWORDS: agricultural catchment; temporal variability; sediment transport; hysteric loops; flood events

Introduction

Suspended sediment transport has been identified as the main global mechanism of fluvial sediment transport. Walling and Webb (1986) estimated that the global amount of suspended sediment transport is about 3.5 times higher than that of solutes, while the bedload represents only a small component of fluvial transport. Suspended sediment transport from agricultural catchments to stream networks is responsible for aquatic habitat degradation, reservoir sedimentation and the transport of sediment-bound pollutants (pesticides, particulate nutrients, heavy metals and other toxic substances). Quantifying and understanding the dynamics of suspended sediment transfer from agricultural land to watercourses is essential in controlling soil erosion and in implementing appropriate mitigation practices to reduce stream suspended sediment and associated

pollutant loads, and hence improve surface water quality downstream (Heathwaite *et al.*, 2005). Appropriate assessment of suspended sediment yield is of particular importance for the purpose of catchment management and therefore interest in the dynamics of suspended sediment transport has increased in recent decades (Alexandrov *et al.*, 2003a).

So far, many studies on suspended sediment transport dynamics have been conducted in small-scale agricultural catchments of less than 100 km² (Gao *et al.*, 2007; Lefrançois *et al.*, 2007; Estrany *et al.*, 2009; Deasy *et al.*, 2009). However, little attention has been paid to sediment dynamics in large agricultural catchments, where there are many difficulties such as spatiotemporal variability in climatic conditions, land use and soil texture. Moreover, field measurements and collection of data on suspended sediment are generally difficult tasks, rarely achieved over long timescales in large

catchments. Understanding of the catchment-scale dynamics of suspended sediment transport is limited by this lack of data and by the high spatial and temporal variability of sediment output, which in turn is associated with various factors such as precipitation characteristics, the connectivity of sediment sources varying with physical settings and human activities, changes in contributing areas and hydraulic boundary conditions (Schmidt and Morche, 2006).

Analysis of the relationships between sediment transport, precipitation and discharge characteristics can help in understanding the factors and processes determining sediment responses (Zabaleta *et al.*, 2007; Nadal-Romero *et al.*, 2008). The study of hysteretic loops in a single flood event also helps to better interpret the spatial distribution of catchment sediment sources within a drainage system (Peart and Walling, 1982; Dickinson and Bolton, 1992; Kostrenzewski *et al.*, 1994; Lefrançois *et al.*, 2007).

The Gascogne area, southwest France, located in highly contrasting zones with various climatic influences (the mountain region, the Atlantic and the Mediterranean), has been dominated by anthropogenic activities, particularly intensive agriculture, causing severe erosion in recent decades. This poses a major threat to surface water quality, since sediment transport within the catchment is the main factor in transporting contaminant sediments. Therefore, the 1110 km² Save catchment located in the Gascogne area was selected for this study.

The objective of this study was to analyse the temporal variability in suspended sediment transport and yield in a large agricultural catchment. Analyses were also undertaken to assess the relationships between precipitation, discharge and

suspended sediment transport, and to interpret sediment delivery processes using suspended sediment-discharge hysteresis patterns.

Materials and Methods

Study area

The Save catchment, located in the area of Coteaux Gascogne, is an agricultural catchment of 1110 km² and has its source in the piedmont zone of the Pyrenees Mountains (southwest France) at an altitude of 600 m, joining the Garonne River after a 140 km course with a linear shape and an average slope of 3.6‰ (Figure 1).

This catchment lies on detrital sediments from the Pyrenees Mountains. It is bound on the east by the Garonne River, on the south by the Pyrenees and on the west by the Atlantic Ocean (Echanchu, 1988). Throughout the Oligocene and Miocene, this catchment served as an emergent zone of subsidence that received sandy, clay and calcareous sediments derived from the erosion of the Pyrenees Mountains, which were in an organic phase at that time. The heterogeneous materials were of low energetic value and produced a thick detrital formation of molasse type in the Miocene. From the Pleistocene onwards, the river became channelized, cutting broad valleys in the molasse deposits and leaving terraces of coarse alluvium (Revel and Guisresse, 1995). The substratum of the catchment consists of impervious Miocene molassic deposits.

In this area, which has been cultivated since the Middle Ages, mechanical erosion by ploughing has had a greater

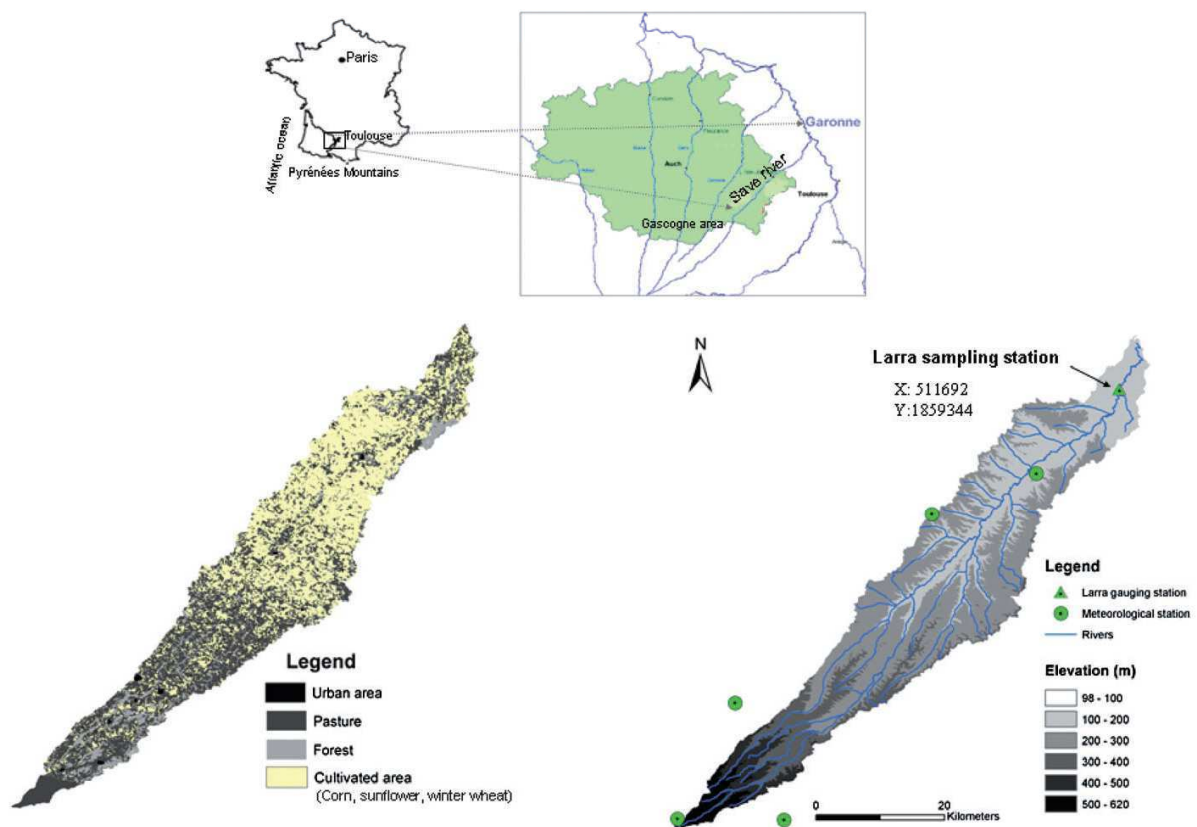


Figure 1. Location, land use and topographical maps of the Save catchment. This figure is available in colour online at wileyonlinelibrary.com/journal/espl

impact on downward soil displacement than water erosion, with a major impact on surface relief, mainly on levelling and soil distribution (Guiesse and Revel, 1995). Very weak erosion has led to the development of calcic luvisols (UN FAO soil units) on the tertiary substratum and local rendosols on the hard calcareous sandstone beds. On hillsides with very gentle slope, the calcic cambisols have been subjected to moderate erosion. Non-calcic silty soils, locally named *boulbènes*, represent less than 10% of the soil in this area. Calcic soils are dominated by a clay content ranging from 40% to 50%, while non-calcic soils are silty (50–60%). The upstream part of the catchment is a hilly agricultural area mainly covered with pastures and small amount of forest, while the lower part is flat and devoted to intensive agriculture, mostly pasture and a rotation of corn, sunflower and winter wheat (90% of the area used for agricultural purposes) (Figure 1).

The climatic conditions are oceanic, with annual precipitation of 700 to 900 mm and annual evaporation of 500 to 600 mm. The dry period runs from June to August (the month with maximum deficit) and the wet period from October to May (Ribeyex-Claret, 2001). The hydrology regime of the catchment is mainly pluvial, i.e. regulated by rainfall (Echanchu, 1988), with maximum discharge in May and low flows during summer (July to September).

The catchment substratum is relatively impermeable due to its high clay content. Consequently, the river discharge is mainly supplied by surface and subsurface runoff, and groundwater is limited to alluvial and colluvial phreatic aquifers. The maximum discharge for the long-term period (1985–2008) is $210 \text{ m}^3 \text{ s}^{-1}$ (14 June 2000), while summer discharge sustained by a nested canal at the catchment head is $0.004 \text{ m}^3 \text{ s}^{-1}$ at a point 100 km downstream since water is used for irrigation along its course. The mean monthly 31-year discharge (1965–2006) is $6.29 \text{ m}^3 \text{ s}^{-1}$.

Instrumentation and sampling method

A Sonde YSI 6920 (YSI Incorporated, Ohio, USA) measuring probe and Automatic Water Sampler (ecoTech Umwelt-Meßsysteme GmbH, Bonn, Germany) with 24 bottles of one litre were installed at the Save catchment outlet (Larra bridge) in January 2007. The Sonde was positioned near the bank of the river under the bridge, where homogeneity of water movement was properly considered for all hydrological conditions. The pump inlet was placed next to the Sonde pipe. The dissolved oxygen content, electrical conductivity, nitrate, pH, turbidity and water level were recorded at 10-minute intervals.

The values of the different parameters in water were detected by sensors on the Sonde YSI and the data then transferred to the ecoTech memory. We programmed the Sonde to pump water when there were water level variations, Δx (in centimetres), ranging from 10 cm to 30 cm, based on seasonal hydrological conditions for both the rising and falling stage. This sampling method provided high sampling frequency during storm events. Manual sampling was also carried out using a two litre bottle lowered from the Larra bridge, near the Sonde position, at weekly intervals when water levels were not remarkably varied. During the study period, several technical problems such as sensor derivation and crushing led to occasional difficulties in measuring continuous water turbidity. We missed continuous measurements for some flood periods (15% of the total study period), but we carried out intensive manual sampling, particularly during the flood events, in order to get reliable estimates of suspended sediment load during the missing time.

Data source, treatment and analysis

Hydro-climatological data

Rainfall data from five meteorological stations in the catchment (Figure 1) were obtained from Meteo France. The mean total rainfall depth and intensity in the whole catchment were derived using the Thiessen Polygon method. Total annual rainfall during the study period in 2007 and 2008 amounted to 603 and 787 mm, respectively. Data on hourly discharge were obtained from CACG (Compagnie d'Aménagement des Coteaux de Gascogne), which is responsible for hydrological monitoring in the Gascogne region.

The discharge was plotted by the rating-curve in which water level was measured hourly by pressure at Larra gauging station in the form of a rectangular weir (length 12 m), then transferred by teletransmission. The mean total water yield of the two study years, 2007 and 2008, was 98 mm and 120 mm, respectively. These values are below the long-term mean value of 136 mm for the period 1985–2008. A year was considered dry if the annual water yield was below the long-term value. Within this context, both years can be classified as dry but the first year 2007 is very dry, since no major floods occurred in autumn. During the whole study period, between January 2007 and March 2009, there were 20 flood events and we had a reliable total of 17 recorded flood events with continuous measurement of turbidity (Figure 2). Mean discharge during the first year was $3.45 \text{ m}^3 \text{ s}^{-1}$ and $4.23 \text{ m}^3 \text{ s}^{-1}$

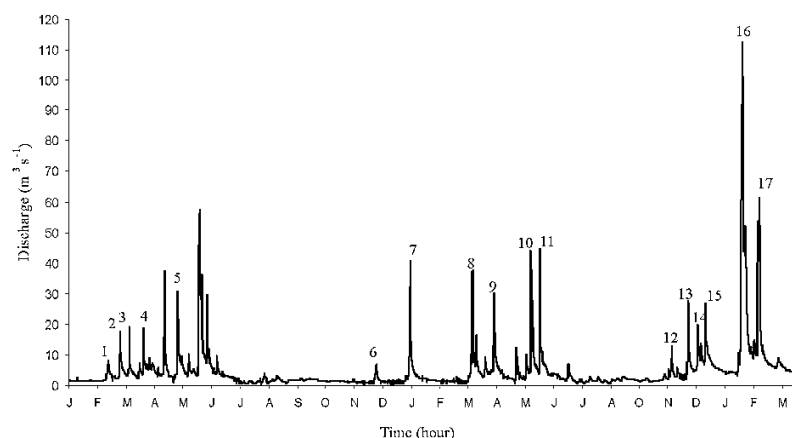


Figure 2. Hourly discharge (in $\text{m}^3 \text{ s}^{-1}$) within 17 recorded flood events between January 2007 and March 2009.

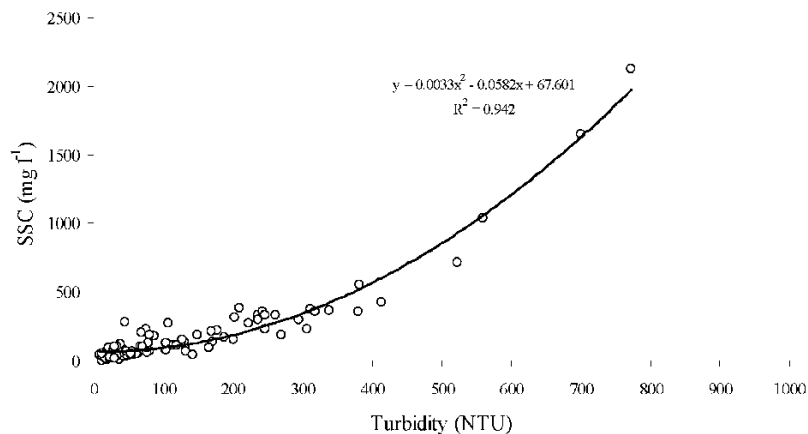


Figure 3. Relationship between recorded turbidity (in NTU) and suspended sediment concentration, SSC (in mg l^{-1}) at Larra sampling station.

during the second year. These values are below the mean annual discharge of the long-term discharge (1985–2008), which was $4.79 \text{ m}^3 \text{ s}^{-1}$. Maximum instantaneous discharge during floods ranged from $6.75 \text{ m}^3 \text{ s}^{-1}$ (observed on 11 December 2007) to $112.60 \text{ m}^3 \text{ s}^{-1}$ (27 January 2009).

Suspended sediment concentration (SSC) and turbidity data processing

During the study period, we obtained 246 water samples through our manual and automatic sampling methods. These water samples were analysed in the laboratory to determine suspended sediment concentration (SSC) using a nitrocellulose filter (GF 0.45 μm) and drying at $40 \text{ }^\circ\text{C}$ for 48 hours. Volumes of water ranging from 150 to 1000 ml were filtered according to particle load. SSC data determined from samples collected manually and by automatic sampling over a range of hydrological conditions and turbidity levels throughout the study period were used to generate a calibration equation between turbidity and SSC data.

The relationship between SSC and turbidity is generally a power function $\text{SSC} = a(\text{Turbidity})^n$ (Gippel, 1995; Lewis, 2003). However, in this case, the SSC–turbidity relationship was polynomial because of the light weight of the particles. Figure 3 illustrates the SSC–turbidity relationship for the Save catchment (best fitted with a second-order positive polynomial equation $\text{SSC} = 0.0033(\text{Turbidity})^2 - 0.0582(\text{Turbidity}) + 67.601$, where SSC is measured in mg l^{-1} and turbidity in NTU (nephelometric turbidity units). Continuous SSC data were derived from this equation for the turbidity range between 0 and 800 NTU, beyond which turbidity saturation occurred. For values of turbidity higher than 800 NTU (5% of flood periods) and during missing continuous measurements of turbidity, a linear interpolation method was applied between two close sampling points to construct the continuous SSC series.

Calculation of fluxes

High frequency SSC records were derived from the relationship between SSC and turbidity. The sediment loads were calculated as the product of the hourly discharge and the corresponding SSC:

$$F = 0.0864 \times Q_t \times \text{SSC}_t$$

$$\begin{cases} \text{SSC}_t = f(\text{NTU}) (0 < \text{NTU} < 800) \\ \text{SSC}_t = \text{Interpolation}[\text{SSC}_{t-1}; \text{SSC}_{t+1}] \end{cases}$$

where F is daily suspended sediment flux (in tonnes per day); Q_t is the hourly water discharge (in $\text{m}^3 \text{ s}^{-1}$), SSC_t is the corresponding suspended sediment concentration (in mg l^{-1}) and 0.0864 is the conversion factor. Accumulated suspended sediment fluxes (monthly to annual load) were calculated as the sum of fluxes during the period considered.

Statistical analyses

To assess the relationships between precipitation, discharge and sediment transport, statistical analyses were performed. A database was generated for each flood event and contained four groups of variables: antecedent conditions to the flood conditions, precipitation, discharge and suspended sediment during the flood. Variables used in the characterization of floods are summarized in Table I. Antecedent conditions are described by accumulated precipitation one day before the flood (P1d), five days before (P5d), and ten days before (P10d), by beginning baseflow (Q_b) before the flood and by the antecedent flood corresponding to the flood (Q_a).

Precipitation that caused the flood was characterized by mean total precipitation (P_t) and hourly maximum intensity of the precipitation (I_{max}). Total water yield (W_t) during the flood was expressed by the total water depth of the event, total duration of the event (T_d), and mean (Q_m) and maximum discharge (Q_{max}) corresponding to the time of rise to reach the peak discharge (T_r). The discharge speed to reach the peak flow during a flood event is defined by flood intensity, I_f [$I_f = (Q_{\text{max}} - Q_b)/T_r$]. Sediment load was expressed as the mean SSC (SSC_m) derived from the SSC–turbidity relationship, the maximum SSC of the event (SSC_{max}) and the total suspended sediment yield transported during the flood event (SST). The relationships between all these variables were investigated using statistical techniques (Pearson correlation matrix) in the STATISTICA package.

Analysis of SSC–discharge dynamics

Relationships between SSC and discharge during flood events were studied using continuous measurements. We use the term ‘flood’ to mean a complete hydrological event with rising and recession limbs. The typology of the SSC–discharge relationship during floods generally depends on the simultaneity or interval between the SSC peak and the discharge maximum. Typology interpretation is not unique, but varies according to

Table I. Names, abbreviations and units for the variables used to characterize flood events and to perform Pearson correlation matrix and factorial analysis

	Abbreviation	Unit
<i>Antecedent conditions</i>		
Accumulated precipitation 1 day before the flood	P1d	mm
Accumulated precipitation 5 days before the flood	P5d	mm
Accumulated precipitation 10 days before the flood	P10d	mm
Baseflow before the flood	Qb	m ³ s ⁻¹
Antecedent maximum discharge	Qa	m ³ s ⁻¹
<i>Flood event conditions</i>		
Flood duration	Fd	hours
Time of rise (time to reach maximum discharge)	Tr	hours
Total precipitation during the flood	Pt	mm
Maximum rainfall intensity of the flood	Imax	mm h ⁻¹
Flood intensity	If	m ³ min ⁻²
Total water yield	Wt	mm
Mean discharge	Qm	m ³ s ⁻¹
Maximum discharge	Qmax	m ³ s ⁻¹
Mean suspended sediment concentration	SSCm	mg l ⁻¹
Maximum suspended sediment concentration	SSCmax	mg l ⁻¹
Total suspended sediment yield in tonnes	SST	tonnes

the study context. We used a typology with three classes, inspired by Williams (1989).

In the first class, peaks of SSC and discharge arrive simultaneously. The SSC–discharge plot is symmetrical between rising and falling limbs, with little or no hysteresis. In the second class, the SSC peak arrives before the discharge peak and the relationship between SSC and discharge describes a clockwise hysteretic loop. In the third class, the SSC peak arrives later than the discharge peak and the SSC–discharge relationship describes an anticlockwise hysteretic loop (Williams, 1989). Typology interpretation can also depend on other flood characteristics. We complemented this typology with an analysis of the range of SSC versus discharge during the flood. The SSC maxima depended simultaneously on stream transport capacity and discharge, and also on the availability of particles to be mobilized by the discharge (Lefrançois *et al.*, 2007). We focused on SSC maxima versus discharge to compare the variation in particle availability during the different flood events. During recession flow, a decrease in discharge leads to sediment deposition. We focused on SSC at the discharge maxima to compare the deposition capacity of the stream during the falling stage of different flood events.

Results

General description of flood events analysed

During the study period, 17 flood events were analysed (Figure 3): six events occurred in winter (January to March), five in spring (March to June) and six in autumn (October to December). The longest event (event 16; 351 hours) occurred on 27 January 2009 with total rainfall depth 74.54 mm, reaching an hourly peak discharge of 116.6 m³ s⁻¹. This event is noteworthy since there was a 10-year return period and it represented a major flood event in winter 2009. During this event, sediment transport reached 23 374 tonnes. However, the event that the maximum sediment transport (event 10) took place in early June 2008, when the flood intensity was the highest of all the events observed during the study period. A total of 41 750 tonnes of sediment were transported during this extreme episode. Table II summarizes the main characteristics of flood duration, time of rise, flood intensity, precipitation,

discharge and SSC associated with the floods analysed, which are described in detail later.

- The duration of the flood events varied between 105 and 351 hours, with an average value of 191 hours (Table II). Seven events were longer than average duration, while 10 events were shorter. The event on 1 June 2008 took the shortest time (16 hours) to reach the peak, while the general rising time of floods in our observed events varied from 16 hours (minimum) to 84 hours (maximum), with an average value of 41 hours. Sediment transport in early June 2008 showed the most extreme value observed during the study period (41 750 tonnes).
- The maximum discharge during flood events varied from 6.75 m³ s⁻¹ to 112.60 m³ s⁻¹, with an average peak value of 33 m³ s⁻¹ (median = 27.57 m³ s⁻¹; standard deviation (SD) = 25.05 m³ s⁻¹). Rainfall amount varied from 7.46 mm to 74.54 mm (median = 20.25 mm; SD = 17.18 mm). Average rainfall intensity in the whole catchment ranged between 1.32 and 17.23 mm h⁻¹ (median = 3.97 mm h⁻¹; SD = 3.72 mm h⁻¹).
- Peak SSC during flood events varied from 158 mg l⁻¹, recorded on 13 February 2007, to 15.74 g l⁻¹ on 1 June 2008 (median = 691 mg l⁻¹; SD = 565 mg l⁻¹). A significant quantity of suspended sediment was transported during floods, mainly in spring season when flood magnitude was significant. The sediment load ranged from 177 to 41 750 tonnes (median = 1642 tonnes; SD = 5820 tonnes), indicating that 65% of each event transported more than 1000 tonnes.
- In terms of the typology described in the previous section, 68% of total sediment transport during all flood events demonstrated clockwise hysteresis, 29% anticlockwise and 3% simultaneity of SSC and discharge.

Temporal variability in suspended sediment transport

Within-event sediment variability

So far, due to differences between the catchments, there is only partial understanding of the internal dynamics of suspended sediment variability, even though many studies have been conducted on SSC–discharge relationships for individual

Table II. General characteristics of all flood events observed in the Save catchment during the study period (January 2007 to March 2009)^a

Event	Flood event date	Season	Flood duration (hours)	Time of rise (hours)	Flood intensity (m ³ min ⁻²)	Total rainfall (mm)	Rainfall intensity (mm h ⁻¹)	Baseflow before flood (m ³ s ⁻¹)	Mean discharge (m ³ s ⁻¹)	Maximum discharge (m ³ s ⁻¹)	Total water yield (hm ³)	Mean SSC (mg l ⁻¹)	Peak SSC (mg l ⁻¹)	Total sediment yield (tonnes)	Class ^b
1	13/02/2007	Winter	132	55	0.11	15.59	4.79	1.89	4.20	7.97	2.13	73	158	177	C
2	27/02/2007	Winter	140	30	0.47	9.59	1.37	3.61	6.67	17.62	3.82	168	468	338	S
3	09/03/2007	Winter	164	41	0.37	7.46	1.32	3.83	6.05	19.11	4.12	164	442	856	AC
4	25/03/2007	Spring	139	21	0.72	12.58	2.64	3.83	7.74	18.94	3.68	152	361	689	AC
5	02/05/2007	Spring	200	21	1.27	20.25	2.55	3.61	10.30	30.36	5.79	243	813	2200	AC
6	11/12/2007	Autumn	128	46	0.08	9.24	2.80	3.16	3.46	6.75	1.71	136	212	190	C
7	19/01/2008	Winter	184	43	0.87	19.87	3.42	3.16	10.74	40.64	7.34	652	1380	4801	C
8	28/03/2008	Spring	228	84	0.42	39.27	2.79	2.56	10.39	37.60	8.56	562	1160	4820	AC
9	21/04/2008	Spring	189	22	1.19	19.38	3.97	4.06	9.60	30.20	7.1	650	1536	4385	C
10	01/06/2008	Spring	228	16	2.48	49.95	17.23	4.28	15.70	44.02	12.75	1597	15743	41750	Complex
11	12/06/2008	Spring	259	29	1.40	28.47	8.46	4.28	15.01	44.80	12.61	850	1322	9077	AC
12	08/11/2008	Autumn	105	46	0.22	23.83	4.65	2.96	6.18	12.97	2.4	159	466	513	C
13	26/11/2008	Autumn	191	43	0.53	35.92	4.44	4.90	9.08	27.57	3.42	1618	494	2959	S
14	06/12/2008	Autumn	126	54	0.28	27.68	5.31	4.90	10.12	19.77	3.21	278	569	1018	AC
15	14/12/2008	Autumn	256	27	0.73	13.32	1.56	6.95	11.63	26.74	6.01	128	501	1085	AC
16	27/01/2009	Winter	351	69	1.57	74.54	4.13	4.06	34.50	112.60	43.71	337	2003	23374	C
17	11/02/2009	Winter	233	54	0.94	32.88	4.16	9.99	25.94	60.66	19.71	396	1030	6867	C

^a Maximum values shown in bold typeface and minimum values shown in bold/italic typeface.

events (Mossa, 1996; Williams, 1989; Sickingabula, 1998; Rovira and Batalla, 2006). The scatter in SSC reported is attributed to the exhaustion of sediment available in the channel or to differences in sediment availability at the beginning and end of the flood (Walling and Webb, 1982; Steegen *et al.*, 2000; Steegen and Govers, 2001; Hudson, 2003). As a result, SSC and discharge during a flood often present hysteretic behaviour, related to a time lag between peak discharge and sediment transport. For clockwise hysteresis, SSC on the rising limb of a storm hydrograph is higher than that measured at equivalent flows on the falling limb (Rovira and Batalla, 2006). For instance, in event 16 (27 January 2009), the 50 m³ s⁻¹ discharge of the rising limb contained 1817 mg l⁻¹, while the 50.28 m³ s⁻¹ discharge of the falling limb discharge contained only 881 mg l⁻¹. The beginning of the discharge wave is supplied by easily available sediment in the channel and nearby source areas. As SSC reaches its maximum value before peak discharge, it is obvious that reduction in the amount of available sediment occurred on the falling limb. Moreover, an increase of portion of baseflow on the falling limb may cause dilution of SSC. In the case of anticlockwise hysteresis, the SSC for a given discharge on the falling limb is higher than for the same discharge on the rising limb (Salant *et al.*, 2008). As can be seen from flood event 4 (25 March 2007), the same discharge of 9.59 m³ s⁻¹ contained 251 mg l⁻¹ for the falling limb and 71 mg l⁻¹ for the rising limb. The suspended sediment transport in the Save catchment was also influenced by sediment exhaustion, as can be observed from three successive events which appear to show a progressive exhaustion of sediment supply (events 13, 14 and 15) and a decrease in sediment availability in the channel. These successive events were recorded on 26 November 2008 (Q_{max} = 27.57 m³ s⁻¹; SSC_{max} = 1613 mg l⁻¹), 6 December 2008 (Q_{max} = 19.77 m³ s⁻¹; SSC_{max} = 569 mg l⁻¹), and 14 December 2008 (Q_{max} = 26.74 m³ s⁻¹; SSC_{max} = 501 mg l⁻¹).

Seasonal, annual and inter-annual variability

In terms of the temporal dynamics in suspended sediment transport, the Save catchment showed strong seasonal, annual and inter-annual variability during the study period (Figure 4). These seasonal variations can be analysed by considering seasonal climatic variations and weather forcing. Sediment yield in both years increased sharply in spring and slightly during summer and autumn. As can be seen in Figure 4, sediment transport from June to December 2007 nearly remained constant due to the absence of major flood events. The slope breaks of the sediment and discharge curve in early June 2008 showed drastically different conditions, since the sediment delivery during these extreme flood events reached 50 000 tonnes (63% of the annual sediment budget).

Suspended sediment transport in autumn 2007 (October to December) was only 2% of annual sediment load, whereas in autumn 2008 it was 13% of annual load. This was because there was only a minor flood event (Q_{max} = 6.75 m³ s⁻¹) in autumn 2007, while many flood events reaching peak discharge of 27.57 m³ s⁻¹ occurred during autumn 2008. The sediment was strongly transported during spring (March to June), a period when there were many flood events with strong flood intensity and high amplitude occurring together with tillage operations in this agricultural catchment. In spring 2007, 79% of annual sediment load was transported, while spring 2008 accounted for 70% of annual sediment load. During summer, there were no major rainfall events that could cause floods and therefore sediment transport in summer 2007 and 2008 represented only 2% and 9% of the annual budget, respectively. During the study period there was significant seasonal variability, with sediment transport during autumn

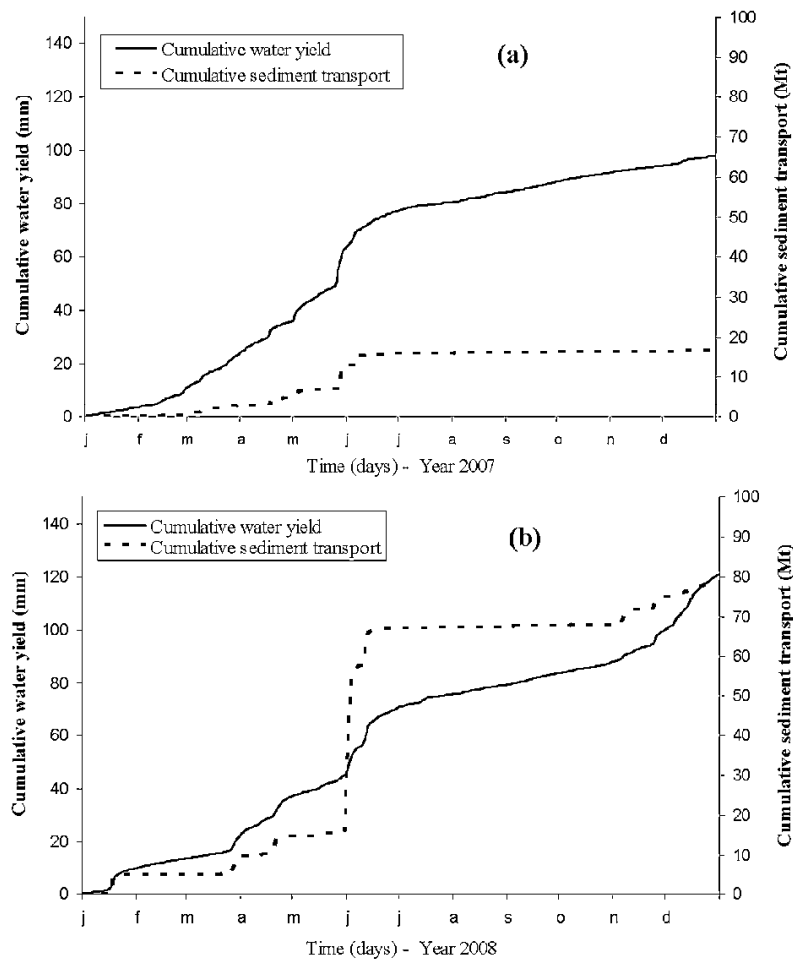


Figure 4. Cumulative water yield (in millimetres) and sediment transport (Mt) during (a) 2007 and (b) 2008.

2007 being significantly different from that in the corresponding season in 2008. Similar variations were observed in winter 2007, 2008 and 2009. Sediment transport during flood events in winter 2009 was strongly significant due to the high magnitude of two flood events (event 16 and 17), which yielded 30241 tonnes, equivalent to 182% and 39% of mean total annual load in 2007 and 2008, respectively.

The sediment transport in 2007 accounted for 16614 tonnes (85% of annual load transport during floods for 16% of annual duration) while transport in 2008 amounted to 77960 tonnes (95% of annual load transport during floods for 20% of annual duration). Although there was only a non-significant difference of 18% between total water yield in 2007 (98 mm) and 2008 (120 mm), the sediment yield in 2008 was 4.7 times higher than in 2007. In one extremely eroding event in early June 2008 (event 10), sediment transport contributed 63% of the total annual sediment budget.

Relationships between precipitation, discharge and sediment variables

In order to assess the relationships between precipitation, discharge and suspended sediment transport, which might explain the hydrological and sedimentological responses

during the flood events in the Save catchment, a Pearson correlation matrix and factorial analysis that included all the above-mentioned variables (Table III) were generated for the 16 flood events. Event 10 (1 June 2008) was excluded from the matrix because it was an extraordinary event.

Table III shows the relationships between precipitation, discharge and suspended sediment transport in the Save catchment. Total precipitation (Pt) showed significant correlations with mean discharge (Q_m) ($R = 0.83$), maximum discharge (Q_{max}) ($R = 0.87$), total water yield (Wt) ($R = 0.85$), maximum suspended sediment concentration (SSC $_{max}$) ($R = 0.76$) and suspended sediment transport (SST) ($R = 0.89$). The discharge variables, Q_m and Q_{max} , were well correlated with total rainfall (Pt), but antecedent discharge (Q_a) and baseflow (Q_b) had only slight correlations with total precipitation (Pt).

Maximum suspended sediment (SSC $_{max}$) and suspended sediment transport (SST) showed strong relationships with total precipitation (Pt). SSC $_{max}$ was well correlated with flood intensity (If) ($R = 0.72$) and flood duration (Fd) ($R = 0.72$). SST was found to be significantly correlated with total water yield (Wt) ($R = 0.97$) and discharge variables (Q_m and Q_{max}). Weaker correlations were found between sediment variables and maximum rainfall intensity (Imax). Suspended sediment did not show any relationship with antecedent flow (Q_a , Q_b) or antecedent precipitation (P1d, P5d and P10d).

Table III. Pearson correlation matrix among all variables ($n = 16$)

	Fd	Tr	If	Pt	Imax	P1d	P5d	P10d	Qa	Qb	Qm	Qmax	Wt	SSCm	SSCmax	SST
Fd	1.00															
Tr	0.23	1.00														
If	0.78	-0.25	1.00													
Pt	0.72	0.61	0.50	1.00												
Imax	0.16	0.12	0.27	0.37	1.00											
P1d	0.04	-0.42	0.31	-0.23	-0.36	1.00										
P5d	-0.06	-0.18	0.03	-0.28	-0.28	0.79	1.00									
P10d	-0.12	-0.39	0.13	-0.27	0.38	0.22	0.45	1.00								
Qa	0.29	0.16	0.32	0.29	0.28	-0.39	-0.33	-0.04	1.00							
Qb	0.36	-0.09	0.28	0.13	0.02	-0.38	-0.42	-0.19	0.69	1.00						
Qm	0.84	0.34	0.71	0.83	0.25	-0.16	-0.36	-0.29	0.53	0.52	1.00					
Qmax	0.88	0.37	0.75	0.87	0.21	-0.05	-0.24	-0.26	0.37	0.32	0.96	1.00				
Wt	0.84	0.40	0.68	0.85	0.20	0.07	0.29	0.29	0.34	0.28	0.96	0.98	1.00			
SSCm	0.43	0.05	0.55	0.35	0.56	-0.08	0.09	0.39	0.26	0.07	0.29	0.38	0.24	1.00		
SSCmax	0.72	0.21	0.72	0.76	0.35	-0.04	-0.05	0.00	0.21	0.15	0.66	0.77	0.66	0.76	1.00	
SST	0.85	0.39	0.72	0.89	0.33	-0.04	-0.23	-0.17	0.24	0.14	0.90	0.97	0.97	0.40	0.77	1.00

Note: Correlation is significant at $p < 0.01$ level for bold numbers and $p < 0.05$ for italics.

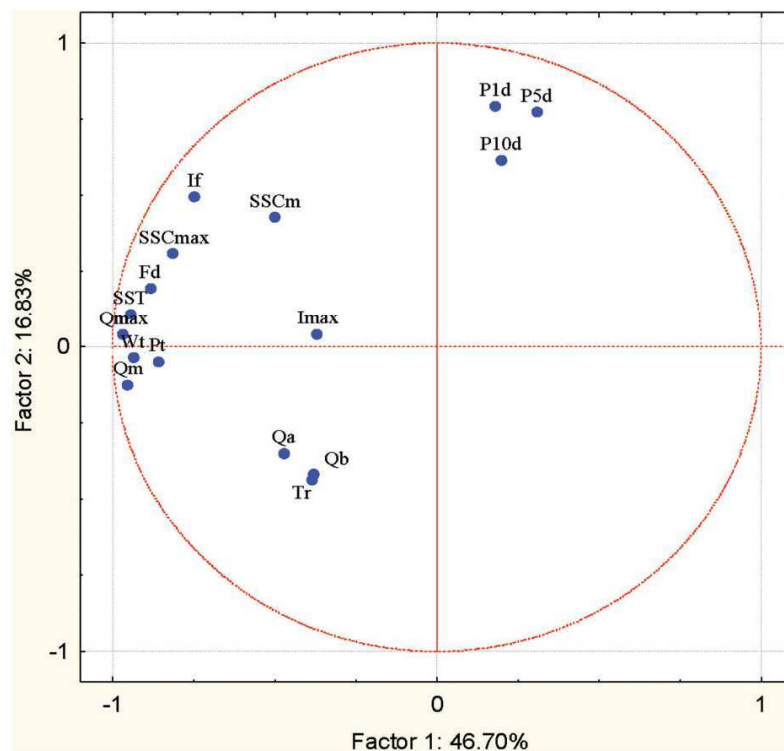


Figure 5. Location of variables included in the correlation matrixes in the factorial plane of principal component analysis. The figure is available in colour online at wileyonlinelibrary.com/journal/espl

Taking all these data into account, principal component analysis (PCA) was performed. This analysis (Figure 5) grouped in the first factor Fd, Qm, Qmax, Pt, Wt and SST, explaining 46.70% of the variance. In the second factor, If, SSCm, SSCmax and Imax were grouped, explaining 16.83% of the variance. In a 1–2 factorial plane, total sediment yield during flood events (SST) showed a strong relationship with these two factors, although the correlation was better with factor one, and no relationship was found with antecedent conditions to the flood event. The results indicate a direct response of the catchment to rainfall events in terms of discharge and suspended sediment transport during flood events.

SSC–discharge hysteresis patterns

The behaviour of suspended sediment and changes in SSC during flood events are not only a function of energy conditions, i.e. sediment is stored at low flow and transported under high flow conditions, but are also related to variations in sediment supply and sediment depletion. These changes in sediment availability result in so-called hysteresis effects (Asselman, 1999).

The relationship between discharge and SSC was analysed for all the individual flood events observed in the Save catchment. In general, we found highly variable relationships

between discharge and sediment response during different seasonal flood events (Figure 6). The different patterns of hysteresis express various probable sources of sediment spreading throughout the catchment. Seven of 17 flood events recorded during the study period showed clockwise hysteretic loops (class 2) (Figure 6b), while seven events displayed anticlockwise hysteretic loops (class 3) (Figure 6c). Two events presented class 1 behaviour (Figure 6a), indicating that SSC and discharge arrived simultaneously. However, one event (event 10, which occurred in early June 2008), showed complex mixing of clockwise and anticlockwise loops (Figure 6d) when there were multiple peaks of discharge together with multiple peaks of SSC during a flood event, coinciding with extreme rainfall intensity.

Discussion

Temporal variability of suspended sediment transport and yield

The analysis of the SSCs collected at different temporal scales (within events, seasonal and annual variability) in the Save catchment provides an insight into the characteristics of the suspended sediment load variability in a large agricultural catchment in southern Pyrenees region. Increasing SSC on the falling limb during floods may be related to sources of relatively more available sediment with lower soil aggregate stability. Such sediment sources are located at the far end of the area contributing to surface runoff, and thus sediment reaches the stream mainly during the falling limb. This may be due to soil particles, eroded within the catchment, not reaching the stream during previous rainfall-runoff events and settling on the slope, before being transported by surface runoff into the stream during the next event. The variability in event sediment transport during successive peaks of similar magnitude is influenced by sediment exhaustion effects. The Save catchment shows a pattern similar to that observed in other catchments in the Mediterranean region, e.g. in the Tordera catchment (Rovira and Batalla, 2006). An example is the progressive reduction in suspended load at different temporal scales (within floods and within multiple-peak events, during a succession of events, and seasonally) related to the exhaustion of sediment availability. Alexandrov *et al.* (2003b) observed that due to a sediment exhaustion effect, SSC levels during secondary floods in the Nahal Eshtemoa basin (Israel) were lower than those observed during a primary flood. This can be attributed to the role of in-channel sediment storage, which controls suspended sediment transport during inter-flood periods of stable flow (Smith and Dragovich, 2008). Therefore, after a period of relatively high sediment transport (supply-rich floods), sediment becomes less and less available from the channel (exhaustion phenomenon) and sediment concentrations recorded during successive floods events are consequently lower (Walling, 1978).

The total specific sediment yields in 2007 and 2008 amounted to 15 t km⁻² and 70 t km⁻², respectively. This may be linked to the different characteristics of flood events, such as flood duration, rainfall intensity and flood amplitude, and other controlling factors related to soil conditions and agricultural practices in the Save catchment during both study years. The first hydrological year of the study (2007) was very dry, since there were very few rainfall events during autumn and less sediment was transported during floods with low duration and flood magnitude. Flood intensity is also a main factor to determine sediment transport. The maximum flood intensity

in 2007 was only 1.27 m³ min⁻², while one event in spring 2008 exhibited the maximum flood intensity of 2.48 m³ min⁻², yielding a suspended sediment load of 63% of annual sediment yield in 2008. Sediment was slightly transported by baseflow during summer (2% of annual load in 2007, 9% in 2008). Although there were some rainfall events in summer during the study period, soil conditions were dry and little runoff was generated, as large amounts of rainfall infiltrated into the soil.

The annual total specific sediment yields in the Save catchment (15–70 t km⁻²) are within the range of specific yields reported for the Garonne River, which vary from 11 to 74 t km⁻² yr⁻¹ (Coynel, 2005), but lower than the values for Mediterranean basins of the Iberian Peninsula (100–200 t km⁻² yr⁻¹) reported by Walling and Webb (1996). Located in the same Gascogne region as the Save catchment, with the same climatic conditions, geology (molasse) and agricultural land use, the 1330 km² Baïs catchment and the 970 km² Gers catchment have specific sediment yields (63 and 41 t km⁻² yr⁻¹, respectively) that are of a similar order of magnitude to that of the Save catchment (Maneux *et al.*, 2001). In comparison with other French catchments of similar size in the Mediterranean area, the Save values are higher than those reported for the 1100 km² Dronne upstream catchment (8–13 t km⁻² yr⁻¹) but similar to those in the 1172 km² upstream catchment at Ariège (57–59 t km⁻² yr⁻¹) (Veyssy, 1998). The Save values are also comparable to those of the 900 km² Tordera catchment (50 t km⁻² yr⁻¹) in northeast Spain (Rovira and Batalla, 2006), but much lower than the 414 t km⁻² yr⁻¹ reported for the 445 km² Isábena catchment (southern central Pyrenees). However, the latter catchment is highly erodible and experiences frequent floods (López-Tarazon *et al.*, 2009).

Sediment delivery process using SSC–discharge hysteresis

SSC–discharge hysteresis patterns are the outcome of the complex interaction of processes and controls that determine event discharge and catchment erosion and sediment transport. These patterns reflect the combination of sediment supply from dominant sources with the capacity of flows to transport the supplied sediment to the catchment outlets. Sediment delivery processes can be interpreted using SSC–discharge hysteresis patterns. For class 1, only two events were recorded in late winter and mid-autumn (events 2 and 13). This class is classically interpreted as the mobilization and transport of particles with unrestricted availability during the flood for the range of discharge concerned (Jansson, 2002). So far, there is little literature describing the sediment sources from this class. However, according to Hudson (2003), at low discharge sediment could come from fine deposited sediment, whereas at high discharge sediment could originate from coarser deposited sediment and/or from bank and channel hydrological erosion. When discharge is principally linked to surface runoff, sediment could originate from remote areas, particularly via surface soil erosion (Lefrançois *et al.*, 2007). Topsoil sources are therefore likely to dominate drain flow sediment in agricultural catchments (Foster *et al.*, 2003).

Clockwise hysteretic loops (class 2), which were observed in seven events in the Save catchment, generally occurred in late winter and mid-autumn, particularly in November when early seasonal rainfall started. During the periods when sediment was stored in the channel and distributed within the catchment tributaries, these sediments were transported only

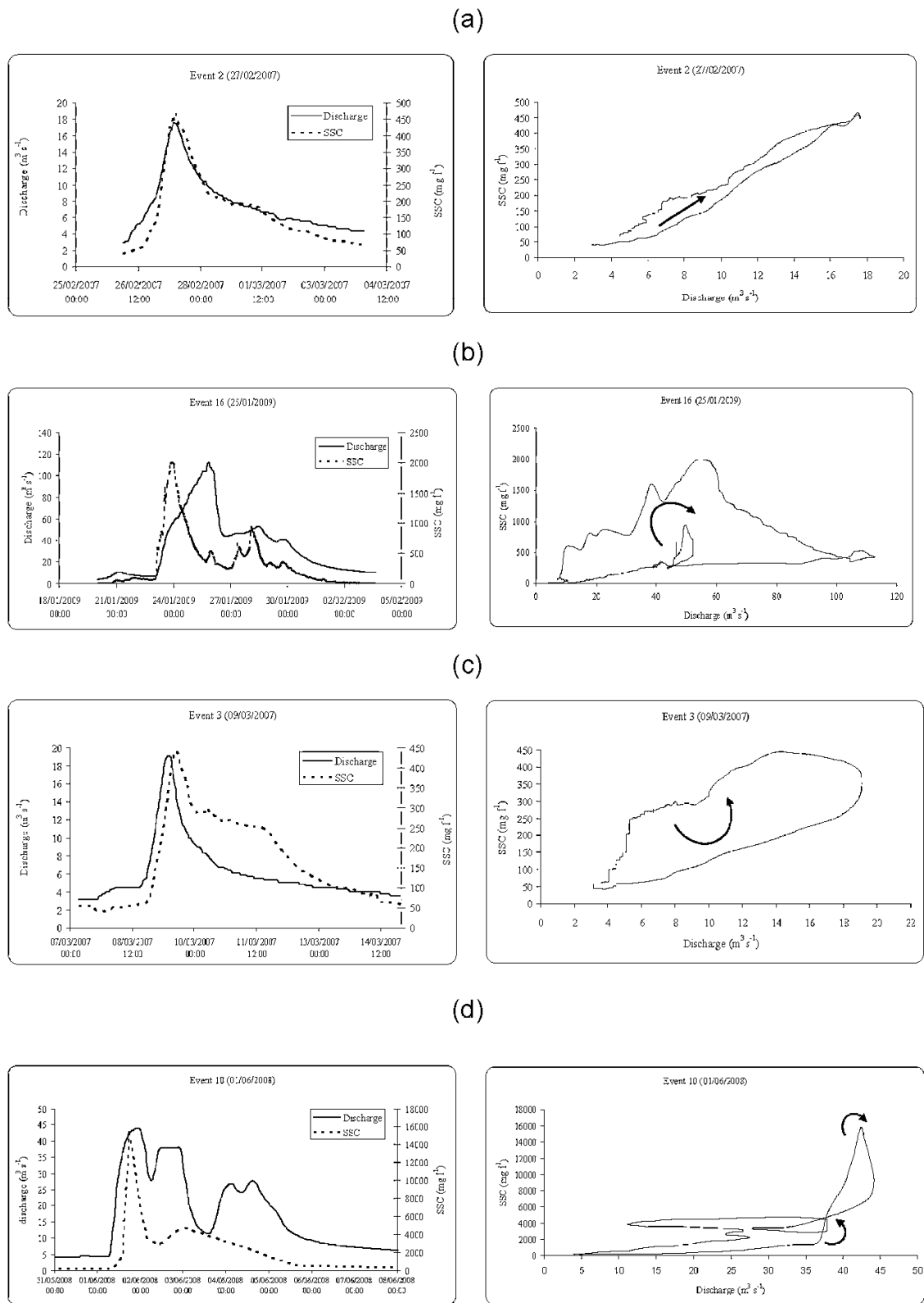


Figure 6. Examples of different types of hysteresis observed in the Save catchment during the study period (2007–2009).

after there were flood events with sufficient transport capacity. Therefore, this class could be explained by the transport of nearby available sediment and deposited sediment within the riverbed during the previous season. This can be also classically interpreted as the mobilization of particles with restricted availability during the flood event for the range of discharge concerned. Particles are believed to come from the removal of sediment deposited in the channel, with decreasing availability during the event (Lenzi and Lorenzo, 2000; Steegen *et al.*, 2000; Jansson, 2002; Goodwin *et al.*, 2003). Particle production by erosion cannot resupply the decrease in sediment stock deposits. The hypothesis of an important contribution by hillslope soils can be dismissed. Various patterns of hysteresis have been reported previously in the literature, with clockwise hysteretic loops being the most common (Walling, 1977; Klein, 1984; Williams, 1989; Jansson, 2002; Hudson, 2003; Rovira and Batalla, 2006). Klein (1984) assumed that clockwise hysteresis occurred when the sediment source area is the channel itself or an adjacent area located close to the catchment outlet, with runoff triggering the movement of sediment accumulated in the channel during the previous seasons and with little or no contribution from the tributaries. López-Tarazon *et al.* (2009) also emphasized that the clockwise phenomenon was found preferentially when rainfall was mostly located near the catchment outlet. For instance, in the Save catchment, this was the case for clockwise flood events in early autumn (events 1 and 12) and late winter (events 7, 16 and 17). For event 6, which happened on 11 December 2007 (late autumn), clockwise flood events were also found, since there was only one flood event during this season and sediment was apparently transported from deposited sediment along the channel. The role of agricultural practices in downstream areas of the Save catchment, which are mainly dominated by a crop rotation of corn, sunflower and winter wheat, was also a key determinant of sediment sources. Tillage activities here are generally carried out in April and September. Soil was eroded and then transported to the stream networks near the catchment outlet, characterized by a clockwise pattern when there were flood events reaching the capacity to bring those sediments to the outlet.

Heidel (1956) and Williams (1989) reported that for small streams, the maximum SSC usually occurs prior to peak discharge. However, other authors have suggested that clockwise hysteresis reflects a progressive decline in sediment availability during the flood event or an early-stage depletion of suspended sediment (Van Sickle and Beschta, 1983; Klein, 1984; Lenzi and Lorenzo, 2000; Sayer *et al.*, 2006). These explanations are considered to be unlikely in the Save catchment, as they imply events related to high water volume associated with the hydrological response across the entire catchment (Nadal-Romero *et al.*, 2008). In contrast, the arrival of clean water from the forested headwater area in the Save catchment could partly dilute flow to reduce SSC but not total transport.

Regarding class 3, anticlockwise hysteretic loops take place when sediment sources are widely spread throughout the catchment and sediment is not rapidly exhausted. Due to the very long thin shape of the Save catchment, sediment transport from upstream and far tributaries may take a long time to reach the catchment outlet. This type of hysteretic loop was mainly found in the Save catchment in spring and late autumn, when there were high flood magnitudes with the sufficient capacity to transport sediments from distant areas of the upstream catchment to the outlet. As the upstream part of the catchment is a hilly agricultural area mainly dominated by pastures and a small amount of forest cover (Figure 1), the source of sediment could be distant sediments, hillslope soil erosion and upstream areas (Braisington and Richards, 2000; Goodwin *et*

al., 2003; Orwin and Smart, 2004). Tillage in upland pasture areas of the Save catchment is generally performed in April, a period of strong rainfall causing the major floods in the spring season. Thus sediment yield could be strongly transported from far upstream in an anticlockwise pattern. Suspended sediment can also originate from processes with slow dynamics (slower than the discharge rise), e.g. banks may collapse when bank material is sufficiently saturated. Williams (1989) suggested that anticlockwise hysteresis results from at least one of the following causes: (i) a difference between the flood wave velocity and the mean flow velocity that carries the suspended sediment, (ii) a high soil erodibility in combination with a prolonged erosion process during the flood, and (iii) a seasonal distribution of sediment production within the drainage basin. Although there was no serious investigations of bank collapse along the Save river, bank erosion was taken into account in supplying sediment sources, particularly during major floods with high flood intensity, e.g. the event in early spring 2008 ($I_f = 2.48 \text{ m}^3 \text{ min}^{-2}$).

Conclusions

The dynamics of suspended sediment transport and sediment yield were analysed at different temporal scales with high resolution through two years of data collection. Analysis of the variability in SSC at different temporal scales (event, seasonal, annual and inter-annual) monitored at catchment outlet (Larra sampling station) provided insights into the characteristics of suspended sediment transport in the Save catchment in southwest France. The temporal dynamics of suspended sediment transport in the Save catchment showed strong within-event, seasonal, annual and inter-annual variability. The sediment was strongly transported during spring, when many flood events with high magnitude and intensity occurred and tillage work was performed. Sediment transport in 2007 yielded 16 614 tonnes (85% of annual load transport during floods for 16% of annual duration), while the 2008 yield was 77 960 tonnes (95% of annual load transport during floods for 20% of annual duration).

Statistical analyses revealed a significant correlation between total precipitation, peak discharge, total water yield and sediment variables during the flood events, but no relationship with antecedent conditions. These results indicate a direct response of the catchment to rainfall events, discharge and flood intensity, as well as suspended sediment transport during the flood events. The variability over different temporal scales of discharge and SSC resulted in different hysteretic patterns. Two classes (classes 2 and 3) were the most common types observed in the Save catchment. Clockwise hysteresis (class 2) mainly occurred in late winter and mid-autumn, particularly in November, while anticlockwise hysteresis (class 3) was mostly found in spring and late autumn. The hysteretic shapes obtained for all flood events reflected the distribution of probable sediment sources throughout the catchment. Of sediment transport during all flood events, clockwise hysteretic loops represented 68% from river deposited sediments and nearby sources areas, anticlockwise 29% from distant source areas, and simultaneity of SSC and discharge 3%.

With only two years of recordings, it is difficult to characterize inter-annual variability in a large agricultural catchment like the Save due to strong seasonal and annual hydrological variations. Therefore, modelling work should be conducted to characterize long-term variability in flux and to study past soil erosion following the identification of critical sediment source areas in the catchment.

Acknowledgements—This research was financially supported by a doctoral research scholarship from the French government in cooperation with Cambodia. This study was performed within the framework of the GIS-ECOBAG, Programme P2 “Garonne Moyenne” and “IMAGES”, and supported by funds from CPER and FEDER (grants n°OPI2003-768) of the Midi-Pyrenees Region and Zone Atelier Adour Garonne (ZAAG) of PEVS/CNRS347 INSUE. We sincerely thank the CACG for discharge data and Meteo France for meteorological data. The authors would like to thank Gael Durbe and ECOLAB staff for access to the site and assistance with monitoring instruments. The authors would also like to acknowledge helpful comments from Alexandra Coynel and Eric Maneux and particularly from two anonymous referees whose comments greatly improved the manuscript.

References

- Alexandrov Y, Laronne JB, Reid I. 2003a. Suspended sediment concentration and its variation with water discharge in a dryland ephemeral channel, northern Negev, Israel. *Journal of Arid Environments* **53**: 73–84.
- Alexandrov Y, Laronne JB, Reid I. 2003b. *Suspended Sediment Transport in Flash Floods of the Semiarid Northern Negev, Israel*. IAHS Publication 278. IAHS Press: Wallingford; 346–352.
- Asselman NEM. (1999). Suspended sediment dynamics in a large basin: the River Rhine. *Hydrological Processes* **13**: 1437–1450.
- Braisington J, Richards K. 2000. Suspended sediment dynamics in small catchments in the Nepal Middle Hills. *Hydrological Processes* **14**: 2559–2574.
- Coynel A. 2005. *Erosion mécanique des sols et transferts géochimiques dans le bassin Adour-Garonne*, PhD Thesis, University of Bordeaux.
- Deasy C, Brazier RE, Heathwaite AL, Hodgkinson R. 2009. Pathways of runoff and sediment transfer in small agricultural catchments. *Hydrological Processes* **23**: 1349–1358.
- Dickinson A, Bolton A. 1992. *A Program of Monitoring Sediment Transport in North Central Luzon, the Philippines, Erosion and Sediment Transport Monitoring Programs in River Basins*. IAHS Publication 210. IAHS Press: Wallingford; 483–492.
- Echanchu D. 1988. *Géochimie des eaux du bassin de la Garonne. Transferts de matières dissoutes et particulières vers l’océan atlantique*, PhD Thesis, University of Paul Sabatier, Toulouse.
- Estrany J, Garcia C, Batalla RJ. 2009. Suspended sediment transport in a small Mediterranean agricultural catchment. *Earth Surface Processes and Landforms* **34**: 929–940.
- Foster IDL, Chapman AS, Hodgkinson RA, Jones AR, Lees JA, Turner SE, Scott M. 2003. Changing suspended sediment and particulate phosphorus loads and pathways in underdrained lowland agricultural catchment; Herefordshire and Worcestershire, UK. *Hydrobiologia* **494**(1–3): 119–126.
- Gao P, Pasternack GB, Bali KM, Wallender WW. 2007. Suspended-sediment transport in an intensively cultivated watershed in south-eastern California. *Catena* **69**: 239–252.
- Gippel CJ. 1995. Potential of turbidity monitoring for measuring the transport of suspended solids in streams. *Hydrological Processes* **9**: 83–97.
- Goodwin TH, Young AR, Holmes GR, Old GH, Hewitt N, Leeks GJL, Packman JC, Smith BPG. 2003. The temporal and spatial variability of sediment transport and yields within the Bradford Beck catchment, West Yorkshire. *The Science of the Total Environment* **311**–**316**: 475–494.
- Guiesse M, Revel JC. 1995. Erosion due to cultivation of calcareous clay soils on hillsides in south-west France. II. Effect of ploughing down the steepest slope. *Soil Tillage* **35**(3): 157–166.
- Heathwaite AL, Dils RM, Liu S, Carvalho L, Brazier RE, Pope L, Hughes M, Phillips G, May L. 2005. A tiered risk-based approach for predicting diffuse and point source phosphorus losses in agricultural areas. *The Science of the Total Environment* **344**(1–3): 225–239.
- Heidel SG. 1956. The progressive lag of sediment concentration with flood waves. *Transactions – American Geophysical Union* **3**(1): 56–66.
- Hudson PF. 2003. Event sequence and sediment exhaustion in the lower Panuco Basin, Mexico. *Catena* **52**: 57–76.
- Jansson MB. 2002. Determining sediment source areas in a tropical river basin, Costa Rica. *Catena* **47**: 63–84.
- Klein M. 1984. Anti-clockwise hysteresis in suspended sediment concentration during individual storms. *Catena* **11**: 251–257.
- Kostrenzowski A, Stach A, Zwolinski Z. 1994. Transport of suspended load in the Parseta River during the flash flood of June 1988, Poland. *Geographia Polonica* **63**: 63–73.
- Lefrançois J, Grimaldi C, Gascuel-Oudoux C, Gilliet N. 2007. Suspended sediment and discharge relationship to identify bank degradation as a main sediment source on small agricultural catchments. *Hydrological Processes* **21**: 2923–2933.
- Lenzi MA, Lorenzo M. 2000. Suspended sediment load during floods in a small stream of the Dolomites (northeastern Italy). *Catena* **39**: 267–282.
- Lewis J. 2003. Turbidity controlled sampling for suspended sediment load estimation. In *Erosion and Sediment Transport Measurement in Rivers: Technological and Methodological Advances*, Bogen J, Fergus T, Walling DE (eds), Proceedings of the Oslo Workshop, June 2002, IAHS Publication 283. IAHS Press: Wallingford; 13–20.
- López-Tarazon JA, Batalla RJ, Vericat D, Francke T. (2009). Suspended sediment in a highly erodible catchment: The River Isábena (southern Pyrenees). *Geomorphology* **109**: 210–221.
- Maneux E, Probst JL, Veyssy E, Etcheber H. 2001. Assessment of dam trapping efficiency from water residence time: Application to fluvial sediment transport in the Adour, Dordogne, and Garonne River basins (France). *Water Resources Research* **37**: 801–811.
- Mossa J. 1996. Sediment dynamics of the lowermost Mississippi River. *Engineering Geology* **45**: 457–479.
- Nadal-Romero E, Latron J, Marti-Bono C, Regués D. 2008. Temporal distribution of suspended sediment transport in a humid Mediterranean badland area: The Araguás catchment, Central Pyrenees. *Geomorphology* **97**: 601–616.
- Orwin JF, Smart CC. 2004. The evidence for paraglacial sedimentation and its temporal scale in the deglaciating basin of Small River Glacier, Canada. *Geomorphology* **58**: 175–202.
- Pearl MR, Walling DE. 1982. Particle size characteristics of fluvial suspended sediment. In *Recent Developments in the Explanation and Prediction of Erosion and Sediment Yield*. IAHS Publication 137. IAHS Press: Wallingford; 397–407.
- Revel JC, Guiesse M. 1995. Erosion due to cultivation of calcareous clay soils on the hillsides of south west France. I. Effect of former farming practices. *Soil Tillage Research* **35**(3): 147–155.
- Ribeyeix-Claret C. 2001. *Agriculture et Environnement en Gascogne Gersoise. Erosion du sol et pollution diffuse par phosphore. Le cas du bassin versant d’Audradé (Gers)*, PhD Thesis, University of Toulouse.
- Rovira A, Batalla R. 2006. Temporal distribution of suspended sediment transport in a Mediterranean basin: The Lower Tordera (NE Spain). *Geomorphology* **79**: 58–71.
- Salant N, Hassan M, Alonso C. 2008. Suspended sediment dynamics at high and low storm flows in two small watersheds. *Hydrological Processes* **22**: 1573–1587.
- Sayer AM, Walsh RPP, Bidin K. 2006. Pipeflow suspended sediment dynamics and their contribution to stream sediment budgets in small rainforest catchment, Sabah, Malaysia. *Forest Ecology and Management* **224**: 119–130.
- Schmidt KH, Morche D. 2006. Sediment output and effective discharge in two small high mountain catchments in the Bavarian Alps, Germany. *Geomorphology* **80**: 131–145.
- Sichingabula HM. 1998. Factors controlling variations in suspended sediment concentration for single-valued sediment rating curves, Fraser River, British Columbia, Canada. *Hydrological Processes* **12**: 1869–1894.
- Smith HG, Drogovich D. 2008. Sediment budget analysis of slope-channel coupling and in-channel sediment storage in an upland catchment, south-eastern Australia. *Geomorphology* **101**: 643–654.
- Steegeen A, Govers G, Nachtergaele J, Takken I, Beuselinck L, Poesen J. 2000. Sediment export by water from an agricultural catchment in the Loam Belt in central Belgium. *Geomorphology* **33**: 25–36.

- Steegeen A, Govers G. 2001. Correction factors for estimating suspended sediment export from loess catchments. *Earth Surface Processes and Landforms* **26**: 441–449.
- Van Sickle J, Beschta RL. 1983. Supply-based models of suspended sediment transport in streams. *Water Resources Research* **19**(3): 768–778.
- Veyssey E. 1998. *Transfers des matières organiques des bassins versants aux estuaries*, PhD Thesis, University of Bordeaux.
- Walling DE. 1977. Assessing the accuracy of suspended sediment rating curves for a small basin. *Water Resources Research* **13**: 531–538.
- Walling DE. 1978. Suspend sediment and solute response characteristics of River Exe, Devon, England. In *Research in Fluvial Systems*, Davidson-Arnott R, Nickling W (eds). Geoabstracts: Norwich; 167–197.
- Walling DE, Webb BW. 1982. Sediment availability and the prediction of storm-period sediment yields. In *Recent Development in the Explanation and Prediction of Erosion and Sediment Yield*. IAHS Publication 137. IAHS Press: Wallingford; 327–337.
- Walling DE, Webb BW. 1986. Solutes in river systems. In *Solute Process*, Trudgill ST (ed.). John Wiley & Sons: Chichester; 251–320.
- Walling DA, Webb BW. 1996. *Erosion and Sediment Yield: A Global Overview*. IAHS Publication 236. IAHS Press: Wallingford; 3–19.
- Williams GP. 1989. Sediment concentration versus water discharge during single hydrologic events in rivers. *Journal of Hydrology* **111**: 89–106.
- Zabaleta A, Martínez M, Uriarte JA, Antigüedad U. 2007. Factors controlling suspended sediment yield during runoff events in small headwater catchments of the Basque Country. *Catena* **71**: 179–190.

Chapter 5

Fluvial transport of suspended sediment and organic carbon in a large agricultural catchment during flood events, in southwest France

*This chapter describes the fluvial transport and relationship between suspended sediment and organic carbon (DOC and POC) within the agricultural catchment context. The fluxes were estimated during each flood event. Their relationship of discharge and hydro-climatic variables is studied in order to comprehend the hydrological processes controlling the transport. The analysis of each hysteresis pattern during different seasonal floods was examined. This chapter was written in the form of publication which was accepted in **Hydrological Processes**.*

Fluvial transport of suspended sediment and organic carbon in a large agricultural catchment during flood events, southwest France

Chantha Oeurng¹, Sabine Sauvage^{1,2}, Alexandra Coynel³, Eric Maneux⁴, Henri Etcheber³, José-Miguel Sánchez-Pérez^{1,2}.

1-Université de Toulouse ; INPT ; UPS ; ECOLAB (Laboratoire Ecologie Fonctionnelle); Ecole Nationale Supérieure Agronomique de Toulouse (ENSAT) Avenue de l'Agrobiopole BP 32607 Auzeville Tolosane 31326 CASTANET TOLOSAN Cedex France.

2-CNRS ; ECOLAB (Laboratoire Ecologie Fonctionnelle) ; 31326 CASTANET TOLOSAN Cedex France.

3-Université de Bordeaux, UMR CNRS 5805 EPOC; Equipe Traceurs Géochimiques et Minéralogiques, Talence, France

4-ADERA, Cellule de transfert GEOTRANSFERT, Centre Condorcet, 33608 Pessac Cedex, France.

Corresponding author: sabine.sauvage@ensat.fr

Abstract

Water draining from a large agricultural catchment in south-west France was sampled over an 18-month period to determine the temporal variability in suspended sediment (SS) and dissolved (DOC) and particulate (POC) organic carbon transport during flood events, with quantification of fluxes and controlling factors, and to analyse the relationships between discharge and SS, DOC and POC. A total of 15 flood events were analysed, providing extensive data on SS, POC and DOC during floods. There was high variability in SS, POC and DOC transport during different seasonal floods, with SS varying by event from 513 to 41 750 t; POC from 12 to 748 t and DOC from 9 to 218 t. Overall, 76% and 62% of total fluxes of POC and DOC occurred within 22% of the study period. POC and DOC export from the Save catchment amounted to 3090 t and 1240 t, equivalent to $1.8 \text{ t km}^{-2} \text{ y}^{-1}$ and $0.7 \text{ t km}^{-2} \text{ y}^{-1}$, respectively. Statistical analyses showed that total precipitation, flood discharge and total water yield were the major factors controlling SS, POC and DOC transport from the catchment. The relationships between SS, POC and DOC and discharge over temporal flood events resulted in different hysteresis patterns, which were used to deduce dissolved and particulate origins. In both clockwise and anticlockwise hysteresis, POC followed the same patterns as discharge and SS. The DOC-discharge relationship was mainly characterised by alternating clockwise and anticlockwise hysteresis due to dilution effects of water originating from different sources in the whole catchment.

Key words:

Agricultural catchment; suspended sediment; dissolved organic carbon; particulate organic carbon; flood events; hysteresis.

5.1. Introduction

Studies of fluvial suspended sediment and organic carbon transport through streams and rivers provide information on the rate of continental erosion, global carbon cycling and the contribution of terrestrial carbon to aquatic systems and oceans (Meybeck, 1982, 1993; Robertson et al., 1996; Sarin et al., 2002). The transportation of organic carbon from terrestrial ecosystems by rivers and hydrological fluxes to the oceans plays an important role in regional budgets of organic carbon entering the continent-ocean interface (Sarin et al., 2002). At the terrestrial scale, the previous estimations of global fluxes of organic carbon brought by the rivers are in the order of 400×10^6 C per year in which $170 - 195 \times 10^6$ C in particulate form (Ludwig et al., 1996; Meybeck and Vörösmarty, 1999) and $200 - 215 \times 10^6$ C in dissolved form (Meybeck and Vörösmarty, 1999).

Intensive agriculture has led to environmental degradation through soil erosion and carbon losses from agricultural land to stream networks (Sharma and Rai, 2004). Suspended sediment (SS) transport from agricultural catchments to watercourses is responsible for aquatic habitat degradation, reservoir sedimentation and the transport of sediment-associated pollutants (pesticides, particulate nutrients, heavy metals and other toxic substances) (Valero-Garcés et al., 1999; Heaney et al., 2001; Verstraeten and Poesen, 2002). Total organic carbon (TOC), comprising dissolved organic carbon (DOC) and particulate organic carbon (POC), is not only an important factor in stream water quality, but also an indicator of organic contamination (Ni et al., 2008). There is a general lack of studies determining organic carbon concentrations and fluxes in lowland agricultural catchments, particularly during flood events where there are many difficulties such as spatiotemporal variability in climatic conditions, different land uses and soil textures. Studies on river ecosystems have demonstrated that river discharge, primary production and litter pool sizes in catchments and the type and extent of agriculture in catchments are major processes influencing organic carbon fluxes in rivers (Robertson et al., 1996). Agriculture can significantly affect hydrological processes and organic carbon and nutrient transport in many ways. For instance, landuse changes and tillage practices affect the hydrological response of a system, and thus nutrient flux, through changes in land cover, infiltration, evapotranspiration and soil characteristics (Robertson et al., 1996). These changes are followed by feedback mechanisms for water, organic carbon and other chemical substances that bring further changes in these linked processes (Alexander and Smith, 1990).

There is a wide range of existing literature investigating fluvial export of organic carbon from peatland environments (Hope et al., 1997; Dawson et al., 2002; Worrall et al., 2003; Pawson et al., 2008). Similar studies have been conducted in forest environments (Meybeck, 1993; Molot and Dillon, 1996; Kao and Liu, 1997; Meybeck and Vörösmarty, 1999; Shibata et al., 2001). However, little attention has been paid to fluvial transport of organic carbon in large agricultural catchments, particularly during flood events when sediment transport can be significant.

The Gascogne area of southern Europe encompasses highly contrasting zones with various climatic influences (mountains, the Atlantic and the Mediterranean) and is dominated by anthropogenic activities, particularly intensive agriculture, causing severe erosion in recent decades. This is posing a major threat to surface water quality, since sediment transport within the catchment is the main factor mobilising aquatic contaminants and associated particulate organic carbon. For example, Oeurng et al. (2010) showed that sediment export during floods in the Save agricultural catchment in 2007 and 2008 represented 85% and 95% of annual loads (16% and 20% of annual duration), respectively. Within these floods, there was one extreme event which transported 63% of the total load. Moreover, Pawson et al. (2008) found that POC export from a peatland catchment in southern Pennines, UK, accounted for 95% of flux in only 8% of the total study period. These results demonstrate the major role of floods in delivering sediment associated with particulate organic carbon transport from catchments. During flood events, hysteresis effect is often observed in sediment/nutrient concentrations and discharge relationships (Asselman, 1999). When the concentration peak at the rising limb arrives before the discharge peak, it describes a clockwise hysteretic loop. When it arrives after the discharge peak, it describes an anticlockwise hysteretic loop (Williams, 1989). However, when there are multiple peaks within a flood event, a complicated mix of clockwise and anticlockwise hysteretic loops occurs. Hysteresis patterns have been used in previous studies to indicate changing sources of sediment and nutrient supply to rivers during flood events (Lefrançois et al., 2007; Nadal-Romero et al., 2008; House and Warwick, 1998; Bowes et al., 2005; Stutter et al., 2008).

The overall aim of the present study was to gain a deeper understanding of fluvial transport of SS and TOC from a large agricultural catchment during flood events. Specific objectives were to:

- Study the temporal variability in suspended sediment, POC and DOC transport during flood events, including quantification of fluxes and controlling factors.
- Analyse the relationship between discharge and SS, DOC and POC concentrations.

5.2. Materials and methods

5.2.1. Study area

The Save agricultural catchment is located in the area of Coteaux Gascogne, with an area of 1110 km² (Figure 5-1). The Save river has its source in the piedmont zone of the Pyrenees Mountains (south-west France) at an altitude of 600 m, joining the Garonne River after a 140 km course with a linear shape and an average slope of 3.6‰.

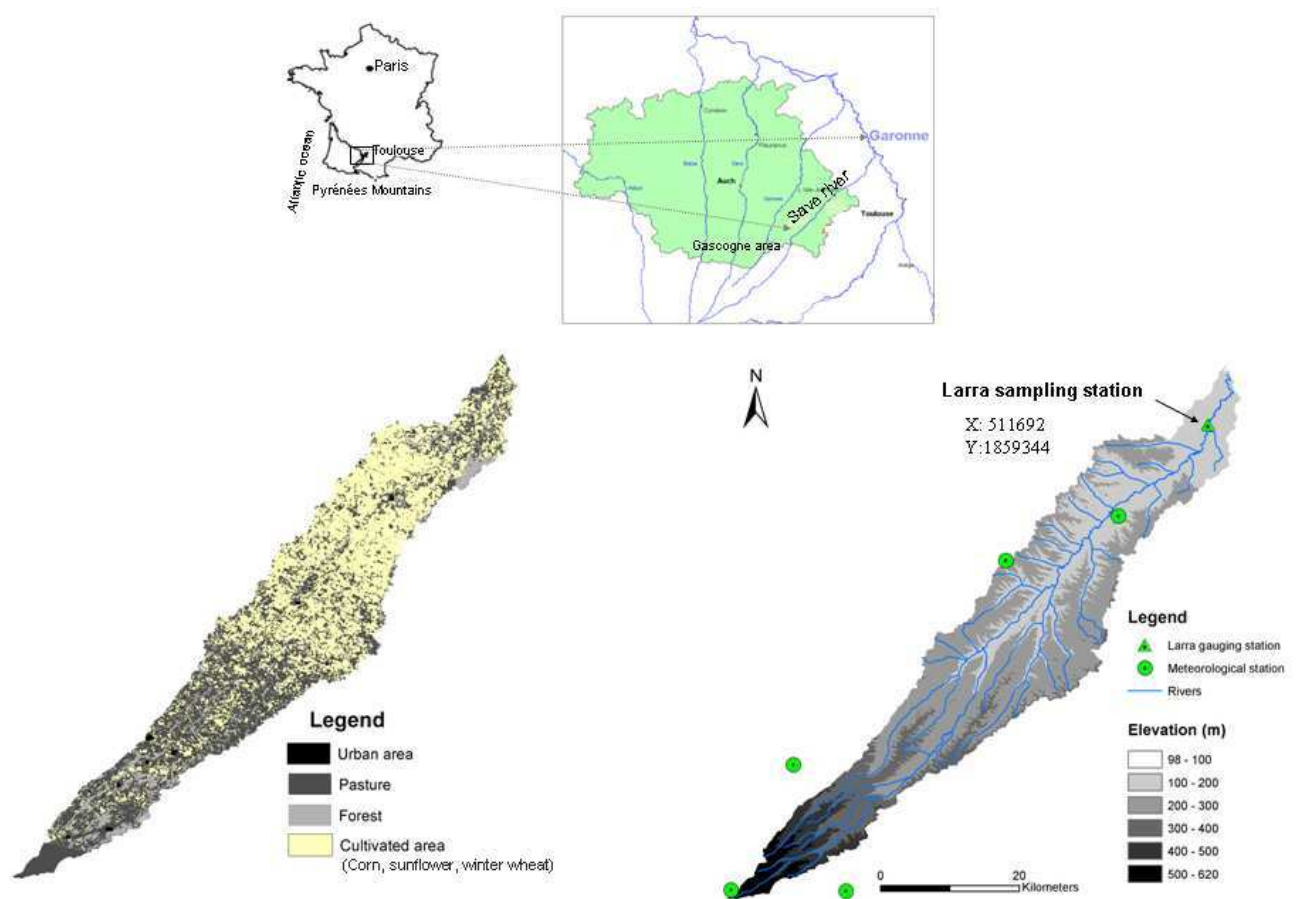


Figure 5-1. Location, landuse and topographical maps of the Save catchment.

This catchment lies on detrital sediments from the Pyrenees Mountains. It is bordered on the east by the Garonne River, on the south by the Pyrenees and on the west by the Atlantic Ocean. Calcic luvisols (UN FAO soil units) have developed on the tertiary substratum and local rendosols on the hard calcareous sandstone beds. The calcic cambisols that developed on hillsides with very gentle slopes have been subjected to moderate erosion. Calcic soils represent dominantly more than 90% in the whole catchment with a clay content ranging from 40% to 50%. Non-calcic silty soils, locally named *boulbènes*, represent less than 10% of the soil in this area (50-60% silt) (Revel and Guiresse, 1995). The upstream part of the catchment is a hilly agricultural area mainly covered with pastures and little forest, while the lower part is flat and devoted to intensive agriculture, mostly sunflower and winter wheat in rotation (90% of the area used for agricultural purposes) (Figure 5-1).

The climatic conditions are oceanic, with annual precipitation of 700-900 mm and annual evaporation of 500-600 mm. The dry period runs from July to September (the month with maximum deficit) and the wet period from October to June. The mean temperature of the catchment is 13°C, with a minimum in January (5°C on average) and a maximum in August (20°C on average). The hydrological regime of the catchment is mainly pluvial, i.e. regulated by rainfall, with maximum discharge in May and low discharge during summer (July to September). The catchment substratum is relatively impermeable due to its high clay content and consequently river discharge is mainly supplied by surface and subsurface runoff, while groundwater is limited to alluvial and colluvial phreatic aquifers (Echanchu, 1988). The maximum instantaneous discharge in the past 40 years (1965-2006) was 620 m³ s⁻¹ (1 July 1977). During low flow periods, the Save River is sustained by about 1 m³ s⁻¹ from the Neste canal at the upstream area.

5.2.2. Instrumentation and sampling method

A Sonde YSI 6920 (YSI Incorporated, Ohio, USA) measuring probe and Automatic Water Sampler (ecoTech Umwelt-Meßsysteme GmbH, Bonn, Germany) with 24 1-litre bottles has been installed at the Save catchment outlet (Larra bridge) since January 2007 for water quality monitoring. The Sonde was calibrated at the laboratory for turbidity with two points (0 and 1000 NTU) and recalibrated each three months in order to avoid sensor derivation. The Sonde is positioned near the bank of the river under the bridge, where homogeneity of water movement is considered appropriate for all hydrological conditions. The pump inlet is placed next to the Sonde pipe. The turbidity and water level are recorded at 10-min intervals.

The turbidity values in water are detected by sensor on the Sonde YSI and the data are then transferred to the ecoTech memory. The Sonde is programmed to activate the automatic water sampler to pump water at water level variations $\Delta x(\text{cm})$ ranging from 10 cm to 30 cm, depending on seasonal hydrological conditions for both the rising and falling stage (Oeurng et al., 2010). This sampling method provides high sampling frequency during storm events (3 minutes to 24 h per sample during floods). In the present study, manual sampling was also carried out using a 2-litre bottle lowered from the Larra bridge, near the Sonde position, at weekly intervals when water levels were not markedly varied. A total of 208 water samples were taken by automatic and manual sampling during the study period (January 2008 to June 2009).

5.2.3. Data sources and treatment

Hydro-meteorological data

Hourly rainfall data from five meteorological stations in the catchment (Figure 5-1) were obtained from Meteo France. Data on mean total rainfall depth and intensity in the whole catchment were derived using the Thiessen Polygon method (Thiessen, 1911). Data on hourly discharge at Larra hydrometric station were obtained from CACG (Compagnie d'Aménagement des Coteaux de Gascogne), which is responsible for hydrological monitoring in the Gascogne region. The discharge was plotted by the rating curve in which water level was measured hourly by pressure with the form of a rectangular weir (length 12 m), then transferred by teletransmission.

Laboratory analysis

Water samples pumped by automatic sampling were generally collected from the field once a week but during high flood periods they were collected twice a week. The water samples were filtered in the laboratory using pre-weighed glass microfibre filter paper (Whatman GF/F 0.7 μm). Volumes of water ranging from 150 ml to 1000 ml were filtered according SS concentration. The sediment retained on the filter paper was dried for 48 h at 60 °C to ensure accurate sediment weight. The filters were then weighed to determine suspended sediment concentration (SSC).

- Sediment analysis for POC

The dried filters containing SS (4 mg to 150 mg) were acidified with HCL 2N in order to remove carbonates and dried at 60 °C for 24 h. POC analyses were carried out using a LECO

CS200 analyser (Etcheber et al., 2007). POC content is expressed as a percentage of dry weight of sediment, abbreviated to POC%, and POC concentration as expressed in mg l^{-1} .

- Water analysis for DOC

The water samples filtered through 0.7 μm filter paper were acidified with HCL (12N; $\text{pH}=2$) and kept cold at 4 $^{\circ}\text{C}$ until analyses were performed as soon as possible. The analyses were carried out with a Shimadzu TOC-5000 analyser using the high temperature catalytic oxidation method (HTCO).

5.2.4. SS concentration data and calculation of fluxes

Continuous data on SS concentration were generated from the relationship between SS and turbidity, with the interpolation method used for missing points (Oeurng et al., 2010). The SS load was calculated using high data resolution. The organic carbon flux for flood events and annual period was calculated using the Walling and Webb (1985) method recommended by the Paris Commission for estimating river loads:

$$\text{Load} = V \times \frac{\sum_{i=1}^n (C_i \times Q_i)}{\sum_{i=1}^n Q_i}$$

Where C_i is the concentration for each instantaneous sample point (mg l^{-1}), Q_i is the discharge at each sampling point ($\text{m}^3 \text{s}^{-1}$), V is the water volume over the period considered (m^3) and n is the number of samples. This is the preferred method for flux estimates given the available data (Littlewood, 1992) and is common in the literature for estimates of organic carbon loads (e.g. Hope et al., 1997; Dawson et al., 2002; Worrall et al., 2003; Worrall and Burt, 2005).

5.2.5. Statistical analyses

Statistical analyses were performed using statistical techniques (Pearson correlation matrix) and Principal Component Analysis (PCA) by the STATISTICA package. The relationships between SS, POC, DOC and hydro-climatological variables were analysed in order to determine the factors controlling SS, POC and DOC transport during flood events. A database was generated for each flood event and contained two main groups of variables: antecedent variables to the flood conditions and flood variables (precipitation, discharge, sediment and organic carbon) during the events (Table 5-1). The antecedent variables used were accumulated precipitation one day before the flood (P1d, mm), five days before (P5d), and ten days before (P10d); initial baseflow (Q_b) before the flood started; and the antecedent flood corresponding to the current flood (Q_a).

Table 5-1. Names, abbreviations and units for the variables used to characterise flood events and to perform Pearson correlation matrix and factorial analysis

<i>Antecedent conditions</i>		
	<i>Abbreviation</i>	<i>Unit</i>
Precipitation 1 day before the event	P1d	mm
Precipitation 5 days before the event	P5d	mm
Precipitation 10 days before the event	P10d	mm
Baseflow before the event	Qb	m ³ s ⁻¹
Antecedent peak discharge	Qa	m ³ s ⁻¹
<i>Flood event conditions</i>		
Flood duration	Fd	h
Time of rise	Tr	h
Total precipitation during the event	Pt	mm
Maximum rainfall intensity of the event	Imax	mm h ⁻¹
Flood intensity ((Qmax - Qb)/time of rise)	If	m ³ min ⁻²
Total water yield	Wt	Hm ³
Mean discharge	Qm	m ³ s ⁻¹
Maximum discharge	Qmax	m ³ s ⁻¹
Mean suspended sediment concentration	SSCm	mg l ⁻¹
Maximum suspended sediment concentration	SSCmax	mg l ⁻¹
Total suspended sediment yield	SSt	t
Mean dissolved organic carbon	DOCm	mg l ⁻¹
Max.dissolved organic carbon	DOCmax	mg l ⁻¹
Dissolved organic carbon yield	DOct	t
Mean particulate organic carbon	POCm	mg l ⁻¹
Max.particulate organic carbon	POCmax	mg l ⁻¹
Particulate organic carbon yield	POCt	t

A Pearson correlation matrix and factorial analysis that included all the above-mentioned variables (Table 5-1) were generated for 13 flood events (event 1 excluded due to lack of DOC and POC data). Event 4 (1 June 2008) was also excluded from the matrix because it was an extraordinary event making a high contribution to total variance. Flood variables were described by the precipitation that caused the flood, i.e. mean total precipitation (Pt) and hourly maximum intensity of the precipitation (Imax). Total water yield (Wt) during the flood was expressed by the total water depth of the event, total duration of the event (Td), and mean discharge (Qm) and maximum discharge (Qmax) corresponding to the time of rise to reach the peak discharge (Tr). The discharge speed to reach the peak flow during flood events was defined by flood intensity If ($If = (Q_{max} - Q_b) / Tr$). Suspended sediment was expressed as the mean concentration (SSCm), the maximum concentration (SSCmax) and the total suspended sediment yield during the flood event (SSt). Dissolved and particulate organic carbon loads during floods were expressed by mean values (DOCm, POCm), maximum values (DOCmax, POCmax) and their yield (DOct; POct).

5.3. Results

5.3.1. Hydrometeorology during the study period

The term ‘flood’ is used here to represent a complete hydrological event with rising and receding limbs. Major rainfall events generally occurred in autumn (October to December) and particularly in spring (March to June) and minor rainfall events in summer (July to October). During the whole observation period, 15 flood events were recorded (3 in winter, 8 in spring and 4 in autumn) (Figure 5-2). The duration of these flood events ranged from 95 h to 351 h, with a mean value of 188 h. The longest event (event 10; 351h) occurred on 27 January 2009, with total precipitation of 74.5 mm in the whole catchment. This event was unusual since it had a 10-year return period and it represented the biggest flood during the whole study period. Maximum hourly discharge during observed flood events varied from 12.97 m³ s⁻¹ (8 November 2008) to 112.60 m³ s⁻¹ (27 January 2009). Mean daily discharge in the whole study period was 6.28 m³ s⁻¹. Table 5-2 summarises all flood characteristics during the observed flood events and their antecedent conditions. Total rainfall in the catchment for the whole study period (January 2008-June 2009) was 1152 mm (i.e. 768 mm y⁻¹). The maximum rainfall intensity reached 17 mm h⁻¹ in event 4 (1 June 2008). The mean total water yield of the whole study period (January 2008 to June 2009) was 178 mm y⁻¹ higher than the long-term mean value of 136 mm for the period 1985-2008.

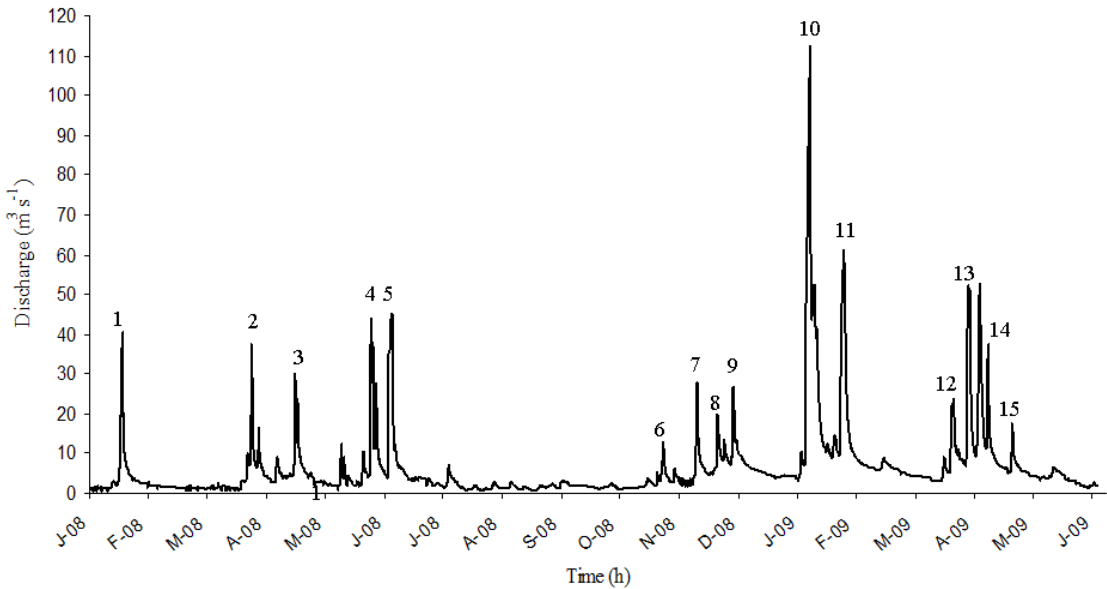


Figure 5-2: Hourly discharge in the 15 flood events observed during the study period (January 2008 to June 2009) at Larra sampling station.

Table 5-2. Summary of the main flood characteristics recorded during the study period in Save catchment

N°	Flood date	Season	P1d (mm)	P5d (mm)	P10d (mm)	Qb (m ³ s ⁻¹)	Qa (m ³ s ⁻¹)	Fd (h)	Tr (h)	Pt (mm)	Imax (m h ⁻¹)	If (m ³ min ⁻²)	Wt (Hm ³)	Qm (m ³ s ⁻¹)	Qmax (m ³ s ⁻¹)
1	19/01/2008	winter	17.7	27.7	41.6	3.16	6.75	184	43	19.9	3.4	0.87	7.34	10.74	40.64
2	28/03/2008	spring	7.2	24.9	26.8	2.56	40.64	228	84	39.3	2.8	0.42	8.56	10.39	37.60
3	21/04/2008	spring	13.3	22.4	51.3	4.06	37.60	189	22	19.4	4.0	1.19	7.1	9.60	30.20
4	01/06/2008	spring	24.0	48.9	61.1	4.28	30.20	228	16	50.0	17.2	2.48	12.75	15.70	44.02
5	12/06/2008	spring	7.5	14.6	54.5	4.28	44.02	259	29	28.5	8.5	1.40	12.61	15.01	44.80
6	08/11/2008	autumn	3.1	14.5	47.3	2.96	44.80	105	46	23.8	4.6	0.22	2.4	6.18	12.97
7	26/11/2008	autumn	3.3	13.1	14.7	4.90	12.97	191	43	35.9	4.4	0.53	3.42	9.08	27.57
8	06/12/2008	autumn	4.2	9.6	32.7	4.90	27.57	126	54	27.7	5.3	0.28	3.21	10.12	19.77
9	14/12/2008	autumn	11.7	22.6	41.0	6.95	19.77	256	27	13.3	1.6	0.73	6.01	11.63	26.74
10	27/01/2009	winter	11.5	11.7	13.0	4.06	26.74	351	69	74.5	4.1	1.57	43.71	34.50	112.60
11	11/02/2009	winter	0.2	7.7	12.6	9.99	112.60	233	54	32.9	4.2	0.94	19.71	25.94	60.66
12	14/04/2009	spring	17.6	48.3	49.1	5.10	60.66	141	29	29.5	4.5	0.64	7.15	14.08	23.80
13	22/04/2009	spring	3.1	9.2	51.5	6.75	23.80	112	36	19.3	4.2	1.26	9.80	24.31	52.24
14	02/05/2009	spring	9.6	25.1	38.9	11.00	52.80	116	22	1.1	0.7	1.20	7.18	15.90	37.47
15	15/05/2009	spring	11.3	12.7	13.2	5.10	37.47	95	26	13.0	1.9	0.48	3.31	9.68	17.62

*Maximum values for bold numbers and minimum values for bold-italic

5.3.2. SS, POC and DOC concentrations and relationship with discharge

Delivered SS characteristics increased with seasonal discharge and varied widely during the observation period. For all hydrological periods (flood and non-flood events), SS concentration ranged between 6 and 15 743 mg l⁻¹. Maximum SS concentration during flood events reached 15 743 mg l⁻¹ (observed in event 4), while the minimum value was 391 mg l⁻¹, observed on 14 April 2009 (event 12). Mean discharge-weighted SS concentration for the whole period (estimated as the mean of all measurements including base flows and floods) was 535 mg l⁻¹.

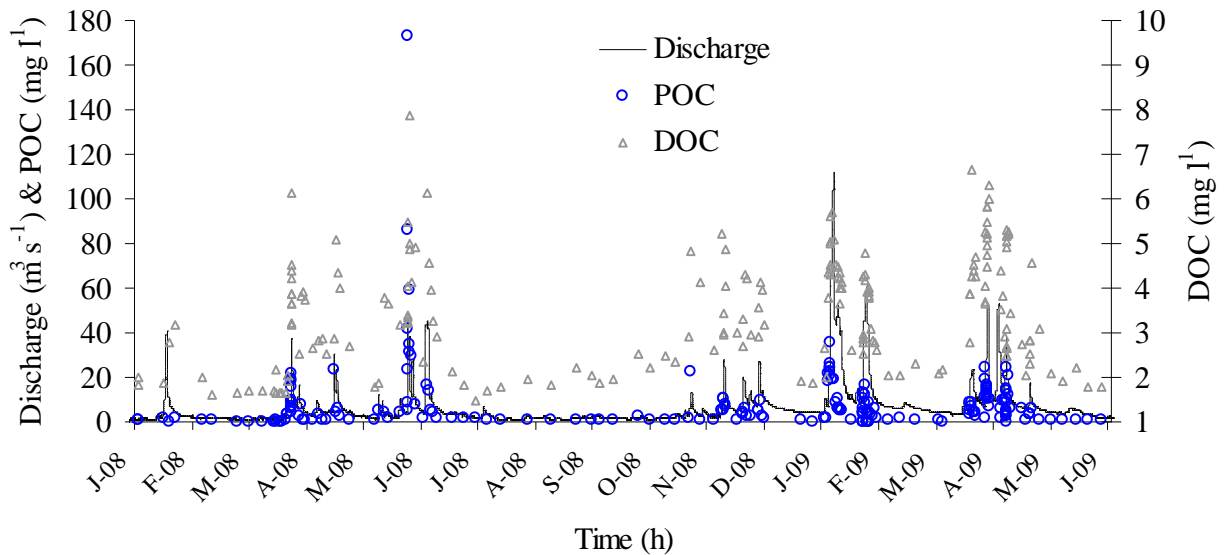


Figure 5-3. Temporal variability in particulate (POC) and dissolved (DOC) organic carbon during the study period (January 2008, June 2009).

Maximum POC and DOC concentrations were recorded during flood events (Figure 5-3), whereas minimum concentrations occurred during base flow periods. POC concentration during all hydrological conditions at the catchment outlet ranged from 0.1 to 173.2 mg l⁻¹ (discharge-weighted mean value of 14 mg l⁻¹) and DOC concentration from 1.5 to 7.9 mg l⁻¹ (discharge-weighted mean value of 4.1 mg l⁻¹). There was a trend for decreasing POC% with increasing discharge and SS concentration during flood events, with POC% ranging from 0.9 to 8% (mean value 2.25%) (Figure 5-4). The Save catchment showed a good relationship between discharge and DOC concentration ($R^2=0.50$) during all hydrological conditions, but a weak relationship between discharge and POC concentration ($R^2=0.18$) (Figure 5-5).

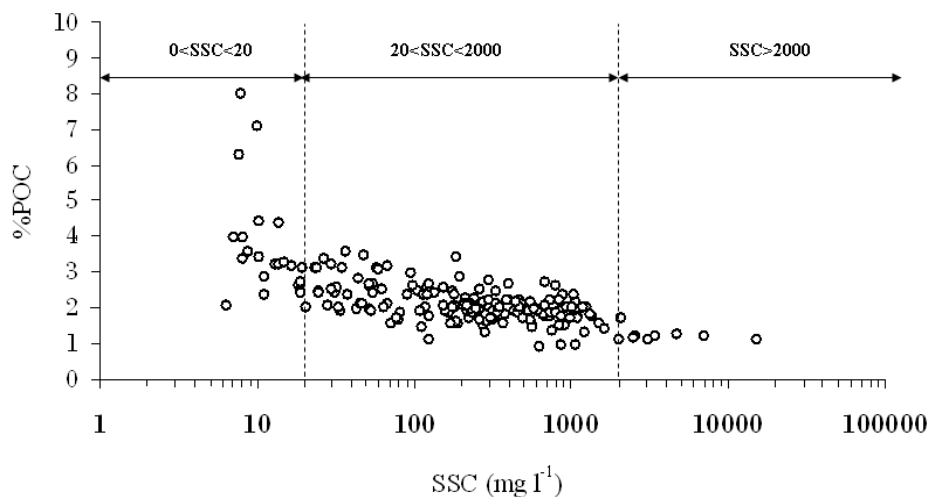


Figure 5-4. Relationship between POC contents (% of dry weight) and suspended sediment concentrations (mg l⁻¹) from the Save catchment at Larra sampling station

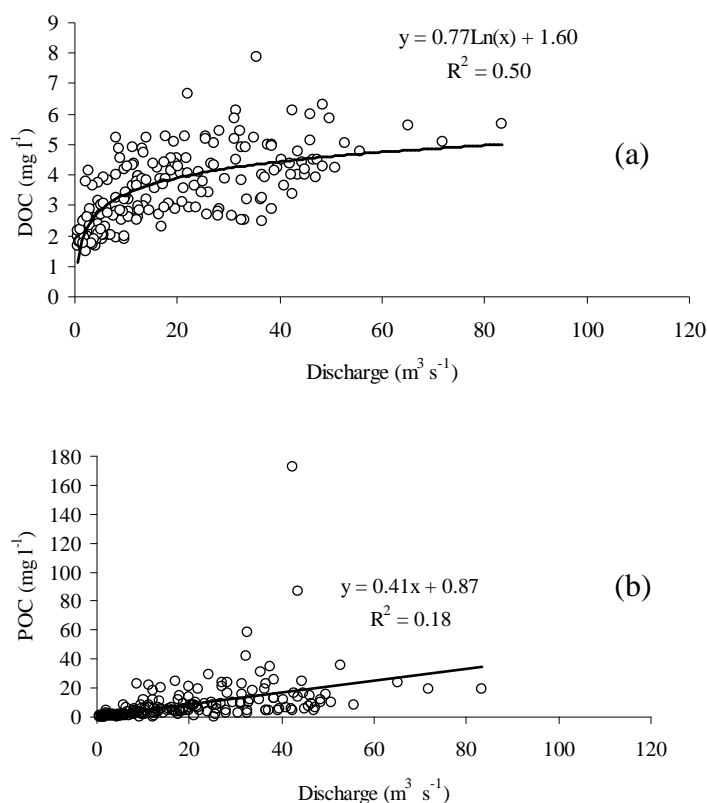
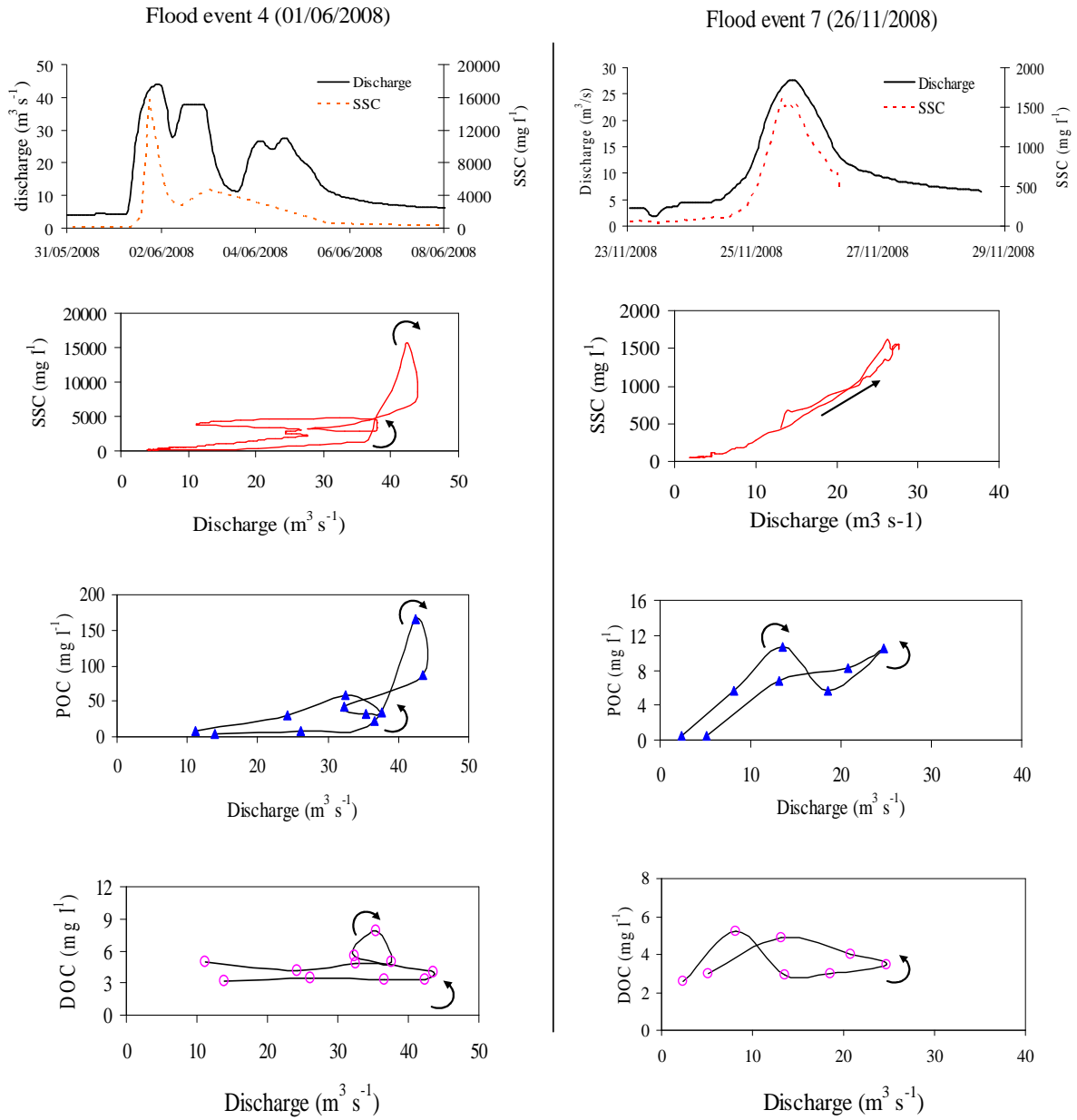


Figure 5-5. Relationship between discharge and DOC (a) and POC (b).

In the present study, complex mixes of clockwise and anticlockwise loops were observed when there were multiple peaks of discharge together with multiple peaks of SSC during a flood event, coinciding with extreme rainfall intensity, e.g. in flood event 4. The relationship between POC/DOC and discharge showed clockwise, anticlockwise and mixed hysteresis due

to temporal variability in concentrations during flood events in different seasons (Figure 5-6), as also observed for sediment concentration and discharge by Oeurng et al. (2010).



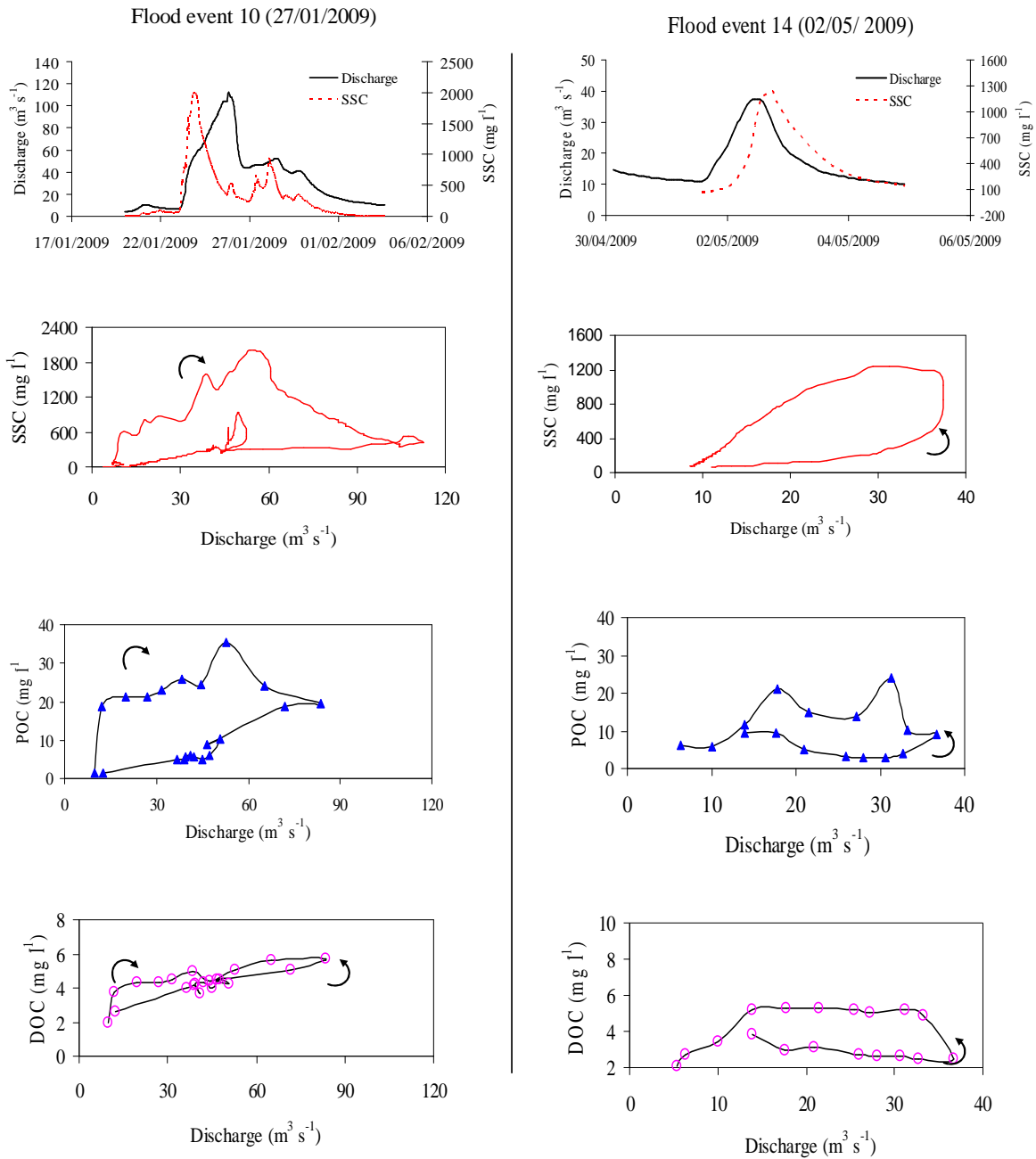


Figure 5-6. Relationship between discharge and suspended sediment (SS), particulate organic carbon (POC) and dissolved organic carbon (DOC), showing different hysteresis patterns.

5.3.3. SS, POC and DOC fluxes

The results clearly demonstrated the temporal variability in SS, DOC and POC transport during seasonal flood events (Table 5-3). The SS, DOC and POC loads transported during autumn were less than those in winter and spring due to lower flood magnitude. The transport rates during observed floods showed that SS load (per event) varied from 513 to 41 750 t; POC load from 12 to 748 t and DOC load from 9.3 to 218 t. The POC and DOC transported

during flood events represented 76% and 62% of their total loads and occurred within 22% of the study period (January 2008-June 2009). The maximum SS and POC loads recorded in flood events occurred during spring flood (event 4), while the maximum DOC load was recorded during the flood of the longest duration (event 10). During the whole study period, POC from the Save catchment amounted to 3090 t and DOC export to 1240 t, representing 1.8 t km⁻² y⁻¹ and 0.7 t km⁻² y⁻¹, respectively. The POC load ranged from 1.6 to 7.7% of sediment transport from the catchment during flood events and represented 2.5% of total sediment export during the whole study period.

Table 5-3. TSS, DOC, POC concentrations and transport rates during 15 studied flood events

N ^o	Flood date	Season	SSC _m (mg l ⁻¹)	SSC _{max} (mg l ⁻¹)	SS _t (t)	DOC _m (mg l ⁻¹)	DOC _{max} (mg l ⁻¹)	DOC _t (t)	POC _m (mg l ⁻¹)	POC _{max} (mg l ⁻¹)	POC _t (t)
1	19/01/2008	winter	652	1380	4801	NA	NA	NA	NA	NA	NA
2	28/03/2008	spring	562	1160	4820	4.0	6.1	34	11.5	24.1	98
3	21/04/2008	spring	650	1536	4385	3.8	5.1	25	13.0	23.8	85
4	01/06/2008	spring	1597	15743	41750	4.5	7.9	58	58.0	173.2	748
5	12/06/2008	spring	850	1322	9077	5.0	6.1	70	12.5	17.6	176
6	08/11/2008	autumn	159	466	<i>513</i>	4.3	4.8	10	16.8	21.9	39
7	26/11/2008	autumn	494	1618	2959	3.6	5.2	22	7.4	10	46
8	06/12/2008	autumn	278	569	1018	3.3	4.3	15	4.4	5.6	20
9	14/12/2008	autumn	<i>128</i>	501	1085	3.6	<i>4.1</i>	38	4.9	6.9	52
10	27/01/2009	winter	337	2003	23374	5.0	5.7	218	16.2	36.2	706
11	11/02/2009	winter	396	1030	6867	3.4	4.8	75	7.2	16.8	157
12	14/04/2009	spring	268	<i>391</i>	1690	4.5	6.7	32	5.5	8.6	39
13	22/04/2009	spring	678	1055	5029	5.2	6.3	51	12.6	24.8	123
14	02/05/2009	spring	344	1246	3113	3.8	5.3	25	8.8	24.2	58
15	15/05/2009	spring	204	434	666	2.8	4.6	9	3.6	6.1	12

*Maximum values for bold numbers and minimum values for bold-italic

5.3.4. Relationship among POC, DOC and hydro-climatological variables.

Table 5-4 shows the relationships between hydro-climatological, DOC and POC variables in the Save catchment. Total precipitation (Pt) showed a moderate correlation with mean discharge (Q_m) (R=0.56) and good correlations with maximum discharge (Q_{max}) (R=0.73) and total water yield (W_t) (R=0.79). Antecedent flood discharge (Q_a) and baseflow (Q_b) had weak correlations with total precipitation (Pt).

Table 5-4. Pearson correlation matrix among all variables (n=13)

	Fd	Tr	If	Pt	Imax	P1d	P5d	P10d	Qa	Qb	Qm	Qmax	Wt	SSCm	SSCmax	SSCT	DOCm	DOCmax	DOct	POCm	POCmax	POCt	
Fd	1.00																						
Tr	0.42	1.00																					
If	0.50	-0.20	1.00																				
Pt	0.71	0.73	0.22	1.00																			
Imax	0.21	0.10	0.15	0.37	1.00																		
P1d	0.12	-0.38	0.20	-0.03	-0.26	1.00																	
P5d	-0.11	-0.25	-0.10	-0.17	-0.20	0.75	1.00																
P10d	-0.28	-0.50	0.16	-0.45	0.30	0.23	0.39	1.00															
Qa	0.00	0.05	0.06	-0.05	0.04	-0.17	0.09	-0.13	1.00														
Qb	-0.14	-0.36	0.30	-0.44	-0.42	-0.16	-0.06	-0.11	0.48	1.00													
Qm	0.53	0.29	0.72	0.56	0.07	-0.07	-0.26	-0.28	0.26	0.34	1.00												
Qmax	0.72	0.43	0.74	0.73	0.11	-0.02	-0.29	-0.34	0.10	0.12	0.93	1.00											
Wt	0.76	0.44	0.66	0.79	0.13	0.08	-0.22	-0.37	0.15	0.03	0.89	0.97	1.00										
SSCm	0.22	0.01	0.53	0.10	0.54	-0.18	-0.16	0.31	-0.04	-0.14	0.16	0.24	0.10	1.00									
SSCmax	0.60	0.26	0.67	0.54	0.17	-0.07	-0.27	-0.24	-0.15	-0.04	0.49	0.70	0.62	0.58	1.00								
SSCT	0.77	0.43	0.71	0.81	0.25	0.07	-0.26	-0.30	-0.01	-0.11	0.82	0.96	0.97	0.27	0.74	1.00							
DOCm	0.29	0.12	0.57	0.40	0.49	0.05	0.10	0.49	-0.13	-0.23	0.49	0.51	0.45	0.47	0.35	0.54	1.00						
DOCmax	0.11	0.13	0.39	0.30	0.34	0.22	0.43	0.33	0.04	-0.20	0.31	0.31	0.24	0.57	0.30	0.32	0.76	1.00					
DOct	0.78	0.42	0.66	0.80	0.18	0.10	-0.22	-0.32	0.02	-0.04	0.86	0.96	0.99	0.11	0.62	0.98	0.52	0.26	1.00				
POCm	0.29	0.30	0.42	0.41	0.32	-0.16	-0.20	0.27	-0.10	-0.38	0.29	0.46	0.44	0.39	0.53	0.54	0.70	0.38	0.45	1.00			
POCmax	0.38	0.36	0.62	0.44	0.01	-0.05	-0.16	0.05	0.03	-0.07	0.57	0.71	0.65	0.37	0.69	0.71	0.62	0.41	0.62	0.87	1.00		
POCt	0.75	0.45	0.64	0.82	0.17	0.11	-0.24	-0.32	-0.05	-0.13	0.81	0.95	0.97	0.11	0.66	0.98	0.51	0.25	0.99	0.53	0.69	1.00	

*Correlation is significant at $P<0.01$ level for bold numbers and $P<0.05$ for italics

Organic carbon concentration (POC_m, POC_{max}, DOC_m, DOC_{max}) had weak relationships with total precipitation (Pt) and maximum rainfall intensity (I_{max}). DOC_m was fairly well correlated with flood intensity (IF) (R=0.57), while POC_{max} showed a moderate correlation with If (R=0.62). DOC_{max} was slightly correlated with Q_{max}, while POC_{max} was more strongly correlated with this parameter (R=0.71). SS_t, DOCT and POCT showed significant correlations with flood duration (Fd), total precipitation (Pt), flood discharge (Q_m; Q_{max}) and total water yield (Wt) (Table 5-4). SS, POC and DOC variables did not show any relationship with antecedent flow (Q_a, Q_b) or antecedent precipitation (P1d, P5d and P10d). In Principal Component Analysis (PCA) taking samples and variables into account, two factors explained 59.10% of total variance, with factor 1 representing 44.25%. Factor 1 was characterised by high negative Eigen-value for total rainfall (Pt), flood duration, flood discharge (Q_m; Q_{max}) and total water yield (Wt), which indicates the response of SS, POC and DOC load transport during flood events. Four factors were retained for rotational analysis. A summary of varimax rotated factors for all variables is given in Table 5-5. The first four axes absorbed 79.10% of the total variance.

Table 5-5. Summary of varimax rotated factor for all variables presented in Table 5-1 (Eigen-values <0.50 were excluded)

Variables	Factor 1	Factor 2	Factor 3	Factor 4
Fd	-0.76	–	–	–
Tr	–	–	0.58	–
If	-0.72	–	-0.51	–
Pt	-0.80	–	–	–
I _{max}	–	–	–	–
P1d	–	–	–	0.75
P5d	–	–	–	–
P10d	–	–	–	–
Q _a	–	–	–	–
Q _b	–	–	-0.74	-0.51
Q _m	-0.83	–	–	–
Q _{max}	-0.96	–	–	–
Wt	-0.94	–	–	–
SSC _m	–	-0.59	–	–
SSC _{max}	-0.77	–	–	–
SST	-0.98	–	–	–
DOC _m	-0.63	-0.66	–	–
DOC _{max}	–	-0.67	–	–
DOCT	-0.95	–	–	–
POC _m	-0.63	–	–	–
POC _{max}	-0.78	–	–	–
POCT	-0.95	–	–	–
Variance explained	44.30	14.80	10.90	9.10
Cumulative variance	44.30	59.10	70.00	79.10

Bold number for value ≥ 0.80

5.4. Discussion

5.4.1. Temporal variability in SS, POC and DOC transport and yield

SS, POC and DOC concentrations recorded during different seasonal flood events provide an insight into the temporal variability in these parameters in the Save agricultural catchment. Maximum SS, POC and DOC concentrations generally increased with increasing magnitude of flood events, particularly in spring, yielding SS, POC and DOC fluxes with strong variability. Based on the statistical analyses, there were strong correlations between total precipitation (Pt), flood duration (Fd), flood discharge (Qm; Qmax), total water yield (Wt) and suspended sediment and organic carbon fluxes (SS_t, POCT and DOCT). These variables could be the main factors controlling SS, POC and DOC transport. Cooper et al. (2007) also attributed DOC transport to flood event magnitude. However, the availability of SS and organic carbon sources is also important in determining the temporal variability. The variability in sediment transport during successive peaks of similar magnitude is influenced by sediment exhaustion effects. After a period of relatively high sediment transport (supply-rich floods), sediment becomes less and less available (exhaustion phenomenon), and the sediment concentrations recorded during successive months are consequently lower (Walling, 1978). This was seen in successive floods (events 7, 8 and 9) during autumn 2008, recorded on 26 November 2008 (Q_{max} = 27.57 m³ s⁻¹; SSC_{max} = 1613 mg l⁻¹), 6 December 2008 (Q_{max} = 19.77 m³ s⁻¹; SSC_{max} = 569 mg l⁻¹), and 14 December 2008 (Q_{max} = 26.74 m³ s⁻¹; SSC_{max} = 501 mg l⁻¹). These exhaustion effects have been described by many previous studies (Walling, 1978; Alexandrov et al., 2003; Rovira and Batalla, 2006).

The highest POC concentrations were measured in the flood event with the highest rainfall intensity (17.2 mm h⁻¹). However the maximum discharge during this flood event amounted to 44.02 m³ s⁻¹, while the flood on 27 January 2009, with discharge of 112.60 m³ s⁻¹, transported only 36.20 mg l⁻¹ of POC. This shows that the level of peak discharge does not always control the peak of POC, as it can also be affected by other factors such as rainfall intensity and flood intensity that determine soil erosion within the catchment during rainfall events. The extreme POC concentration was linked to the highest SS associated with POC%.

DOC also showed strong variability in concentrations during all hydrological conditions. However, it transpired that the level of increase in flood discharge did not solely control the increase in DOC concentration, as similar peaks in DOC were produced by different flood

discharges (Table 3). This is confirmed by the poor statistical relationship between maximum DOC and peak discharge ($R=0.31$). The temporal dynamics of DOC are very complex (Jones et al., 1996) and may be controlled not only by microbial activity in sediments (Bicudo et al., 1998) but also by variations in POC (Vervier et al., 1993; Jones et al., 1995). However during summer, the groundwater dilution of DOC is limited in the Save catchment, since the catchment substratum is relatively impermeable due to its high clay content, and therefore DOC concentrations are not high ($<8 \text{ mg L}^{-1}$). Numerous authors have reported that groundwater may be high in DOC (Wallis et al., 1981; McDowell & Likens, 1988; Vervier et al., 1993; Bernard et al., 1994) and have described groundwater as being a source of organic matter for surface water (Fiebig & Lock, 1991). The mean DOC concentration in the Save catchment is similar to the DOC value of 4.1 mg l^{-1} reported for temperate zones (Meybeck, 1988). Compared with other rivers, the Save DOC range is close to the range ($2\text{-}6 \text{ mg l}^{-1}$) of the Niger River (Martins, 1982), slightly higher than the range ($3\text{-}5 \text{ mg l}^{-1}$) of the Amazon (Richey et al., 1985) and the St. Lawrence River (Pocklington and Tan, 1983) but much lower than the range ($2\text{-}22 \text{ mg l}^{-1}$) of the Indus River (Arain, 1987).

The specific POC yield ($1.8 \text{ t km}^{-2} \text{ y}^{-1}$) of the Save catchment is comparable to the mean of the Garonne River ($1.47 \text{ t km}^{-2} \text{ y}^{-1}$) (Veyssy et al., 1999) and slightly higher than the mean of rivers in Europe ($1.10 \text{ t km}^{-2} \text{ y}^{-1}$) (Ludwig et al., 1996). However, it is lower than the yield of the Amazon River ($2.83 \text{ t km}^{-2} \text{ y}^{-1}$; Richey et al., 1990), and much lower than that of the Nivelle River ($5.3 \text{ t km}^{-2} \text{ y}^{-1}$) (Coynel et al., 2005), which drains a typical Pyrenean mountainous catchment into the Bay of Biscay (Atlantic Ocean). This could be attributed to lower soil erosion generating less POC yield, as POC is associated with sediment. The specific DOC yield of the Save catchment ($0.7 \text{ t km}^{-2} \text{ y}^{-1}$) is 2.5 times higher than that of a Himalayan catchment dominated by agriculture studied by Sharma and Rai (2004), a difference that can be attributed to land conservation preventing soil and carbon losses within the latter. However, peatland catchments, which are rich in organic carbon, have much higher specific DOC yields, e.g. $16.9 \text{ t km}^{-2} \text{ y}^{-1}$ for a catchment in north-east Scotland (Dawson et al., 2002). This value is common in peat-dominated headwater catchments in the UK, where soil carbon is the major source of organic carbon in stream water (Aitkenhead et al., 1999; Dawson et al., 2001).

5.4.2. Discharge, SS, POC and DOC relationships and probable origins

The relationship between sediment concentration and discharge revealed the existence of clockwise, anticlockwise and mixed-shape hysteretic loops (mixing of clockwise and anticlockwise patterns). Interpreting sediment and organic carbon delivery processes using hysteresis patterns could help understand the origins of dissolved and particulate matter in a catchment. Increasing SSC on the falling limb during floods may be related to sources of relatively more available sediment near the catchment outlet. Clockwise hysteresis occurs when the sediment source area is the channel itself or an adjacent area located close to the catchment outlet, with runoff triggering the movement of sediment accumulated in the channel during the previous seasons and with little or no contribution from the tributaries (Klein, 1984). López-Tarazon et al (2009) also reported that the clockwise phenomenon was found preferentially when rainfall was mostly located near the catchment outlet. In the Save catchment, this was the case for clockwise flood events in early autumn and late winter. Anticlockwise hysteretic loops occur when sediment sources are far from the catchment outlet, e.g. soil erosion from hillsides and upstream areas (Braisington and Richards, 2000; Goodwin et al., 2003; Orwin and Smart, 2004). This type of hysteretic loop is mainly found in the Save catchment in spring and late autumn, when there are high flood magnitudes with sufficient capacity to transport sediments from distant areas of the upstream catchment to the outlet (Oeurng et al., 2010). However, it is noted that clear interpretation of sediment sources using hysteresis patterns is limited within this study because the Save catchment is long with only one sampling station at the catchment outlet. Some hysteresis studies from existing literature were used to identify the sediment sources which are close or far referring to the sampling station, mainly in small catchments (Lefrançois et al., 2007; Nadal-Romero et al., 2008).

POC and DOC exhibited different hysteresis behaviour during flood events. This resulted from variability in concentrations during rising and falling limbs of floods. The relationship between discharge and POC for both clockwise and anticlockwise hysteresis followed the same patterns as discharge and SS hysteresis. Examples can be seen in flood events 4, 7, 10 and 15 (Figure 5-6). Although POC% decreased during flood events, POC concentrations remained high with high concentrations of SSC and therefore the hysteresis patterns were similar (Figure 5-6). Generally, POC% decreased as SS increased, following a hyperbolic relationship (Figure 5-4). This is a very typical trend as reported for other rivers (Meybeck, 1982; Ittekkot, 1988, Coynel et al., 2005), and it is attributed to changes in organic matter

sources during the hydrograph through declining organic carbon in eroded materials (Ittekkot and Lanne, 1991). Probst (1992) showed for the Garonne that high POC% corresponds to production of phytoplankton during low flood periods, while low POC content corresponds to POC from soil erosion during high flow periods. In the present study ($SSC < 20 \text{ mg l}^{-1}$, associated with low river discharge), the high POC content could be attributed to the phytoplankton and litter contribution. For the other classes, corresponding to medium or strong sediment mobilisation associated with high river discharge and turbid waters, organic carbon content is low and generally recognised as being of allochthonous origin (Etcheber, 1986; Lin, 1988; Coynel et al., 2005). In this study, POC associated with SSC higher than the 2000 mg l^{-1} can be attributed to the terrigenous origins which mainly originated from the soil.

The relationship between DOC and discharge also showed clockwise, anticlockwise and mixed patterns during the study period, but the mixed patterns were mostly found when the SS peak arrived before peak discharge. An example can be seen in flood events 4 and 10 (Figure 5-6). This could be due to dilution effects between old water before the floods and new water during and after floods. For clockwise patterns, DOC before the flood events was low, but then it was diluted by new water containing higher DOC concentrations from soils which quickly released DOC during storm events before reaching the peak discharge. Many studies have examined the effect of storms on the ability of soils to release DOC and water fluxes are responsible for seasonal changes in DOC concentration in runoff (Kalbitz et al., 2000). The relationship between DOC and discharge showed anti-clockwise hysteresis, with higher DOC concentrations on the falling limb of the high hydrograph than on the rising limb. This indicates that water entering the stream during the early part of the flood events had lower DOC concentrations than water entering the stream after peak discharge (Morel et al., 2009), an effect associated with subsurface water from shallow soil horizons, which is rich in DOC.

5.5. Conclusion

Temporal characteristics of fluvial transport of suspended sediment and organic carbon during flood events were studied in a large agricultural catchment using an extensive dataset with high temporal resolution obtained by manual and automatic sampling. The results showed strong variability in SS and POC and DOC concentrations. Suspended sediment load during different seasonal flood events varied from 513 to 41 750 t; POC load from 12 to 748 t and DOC load from 9 to 218 t. Transport of POC and DOC during flood events amounted to 76%

and 62% of their total fluxes and occurred within 22% of the study period (January 2008-June 2009). These results reveal the important role of floods in mobilising SS, POC and DOC transport from the Save agricultural catchment. Total POC export during the whole study period amounted to 3091 t and total DOC export to 1238 t, representing $1.8 \text{ t km}^{-2} \text{ y}^{-1}$ and $0.7 \text{ t km}^{-2} \text{ y}^{-1}$, respectively.

Statistical analyses revealed strong correlations between total precipitation (Pt), flood discharge and total water yield and SS, POC and DOC, indicating that these variables are the main factors controlling sediment and organic carbon export from the Save catchment. Sediment and organic carbon sources are also important in yielding dissolved and particulate matter during flood events, as successive floods exhaust the amounts available. The relationships between SSC, POC and DOC loads and discharge over different temporal scales during flood events resulted in different hysteresis patterns, which were used to identify their origins. For POC, clockwise and anticlockwise hysteresis followed the same patterns as discharge and SS hysteresis. The relationship between DOC and discharge was mainly dominated by alternating clockwise and anticlockwise hysteresis due to dilution effects of water originating from different sources in the whole catchment.

5.6. Acknowledgements

This research was financially supported by a doctoral research scholarship from the French government in cooperation with Cambodia. The work was performed within the framework of GIS-ECOBAG, Programme P2 Garonne Moyenne and IMAQUES, and supported by funds from CPER and FEDER (grants n°OPI2003-768) of the Midi-Pyrenees Region, Zone Atelier Adour Garonne (ZAAG) of PEVS/CNRS347 INSUE. This work was also performed within the framework of the EU Interreg SUDOE IVB program (SOE1/P2/F146 AguaFlash project, <http://www.aguaflash-sudoe.eu>) and funded by ERDF and Midi-Pyrénées Region. We sincerely thank the CACG for discharge data and Meteo France for meteorological data. The authors would like to thank Ecolab staff for access to the site and assistance with monitoring instruments and in laboratory. Great thanks were particularly delivered to two anonymous referees whose comments improve the manuscript.

5.7. References

- Aitkenhead JA, Hope D, Billett MF. 1999. The relationship between dissolved organic carbon in streamwater and soil organic carbon pools at different spatial scales. *Hydrological Processes* **13**: 1289-1302.
- Alexander RB, Smith RA. 1990. Country-level estimation of nitrogen and phosphorus fertilizer use in the United States, 1945 to 1985. *USGS Open File Report, Reston, VA, Australia*.
- Alexandrov Y, Laronne JB, Reid I. 2003. Suspended sediment transport in flash floods of the semiarid northern Negrev, Israel. *IAHS Publication* **278**: 346-352.
- Arain R. 1987. Persisting trends in carbon and mineral transport monitoring of the Indus River. In: Degens, E. T., Kempe, S. and Gan Weibin (Eds) *Transport of Carbon and Minerals in Major World Rivers, Pt. 4*. Mitt. Geol.-Paläont. Inst. Univ. Hamburg, SCOPE/UNEP Sonderbd **64**: 417-21.
- Asselman NEM. (1999). Suspended sediment dynamics in a large basin: the River Rhine. *Hydrological Processes* **13**: 1437-1450
- Bernard C, Fabre A, Vervier P. 1994. DOC cycling in surface and ground waters interaction zone in a fluvial ecosystem. *Verh. int. Ver. Limnology* **25**: 1410-1413.
- Bicudo DC, Ward AK, Wetzel RG. 1998. Fluxes of dissolved organic carbon within attached aquatic microbiota. *Verh. int. Ver. Limnology* **26**: 1608-1613.
- Bowes MJ, House WA, Hodgkinson RA, Leach DV. 2005. Phosphorus discharge hysteresis during storm events along a river catchment: the River Swale. UK. *Water Research* **39** (5): 751–762.
- Braisington J, Richards K. 2000. Suspended sediment dynamics in small catchments in the Nepal Middle Hills. *Hydrological Processes* **14**: 2559-2574.
- Copper R, Thoss V, Watson H. 2007. Factors influencing the release of dissolved organic carbon and dissolved forms of nitrogen from a small upland headwater during autumn runoff events. *Hydrological Processes* **21**: 622-633.
- Coyne A, Etcheber H, Abril G, Maneux E, Dumas J, Hurtrez JE. 2005. Contribution of small mountainous rivers to particulate organic carbon input in the Bay of Biscay. *Biogeochemistry* **74**: 151-171.
- Dawson, JJC, Backwell C, Billett MF. 2001. Is within stream processing an important control on spatial changes in headwater carbon fluxes?. *Science of the Total Environment* **265**(1-3): 153-167.
- Dawson JC, Billet MF, Neil C, Hill S. 2002. A comparison of particulate, dissolved and gaseous carbon in two contrasting upland streams in the UK. *Journal of Hydrology* **257**: 226-246.

- Echanchu D. 1988. Géochimie des eaux du bassin de la Garonne. Transfers de matières dissoutes et particulaires vers l'océan atlantique. Ph.D thesis, University of Paul Sabatier Toulouse III.
- Etcheber H. 1986. Biogéochimie de la matière organique en milieu estuarien: comportement, bilan, propriétés. Cas de le Gironde. Mem. Inst. Géologie Bassin Aquitaine., Talence, 379 pp.
- Etcheber H, Taillez A, Abril G, Garnier J, Servais P, Moatar F, Commarieu MV. 2007. Particulate organic carbon in the estuarine turbidity maxima of the Gironde, Loire and Seine estuaries: origin and lability. *Hydrobiologia* **558**(1): 247–259.
- Fiebig DM, Lock MA. 1991. Immobilization of dissolved organic matter from groundwater discharging through the stream bed. *Freshwater Biology* **26**: 45-55.
- Goodwin TH, Young AR, Holmes GR, Old GH, Hewitt N, Leeks GJL, Packman JC, Smith BPG. 2003. The temporal and spatial variability of sediment transport and yields within the Bradford Beck catchment, West Yorkshire. *The Science of the Total Environment* 3114-316: 475-494.
- Heaney SI, Foy RH, Kennedy GJ, Crozier WW, O'Connor WC. 2001. Impacts of agriculture on aquatic systems: lessons learnt and new unknowns in Northern Ireland. *Marine and Freshwater Research* **52**: 151–163.
- Hope D, Billet MF, Cresser MS. 1997. Exports of organic carbon from two river systems in NE Scotland. *Journal of Hydrology* **193**: 61-82.
- House WA, Warwick MS. 1998. Hysteresis of the solute concentration/discharge relationship in rivers during storms. *Water Research* **32** (8): 2279–2290.
- Ittekkot V. 1988. Global trends in the nature of organic matter in river suspensions. *Nature* **332**: 436–438.
- Ittekkot V, Lane RW. 1991. Fate of riverine particulate organic matter. Biogeochemistry of Major World Rivers. SCOPE 42. John Wiley, New York: 233-242.
- Jones, JB, Fisher SG, Grimm NB. 1995. Vertical hydrologic exchange and ecosystem metabolism in a Sonoran Desert stream. *Ecology* **76**: 942-952.
- Jones JB, Fisher SG, Grimm NB. 1996. A long-term perspective of dissolved organic carbon transport in Sycamore Creek, Arizona, U.S.A. *Hydrobiologia* **317**: 183-188.
- Kalbitz K, Solinger S, Park JH, Michalzik B, Matzner E. 2000. Controls on the dynamics of dissolved organic matter in soils: A review. *Soil Science* **165**: 277-304.
- Kao SJ, Liu KK. 1997. Fluxes of dissolved and non fossil particulate organic carbon from an Oceania small river (Lanyang His) in Taiwan. *Biogeochemistry* **39**: 255-269.
- Klein M. 1984. Anti-clockwise hysteresis in suspended sediment concentration during individual storms. *Catena* **11**: 251-257.

Lefrançois J, Grimaldi C, Gascuel-Oudou C, Gilliet N. 2007. Suspended sediment and discharge relationship to identify bank degradation as a main sediment source on small agricultural catchments. *Hydrological Processes* **21**: 2923-2933.

Lin RG. 1988. Etude du potentiel de dégradation de la matière organique particulaire au passage eau douce-eau salée: Cas de l'estuaire de la Gironde. Thèse Doctorat no 218, Bordeaux 1, 196 pp.

Littlewood IG. 1992. Estimating constituent loads in rivers: a review, Institute of Hydrology, Wallingford, UK, 81 pp.

López-Tarazon JA, Batalla RJ, Vericat D, Francke T. (2009). Suspended sediment in a highly erodible catchment: The River Isábena (Southern Pyrenees). *Geomorphology* **109**: 210-221.

Ludwig W, Probst JL, Kempe S. 1996. Predicting the oceanic input of organic carbon by continental erosion. *Global Biogeochemical Cycles* **10**: 23–41.

Martins O. 1982. Geochemistry of the Niger River. In: Degens, E. T. (Ed.) Transport of Carbon and Minerals in Major World Rivers, Pt. 1. Mitt. Geol.- Paläont. Inst. Univ. Hamburg, SCOPE/UNEP Sonderbd. **52**: 397-418.

McDowell WH, Likens GE. 1988. Origin, composition and flux of dissolved organic carbon in the Hubbard Brook valley. *Ecological Monograph* **58**: 177-195.

Meybeck M. 1982. Carbon, nitrogen and phosphorus transport by World Rivers. *American Journal of Science* **282**: 401-450.

Meybeck M. 1988. How to establish and use world budgets of riverine materials. In: Lerman, A. and Meybeck, M. (Eds) Physical and Chemical Weathering in Geochemical Cycles, Kluwer Academic Publishers, Dordrecht: 247-72.

Meybeck M. 1993. Riverine transport of atmospheric carbon: sources, global typology and budget. *Water, Air and Soil Pollution* **70**: 443-463.

Meybeck M, Vörösmarty C. 1999. Global transfer of carbon rivers. *Global Change News Letter* **37**: 18-20.

Molot L, Dillon PJ. 1996. Storage of terrestrial carbon in boreal lake sediments and evasion to the atmosphere. *Global Biogeochemical Cycles* **10**: 483-492.

Morel B, Durand P, Jaffrezic, Gruau G, Molenat J. 2009. Sources of dissolved organic carbon during stormflow in a headwater agricultural catchment. *Hydrological Processes* **23**: 2888-2901.

Nadal-Romero E, Regúés D, Latron J. 2008. Relationships among rainfall, runoff, and suspended sediment in a small catchment with badlands. *Catena* **74**: 127–136.

Ni HG, Lu FH, Luo XL, Tian HY, Zeng YE. (2008). Riverine inputs of total organic carbon and suspended particulate matter from the Pearl River Delta to the coastal ocean off South China. *Marine Pollution Bulletin* **56**: 1150–1157.

- Oeurng C, Sauvage S, Sanchez JM. 2010. Dynamics of suspended sediment transport and yield in a large agricultural catchment, southwest France. *Earth Surface Processes and Landforms* **35**: 1289–1301.
- Orwin JF, Smart CC. 2004. The evidence for paraglacial sedimentation and its temporal scale in the deglaciating basin of Small River Glacier, Canada. *Geomorphology* **58**: 175-202.
- Pawson RR, Lord DR, Evans MG, Allott THE. 2008. Fluvial organic carbon flux from an eroding peatland catchment, southern Pennines, UK. *Hydrology and Earth System Science* **12**: 625-634.
- Pocklington R, Tan F. 1983. Organic carbon transport in the St. Lawrence River. In: Degens, E. T., Kempe, S. and Soliman, H. (Eds) Transport of Carbon and Minerals in Major World Rivers, Pt. 2. Mitt, Geol.-Paläont. Inst. Univ. Hamburg, SCOPE/UNEP Sonderbd. **55**: 243-52.
- Probst JL. 1992. Géochimie et hydrologie de l'érosion continentale, Mécanismes, bilan global actuel et fluctuations au cours des 500 derniers millions d'années. *Science Géologie Bulletin Strasbourg* **94**: 1-161.
- Revel JC, Guirese M. 1995. Erosion due to cultivation of calcareous clay soils on the hillsides of south west France. I. Effect of former farming practices. *Soil Tillage. Research.* **35**(3): 147-155.
- Richey JE, Salati E, Dos Santos U. 1985. Biochemistry of the Amazon River: an update. In: Degens, E. T., Kempe, S. and Herrera, R. (Eds) Transport of Carbon and Minerals in Major World Rivers, Pt. 3. Mitt, Geol.-Paläont. Inst. Univ. Hamburg, SCOPE/UNEP Sonderbd. **58**: 245-58.
- Richey JE, Hedges JI, Devol AH, Quay PD. 1990. Biogeochemistry of carbon in the Amazon River. *Limnology Oceanography* **35**: 352–371.
- Rovira A, Batalla R. 2006. Temporal distribution of suspended sediment transport in a Mediterranean basin: the Lower Tordera (NE Spain). *Geomorphology* **79**: 58-71.
- Robertson AI, Boon PI, Bunn SE, Ganf GG, Hergceg AL, Hilman TJ, Walker KF. 1996. A scoping study into the role, importance, source, transportation and cycling of carbon in the riverine environment, Report to the Murray-Darling Basin Commission, Project R6067, MDBC, Canberra.
- Sarin MM, Sudheer AK, Balakrishna K. 2002. Significance of riverine carbon transport: A case study of a large tropical river. Godavari (India). *Science in China, series C* **45**: 97-108.
- Sharma P, Rai SC. 2004. Streamflow, sediment and carbon transport from a Himalayan watershed. *Journal of Hydrology* **289**: 190-203.
- Shibata R, Mitsunashi H, Miyake Y, Nakano S. 2001. Dissolved and particulate carbon dynamics in a cool-temperate forested basin in northern Japan. *Hydrological Processes* **15**: 1817-1828.

Stutter MI, Langan SJ, Cooper RJ. 2008. Spatial contributions of diffuse inputs and within-channel processes to the form of stream water phosphorus over storm events. *Journal of Hydrology* **350** (3–4): 203–214.

Thiessen AH. 1911. Precipitation averages for large areas. *Monthly Weather Review* **39** : 1082– 1084.

Valero-Garcés BL, Navas A, Machín J, Walling D. 1999. Sediment sources and siltation in mountain reservoirs: a case study from the Central Spanish Pyrenees. *Geomorphology* **28**: 23–41.

Verstraeten G, Poesen J. 2002. Regional scale variability in sediment and nutrient delivery from small agricultural catchments. *Journal of Environmental Quality* **31**: 870–879.

Vervier P, Dobson M, Pinay P. 1993. Role of interaction zones between surface and ground waters in DOC transport and processing: considerations for river restoration. *Freshwater Biology* **29**: 275-284.

Veyssy E, Etcheber H, Lin RG, Buat-Menard P, Maneux E. 1999. Seasonal variation and origin of Particulate Organic Carbon in the lower Garonne River at La Re´ole (Southwestern France). *Hydrobiologia* **391**: 113–126.

Walling DE. 1978. Suspend sediment and solute response characteristics of river Exe, Devon, England. In: Davidson-Arnott, R., Nickling, W. (Eds.), *Research in Fluvial Systems. Geoabstracts, Norwich*: 167-197.

Walling DE, Webb BW. 1985. Estimating the discharge of contaminants to coastal waters by rivers: Some cautionary comments. *Marine Pollution Bulletin* **16**: 488-492.

Wallis PM, Hynes HB, Telang SA. 1981. The importance of groundwater in the transportation of allochthonous dissolved organic matter to the stream draining a small mountain basin. *Hydrobiologia* **79**: 77-90.

Williams GP. 1989. Sediment concentration versus water discharge during single hydrologic events in rivers. *Journal of Hydrology* **111**: 89-106.

Worrall F, Reed M, Warburton J, Burt TP. 2003. Carbon budget for a British upland peat catchment. *The Science of Total Environment* **312**: 133-146.

Worrall F, Burt T. 2005. Predicting the future DOC flux from upland peat catchments. *Journal of Hydrology* **300**: 126-139.

Chapter 6

Assessment of hydrology, sediment and particulate organic carbon yield in a large agricultural catchment using the SWAT model

*This chapter addresses the modelling approach to characterise the fluxes of suspended sediment and particulate organic carbon using agro-hydrological model, the SWAT model (Soil and Water Assessment Tool). The simulation of suspended sediment was compared with observed sediment data from the two year observation. The catchment water balance was also evaluated. The fluxes of sediment and POC were estimated via long-term simulation of suspended sediment and POC concentrations. A regression between annual water yield and simulated annual sediment yield was established and potential source areas of erosion were also identified for the studied catchment. This chapter was written in the form of publication which is under review in the *Journal of Hydrology*.*

Assessment of hydrology, sediment and particulate organic carbon yield in a large agricultural catchment using the SWAT model

Chantha Oeurng¹, Sabine Sauvage^{1,2}, José-Miguel Sánchez-Pérez^{1,2}.

(1) Université de Toulouse ; INPT ; UPS ; ECOLAB (Laboratoire Ecologie Fonctionnelle); Ecole Nationale Supérieure Agronomique de Toulouse (ENSAT) Avenue de l'Agrobiopole BP 32607 Auzeville Tolosane 31326 CASTANET TOLOSAN Cedex France.

(2) CNRS ; ECOLAB (Laboratoire Ecologie Fonctionnelle) ; 31326 CASTANET TOLOSAN Cedex France.

Corresponding author: sabine.sauvage@ensat.fr

Abstract

Assessment of catchment hydrology, sediment and associated particulate organic carbon losses from agricultural land to stream networks is important for best water and soil management and for better understanding of the global carbon cycle. In this study, the Soil and Water Assessment Tool (SWAT 2005) was used to simulate discharge and sediment transport at daily time steps within the intensively farmed Save catchment in south-west France. The SWAT model was applied to evaluate catchment hydrology and sediment and associated particulate organic carbon yield using historical flow and meteorological data for the period January 1999-March 2009 and sediment data for January 2007-March 2009. Data on management practices (crop rotation, planting date, fertiliser quantity and irrigation) were also included in the model. Simulated daily discharge and sediment values matched the observed values satisfactorily. The model predicted that mean annual catchment precipitation for the total study period (726 mm) was partitioned into evapotranspiration (78.3%), percolation/groundwater recharge (14.1%) and abstraction losses (0.5%), yielding 7.1% surface runoff. Simulated mean total water yield for the whole simulation period amounted to 138 mm, comparable to the observed value of 136 mm. Simulated annual sediment yield ranged from 4766 t to 123000 t, representing a mean specific sediment yield of 48 t km⁻² y⁻¹. Annual yield of particulate organic carbon ranged from 120 t to 3100 t, representing a mean specific POC yield of 1.2 t km⁻² y⁻¹. A regression between annual water yield and simulated annual sediment yield was developed for this agricultural catchment. Potential source areas of erosion were also identified.

Key words: Save catchment, SWAT 2005, hydrology, sediment yield, particulate organic carbon,

6.1. Introduction

Intensive agriculture has led to environmental degradation through soil erosion and associated carbon losses from agricultural land to stream networks (Sharma and Rai, 2003). The global river network is increasingly being recognised as a major component of the carbon cycle due to the important role of rivers in the terrestrial water cycle, regulating the mobilisation and transfer of components from land to sea. Studies seeking a better understanding of the global carbon cycle have expressed increasing concern over the quantification of sediment and carbon transport by rivers to the sea (Milliman and Syvitski, 1992; Ludwig and Probst, 1998). The erosion of carbon from land and its subsequent transport to sea via rivers represents a major pathway in the global carbon cycle (Kempe, 1979; Degens et al., 1984). Organic carbon is estimated to constitute ~40% of the total flux of carbon carried by the world's rivers (1 Gt yr⁻¹) (Meybeck, 1993).

Effective control of water and soil losses in agricultural catchments requires the use of best management practice (BMP). Quantifying and understanding sediment transfer from agricultural land to watercourses is also essential in controlling soil erosion and in implementing appropriate mitigation practices to reduce stream sediment transport and associated pollutant loads, and hence improve surface water quality downstream (Heathwaite et al., 2005). However, field measurements and collection of data on suspended sediment and particulate organic carbon are generally difficult tasks, rarely achieved over long timescales in large catchments.

Appropriate tools are needed for better assessment of long-term hydrology and soil erosion processes and as decision support for planning and implementing appropriate measures. The tools include various hydrological and soil erosion models, as well as geographical information system (GIS). Due to technological developments in recent years, distributed catchment models are increasingly being used to implement alternative management strategies in the area of water resource allocation and flood control (Setegn, 2009). Many hydrological and soil erosion models are designed to describe hydrology, erosion and sedimentation processes. Hydrological models describe the physical processes controlling the transformation of precipitation to runoff, while soil erosion modelling is based on understanding the physical laws of processes that occur in the natural landscape (Setegn, 2009). Distributed hydrological models, mainly simulating processes such as runoff and the transport of sediment and pollutants in a catchment, are crucial for providing systematic and

consistent information on water availability, water quality and anthropogenic activities in the hydrological regime (Yang et al., 2007). A physically-based distributed model is preferable, since it can realistically represent the spatial variability of catchment characteristics (Mishra et al., 2007). A number of water quality models at catchment scale have been developed, such as AGNPS (Young et al., 1989), CREAMS (Knisel, 1980), EUROSEM (Morgan et al., 1998), ANSWERS (Beasley et al., 1980), HSPF (Donigian et al., 1995), KIREROS (Smith, 1981), WEPP (Nearing et al., 1989), AnnAGPS (Binger and Theurer, 2003), SWAT (Arnold et al., 1998) and SHETRAN (Ewen et al., 2000). Among these models, SWAT (Soil and Water Assessment Tool) is frequently used to assess hydrology and water quality in agricultural catchments. To date, a number of SWAT applications to study hydrology and sediment transport in small and large catchments have been undertaken in different regions, e.g. Miyun reservoir catchment in China (Xu et al., 2009), Lake Pyhäjärvi, Yläneenjoki catchment in Finland (Bärlund et al., 2007; Koskiaho et al., 2007), Tana Lake Basin in Ethiopia (Setegn et al., 2009), two mountainous catchments in Central Iran (Rostamian et al., 2008), Kapgari catchment in India (Behera and Panda, 2006), and many studies in American catchments such as Cottonwood catchment in Minnesota (Hanratty and Stefan, 1998), Upper North Bosque River in Texas (Di Luzio et al., 2002) and Sandusky catchment in Ohio (Grunwald and Qi, 2006). However, there have been few applications in European catchments in which intensive agriculture is increasingly being practised. Moreover, most previous SWAT applications were made on a monthly timescale.

The objective of the present study was to apply the SWAT model to the Save catchment in the Gascogne area of south-west France in order to assess long-term catchment hydrology and sediment-associated particulate organic carbon (POC) transport and to quantify sediment and carbon yields from this agricultural catchment.

6.2. Materials and methods

6.2.1. Study area

The Save catchment in the area of Coteaux Gascogne is a 1110 km² agricultural catchment. The Save river has its source in the piedmont zone of the Pyrenees Mountains (south-west France), joining the Garonne River after a 140 km course with a linear shape and an average slope of 3.6‰ (Figure 6-1A). The altitude ranges from 98 m to 620 m (Figure 6-1B). This catchment lies on detrital sediments from the Pyrenees Mountains. It is bound on the east by the Garonne River, on the south by the Pyrenees and on the west by the Atlantic Ocean.

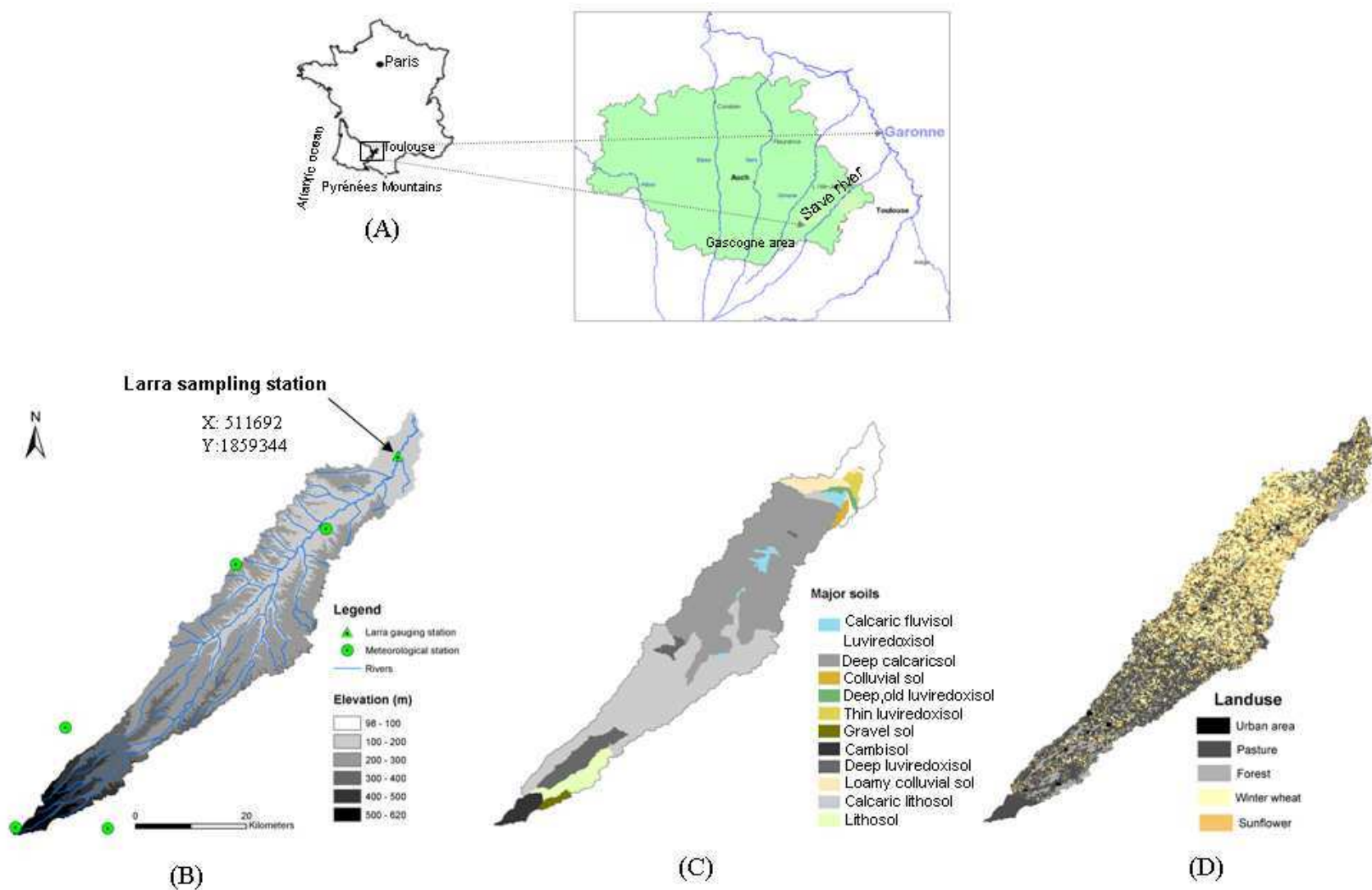


Figure 6-1. (A) Location of study area; (B) Topographical map; (C) Major agricultural landuses (D) Major soil types in the Save catchment.

Throughout the Oligocene and Miocene, this catchment served as an emergent zone of subsidence, receiving sandy, clay and calcareous sediments derived from the erosion of the Pyrenees Mountains, which were in an orogenic phase at that time. The heterogeneous sediment materials were of low energetic value and produced a thick detrital formation of the molasse type in the Miocene. From the Pleistocene onwards, the river became channelised, cutting broad valleys into the molasse deposits and leaving terraces of coarse alluvium (Revel and Guiresse 1995). The substratum of the catchment consists of impervious Miocene molassic deposits.

In this area, which has been cultivated since the Middle Ages, mechanical erosion by ploughing has had a greater impact on downward soil displacement than water erosion, with a major impact on surface relief, mainly on levelling and soil distribution (Guiresse and Revel, 1995). Very weak erosion has led to the development of Calcic Luvisols (UN FAO soil units) on the tertiary substratum and local Rendosols on the hard calcareous sandstone beds. The Calcic Cambisols on hillsides with very gentle slopes have been subjected to moderate erosion. Non-calcic silty soils, locally named *boulbènes*, represent less than 10% of the soils in this area. The calcic soils are dominated by a clay content ranging from 40% to 50%, while the non-calcic soils are silty (50-60%). The major soils of the Save catchment are presented in Figure 6-1C. The upstream part of the catchment is a hilly agricultural area mainly covered with patchy forest and dominant pastures, while the lower part is flat and devoted to intensive agriculture, with sunflower and winter wheat dominating the crop rotation (Figure 6-1D).

The climatic conditions are oceanic, with annual precipitation of 700-900 mm and annual evaporation of 500-600 mm. The dry period runs from June to August (the month with maximum deficit) and the wet period from October to May. The hydrological regime of the catchment is mainly pluvial, i.e. regulated by rainfall, with maximum discharge in May and low flows during summer (July to September).

The catchment substratum is relatively impermeable due to its high clay content. Consequently, the river discharge is mainly supplied by surface and subsurface runoff, and groundwater is limited to alluvial and colluvial phreatic aquifers. The maximum instantaneous discharge for the long-term period (1965-2006) is $620 \text{ m}^3 \text{ s}^{-1}$ (1 July 1997). The mean annual discharge (1965-2006) is $6.29 \text{ m}^3 \text{ s}^{-1}$ (data from Compagnie d'Aménagement des Coteaux de Gascogne, CACG). During low flow, the river discharge is sustained by a nested canal at the catchment head about $1 \text{ m}^3 \text{ s}^{-1}$

6.2.2. Catchment water quality monitoring

A Sonde YSI 6920 (YSI Incorporated, Ohio, USA) measuring probe and Automatic Water Sampler (ecoTech Umwelt-Meßsysteme GmbH, Bonn, Germany) with 24 1-litre bottles has been installed at the Save catchment outlet (Larra bridge) since January 2007 for water quality monitoring. The Sonde is positioned near the bank of the river under the bridge, where the homogeneity of water movement is considered representative of all hydrological conditions. The pump inlet is placed next to the Sonde pipe. The Sonde is programmed to activate the automatic water sampler to pump water at water level variations $\Delta x(\text{cm})$ ranging from 10 cm to 30 cm, depending on seasonal hydrological conditions for both the rising and falling stage. This sampling method provides a high sampling frequency during storm events (3 samples per week to 4 samples per day during flood events). Manual sampling is also carried out using a 2-litre bottle lowered from the Larra bridge, near the Sonde position, at weekly intervals when water levels are not remarkably varied. The total instantaneous water samples from both automatic and manual sampling from January 2007 to March 2009 amounted to 246 samples.

6.2.3. Determination of suspended sediment and POC concentrations

All 246 water samples were analysed in the laboratory to determine suspended sediment concentration (SSC) using a nitrocellulose filter (GF 0.45 μm) and drying at 40 °C for 48 h. Volumes of water ranging from 150 to 1000 ml were filtered according the suspended sediment load. Suspended sediment concentration data were determined for samples collected using the automatic and manual sampling methods described above over a range of hydrological conditions from January 2007 to March 2009 (Oeurng et al., 2010). Daily SSC values were calculated from the mean of instantaneous SSC for a given day.

Particulate organic carbon (POC) was analysed on samples collected from January 2008 to March 2009. Water samples were filtered by glass microfibre filter paper (GF/F 0.7 μm) for determination of particulate organic carbon (POC). The filter paper containing suspended sediment was then acidified with HCL 2N in order to remove carbonates and dried at 60 °C for 24 h. Particulate organic carbon analyses were carried out using a LECO CS200 analyser (Etcheber et al., 2007). The SSC values obtained using the nitrocellulose and glass microfibre filters were identical.

6.3. Modelling approach

6.3.1. The SWAT model

The Soil and Water Assessment Tool (SWAT 2005) was selected for this study primarily because of its many previous applications to assess hydrology and sediment transport in small and large catchments in different regions. The model is a free assessable source and user friendly environment. Furthermore, the SWAT project for the Save catchment may be extended in the future to study the other aspects of nutrient and pesticide transport.

SWAT is physically-based, distributed, agro-hydrological model that operates on a daily time step and is designed to predict the impact of management on water, sediment and agricultural chemical yields in ungauged catchments (Arnold et al., 1998). Major component models include weather, hydrology, soil temperature, plant growth, nutrients, pesticides and land management. The model is capable of continuous simulation in large complex catchments with varying soils and management conditions over long time periods. SWAT uses readily available inputs, has the capability of routing runoff and chemicals through stream and reservoirs, and allows the addition of flows and the inclusion of measured data from point sources.

SWAT can analyse small or large catchments by discretising into sub-basins, which are then further subdivided into hydrological response units (HRUs) with homogeneous land use, soil type and slope. The SWAT system embedded within geographical information system (GIS) can integrate various spatial environmental data, including soil, land cover, climate and topographical features.

6.3.2. Hydrological modelling component in SWAT

SWAT uses a modification of the SCS curve number method (USDA Soil Conservation Service, 1972) to compute surface runoff volume for each HRU. Peak runoff rate is estimated using a modification of the Rational Method (Chow et al., 1988). Daily rainfall data are used for calculations. Flow is routed through the channel using a variable storage coefficient method (Williams, 1969) or the Muskingum routing method (Cunge, 1969). In this work, SCS curve number and Muskingum routing methods, along with daily climate data, were used for surface runoff and streamflow computations. SWAT simulates the hydrological cycle based on the soil and water balance equation as follows:

$$SW_t = SW_0 + \sum_{i=1}^t (R_{\text{day}} - Q_{\text{surf}} - E_a - W_{\text{seep}} - Q_{\text{gw}})_i$$

where SW_t is the final soil water content (mm), SW_0 is the initial soil water content on day i (mm), t is the time (days), R_{day} is the amount of precipitation on day i (mm), Q_{surf} is the amount of surface runoff on day i (mm), E_a is the amount of evapotranspiration on day i (mm), W_{seep} is the amount of water entering the vadose zone from the soil profile on day i (mm), and Q_{gw} is the amount of return flow to the stream on day i (mm).

Groundwater flow contribution to total streamflow is simulated by creating shallow aquifer storage (Arnold & Allen, 1996). Percolation from the bottom of the root zone is considered as recharge to the shallow aquifer. Three methods for estimating potential evapotranspiration are used in SWAT: Priestley and Taylor (1972), Penman (Monteith, 1965) and Hargreaves and Samani (1985). In this study, the Penman method was used to estimate potential evapotranspiration.

6.3.3. Suspended sediment modelling component in SWAT

The sediment from sheet erosion for each HRU is calculated using the Modified Universal Soil Loss Equation (MUSLE) (Williams, 1975).

$$\text{Sed} = 11.8 \times (Q_{\text{surf}} \times q_{\text{peak}} \times A_{\text{hru}})^{0.56} \times K_{\text{USLE}} \times C_{\text{USLE}} \times P_{\text{USLE}} \times LS_{\text{USLE}} \times \text{CFRG}$$

where Sed is the sediment yield (t) on a given day, Q_{surf} is the surface runoff volume (mm ha^{-1}), q_{peak} is the peak runoff rate ($\text{m}^3 \text{s}^{-1}$), A_{hru} is the area of the HRUs (ha), K_{USLE} is the soil erodibility factor, C_{USLE} is the cover and management factor, P_{USLE} is the support practice factor, LS_{USLE} is the USLE topographical factor and CFRG is the coarse fragment factor. Details of the USLE factors can be found in Neitsch et al. (2005).

The sediment concentration is obtained from the sediment yield, which corresponds to flow volume within the channel on a given day. The transport of sediment in the channel is controlled by simultaneous operation of two processes: deposition and degradation. Whether channel deposition or channel degradation occurs depends on the sediment loads from the upland areas and the transport capacity of the channel network. If the sediment load in a channel segment is larger than its sediment transport capacity, channel deposition will be the dominant process. Otherwise, channel degradation occurs over the channel segment. SWAT calculates the maximum amount of sediment that can be transported from the channel segment as a function of the peak channel velocity:

$$\text{conc}_{\text{sed,ch,mx}} = \text{SPCON} \times v^{\text{SPEXP}}$$

where $\text{conc}_{\text{sed,ch,mx}}$ (ton m^{-3}) is the maximum concentration of sediment that can be transported by streamflow (i.e. transport capacity), SPCON is a coefficient defined by the user, SPEXP is an exponent parameter for calculating sediment reentrained in channel sediment routing that is defined by the user ($1 < \text{spexp} < 2$) and v (m s^{-1}) is the peak channel velocity. The peak channel velocity in a reach segment at each time step is calculated from:

$$v = \frac{\text{PRF}}{n} \times R_{\text{ch}}^{2/3} \times S_{\text{ch}}^{1/2}$$

where PRF is the peak rate adjustment factor with a default value of unity, n is manning's roughness coefficient, R_{ch} is the hydraulic radius(m), and S_{ch} is the channel invert slope (m m^{-1}).

The maximum concentration in the reach is compared with the concentration of sediment in the reach at the beginning of the time step, $\text{conc}_{\text{sed,ch,i}}$

If $\text{conc}_{\text{sed,ch,i}} > \text{conc}_{\text{sed,ch,mx}}$, deposition is the dominant process in the reach segment. The net amount of sediment deposited is calculated by:

$$\text{Sed}_{\text{dep}} = (\text{conc}_{\text{sed,ch,i}} - \text{conc}_{\text{sed,ch,mx}}) \times V_{\text{ch}}$$

where sed_{dep} is the amount of sediment deposited in the reach segment (metric tons), $\text{conc}_{\text{sed,ch,i}}$ is the initial sediment that can be transported by water (kg L^{-1} or ton m^{-3}) and V_{ch} is the volume of water in the reach segment (m^3).

If $\text{conc}_{\text{sed,ch,i}} < \text{conc}_{\text{sed,ch,mx}}$, degradation is the dominant process in the reach segment. The net amount of sediment reentrained is calculated by:

$$\text{Sed}_{\text{deg}} = (\text{conc}_{\text{sed,ch,mx}} - \text{conc}_{\text{sed,ch,i}}) \times V_{\text{ch}} \times K_{\text{ch}} \times C_{\text{ch}}$$

where sed_{deg} is the amount of sediment reentrained in the reach segment (metric tons), $\text{conc}_{\text{sed,ch,mx}}$ is the maximum concentration of sediment that can be transported by water (kg l^{-1} or ton m^{-3}), V_{ch} is the volume of water in the reach segment (m^3), K_{ch} (CH_EROD) is the channel erodibility factor ($\text{cm h}^{-1} \text{Pa}^{-1}$), and C_{ch} (CH_COV) is the channel cover factor.

The final amount of sediment in the reach is calculated by:

$$\text{Sed}_{\text{ch}} = \text{sed}_{\text{ch,i}} - \text{sed}_{\text{dep}} + \text{sed}_{\text{deg}}$$

where sed_{ch} is the amount of suspended sediment in the reach (metric tons), $sed_{ch,i}$ is the amount of the suspended sediment in the reach at the beginning of the time period (metric tons) and $sed_{dep, is}$ is the amount of sediment reentrained in the reach segment (metric tons).

The total amount of sediment that is transported out of the reach segment is computed as:

$$sed_{out} = sed_{ch} \times \frac{V_{out}}{V_{ch}}$$

where sed_{out} is the total amount of sediment transported out of the reach (metric tons), sed_{ch} is the amount of suspended sediment in the reach (metric tons), V_{out} is the volume of water leaving the reach segment (m^3) at each time step and V_{ch} is the volume of water in the reach segment (m^3).

6.3.4. Particulate organic carbon modelling

The relationship between SSC and POC concentration was found to have an R^2 value of 0.93 (Figure 6-2). Based on this relationship ($POC=0.01 \text{ SSC} + 1.87$), long-term POC could be computed from simulated SSC obtained from SWAT.

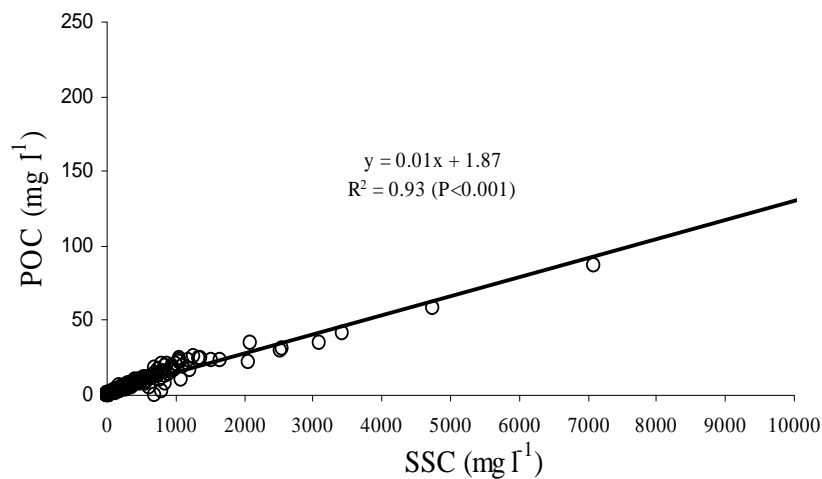


Figure 6-2. Relationship between instantaneous suspended sediment concentration (SSC) and particulate organic carbon (POC) at Larra sampling station.

6.3.5. SWAT data input

The Arc SWAT interface for SWAT version 2005 (Winchell et al., 2007) was used to compile the SWAT input files. The SWAT model requires input on topography, soils, landuse and meteorological data.

- Digital elevation map (DEM) with a resolution of 25 m × 25 m from BD TOPO R IGN France - Cemagref de Bordeaux (UR ADBX)

- Soil data at the scale of 1:80 000 from CACG and digitised by Cemagref de Bordeaux (UR ADBX) (Macary et al., 2006) and soil properties from Lescot and Bordenave. (2009) for the SWAT soil database

- Landuse data from Landsat 2005 (Macary et al. 2006). The management practices were taken into account in the model for simulation. The dominant landuse in the catchment were pasture, sunflower/winter wheat in rotation. The starting dates of plant beginning, amounts, date of fertilizer and irrigation applications were included. For pasture area, there is one rotation of corn during a period of 4 years. Tillage works were practiced during April within this area. For sunflower-winter wheat rotation, the planting date of sunflower is on April 10 then is harvested on July 10. After that, winter wheat begins on October 9 then is harvested on July 10, following year. The rotation of winter wheat-sunflower follows the same pattern by plant begins of winter wheat on October 9 and it is harvested on July 10. For following year, sunflower is planted on April 10, then is harvested on July 10. The soil is uncovered from July through April for this rotation once per two years.

- Meteorological data included 5 rainfall stations with daily precipitation from Meteo France (Figure 6-1A). Some past and missing data were generated for some stations by linear regression equation from the data of the nearest stations with complete measurement. Two stations at the upstream part having a complete measurement of daily minimum and maximum air temperature, wind speed, solar radiation and relative humidity was used to simulate the potential evapotranspiration (PET) in the model by the Penman method.

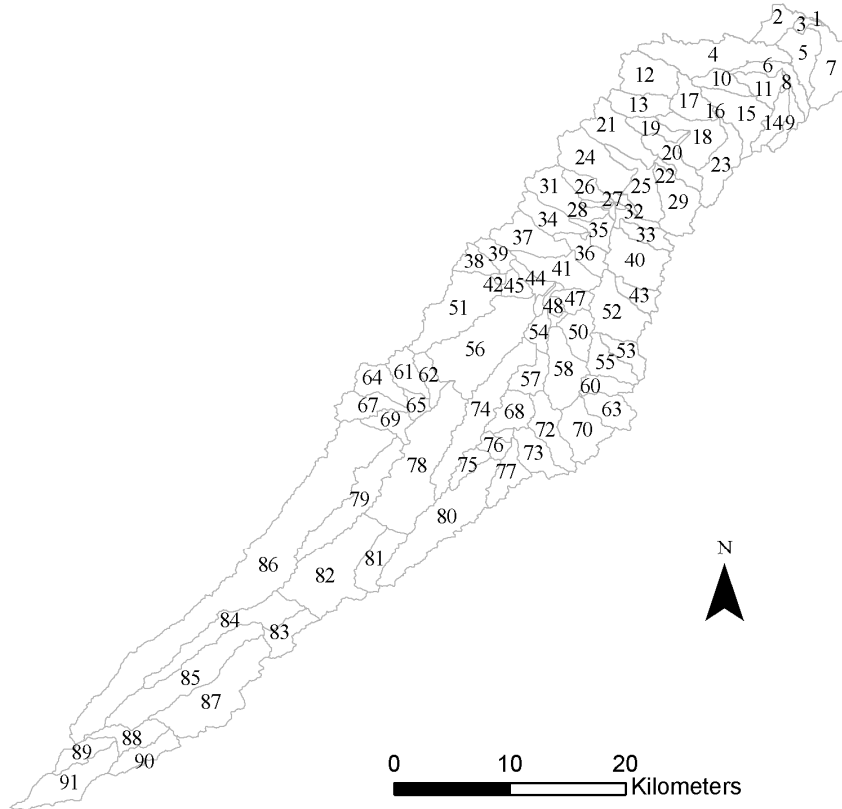


Figure 6-3. Map showing 91 sub-basins in the Save catchment.

The catchment was discretized into 91 subbasins with dominant landuse and soil classification. The main dominant landuses in the Save catchment are pasture, sunflower and winter wheat. The figure 6-3 showed 91 subbasins in the Save catchment.

6.3.6. Model evaluation

The performance of the model in simulating discharge and sediment was evaluated graphically and by Nash-Sutcliffe efficiency (E_{NS}) and coefficient of determination (R^2):

$$E_{NS} = 1 - \frac{\sum_{i=1}^n (O_i - S_i)^2}{\sum_{i=1}^n (O_i - \bar{O})^2}$$

$$R^2 = \left\{ \frac{\sum_{i=1}^n (O_i - \bar{O})(S_i - \bar{S})}{\left[\sum_{i=1}^n (O_i - \bar{O})^2 \right]^{0.5} \left[\sum_{i=1}^n (S_i - \bar{S})^2 \right]^{0.5}} \right\}$$

Where O_i and S_i are the observed and simulated values, n is the total number of paired values, \bar{O} is the mean observed value and \bar{S} is the mean simulated value.

E_{NS} ranges from negative infinity to 1, with 1 denoting perfect agreement between simulated and observed values. Generally E_{NS} is very good when E_{NS} is greater than 0.75, satisfactory when E_{NS} is between 0.36 and 0.75, and unsatisfactory when E_{NS} is lower than 0.36 (Nash and Sutcliffe, 1970; Krause et al., 2005). However, a shortcoming of the Nash-Sutcliffe statistic is that it does not perform well in periods of low flow, as the denominator of the equation tends to zero and E_{NS} approaches negative infinity with only minor simulation errors in the model. This statistic works well when the coefficient of variation for the data set is large (Pandey et al., 2008). The coefficient of determination (R^2) is the proportion of variation explained by fitting a regression line and is viewed as a measure of the strength of a linear relationship between observed and simulated data. R^2 ranges between 0 and 1. If the value is equal to one, the model prediction is considered to be 'perfect'.

6.3.7. Calibration process

The period July-December 1998 served as a warm-up period for the model (allowing state variables to assume realistic initial values for the calibration period). The calibration was carried out at daily time steps using flow data for the hydrological years from January 1999 to March 2009 and suspended sediment data for January 2007-March 2009. The capability of a hydrological model to adequately simulate streamflow and sediment process typically depends on the accurate calibration of parameters (Xu et al., 2009). Parameters can either be estimated manually or automatically. In this study, the calibration was done manually based on physical catchment understanding and sensitive parameters from published literature (e.g. Bärlund et al., 2007; Xu et al., 2009) and calibration techniques from the SWAT user manual. After calibration of flow, calibration of sediment was carried out. The SCS curve number (CN2) is a function of soil permeability, landuse and antecedent soil water conditions. This parameter is important for surface runoff. The baseflow recession coefficient (ALPHA_BF) is a direct index of groundwater flow response to changes in recharge. This parameter is necessary for baseflow calibration. The sensitive parameters for predictions of sediment are a linear parameter for calculating the maximum amount of sediment that can be entrained during channel sediment routing (SPCON), an exponential parameter for calculating the channel sediment routing (SPEXP), and a peak rate adjustment factor (PRF), which is

sensitive to peak sediment. There is no channel protection; however, the channel banks are covered by riparian vegetation along the Save river.

Added to the difficulty of discharge calibration was possibly another disadvantage caused by inaccuracy of instantaneous discharge higher than $40 \text{ m}^3 \text{ s}^{-1}$ at Larra station, generated from the rating curve. Moreover, daily nested discharge data for the Save catchment during water extraction in summer and during the winter period to sustain flow discharge in the Save river also contribute to the uncertainty in baseflow calibration. The parameters used to calibrate discharge and suspended sediment, are presented in Table 6-1.

6.4. Results and Discussion

6.4.1. Discharge simulation and hydrological assessment

Simulations were carried out for the period January 1999-March 2009. Flow and sediment calibration was based on daily simulations. Table 6-1 presents the calibrated parameters for discharge, suspended sediment and the range of SWAT parameter values, while Figure 6-4 graphically illustrates observed and simulated daily discharge at Larra gauging station. Simulated discharge followed a similar trend to observed discharge. However, simulated peak discharge was underestimated during some flood periods such as an event in June 2000, which was the largest flood observed in the study area since 1985 (data from CACG). The underestimation may be due to local rainfall storms not being well represented by the rainfall data used in the hydrological simulations. In any case, SWAT could not accurately simulate the flood discharge when the river overflowed, as in the June 2000 flood. Daily simulated discharge was also overestimated for some periods, e.g. in May 2007. Larger errors occurred when simulated peak and average flows differed significantly from the measured values. It should be noted that the hydrological regime of the Save fluctuates significantly, possibly resulting in difficulty in discharge calibration. The statistical performance was satisfactory, with a daily E_{NS} value of 0.53 and an R^2 value of 0.56. Good statistical performance was hard to achieve for the Save agricultural catchment over a long period of simulation due to strong spatial heterogeneity and lack of accurate data limitation (climate data, agricultural data) within the catchment. Very few studies published to date have shown good results of SWAT model calibration for long periods of daily simulation within an intensively farmed agricultural catchment.

Table 6-1. Parameters used to calibrate flow and sediment at Larra gauging station

Parameters used to calibrate flow					
	Parameter	Definition	Min.Value	Max.Value	Calibrated value
basins.bsn	ESCO	Soil evaporation compensation factor	0	1	0.5
	EPCO	Plant water uptake compensation factor	0	1	1
	ICRK	Crack flow (1=model crack flow in soil)			active
	SURLAG	Surface runoff lag time	0	10	1
*.GW	GW_DELAY	Groundwater delay	0	500	30
	GW_REVAP	Groundwater revap	0.02	0.2	0.05
	RCHRG_DP	Deep aquifer percolation factor	0	1	0.15
	ALPHA_BF	Baseflow alpha factor	0	1	0.5
*.soil	SOL_AWC	Available water capacity of the soil layer	0	1	0.2
*.sub	CH_N1	Manning's "n" value for tributary channels	0.01	0.5	0.025
*.rte	CH_N2	Manning's "n" value for main channel	0.01	0.5	0.04
*.hru	OV_N	Manning's "N" for overland flow	0.01	0.5	0.19
*.mgt	CN2	SCS Curve number	35	98	80 (cultivated) 65 (urban) 70 (forest)
Parameters used to calibrate sediment					
File	Parameter	Definition	Min.Value	Max.Value	Calibrated value
*.bsn	PRF	Peak rate adjustment factor for sediment routing	0	2	0.58
*.rte	CH_COV	Channel cover factor	-0.001	1	1
*.rte	CH_EROD	Channel erodibility factor	-0.05	0.6	0.0001
*.bsn	SPCON	Linear parameters for calculating the channel sediment routing	0.0001	0.01	0.01
*.bsn	SPEXP	Exponent parameter for calculating the channel sediment routing	1	2	2

For the calibrated parameter set, the model predicted that mean annual rainfall for the total simulation period over the area of the catchment (726 mm) is mainly removed through evapotranspiration ET (78.3%), percolation/groundwater recharge (14.1%) and transmission loss/abstraction (0.5%), yielding surface runoff of 7.1%. The computed water balance components indicated rather high mean annual ET rates (78.3% of mean annual rainfall). This value is similar to the ET (72%) of an agricultural catchment in an arid area in Tunisia studied by Ouessar et al. (2009). However, the groundwater recharge rate (14.1% of mean annual rainfall) of the Save catchment was lower than that of the Tunisian catchment (22%). This can be attributed to limitation of groundwater recharge by the Save catchment substratum, which is relatively impermeable due to its high clay content. Simulated mean total water yield for the whole simulation period amounted to 138 mm, which is comparable to the observed value

of 136 mm (1985-2008). In this large intensive agricultural catchment, most rainfall was evapotranspired throughout the year.

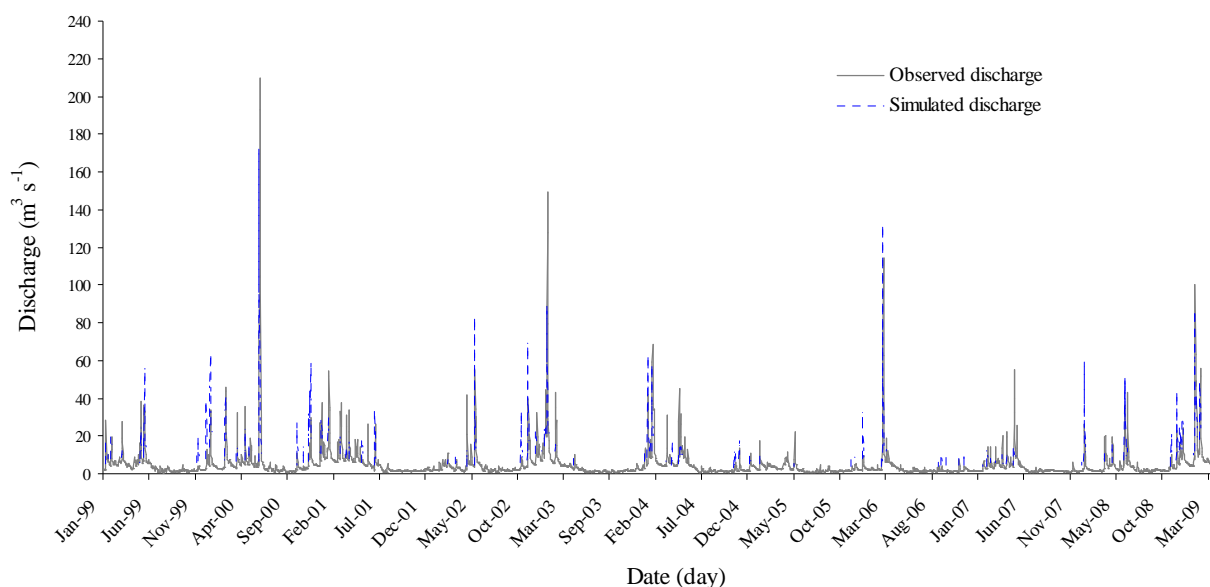


Figure 6-4. Observed and simulated daily discharge at Larra station (January 1999 to March 2009).

6.4.2. Suspended sediment simulation and yield

The observed values of suspended sediment were compared with simulated sediment values for the period January 2007-March 2009. Figure 6-5 shows observed and simulated discharge and observed and simulated suspended sediment concentration during the suspended sediment sampling period at Larra gauging station. Similar trends were found for observed and simulated sediment concentrations. During some floods in June 2007 and January 2008, there were no observed sediment data due to the damage of the sampling instrument. However, the simulated sediment was underestimated and overestimated during some flood events. The underestimation occurred for a flood event in June 2008 when rainfall intensity was extreme, resulting in severe sediment load transport (Oeurng et al., 2010). In practice, high-intensity and even short duration rainfall can generate more sediment than simulated by the model on the basis of daily rainfall (Xu et al., 2009). The statistical analysis showed reasonable agreement between observed and simulated daily values, with an R^2 value of 0.51 (excluding a few extreme observed concentrations). However, at the annual scale, the model predicted annual sediment yield which significantly matched the two years of observed sediment yield data at the outlet (Figure 6-6B).

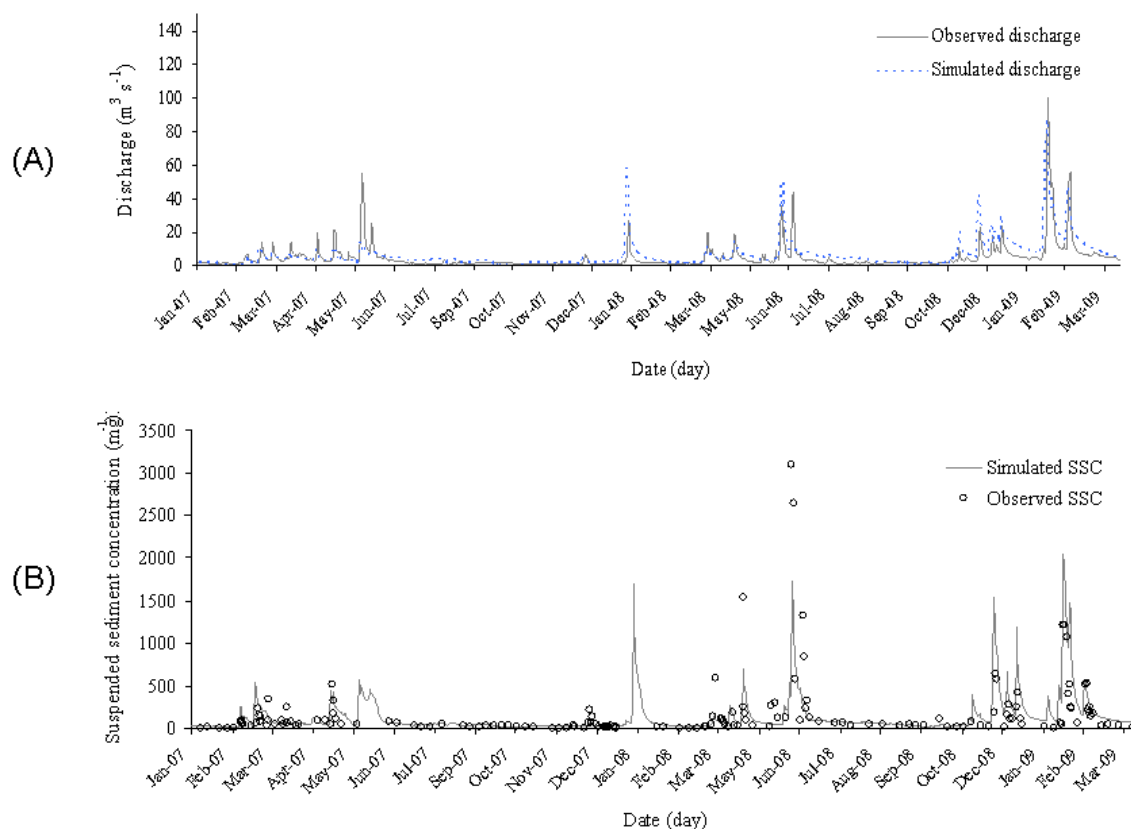


Figure 6-5. Observed and simulated daily discharge (A) and observed and daily simulated suspended sediment concentration (B) at Larra sampling station (January 2007 to March 2009).

Oeurng et al. (2010) showed that one extreme flood event in June 2008 in the Save catchment yielded a sediment load of 63% of the annual sediment yield in 2008. This could indicate that SWAT might not be able to simulate high sediment transport flood events and those event-based models such as AGNPS and ANSWERS should be used instead of continuous simulation models such as SWAT (Xu et al., 2009). Benaman and Shoemaker (2005) analysed high flow sediment event data to evaluate the performance of the SWAT model in the 1178 km^2 Cannonsville catchment and concluded that SWAT tended to underestimate the loads for high loading events (greater than 2000 metric tons). The main disadvantage of SWAT is the very simplified suspended sediment routing algorithm as described in section 2.3.3. Furthermore, SWAT allows all soil eroded by runoff to reach the river directly, without considering sediment deposition remaining on surface catchment areas.

The simulated sediment yield of other years is also presented in Figure 6-6B. The annual sediment yield from the Save catchment showed great variability, ranging from 4766 t to

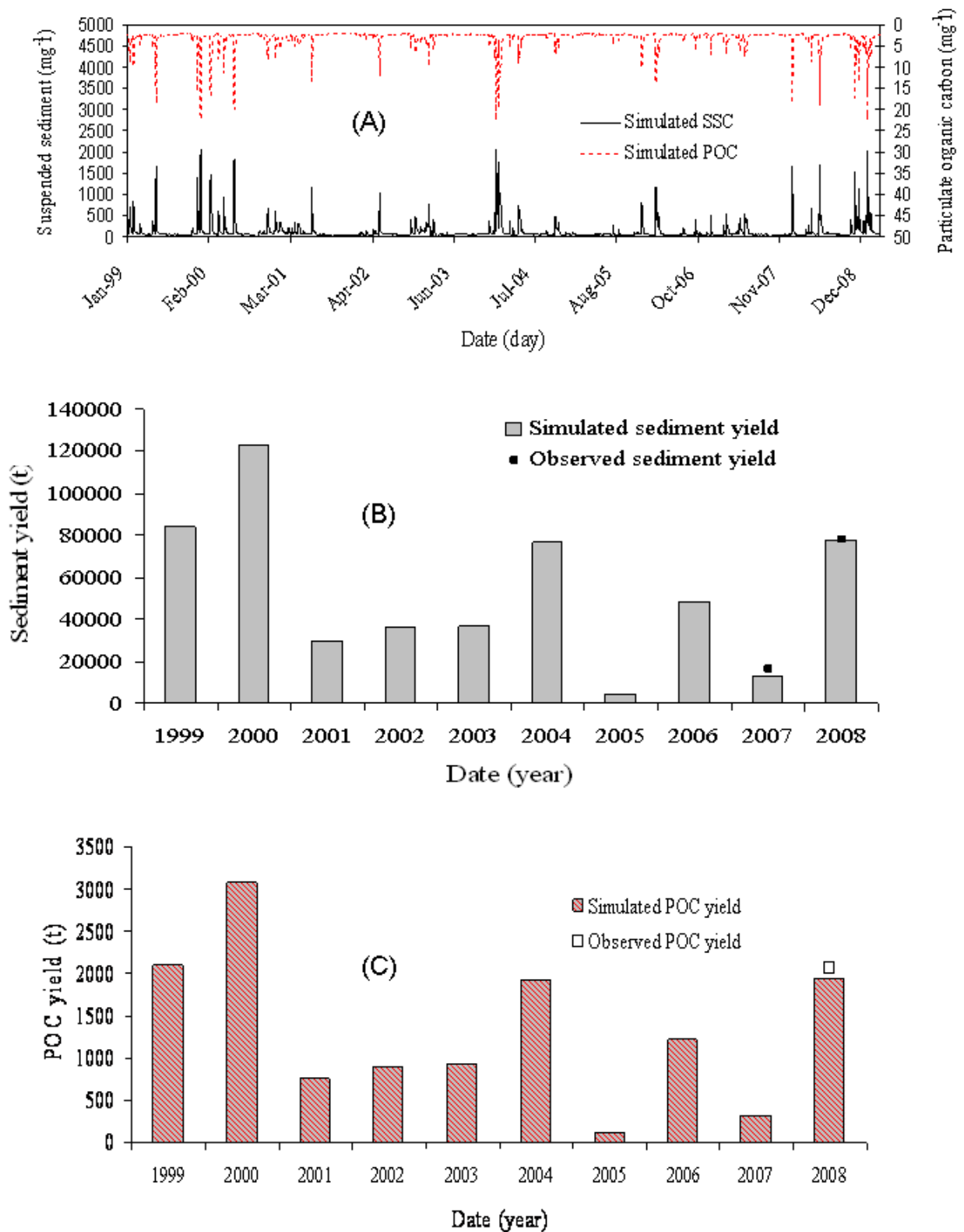


Figure 6-6. (A) Simulated daily suspended sediment concentration (SSC) and particulate organic carbon (POC) (January 1999-March 2009), (B) simulated annual sediment yield (1999-2008) and observed annual sediment yield (2007-2008) and (C) simulated annual particulate organic carbon yield (POC) (1999-2008) and observed annual POC yield (2008).

123000 t, representing a mean specific sediment yield of $48 \text{ t km}^{-2} \text{ y}^{-1}$. The sediment yield in 2000 was the highest of all simulated annual sediment yields and could be attributed to a major flooding period when daily maximum discharge reached $210 \text{ m}^3 \text{ s}^{-1}$. The lowest sediment yield occurred in the driest year (2005), when no major flood events were observed during the whole year. The great variability of sediment yield in the Save catchment mainly resulted from hydrological fluctuations from season to season and year to year. Oeurng et al. (2010) showed that hydro-climatological variables (total precipitation during flood event, flood discharge, flood duration, flood intensity and water yield) are the main factors controlling sediment load transport in the Save catchment. The annual sediment yield from the model was significantly correlated with annual water yield, with an R^2 value of 0.82 (Figure 6-7). Based on this strong regression, annual water yield could be used to estimate annual sediment yield for long-term periods within this catchment.

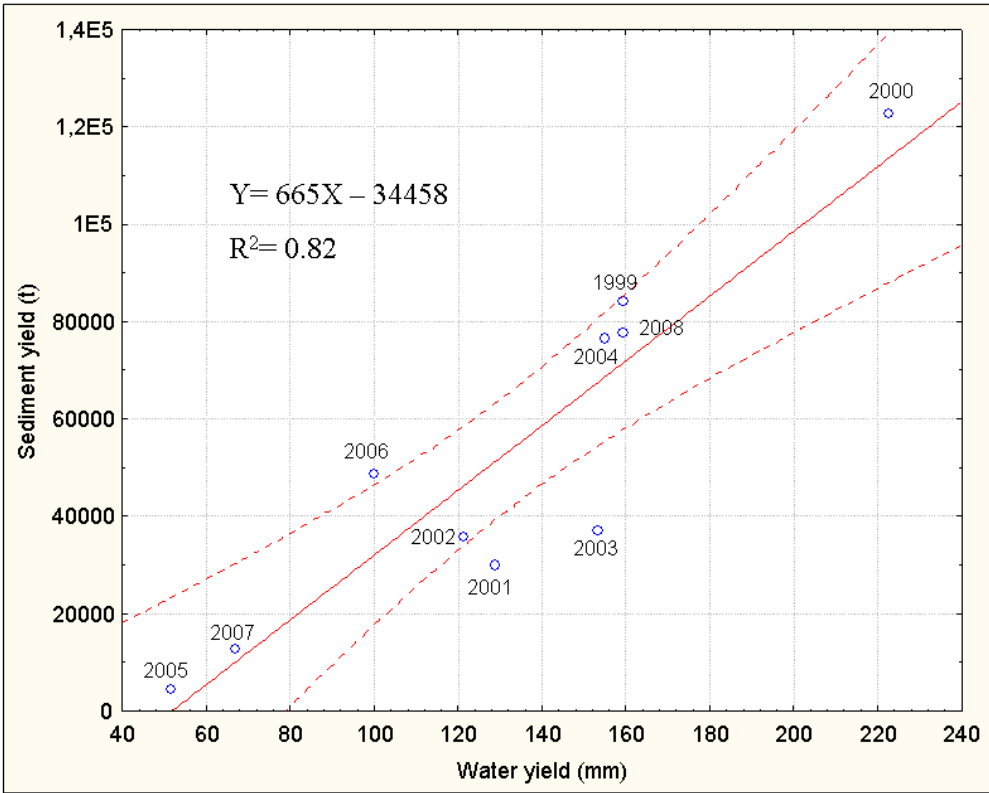


Figure 6-7. Regression between annual water yield and simulated annual sediment yield with 95% confidence interval for the Save catchment

The mean specific sediment yield of $48 \text{ t km}^{-2} \text{ y}^{-1}$ in the Save catchment is within the range reported for the Garonne River ($11\text{-}74 \text{ t km}^{-2} \text{ y}^{-1}$) by Coynel (2005). The 1330 km^2 Baïs catchment and the 970 km^2 Gers catchment, located in the same Gascogne region as the Save catchment and with the same climatic conditions, geology (molasse) and agricultural landuse, also have similar specific sediment yields (63 and $41 \text{ t km}^{-2} \text{ y}^{-1}$, respectively) (Maneux et al., 2001). The Save sediment yield is also similar to that of the 900 km^2 Tordera catchment ($50 \text{ t km}^{-2} \text{ y}^{-1}$) in north-east Spain (Rovira and Batalla, 2006), but much lower than the $414 \text{ t km}^{-2} \text{ y}^{-1}$ reported for the 445 km^2 Isábena catchment (Southern Central Pyrenees) which is highly erodible and experiences frequent floods (López-Tarazon et al., 2009).

6.4.3. POC simulation and yield

Based on the relationship between suspended sediment and particulate organic carbon ($R^2=0.93$), POC was computed from simulated suspended sediment data for the period January 1998-March 2009 (Figure 6-6A). The simulated annual POC yield ranged from 120 t to 3100 t (mean 1327 t; SD 916 t), representing a mean specific POC yield of $1.2 \text{ t km}^{-2} \text{ y}^{-1}$. The 2008 value of 1948 t was statistically similar to the observed annual value of 2060 t (Figure 6-6C). The annual POC yield showed strong variability due to the variability in sediment yield within the catchment. The average specific POC yield of 1.2 t km^{-2} in the Save catchment is similar to that of the Garonne River ($1.47 \text{ t km}^{-2} \text{ y}^{-1}$) (Veyssy et al., 1999) and that of other rivers in Europe (mean $1.10 \text{ t km}^{-2} \text{ y}^{-1}$) (Ludwig et al., 1996). However, it is lower than that of the Amazon River ($2.83 \text{ t km}^{-2} \text{ y}^{-1}$) (Richey et al., 1990).

6.4.4. Identification of critical areas of soil erosion

Using the total simulation results, it was possible to identify areas of significant soil erosion based on the average annual sediment yield for the total hydrological period within each sub-basin. The rate of soil erosion ranged from 0.10 to 6 t ha^{-1} (Figure 6-8). Among the 91 sub-basins within the catchment, numbers 91, 89, 88, 87, 83, 81 were identified as areas with serious soil erosion areas ($3.16 - 6 \text{ t ha}^{-1}$). These are several possible reasons for this. These sub-basins located at high upstream, have the steep slope and experience many major rainfall events, while downstream areas are mostly flat and experience fewer major rainfall events which impacted less soil erosion. Although the downstream areas are intensively cultivated, less soil erosion occurs there than in upstream areas, where high slope, tillage practices in pasture areas and major rainfall events are significant factors contributing to sediment

transport from the Save catchment. Therefore, appropriate strategies should be devised to protect these critical areas where soil erosion is most serious.

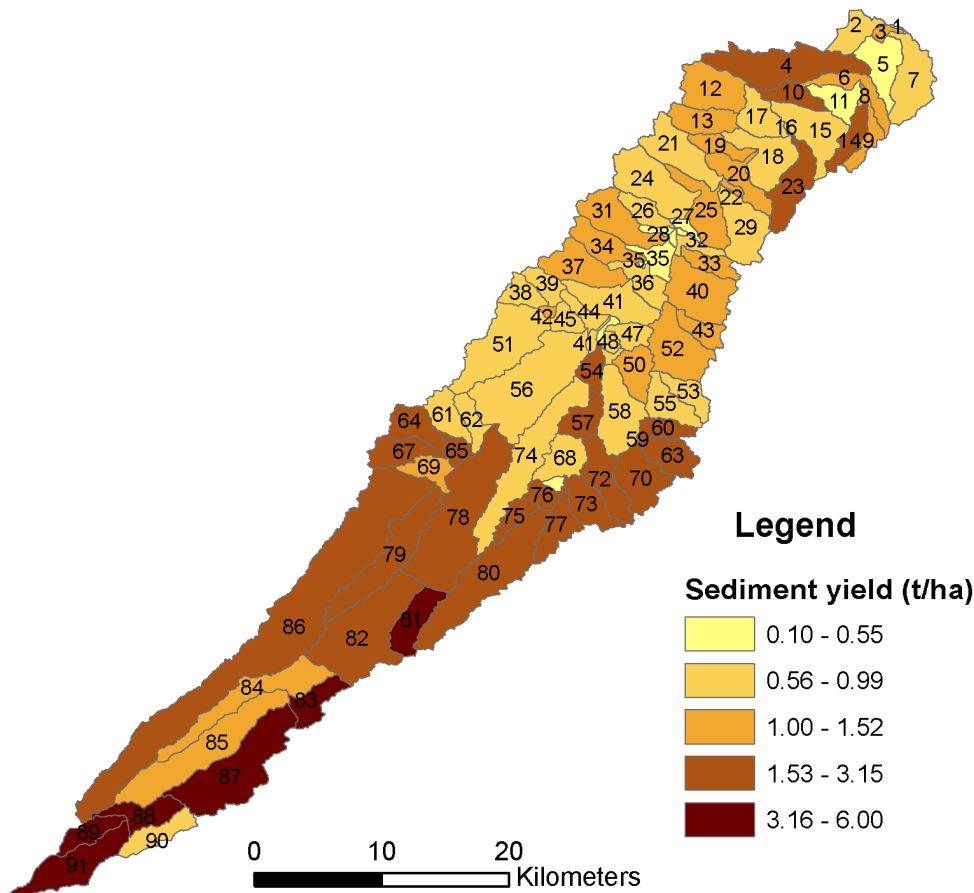


Figure 6-8. Simulated soil erosion within the 91 sub-basins, based on average sediment yield (1999-2008).

6.5. Conclusions

Parameterisation of the model to achieve good simulations of daily flow and sediment transport for long hydrological periods proved to be a laborious task in the Save agricultural catchment. The simulation of daily discharge was better than that of sediment transport. Although the model underestimated and overestimated daily discharge and suspended sediment for some flood events, predictions were within acceptable limits. The hydrological assessment showed that more than two-thirds of the total rainfall received was removed from the Save catchment as evapotranspiration. The water balance component in SWAT proved very useful for examining water management in the catchment, which is dominated by intensive agriculture. The simulated sediment yield at annual scale well matched the

measured sediment yield during the two-year study. The simulated mean total water yield for the whole simulation period amounted to 138 mm (observed value 136 mm) and annual sediment yield varied from 4766 t to 123000 t, representing a mean specific sediment yield of $48 \text{ t km}^{-2} \text{ y}^{-1}$. The annual yield of particulate organic carbon ranged from 120 t to 3100 t, representing a specific POC yield of $1.2 \text{ t km}^{-2} \text{ y}^{-1}$. A regression between annual water yield and simulated annual sediment yield was developed for this agricultural catchment. This relationship can be used for generating long-term sediment yield for the Save catchment in the future, reducing the need for expensive field work. Moreover, potential sources of erosion were also identified.

SWAT can be a useful tool for assessing hydrology and sediment yield over long-term periods. Based on historical flow and climate data, SWAT can generate sediment yield values, which are crucial in identifying past soil erosion patterns within a catchment. Prediction of discharge and soil losses is important for assessing soil degradation and for determining suitable landuse and soil conservation measures for a catchment. The results obtained can be used to mitigate environmental problems within intensively farmed agricultural catchments.

6.6. Acknowledgement

This research was financially supported by a doctoral research scholarship from the French government in cooperation with Cambodia. This work was performed within the framework of the EU Interreg SUDOE IVB program (SOE1/P2/F146 AguaFlash project, <http://www.aguaflash-sudoe.eu>) and funded by ERDF and Midi-Pyrénées Region. We sincerely thank the CACG for discharge data, Meteo France for meteorological data and Cemagref Bordeaux (UR ADBX) for landuse and soil data. The authors would like to thank ECOLAB staff for access to the site and assistance with monitoring instruments and technical support for modelling system.

6.7. References

- Arnold, J.G., Allen, P.M., 1996. Estimating hydrologic budgets for three Illinois watersheds. *Journal of Hydrology* 176 (1–4), 57–77.
- Arnold, J.G., Srinivasan, P., Muttiah, R.S., Williams, J.R., 1998. Large area hydrologic modeling and assessment. Part I. Model development. *Journal of American Water Resources Association* 34, 73–89.
- Bärlund, I., Kirkkala, T., Malve, O., Kämäri, J., 2007. Assessing SWAT model performance in the evaluation of management actions for the implementation of the Water Framework Directive in a Finnish catchment. *Environmental Modelling & Software* 22, 719–724
- Beasley, D.B., Huggins, L.F., Monke, E.J., 1980. ANSWERS: a model for watershed planning. *Transactions of the ASAE*, 938–944.
- Behera, S., Panda, R.K., 2006. Evaluation of management alternatives for an agricultural watershed in a sub-humid subtropical region using a physical process model. *Agriculture Ecosystem. Environment*. 113, 62–72.
- Benaman, J., Shoemaker, C.A., 2005. An analysis of high-flow sediment event data for evaluating model performance. *Hydrological Processes* 19, 605–620.
- Binger, R.L., Theurer, F.D., 2003. AnnAGNPS technical processes: documentation version 3. Available at <http://www.ars.usda.gov/Research/docs.htm>.
- Chow, V.T., Maidment, D.R., Mays, L.W. (Eds.). 1998. *Applied Hydrology*. McGrawHill, New York, USA.
- Coynel, A., 2005. Erosion mécanique des sols et transferts géochimiques dans le bassin AdourGaronne. Ph.D thesis, University of Bordeaux 1.
- Cunge, J.A., 1969. On the subject of a flood propagation method (Muskingum method). *Journal of Hydraulics Research* 7(2): 205-230
- Degens E.T., Kempe S., Spitzky A., 1984. A biogeochemical portrait. In: Hutzinger C.O. (ed.), *Handbook of Environmental Chemistry*. Springer-Verlag publisher, Berlin, pp. 127–215.
- Di Luzio, M., Srinivasan, R., Arnold, J.C., 2002. Integration of watershed tools and SWAT model into BASINS. *American Water Resource Association*, 38(4), 1127–1141.
- Donigian, A.S., Bicknell, B.R., Imhoff, J.C., 1995. Hydrological simulation program-Fortran (HSPF), chap. 12. In *Computer Models of Watershed Hydrology*, Singh VP (ed). Water Resources Publications: Colorado, USA, 395–442.
- Etcheber, H., Taillezm A., Abrilm G., Garnier, J., Servais, P., Moatarm F., Commarieu, M.V., 2007. Particulate organic carbon in the estuarine turbidity maxima of the Gironde, Loire and Seine estuaries: origin and lability. *Hydrobiologia* 558(1): 247–259.

Ewen, J., Parkin, G., O'Connell, P.E., 2000. SHETRAN: distributed river basin flow and transport modeling system. *Hydrologic Engineering* 5, 250–258.

Grunwald, S., Qi, C., 2006. GIS-based water quality modelling in the Sandusky watershed, Ohio, USA. *American Water Resource Association*. 42(4), 957–973.

Guirese, M., Revel, J.C., 1995. Erosion due to cultivation of calcareous clay soils on hillsides in south-west France. II. Effect of ploughing down the steepest slope. *Soil Tillage Research*. 35(3), 157–166.

Hanratty, M.P., Stefan, H.G., 1998. Simulating climate change effects in a Minnesota agricultural watershed. *Environmental Quality* 27(6), 1524–1532.

Hargreaves, G.H., Samani Z.A., 1985. Reference crop evapotranspiration from temperature. *Applied Engineering in Agriculture* 1, 96–99.

Heathwaite, A.L., Dils, R.M., Liu, S., Carvalho, L., Brazier, R.E., Pope, L., Hughes, M., Philips, G., May, L., 2005. A tiered risk-based approach for predicting diffuse and point source phosphorus losses in agricultural areas. *Science of the Total Environment* 344 (1-3), 225-239.

Kempe S., 1979. Carbon in the freshwater cycle. In: Bolin B., Degens E.T., Kempe S. and Ketner P. (eds), *The Global Carbon Cycle*. SCOPE Rep. 13. John Wiley, New York, pp. 317–342.

Koskiaho, J., Tattari, S., Bärlund, I., 2007. Assessment of hydrology and sediment transport and prospects of simulating agri-environmental measures with SWAT. 4th International SWAT conference Proceedings, UNESCO-IHE, Delft, The Netherlands July 4-6, 2007.

Knisel, W.G., 1980. CREAMS, a field scale model for chemicals, runoff, and erosion from agricultural management systems. USDA Conservation Research Report No. 26. Washington, D.C: USDA

Krause, P., Boyle, D.P., Bäse, F., 2005. Comparison of different efficiency criteria for hydrological model assessment. *Advances in Geosciences* 5, 83–87.

Lescot, J.M., Bordenave, P., 2009. A decision support to choose between changes of agricultural practices; A spatially distributed Cost-Effectiveness assessment framework. *Integrated Assessment of Agriculture and Sustainable Development, Setting the Agenda for Science and Policy; AgSAP Conference, 10-12/03/2009, Egmond aan Zee, NLD, 452 – 453.*

López-Tarazon, J.A., Batalla, R.J., Vericat, D, Francke T., 2009. Suspended sediment in a highly erodible catchment: The River Isábena (Southern Pyrenees). *Geomorphology* 109, 210–221.

Ludwig, W., Probst, J.L., Kempe, S., 1996. Predicting the oceanic input of organic carbon by continental erosion. *Global Biogeochemical Cycles* 10, 23–41.

- Ludwig, W., Probst, J.L., 1998. River sediment discharge to the oceans: Present-day controls and global budgets. *American Journal of Science* 298, 265–295.
- Macary, F., Lavie, E., Lucas, G., Riglos, O., 2006. Méthode de changement d'échelle pour l'estimation du potentiel de contamination des eaux de surface par l'azote. *Ingénieries - E A T*, 46, 35-49.
- Maneux, E., Probst, J.L., Veyssy, E., Etcheber, H., 2001. Assessment of dam trapping efficiency from water residence time: Application to fluvial sediment transport in the Adour, Dordogne, and Garonne River basins (France). *Water Resources Research* 37, 801–811.
- Meybeck, M., 1993. Riverine transport of atmospheric carbon: sources, global typology and budget. *Water Air Soil Pollution* 70, 443–463.
- Milliman, J.D., Syvitski, P.M., 1992. Geomorphic/tectonic control of sediment discharge to the ocean: the importance of small mountainous rivers. *Journal of Geology* 100, 525–544.
- Mishra, A., Kar, S., Singh, V.P., 2007. Determination of runoff and sediment yield from a small watershed in sub-humid subtropics using the HSPF model. *Hydrological Processes* 21, 3035–3045.
- Monteith, J.L., 1965. *Evaporation and the environment: in the state and movement of water in living organisms*. XIXth Symposium. Soc. For Exp. Biol., Swansea, Cambridge University Press, 205-234.
- Morgan, R.P.C., Quinton, J.N., Smith, R.E., Govers, G., Poesen, J.W.A., Auerswald, K., Chisci, G., Torri, D., Styczen, M.E., 1998. The European soil erosion model (EUROSEM): a dynamic approach for predicting sediment transport from fields and small catchments. *Earth Surface Processes and Landforms* 23, 527–544.
- Nash, J.E., Sutcliffe, J.V., 1970. River flow forecasting through conceptual models. Part I-a discussion of principles. *Journal of Hydrology* 10, 282–290.
- Neitsch, S.L., Arnold, J.G., Kiniry, J.R., Srinivasan, R., Williams, J.R., 2005. *Soil and Water Assessment Tool, Theoretical Documentation: Version 2005*. USDA Agricultural Research Service and Texas A&M Blackland Research Center: Temple.
- Nearing, M.A., Foster, G.R., Lane, L.J., Finkner, S.C., 1989. A process-based soil erosion model for USDA-water erosion prediction project technology. *Transactions of the ASAE* 32 (5), 1587– 1593.
- Oeurng C., Sauvage, S., Sanchez, J.M., 2010 (in press). Dynamics of suspended sediment transport and yield in a large agricultural catchment, southwest France. *Earth Surface Processes and Lanforms*.
- Ouessar, M., Bruggeman, A., Abdelli, F., Mohtar, R.H., Gabriels, D., Cornelis, W.M., 2009. Modelling water-harvesting systems in the arid south of Tunisia using SWAT. *Hydrology and Earth System Science* 13, 2003–2021.

- Pandey, A., Chowdary, V.M., Mal, B.C., Billib, M., 2008. Runoff and sediment yield modeling from a small agricultural watershed in India using the WEPP model. *Journal of Hydrology* 348 (3–4), 305–319.
- Priestley, C.H.B., Taylor, R.J., 1972. On the assessment of surface heat flux and evaporation using large scale parameters. *Mon. Weather Rev.* 100, 81–92.
- Revel, J.C., Guiresse, M., 1995. Erosion due to cultivation of calcareous clay soils on the hillsides of south west France. I. Effect of former farming practices. *Soil Tillage. Research.* 35(3), 147–155.
- Richey, J.E., Hedges, J.I., Devol, A.H., Quay, P.D., 1990. Biogeochemistry of carbon in the Amazon River. *Limnology Oceanography* 35, 352–371.
- Rovira, A., Batalla, R., 2006. Temporal distribution of suspended sediment transport in a Mediterranean basin: the Lower Tordera (NE Spain). *Geomorphology* 79, 58–71.
- Rostamian, R., Jalth, A., Afyuni, M., Mousavi, S.F., Heidarpour, M., Jalalian, A., Abbaspour, K.C., 2008. Application of a SWAT model for estimating runoff and sediment in two mountainous basins in central Iran. *Hydrological Science* 53(5), 977–988
- Setegn, S.G., Srinivasan, R., Dargahi, B., Melesse, A.M., 2009. Spatial delineation of soil vulnerability in the Lake Tana Basin, Ethiopia. *Hydrological Processes* 23, 3738–3750.
- Smith, R.E., 1981. A kinematic model for surface mine sediment yield. *Transactions of the ASAE*, 1508– 1514.
- USDA Soil Conservation Service., 1972. *National Engineering Handbook, Hydrology Section 4 (Chapters 4–10)*.
- Veyssy, E., Etcheber, H., Lin, R.G., Buat-Menard, P., Maneux, E., 1999. Seasonal variation and origin of Particulate Organic Carbon in the lower Garonne River at La Re´ole (Southwestern France). *Hydrobiologia* 391, 113–126.
- Williams, J.R., 1969. Flood routing with variable travel time or variable storage coefficients. *Transactions of the ASAE* 12(1): 100-103
- Williams, J.R., 1975. Sediment-yield prediction with universal equation using runoff energy factor. *Present and Prospective Technology for Predicting Sediment Yield and Sources: Proceedings of the Sediment Yield Workshop 1975, USDA Sedimentation Lab., Oxford, November 28–30, 1972. ARS-S-40. 244–252.*
- Winchell, M., Srinivasan, R., Di Luzio, M., Arnold J., 2007. *ArcSWAT Interface for SWAT User’s Guide*. Blackland Research Center, Texas Agricultural Experiment station and USDA Agricultural Research Service.
- Wischmeier, W.H., Johnson, C.B., Cross, B.V., 1971. A soil erodibility nomograph for farmland and construction sites. *Journal of Soil and Water Conservation* 26,189–193.

Xu, Z.X., Pang, J.P., Liu, C.M., Li, J.Y., 2009. Assessment of runoff and sediment yield in the Miyun Reservoir catchment by using SWAT model. *Hydrological Processes* 23, 3619–3630

Yang, J., Reichert, P., Abbaspour, K.C., Yang, H., 2007. Hydrological modelling of the Chaohe basin in China: statistical model formulation and Bayesian inference. *Journal of Hydrology* 340, 167–182.

Young, R.A., Onstad, C.A., Bosch, D.D., Anderson, W.P., 1989. AGNPS: a nonpoint-source pollution model for evaluating agricultural watersheds. *Journal of Soil and Water Conservation*, 168–173.

Chapter 7

General Discussion

This chapter provides the general discussion of the results from the chapter 4, 5 and 6 and the model.

7.1. SS, POC and DOC transport dynamics and modelling

The study of the suspended sediment and organic carbon transport collected at different temporal scales with high frequency of extensive dataset in the Save catchment provides an insight into the characteristics of the temporal variability in this agricultural catchment. Maximum SS, POC and DOC concentrations generally increased during high flood magnitudes particularly in spring, yielding SS, POC and DOC fluxes with strong variability. Increasing SS on the falling limb during floods may be related to sources of relatively more available sediment with lower soil aggregate stability. The variability in event sediment transport during successive peaks of similar magnitude is influenced by sediment exhaustion effects. The Save catchment shows a pattern similar to that observed in other catchments in the Mediterranean region, e.g. in the Tordera catchment (Rovira and Batalla, 2006). An example is the progressive reduction in suspended load at different temporal scales (within floods and within multiple-peak events, during a succession of events, and seasonally) related to the exhaustion of sediment availability. The role of in-channel sediment storage also controls suspended sediment dynamics during inter-flood periods of stable flow (Smith and Dragovich, 2008). Therefore, after a period of relatively high sediment transport (supply-rich floods), sediment becomes less and less available from the channel (exhaustion phenomenon) and sediment concentrations recorded during successive floods events are consequently lower (Walling, 1978). The two year study of suspended sediment transport revealed strong temporal variability (16 614 tonnes in 2007 and 77 960 tonnes in 2008) attributed to the hydro-climatic factors such as flood duration, rainfall intensity and flood amplitude, and other controlling factors related to soil conditions and agricultural practices in the Save catchment during both study years. The first hydrological year of the study (2007) was very dry, since there were very few rainfall events during autumn and less sediment was transported during floods with low duration and flood magnitude. Flood intensity is also a main factor to determine sediment transport. Flood events in 2008 were strong with high flood intensity. The maximum flood intensity in 2007 was only $1.27 \text{ m}^3 \text{ min}^{-2}$, while one event in spring 2008 exhibited the maximum flood intensity of $2.48 \text{ m}^3 \text{ min}^{-2}$, yielding a suspended sediment load of 63% of annual sediment yield in 2008. Sediment was slightly transported during summer due to low rainfall events.

DOC also showed strong variability in concentrations during all hydrological conditions. However, it transpired that the level of increase in flood discharge did not solely control the

increase in DOC concentration, as similar peaks in DOC were produced by different flood discharges. This is confirmed by the poor statistical relationship between maximum DOC and peak discharge ($R=0.31$). The temporal dynamic of DOC is very complex (Jones et al., 1996) and can be controlled not only by microbial activity in sediments (Bicudo et al., 1998) and also by variations in POC (Vervier et al., 1993; Jones et al., 1995). Regarding POC dynamics, POC% decreased while SS increased during high flood events. However, POC loads were also transported significantly during floods particularly in spring, attributed to high soil erosion from the catchment.

With only two years of data collection, it is difficult to understand temporal dynamics and to characterise inter-annual variability in a large agricultural catchment like the Save with the context of intensive agriculture due to strong seasonal and annual hydrological variations. Therefore, modelling approach using the SWAT model is very useful to understand long term temporal variability of suspended sediment transport and yield. The model predicted the annual sediment yield (1999-2008) varying from 4766 t to 123000 t, representing a mean specific sediment yield of $48 \text{ t km}^{-2} \text{ y}^{-1}$. During the 10 years of hydrological variations, the flux ratio between the maximum load and minimum load is 26 times, indicating a significant variability of sediment yield exporting from the Save catchment. POC concentration (1999-2008) was computed from the relationship between suspended sediment and POC. As POC is associated with sediment, annual POC fluxes also showed strong temporal variability ranging from 120 t to 3100 t, representing a mean specific POC yield of $1.2 \text{ t km}^{-2} \text{ y}^{-1}$.

The annual total specific sediment yields in the Save catchment (48 t km^{-2}) is within the range of specific yields reported for the Garonne River, which vary from 11 to $74 \text{ t km}^{-2} \text{ y}^{-1}$ (Coynel, 2005), but lower than the values for Mediterranean basins of the Iberian Peninsula (100 to $200 \text{ t km}^{-2} \text{ y}^{-1}$) reported by Walling and Webb (1996). Located in the same Gascogne region as the Save catchment, with the same climatic conditions, geology (molasse) and agricultural landuse, the 1330 km^2 Baïse catchment and the 970 km^2 Gers catchment have specific sediment yields (63 and $41 \text{ t km}^{-2} \text{ y}^{-1}$, respectively) that are of a similar order of magnitude to that of the Save catchment (Maneux et al., 2001). The value of specific POC yield ($1.2 \text{ t km}^{-2} \text{ y}^{-1}$) is comparable to the value range of the Garonne River of $1.47 \text{ t km}^{-2} \text{ y}^{-1}$ (Vessy et al., 1999) and also similar to the rivers in Europe with a mean of $1.10 \text{ t km}^{-2} \text{ y}^{-1}$ (Ludwig et al., 1996). However, this value is lower than Amazon River ($2.83 \text{ t km}^{-2} \text{ y}^{-1}$; Richey et al., 1990). Moreover, the value of the Save agricultural catchment is much lower

than that of the Nivelles River of $5.3 \text{ t km}^2 \text{ y}^{-1}$ (Coynel et al., 2005), draining a typical Pyrenean mountainous catchment, reaching the Bay of Biscay (Atlantic Ocean). The value of specific DOC yield ($0.7 \text{ t km}^{-2} \text{ y}^{-1}$) is 2.5 times higher than that of one Himalayan catchment which is also dominated by agriculture studied by Sharma and Rai (2004) due to landuse conservation which prevented soil and carbon loss within this Himalayan catchment. However, this value is much lower than the peatland catchments; for instance, a catchment in northeast Scotland with specific DOC yield of $16.9 \text{ t km}^2 \text{ y}^{-1}$ (Dawson et al., 2002). This value is common in peat dominated headwater catchments in the UK where soil carbon is the major source of organic carbon to the stream (Aithenhead et al., 1999; Dawson et al., 2001).

7.2. Agro hydrological modelling using the SWAT model

So far lots of models have been developed to study the soil erosion and sediment transport at catchment scale. These models were applied within the different catchment context. In agricultural environment, SWAT has been widely used for assessing water resources and water quality (sediment, nutrients and pesticides). SWAT is semi-distributed model which subdivides a catchment into different subbasins connected by a stream network, and further into hydrological response units (HRUs), which is a combination of the same soil, landuse and slope. The main advantage of HRUs enables to simplify the physical processes in order to integrate some empirical equations into the model such as SCS curve number method and MUSLE erosion/sediment equation. Furthermore, landuse types can be directly modified within the HRUs, which are useful to study the landuse change. SWAT offers many possibilities to take into account the adverse agricultural management practices (tillage, crop planting fertilizer and pesticides applications, irrigation, harvest/kill), water bodies (ponds, reservoirs, wetland etc.), point sources (urban, industries etc.), and exclusion of non-modelled zones. However, this simplification cannot well represent the natural systems into the model such as grid based processes.

7.2.1. Input data and sub-catchment delineation

SWAT requires lots of input data which is important to represent the spatial processes within the model. Basically, SWAT takes the climate data of the closest station to the centre of each subbasin to represent HRU where it is located. In our case, there are only 5 meteorological stations (two at the downstream and three at the upstream). It is therefore difficult to represent the rainfall specialisation at the middle catchment. Another difficulty is that there are only two stations which were used to simulate potential evapotranspiration (PET) since data is

unavailable for other stations. Chaplot et al. (2005) analyzed the effects of rain gauge distribution on SWAT output by simulating the impacts of climatic inputs for a range of 1 to 15 rain gauges in both the Walnut Creek catchment in central Iowa and the upper North Bosque River catchment in Texas. Sediment predictions improved significantly when the densest rain gauge networks were used.

Agricultural management practices and rotation of the crops were taken into account; however, in this study, only dominant landuse (pastures, winter wheat, and sunflower) and dominant soil type were taken into the model. This can decrease the spatial landuse and soil information and it can affect on erosion processes within the Save catchment. Bosch et al. (2004) found that SWAT streamflow estimates for a 22.1 km² tributary catchment of the Little River catchment in Georgia were more accurate using high resolution topographic, land use, and soil data versus low resolution data. In terms of sub-catchment delineation, many studies found that SWAT streamflow predictions were generally insensitive to variations in HRU and/or sub-catchment delineations for catchments ranging in size from 21.3 to 17 941 km² (Bingner et al., 1997; Manguerra and Engel, 1998; Fitz-Hugh and Mackay, 2000; Jha et al., 2004; Chen and Mackay, 2004; Tripathi et al., 2006; and Muleta et al., 2007). Tripathi et al. (2006) and Muleta et al. (2007) further discuss HRU and sub-catchment delineation impacts on other hydrologic components. Haverkamp et al. (2002) report that streamflow accuracy was much greater when using multiple HRUs to characterize each sub-catchment, as opposed to using just a single dominant soil type and land use within a sub-catchment, for two catchments in Germany and one in Texas. However, the gap in accuracy between the two approaches decreased with increasing numbers of sub-catchments.

7.2.2. Challenges in model calibration and evaluation

There are many parameters in the SWAT model; therefore, it is very challenging to calibrate the model. In this case, we can identify the sensitive parameters through manual calibration. SWAT calibration technique can be useful to calibrate the model. The experience on manual calibration is essential for applying auto calibration and sensitivity analysis.

In this study, lots of parameters associated with basin parameters and groundwater parameters were manually tested with maximum, minimum and mean values to assess their sensitivity within the model. The parameters related to the subbasins and the channels were also tested to evaluate the sediment response from the model. In our model calibration, CN is the most

sensitive parameter which played an important role in controlling surface runoff peak. However, the main disadvantage of the SCS method is that the amount of simulated runoff is not sensitive to rainfall intensity. Therefore, the method would compute the same amount of runoff, given the same amount of total rainfall, independent of event duration or the distribution of rainfall intensity during the event (Shen et al., 2009). This could affect the soil erosion resulting from high rainfall intensity during a short rainfall period. Furthermore, the assessment of hydrological and sediment yield modelling at only the Save catchment outlet can result in less representation of processes correctly. It is therefore necessary to consider more gauging stations along the main channel in order to calibrate/validate hydrology and sediment. Added to the difficulty of discharge calibration was possibly another disadvantage caused by inaccuracy of instantaneous discharge higher than $40 \text{ m}^3 \text{ s}^{-1}$ at Larra station, generated from the rating curve. Moreover, inaccurate daily discharge data from Neste canal to the Save catchment under water derivation during summer and winter period to sustain flow discharge in the Save river also contributes to the uncertainty for baseflow calibration.

The main disadvantage of SWAT is the very simplified suspended sediment routing algorithm as described in previous chapter. During the overflow in the river during high flooding period, SWAT could not simulate properly. The high underestimation of suspended sediment load was seen during a flood in early June 2008 when rainfall intensity during this flood was extreme (Oeurng et al., 2010). In practice, high-intensity and even short duration rainfall can generate more sediment than did the model based on daily rainfall (Xu et al., 2009). The model might not be able to daily simulate sediment transport during high sediment loading period; therefore, event-based models such as AGNPS and ANSWERS should be used instead of continuous simulation models such as SWAT (Xu et al., 2009). Benaman and Shoemaker (2005) evaluated the performance of the SWAT model in the 1178 km^2 Cannonsville catchment and concluded that SWAT tended to underestimate the sediment loads for high loading events (greater than 2000 metric tons). Moreover, SWAT does not properly take the bank erosion into account. A parameter (CH_COV) which can address the river bank conditions is only channel cover factor in the model. Through observation, the Save river also experienced bank collapse particularly during flood events, which could contribute more sediment export from this catchment.

At monthly or annual scale, SWAT could provide more satisfied results. For the Save catchment, the model is able to simulate well the two years of annual suspended sediment loads which had strong inter-annual variability in sediment yield. Kaur et al. (2004) also

concluded that SWAT predicted annual sediment yields reasonably well for a Nagwan catchment of 9.58 km² in India. Therefore, SWAT is the agro-hydrological model which is crucial for long-term assessment purposes.

Chapter 8

Conclusion and perspectives

This chapter is finalized by the conclusion summarizing the results of the research findings and remains some perspectives for future works.

8.1. Conclusion

The study of suspended sediment and organic carbon transport in an agricultural catchment provides the understanding of the transport dynamics and factors conditioning the transport processes. This work confirmed the key factors which control the suspended sediment and organic carbon transport. The measurement of sediment load, together with agro-hydrological modelling is crucial for soil and water conservation within the catchment.

Synthesis of research results:

The two year sampling at the Larra station in the Save River outlet enables to collect the interesting dataset. The sediment load during flood events from January 2007 to March 2009 varied from 177 t to 41 750 t. The annual sediment load transport in 2007 and 2008 ranged from 16 614 to 77 960 t (85% to 89 of annual load), which were transported during floods for 16 % to 20 % of annual duration. The organic carbon load during flood events (January 2008 to June 2009) varied from 12 t to 748 t for particulate organic carbon (POC) and from 9 t to 218 t for dissolved organic carbon (DOC). The total export of POC and DOC from the Save agricultural catchment amounted to 3 091 t and 1 238 t, representing the specific yields of 1.8 t km⁻² y⁻¹ and 0.7 t km⁻² y⁻¹, respectively.

The analysis of suspended sediment load during flood events could allow understanding the fundamental processes which result in sediment responses from the catchment. Within the context of water quality monitoring, the estimation of suspended sediment load is essential. Different sediment dynamics reflect different sediment availability from the catchment. The results of this study showed that the sediment and organic carbon transport in the Save catchment, varied significantly in time (infra-daily, seasonally and inter-annually). The role of spring floods impacted on sediment and organic carbon load transport, which considerably contributed to annual load, and could be explained mainly by the hydro-climatic factors. The application of statistical approach: correlations and Principle Component Analysis, could identify the hydro-climatic factors controlling SS, POC and DOC load transport from the Save catchment. Better correlations were found between total precipitation, flood discharge, water yield and SS, POC and DOC load transport, but no relationship with antecedent conditions. The hysteresis analysis at flood time scale with high data resolution enabled to estimate the sediment sources: 68% from river deposited sediments and nearby source area, 29% from distant source areas and simultaneity of SS and discharge 3%.

The two-year sampling could not explain the long-term variability but retrospective modelling would allow predicting the value range from different hydrological years. Despite the satisfactory results of sediment modelling at daily timestep, SWAT could wells simulation two years' annual sediment yield which were similar to the observed values. In this case, the model was essentially used to estimate long-term sediment yield, taking into account agricultural management practices and hydro-climatic conditions within the catchment. The modeling results showed that the simulated total water yield of 138 mm was close to the observed value of 136 mm for hydrological periods (1999-2008). During the whole simulation periods, the simulated annual sediment yield varied from 4 766 t to 123 000 t, representing a specific sediment yield of $48 \text{ t km}^{-2} \text{ y}^{-1}$ and simulated annual POC yield ranged from 120 t to 3 100 t, representing a specific POC yield of $1.2 \text{ t km}^{-2} \text{ y}^{-1}$. We used the model to reconstruct the past sediment chronic. According to this result, we could establish a good empirical correlation between annual water yield and annual sediment yield. Consequently, this relation is crucial to generate sediment yield by using only water yield. Furthermore, the potential areas of soil erosion were identified within the Save catchment. As a result, this could help characterize the sediment sources at the catchment scale. Therefore, SWAT was tested to evaluate catchment hydrology and long-term sediment yield, particularly in an agricultural catchment like the Save catchment.

8.2. Perspectives

This work remains several perspectives for future research. The data acquisition from more sampling points along the main river such as at the middle route should be considered in order to have better understanding of sediment and organic carbon dynamics within the Save catchment. These data would be also beneficial for model calibration/validation. The modelling project of the Save catchment using the SWAT model provides the possibilities to extend this work for other problematic concerning with modelling of nitrate and pesticide transport. Since particulate pesticide is associated with SS and POC, this work could contribute to the future study of pesticide transport in this agricultural catchment. These perspectives could be also oriented to study the impact of agricultural practice scenarios on sediment and contaminant transport at catchment scale. These works would be beneficial to the catchment manager in order to evaluate the impacts of agricultural practices, particularly to minimize soil erosion and reduce diffuse pollution from agriculture-dominated catchments. Moreover, it is interesting to focus on the role of climate change which can impact on sediment associated with contaminants transport at catchment scale.

Another research perspective would be to improve the sediment simulations by developing the model which can integrate the physical processes and distributed approach so as to better simulate the suspended sediment transport at daily time step until hourly time step. To answer this question, the development of the mechanistic MOHID model (<http://www.mohid.com/>) will be considered since the model takes into account the distributed and mechanic processes rather than the SWAT model. The MOHID model will include the erosion/deposition on the catchment into account and allows improving the simulation of sediment transport at different temporal scales. This type of the model could ameliorate the simulation from daily to hourly time scale, particularly flood time scale when a large of sediments associated with contaminants (pesticides, metals, particulate organic carbon) mobilize to the catchment outlet. Such a model would be indispensable for catchment manager to predict the water pollution and minimize these impacts.

The last research perspective from this work would be the SWAT model applications for other catchments in the future, particularly the catchments in Cambodia in order to better manage water resources and help the development of agriculture which is the indispensable sector of the country. When the agricultural activities start to significantly increase from year to year, soil erosion problems and diffuse pollutions resulting from agricultural practices would be key factors on surface water degradation. It is therefore to envisage the different scenarios of agricultural practices using the modelling approach such as SWAT or MOHID model so as to choose a better scenario in response to the context of sustainable development.

Conclusion générale

Ce travail a permis la récolte d'un jeu de données important sur 2 ans à la sortie d'un bassin versant agricole, sud-ouest de la France. Cette étude, sur le transport des matières en suspension et du carbone organique à l'échelle du bassin versant agricole, a permis de quantifier la dynamique du transport de ces matières et de comprendre les facteurs qui la conditionnent. Ce travail a donc confirmé ou précisé l'effet de plusieurs facteurs clefs qui contrôlent le transport des MES et du carbone organique. L'analyse des flux de MES à l'échelle de la crue permet de mettre en évidence les processus fondamentaux qui régissent le transfert des sédiments sur le bassin versant. Dans un contexte de suivi de la qualité de l'eau, le suivi des MES repose principalement sur l'estimation des flux de MES. Ces dynamiques de MES reposent sur des disponibilités en particules différentes. Le problème de la quantification des matières est lié à la grande variabilité spatiale et temporelle des concentrations et de flux de MES, fonction de l'événement hydrologique et des caractéristiques naturelles et/ou anthropiques du bassin. Les résultats de cette étude ont montré que le transport de MES et du carbone sur le bassin versant de la Save est très variable dans le temps (réponse infra journalière, saisonnière et interannuelle). Les flux annuels sont également très variables entre les années. Le rôle des crues saisonnières sur le flux de MES a montré que les crues de printemps étaient plus fortes que les autres, et transportent beaucoup de MES et de carbone par rapport au flux annuel, car elles sont liées principalement aux conditions hydro-climatiques. L'utilisation des approches statistiques, les statistiques de corrélations et l'Analyse en Composante Principale, a permis d'identifier les facteurs hydro-climatiques qui peuvent contrôler le transport de ces matières à l'échelle du bassin versant.

Les mesures réalisées durant deux ans n'ont pour l'instant pas permis de mettre en évidence une variabilité sur le long terme. Pour cela, l'utilisation de modèle permet de prédire les variations interannuelles pour les différentes années hydrologiques. Nous avons pour l'instant utilisé le modèle SWAT (<http://swatmodel.tamu.edu/>), calibré sur la période de mesure, pour reconstruire des chroniques passées des MES. A partir de ces simulations, on a pu établir la relation empirique entre le flux d'eau annuel et le flux annuel de MES sur le long terme. Cette relation est utile pour générer le flux de MES en n'utilisant que le flux d'eau. De plus, les zones potentielles de sources d'érosion ont été identifiées pour la Save. Cela permet de caractériser les sources de MES à l'échelle du bassin versant.

Ce travail ouvre un certain nombre de perspectives de recherche intéressantes. Les travaux de modélisation à l'aide du modèle SWAT sur la Save seront prolongés sur d'autres problématiques, concernant la modélisation du transfert des nitrates et des pesticides. Ces perspectives peuvent s'orienter notamment vers l'étude de l'impact de scénarios agricoles sur le transport de MES et d'autres contaminants vers l'exutoire du bassin versant. Ces travaux sont nécessaires pour les gestionnaires du bassin afin d'évaluer les impacts des pratiques agricoles, notamment pour minimiser l'érosion du sol et limiter les pollutions diffuses dans le bassin versant agricole. De plus, on s'intéresse également au rôle du changement climatique sur le transport des contaminants associés aux MES et des nutriments à l'échelle du bassin versant.

Enfin, ce travail a fait l'objet de 3 publications dont une publication acceptée et 2 publications soumises.

References

- Abaci O, Thanos Papnicolaou AN. 2009. Long-term effects of management practices on water-driven soil erosion in an intense agricultural sub-watershed: monitoring and modelling. *Hydrological Processes* **23**: 2818–2837
- Aitkenhead JA, Hope D, Billett MF. 1999. The relationship between dissolved organic carbon in streamwater and soil organic carbon pools at different spatial scales. *Hydrological Processes* **13**: 1289–1302.
- Aksoy H, Kavvas ML. 2005. A review of hillslope and watershed scale erosion and sediment transport models. *Catena* **64**: 247–271.
- Alan JD. 1995. Stream ecology: structure and function of running waters. Chapman & Hall, London.
- Arain R. 1987. Persisting trends in carbon and mineral transport monitoring of the Indus River. In: Degens, E. T., Kempe, S. and Gan Weibin (Eds) Transport of Carbon and Minerals in Major World Rivers, Pt. 4. Mitt. Geol.-Paläont. Inst. Univ. Hamburg, SCOPE/UNEP Sonderbd **64**: 417-21.
- Alexander RB, Smith RA. 1990. Country-level estimation of nitrogen and phosphorus fertilizer use in the United States, 1945 to 1985. *USGS Open File Report, Reston, VA, Australia*.
- Alexandrov Y, Laronne JB, Reid I. 2003a. Suspended sediment concentration and its variation with water discharge in a dryland ephemeral channel, northern Negev, Israel. *Journal of Arid Environments* **53**: 73–84.
- Alexandrov Y, Laronne JB, Reid I. 2003b. Suspended sediment transport in flash floods of the semiarid northern Negev, Israel. *IAHS Publication* **278**: 346–352.
- Arnold JG, Allen PM. 1996. Estimating hydrologic budgets for three Illinois watersheds. *Journal of Hydrology* **176** (1–4): 57–77.
- Arnold JG, Srinivasan P, Muttiah RS, Williams JR. 1998. Large area hydrologic modeling and assessment. Part I. Model development. *Journal of American Water Resources Association* **34**: 73–89.
- Asselman NEM. (1999). Suspended sediment dynamics in a large basin: the River Rhine. *Hydrological Processes* **13**: 1437–1450.
- Aumont O, Orr JC, Monfray P, Ludwig W, Amiotte-Suchet P, Probst JL. 2001. Riverine-driven interhemispheric transport of carbon. *Global Biogeochemical Cycles* **15**: 393–405.
- Bärlund I, Kirkkala T, Malve O, Kämäri J. 2007. Assessing SWAT model performance in the evaluation of management actions for the implementation of the Water Framework Directive in a Finnish catchment. *Environmental Modelling & Software* **22**: 719–724.

- Bauer JE, Druffel ERM. 1998. Ocean margins as a significant source of organic matter to the deep open ocean. *Nature* **46**: 1–10.
- Beasley DB, Huggins LF, Monke EJ. 1980. ANSWERS: a model for watershed planning. *Trans. ASAE* **23** (4): 938–944.
- Behera S, Panda RK. 2006. Evaluation of management alternatives for an agricultural watershed in a sub-humid subtropical region using a physical process model. *Agriculture Ecosystem Environment* **113**: 62–72.
- Benaman J, Shoemaker CA. 2005. An analysis of high-flow sediment event data for evaluating model performance. *Hydrological Processes* **19**: 605–620.
- Bernard C, Fabre A, Vervier P. 1994. DOC cycling in surface and ground waters interaction zone in a fluvial ecosystem. *Verh. int. Ver. Limnology* **25**: 1410–1413.
- Bicknell BR, Imhoff JC, Kittle JL Jr, Donigian AS Jr, Johanson RC. 1997. Hydrological Simulation Program–FORTRAN, User’s Manual for Release–11. EPA/600/R–97/080. USEPA Environmental Research Laboratory: Athens, GA.
- Bicudo DC, Ward AK, Wetzel RG. 1998. Fluxes of dissolved organic carbon within attached aquatic microbiota. *Verh. int. Ver. Limnology* **26**: 1608–1613.
- Binger RL, Theurer FD. 2003. AnnAGNPS technical processes: documentation version 3. Available at <http://www.ars.usda.gov/Research/docs.htm>.
- Bingner RL. 1996. Runoff simulated from Goodwin Creek watershed using SWAT. *Trans. ASAE* **39**(1): 85–90.
- Bosch DD, Sheridan JM, Batten HL, Arnold GC. 2004. Evaluation of the SWAT model on a coastal plain agricultural watershed. *Trans. ASAE* **47**(5): 1493–1506.
- Bowes MJ, House WA, Hodgkinson RA, Leach DV. 2005. Phosphorus discharge hysteresis during storm events along a river catchment: the River Swale. UK. *Water Research* **39** (5): 751–762.
- Braisington J, Richards K. 2000. Suspended sediment dynamics in small catchments in the Nepal Middle Hills. *Hydrological Processes* **14**: 2559–2574.
- Chanson H. 2004 (2nd edition). The Hydraulics of open channel flow: An introduction. 634 pages.
- Chaplot V, Saleh A, Jaynes DB. 2005. Effect of the accuracy of spatial rainfall information on the modeling of water, sediment, and NO₃-N loads at the watershed level. *Journal of Hydrology* **312**(1–4): 223–234.
- Chow VT, Maidment DR, Mays LW. (Eds.). 1998. Applied Hydrology. McGrawHill, New York, USA.

- Copper R, Thoss V, Watson H. 2007. Factors influencing the release of dissolved organic carbon and dissolved forms of nitrogen from a small upland headwater during autumn runoff events. *Hydrological Processes* **21**: 622–633.
- Coynel A, Etcheber H, Abril G, Maneux E, Dumas J, Hurtrez JE. 2005. Contribution of small mountainous rivers to particulate organic carbon input in the Bay of Biscay. *Biogeochemistry* **74**: 151–171.
- Coynel A. 2005. Erosion mécanique des sols et transferts géochimiques dans le bassin AdourGaronne. Ph.D thesis, University of Bordeaux 1.
- Crawford, CG. 1991. Estimation of Suspended–Sediment Rating Curves and Mean Suspended–Sediment Loads. *Journal of Hydrology* **129** (1–4): 331–348.
- Cunge JA. 1969. On the subject of a flood propagation method (Muskingum method). *Journal of Hydraulics Research* **7**(2): 205–230.
- Dawson, JC, Backwell C, Billett MF. 2001. Is within stream processing an important control on spatial changes in headwater carbon fluxes?. *Science of the Total Environment* **265**(1–3): 153–167.
- Dawson JC, Billet MF, Neil C, Hill S. 2002. A comparison of particulate, dissolved and gaseous carbon in two contrasting upland streams in the UK. *Journal of Hydrology* **257**: 226–246.
- Deasy C, Brazier RE, Heathwaite AL, Hodgkinson R. 2009. Pathways of runoff and sediment transfer in small agricultural catchments. *Hydrological Processes* **23**: 1349–1358.
- Degens ET, Kempe S, Spitzky A. 1984. A biogeochemical portrait. In: Hutzinger C.O. (ed.), *Handbook of Environmental Chemistry*. Springer–Verlag publisher, Berlin, pp. 127–215.
- Di Luzio M, Srinivasan R, Arnold JC. 2002. Integration of watershed tools and SWAT model into BASINS. *American Water Resource Association* **38**(4): 1127–1141.
- Dickinson A, Bolton A. 1992. A program of monitoring sediment transport in north central Luzon, the Philippines, Erosion and Sediment Transport Monitoring Programs in River Basins. *IHAS Publication* **210**: 483–492.
- Dinehart RL, Burau JR. 2005. Repeated surveys by acoustic Doppler current profiler for flow and sediment dynamics in a tidal river. *Journal of Hydrology* **314**(1–4): 1–21.
- Donigian AS, Bicknell BR, Imhoff JC. 1995. Hydrological simulation program–Fortran (HSPF), chap. 12. In *Computer Models of Watershed Hydrology*, Singh VP (ed). Water Resources Publications: Colorado, USA: 395–442.
- Downing J. 2005. *Environmental Instrumentation and Analysis Handbook*. Chapitre **24**: Turbidity monitoring, pp. 511–546. John Wiley and Sons.

- Echanhu D. 1988. Géochimie des eaux du bassin de la Garonne. Transfers de matières dissoutes et particulaires vers l'océan atlantique. Ph.D thesis, University of Paul Sabatier Toulouse III.
- Esser G, Kohlmaier, GH. 1989. Biogeochemistry of major work rivers, modelling terrestrial sources of nitrogen, phosphorous, sulphur and organic carbon to rivers, General Ecology Group, University of Freiburg, Germany.
- Estrany J, Garcia C, Batalla RJ. 2009. Suspended sediment transport in a small Mediterranean agricultural catchment. *Earth Surface Processes and Landforms* **34**: 929–940.
- Etcheber H. 1986. Biogéochimie de la matière organique en milieu estuarien: comportement, bilan, propriétés. Cas de le Gironde. Mem. Inst. Géologie Bassin Aquitaine., Talence, 379 pp.
- Etcheber H, Taillezm A, Abrilm G, Garnier J, Servais P, Moatarm F, Commarieu MV. 2007. Particulate organic carbon in the estuarine turbidity maxima of the Gironde, Loire and Seine estuaries: origin and lability. *Hydrobiologia* **558**(1): 247–259.
- Ewen J, Parkin G, O'Connel PE. 2000. SHETRAN: distributed river basin flow and transport modeling system. *Hydrologic Engineering* **5**: 250–258.
- Fenn CR, Gurnell AM, Beecroft IR. 1985. An Evaluation of the Use of Suspended Sediment Rating Curves for the Prediction of Suspended Sediment Concentration in a Proglacial Stream. *Geografiska Annaler. Series A, Physical Geography* **67** (1–2): 71–82.
- Ferguson RI. 1986. River loads underestimated by rating curves. *Water Resources Research* **22** (1): 74–76.
- Ferro V, Minacapilli M. 1995. Sediment delivery processes at basin scale. *Hydrological Sciences Journal – Journal des Sciences Hydrologiques* **40**(6): 703–717.
- Fiebig DM, Lock MA. 1991. Immobilization of dissolved organic matter from groundwater discharging through the stream bed. *Freshwater Biology* **26**: 45–55.
- FitzHugh TW, Mackay DS. 2000. Impacts of input parameter spatial aggregation on an agricultural non–point source pollution model. *Journal of Hydrology* **236**(1–2): 35–53.
- Flanagan DC, Nearing MA. 1995. USDA–Water Erosion Prediction Project: Hillslope Profile and Watershed Model Documentation. NSERL Report No. 10. USDA–ARS National Soil Erosion Research Laboratory, West Lafayette.
- Foster IDL, Chapman AS, Hodgkinson RA, Jones AR, Lees JA, Turner SE, Scott M. 2003. Changing suspended sediment and particulate phosphorus loads and pathways in underdrained lowland agricultural catchment; Herefordshire and Worcestershire, UK. *Hydrobiologia* **494**(1–3): 119–126.

- Fuhrer GL, Gilliom RJ, Hamilton PA, Morace JL, Nowell LH, Rinella JF, Stoner JD, Wentz DA. 1999. The quality of our nation's water: nutrients and pesticides, US Geological Survey Circular 1225, USA.
- Gafrej R. 1993. Modélisation conceptuelle du transfert des matières en suspension: effets d'échelles spatio-temporelles. Thèse de doctorat, Université de Paris 6.
- Galloway JN, Schlesinger WH, Levy H, Michaels A, Schnoor JL. 1995. Nitrogen fixation: anthropogenic enhancement – environmental response. *Global Biogeochemical Cycles* **9**: 235–252.
- Gao P, Pasternack GB, Bali KM, Wallender WW. 2007. Suspended-sediment transport in an intensively cultivated watershed in southeastern California. *Catena* **69**: 239–252.
- Gippel CJ. 1995. Potential of turbidity monitoring for measuring the transport of suspended solids in streams. *Hydrological Processes* **9**: 83–97.
- Goodwin TH, Young AR, Holmes GR, Old GH, Hewitt N, Leeks GJL, Packman JC, Smith BPG. 2003. The temporal and spatial variability of sediment transport and yields within the Bradford Beck catchment, West Yorkshire. *The Science of the Total Environment* 3114–3116: 475–494.
- Grunwald S, Qi C. 2006. GIS-based water quality modelling in the Sandusky watershed, Ohio, USA. *American Water Resource Association* **42**(4): 957–973.
- Guirese M, Revel JC. 1995. Erosion due to cultivation of calcareous clay soils on hillsides in south-west France. II. Effect of ploughing down the steepest slope. *Soil Tillage Research* **35**(3): 157–166.
- Hann MJ, Morgan RPC. 2006. Evaluating erosion control measures for bio restoration between the time of soil reinstatement and vegetation establishment. *Earth Surface Processes and Landforms* **31**: 589–597.
- Hanratty MP, Stefan HG. 1998. Simulating climate change effects in a Minnesota agricultural watershed. *Environmental Quality* **27**(6): 1524–1532.
- Hargreaves GH, Samani ZA. 1985. Reference crop evapotranspiration from temperature. *Applied Engineering in Agriculture* **1**: 96–99.
- Haritashya UK, Singh P, Kumar N, Gupta RP. 2005. Suspended sediment from the Gangotri Glacier: Quantification, variability and associations with discharge and air temperature. *Journal of Hydrology* **327** (1–2): 55–67.
- Harrison KW, Broecker W, Bonani G. 1993. A strategy for estimating the impact of CO₂ fertilization on soil carbon storage. *Global Biogeochemical Cycles* **7**: 69–80.

- Haverkamp S, Srinivasan R, Frede HG, Santhi C. 2002. Subwatershed spatial analysis tool: Discretization of a distributed hydrologic model by statistical criteria. *Journal of American Water Resources Association* **38** (6): 1723–1733.
- Heaney SI, Foy RH, Kennedy GJ, Crozier WW, O'Connor WC. 2001. Impacts of agriculture on aquatic systems: lessons learnt and new unknowns in Northern Ireland. *Marine and Freshwater Research* **52**: 151–163.
- Heathwaite AL, Dils RM, Liu S, Carvalho L, Brazier RE, Pope L, Hughes M, Philips G, May L. 2005. A tiered risk-based approach for predicting diffuse and point source phosphorus losses in agricultural areas. *Science of the Total Environment* **344** (1–3): 225–239.
- Heidel SG. 1956. The progressive lag of sediment concentration with flood waves. *Transactions – American Geophysical Union* **3**(1): 56–66.
- Hélie JF, Hillaire-Marcel C. 2006. Sources of particulate and dissolved organic carbon in the St Lawrence River: isotopic approach. *Hydrological Processes* **20**: 1945–1959.
- Hjulstrom F. 1935. Studies of the morphological activity of rivers as illustrated by river Fyris. *Bulletin of the Geological Institution* **25**: 221–455.
- Hoitink AJF, Hoekstra P. 2005. Observations of suspended sediment from ADCP and OBS measurements in a mud-dominated environment. *Coastal Engineering* **52**(2): 103–118.
- Holdaway GP, Thorne PD, Flatt D, Jones SE, Prandle D. 1999. Comparison between ADCP and transmissometer measurements of suspended sediment concentration. *Continental Shelf Research* **19** (3): 421–441.
- Hope D, Billet MF, Cresser MS. 1997. Exports of organic carbon from two river systems in NE Scotland. *Journal of Hydrology* **193**: 61–82.
- Horowitz AJ. 2003. An evaluation of sediment rating curves for estimating suspended sediment concentrations for subsequent flux calculations. *Hydrological Processes* **17** (17): 3387–3409.
- House WA, Warwick MS. 1998. Hysteresis of the solute concentration/discharge relationship in rivers during storms. *Water Research* **32** (8): 2279–2290.
- Hudson PF. 2003. Event sequence and sediment exhaustion in the lower Panuco Basin, Mexico. *Catena* **52**: 57–76.
- Itakura H, Kishi T. 1980. Open channel flow with suspended sediments. *Journal of the Hydraulics Division, ASCE* **106**: 1325–1343.
- Ittekkot V, Laane RW. 1991. Fate of riverine particulate organic matter. *Biogeochemistry of Major World Rivers*. SCOPE 42. John Wiley, New York: 233–242.

- Ittekkot V. 1988. Global trends in the nature of organic matter in river suspensions. *Nature* **332**: 436–438.
- Jansson MB. 2002. Determining sediment source areas in a tropical river basin, Costa Rica. *Catena* **47**: 63–84.
- Jha M, Gassman PW, Secchi S, Gu R, Arnold J. 2004. Effect of watershed subdivision on SWAT flow, sediment, and nutrient predictions. *Journal of American Water Resources Association* **40**(3): 811–825.
- Jones JB, Fisher SG, Grimm NB. 1996. A long-term perspective of dissolved organic carbon transport in Sycamore Creek, Arizona, U.S.A. *Hydrobiologia* **317**: 183–188.
- Jones, JB, Fisher SG, Grimm NB. 1995. Vertical hydrologic exchange and ecosystem metabolism in a Sonoran Desert stream. *Ecology* **76**: 942–952.
- Kalbitz K, Solinger S, Park JH, Michalzik B, Matzner E. 2000. Controls on the dynamics of dissolved organic matter in soils: A review. *Soil Science* **165**: 277–304.
- Kao SJ, Liu KK. 1997. Fluxes of dissolved and non fossil particulate organic carbon from an Oceania small river (Lanyang His) in Taiwan. *Biogeochemistry* **39**: 255–269.
- Kasai M, Marutani T, Reid L, Trustrum NA. 2001. Estimation of temporally average aged sediment delivery ration using aggradational terraces in headwater catchments of the Waipaoa River, North Island, New Zealand. *Earth Surface Processes and Landforms* **26**: 1–16.
- Kaur R, Singh O, Srinivasan R, Das SN, Mishra K. 2004. Comparison of a subjective and a physical approach for identification of priority areas for soil and water management in a watershed: A case study of Nagwan watershed in Hazaribagh District of Jharkhand, India. *Environmental Modelling Assessment* **9**(2): 115–127.
- Kazama S, Suzuki K, Sawamoto M. 2005. Estimation of rating-curve parameters for sedimentation using a physical model. *Hydrological Processes* **19**: 3863–3871.
- Kempe S. 1979. Carbon in the freshwater cycle. In: Bolin B, Degens ET, Kempe S. and Ketner P. (eds), *The Global Carbon Cycle*. SCOPE Rep. 13. John Wiley, New York, pp. 317–342.
- Kieber OJ, McDaniel J, Mopper K. 1989. Photochemical source of biological substrates in seawater: implication for carbon cycling. *Nature* **341**: 637–639.
- Kinnell PIA. 2003. Event erosivity factor and errors in erosion predictions by some empirical models. *Australian Journal of Soil Research* **41**: 991–1003.
- Klein M. 1984. Anti-clockwise hysteresis in suspended sediment concentration during individual storms. *Catena* **11**: 251–257.

- Knisel WG. 1980. CREAMS, a field scale model for chemicals, runoff, and erosion from agricultural management systems. USDA Conservation Research Report No. 26. Washington, D.C: USDA.
- Koskiaho J, Tattari S, Bärlund I. 2007. Assessment of hydrology and sediment transport and prospects of simulating agri–environmental measures with SWAT. 4th International SWAT conference Proceedings, UNESCO–IHE , Delft, The Netherlands July 4–6, 2007.
- Kostaschuk R, Best B, Villard P, Peakall J, Franklin M. 2005. Measuring flow velocity and sediment transport with an acoustic Doppler current profiler. *Geomorphology* **68**: 25–37.
- Kostrenzewski A, Stach A, Zwolinski Z. 1994. Transport of suspended load in the Parseta River during the flash flood of June 1988, Poland. *Geographia Polonica* **63**: 63–73.
- Krause P, Boyle DP, Bäse F. 2005. Comparison of different efficiency criteria for hydrological model assessment. *Advances in Geosciences* **5**: 83–87.
- Lee YH, Singh VP. 2005. Tank model for sediment yield. *Water Resources Management* **19**(4): 349–362.
- Lefrançois J, Grimaldi C, Gascuel–Odoux C, Gilliet N. 2007. Suspended sediment and discharge relationship to identify bank degradation as a main sediment source on small agricultural catchments. *Hydrological Processes* **21**: 2923–2933.
- Lenzi MA, Lorenzo M. 2000. Suspended sediment load during floods in a small stream of the Dolomites (northeastern Italy). *Catena* **39**: 267–282.
- Lescot JM, Bordenave P. 2009. A decision support to choose between changes of agricultural practices; A spatially distributed Cost–Effectiveness assessment framework. Integrated Assessment of Agriculture and Sustainable Development, Setting the Agenda for Science and Policy; AgSAP Conference, 10–12/03/2009, Egmond aan Zee, NLD: 452 – 453.
- Lewis J. 2003. Turbidity–controlled sampling for suspended sediment load estimation. In: Bogen J, Fergus T, Walling DE. (Eds.). Erosion and Sediment Transport Measurement in Rivers: Technological and methodological advances. Proc. Oslo Workshop, June 2002. *IAHS Publication* **283**: 13–20.
- Lin RG. 1988. Etude du potentiel de dégradation de la matière organique particulaire au passage eau douce–eau salée: Cas de l’estuaire de la Gironde. Thèse Doctorat no 218, Bordeaux 1: 196 pp.
- Littlewood IG. 1992. Estimating constituent loads in rivers: a review, Institute of Hydrology.

- López-Tarazon JA, Batalla RJ, Vericat D, Francke T. (2009). Suspended sediment in a highly erodible catchment: The River Isábena (Southern Pyrenees). *Geomorphology* **109**: 210–221.
- Lowett S, Price P. 1999. Riparian Land Management Technical Guidelines, Land and Water Resources Research and Development Corporation, Canberra.
- Lu H, Moran CJ, Prosser IP. 2006. Modelling sediment delivery ratio over the Murray Darling Basin. *Environmental Modelling and Software* **21**(9): 1297–1308.
- Ludwig W, Probst JL, Kempe S. 1996. Predicting the oceanic input of organic carbon by continental erosion. *Global Biogeochemical Cycles* **10**: 23–41.
- Ludwig W, Probst JL. 1998. River sediment discharge to the oceans: Present-day controls and global budgets. *American Journal of Science* **298**: 265–295.
- Macary F, Lavie E, Lucas G, Riglos O. 2006. Méthode de changement d'échelle pour l'estimation du potentiel de contamination des eaux de surface par l'azote. *Ingénieries – E A T*, **46** : 35–49.
- Maltby L. 1992. Detritus processing. In Calow, P. and Petts, G.E.(Eds), *The Rivers Handbook* Blackwell Scientific, Oxford.
- Maner SB. 1958. Factors influencing sediment delivery rates in the Red Hills physiographic area. *Transactions of the American Geophysical Union* **39**: 669–675.
- Maneux E, Probst JL, Veyssy E, Etcheber H. 2001. Assessment of dam trapping efficiency from water residence time: Application to fluvial sediment transport in the Adour, Dordogne, and Garonne River basins (France). *Water Resources Research* **37**: 801–811.
- Manguerra HB, Engel BA. 1998. Hydrologic parameterization of watersheds for runoff prediction using SWAT. *Journal of American Water Resources Association* **34**(5): 1149–1162.
- Martins O. 1982. Geochemistry of the Niger River. In: Degens, E. T. (Ed.) *Transport of Carbon and Minerals in Major World Rivers*, Pt. 1. Mitt. Geol.- Paläont. Inst. Univ. Hamburg, SCOPE/UNEP Sonderbd. **52**: 397-418.
- Marutani T, Kasai M, Reid LM, Trustrum NA. 1999. Influence of storm-related sediment storage on the sediment delivery from tributary catchments in the upper Waipaoa River, New Zealand. *Earth Surface Processes and Landforms* **24**: 881–896.
- McDowell WH, Likens GE. 1988. Origin, composition and flux of dissolved organic carbon in the Hubbard Brook valley. *Ecological Monograph* **58**: 177–195.
- McDowell WH. 2002. Connecticut River airshed-watershed consortium comprehensive scientific literature review of land surface-groundwater interface research. In partial fulfillment of the US Environmental Protection Agency Cooperation Agreement X-98145801, April 2002, USA.

- McHenry JR, Coleman NL, Willis AC, Sansom OW, Carrol BR. 1970. Effect of concentration gradients on the performance of a nuclear sediment concentration gage. *Water Resources Research* **6**(2): 538–548.
- Meybeck M, Vörösmarty C. 1999. Global transfer of carbon rivers. *Global Change News Letter* **37**: 18–20.
- Meybeck M. 1982. Carbon, nitrogen and phosphorus transport by World Rivers. *American Journal of Science* **282**: 401–450.
- Meybeck M. 1988. How to establish and use world budgets of riverine materials. In: Lerman, A. and Meybeck, M. (Eds) *Physical and Chemical Weathering in Geochemical Cycles*, Kluwer Academic Publishers, Dordrecht: 247-72.
- Meybeck M. 1993. Riverine transport of atmospheric carbon: sources, global typology and budget. *Water, Air and Soil Pollution* **70**: 443–463.
- Milliman JD, Syvitski PM. 1992. Geomorphic/tectonic control of sediment discharge to the ocean: the importance of small mountainous rivers. *Journal of Geology* **100**: 525–544.
- Minella JPG, Merten GH, Reichert JM, Clarke RT. 2008. Estimating suspended sediment concentrations from turbidity measurements and the calibration problem. *Hydrological Processes* **22**: 1819–1830.
- Mishra A, Kar S, Singh VP. 2007. Determination of runoff and sediment yield from a small watershed in sub-humid subtropics using the HSPF model. *Hydrological Processes* **21**: 3035–3045.
- Molot L, Dillon PJ. 1996. Storage of terrestrial carbon in boreal lake sediments and evasion to the atmosphere. *Global Biogeochemical Cycles* **10**: 483–492.
- Monteith JL. 1965. Evaporation and the environment: in the state and movement of water in living organisms. XIXth Symposium. Soc. For Exp. Biol., Swansea, Cambridge University Press, 205–234.
- Morel B, Durand P, Jaffrezic, Gruau G, Molenat J. 2009. Sources of dissolved organic carbon during stormflow in a headwater agricultural catchment. *Hydrological Processes* **23**: 2888–2901.
- Morgan RPC, Quinton JN, Smith RE, Govers G, Poesen JWA, Auerswald K, Chisci G, Torri, D, Styczen ME. 1998. The European soil erosion model (EUROSEM): a dynamic approach for predicting sediment transport from fields and small catchments. *Earth Surface Processes and Landforms* **23**: 527–544.
- Morgan RPC. 2005 (3rd edition). *Soil erosion and conservation*. 316 p.
- Mossa J. 1996. Sediment dynamics of the lowermost Mississippi River. *Engineering Geology* **45**: 457–479.

- Mou J, Meng Q. 1980. Sediment delivery ratio as used in the computation of the watershed sediment yield. *Chinese Society of Hydraulic Engineering: Beijing*.
- Muleta MK, Nicklow JW, Bekele EG. 2007. Sensitivity of a distributed watershed simulation model to spatial scale. *Journal of Hydrologic Engineering* **12**(2): 163–172.
- Nadal–Romero E, Latron J, Marti–Bono C, Regüés D. 2008. Temporal distribution of suspended sediment transport in a humid Mediterranean badland area: The Araguás catchment, Central Pyrenees. *Geomorphology* **97**: 601– 616.
- Nash JE, Sutcliffe JV. 1970. River flow forecasting through conceptual models. Part I—a discussion of principles. *Journal of Hydrology* **10**: 282–290.
- Nearing MA, Foster GR, Lane LJ, Finkner SC. 1989. A process–based soil erosion model for USDA–water erosion prediction project technology. *Transactions of the ASAE* **32** (5): 1587– 1593.
- Neff JC, Asner GP. 2001. Dissolved organic carbon in terrestrial ecosystems: synthesis and a model. *Ecosystems* **4**: 29–48.
- Neitsch SL, Arnold JG, Kiniry JR, Srinivasan R, Williams JR. 2005. Soil and Water Assessment Tool, Theoretical Documentation: Version 2005. USDA Agricultural Research Service and Texas A&M Blackland Research Center: Temple.
- Ni HG, Lu FH, Luo XL, Tian HY, Zeng YE. (2008). Riverine inputs of total organic carbon and suspended particulate matter from the Pearl River Delta to the coastal ocean off South China. *Marine Pollution Bulletin* **56**: 1150–1157.
- Oeurng C, Sauvage S, Sanchez JM. 2010. Dynamics of suspended sediment transport and yield in a large agricultural catchment, southwest France. *Earth Surface Processes and Landforms* **35**: 1289–1301.
- Orwin JF, Smart CC. 2004. The evidence for paraglacial sedimentation and its temporal scale in the deglaciating basin of Small River Glacier, Canada. *Geomorphology* **58**: 175–202.
- Ouassar M, Bruggeman A, Abdelli F, Mohtar RH, Gabriels D, Cornelis WM. 2009. Modelling water–harvesting systems in the arid south of Tunisia using SWAT. *Hydrology and Earth System Science* **13**: 2003–2021.
- Outeiro L, Úbedal X, Farguell J. 2010 (in press). The impact of agriculture on solute and suspended sediment load on a Mediterranean watershed after intense rainstorms. *Earth Surface Processes and Landforms*.
- Pandey A, Chowdary VM, Mal BC, Billib M. 2008. Runoff and sediment yield modeling from a small agricultural watershed in India using the WEPP model. *Journal of Hydrology* **348** (3–4): 305–319.

- Pawson RR, Lord DR, Evans MG, Allott THE. 2008. Fluvial organic carbon flux from an eroding peatland catchment, southern Pennines, UK. *Hydrology and Earth System Science* **12**: 625–634.
- Peart MR, Walling DE. 1982. Particle size characteristics of fluvial suspended sediment. Recent Developments in the Explanation and Prediction of Erosion and Sediment Yield. *IAHS Publication* **137**: 397–407.
- Phillips JM, Walling DE. 1995. Measurement in situ of the effective particle size characteristics of fluvial suspended sediment by means of a field portable laser backscatter probe: some preliminary results. *Maritime Freshwater Resources* **46**: 349–357.
- Picouet C, Hingray B, Olivry JC. 2009. Modelling the suspended sediment dynamics of a large tropical river: the Upper Niger River basin at Banankoro. *Hydrological Processes* **23**: 3193–3200.
- Pidwirny MJ. 2000. The carbon cycle, Ph.D. studies by Michael J. Pidwirny, Department of Geography, Okanagan University College, Canada.
- Pocklington R, Tan F. 1983. Organic carbon transport in the St. Lawrence River. In: Degens, E. T., Kempe, S. and Soliman, H. (Eds) Transport of Carbon and Minerals in Major World Rivers, Pt. 2. Mitt, Geol.-Paläont. Inst. Univ. Hamburg, SCOPE/UNEP Sonderbd. **55**: 243-52.
- Priestley CHB, Taylor RJ. 1972. On the assessment of surface heat flux and evaporation using large scale parameters. *Mon. Weather Rev.* **100**: 81–92.
- Probst JL. 1992. Géochimie et hydrologie de l'érosion continentale, Mécanismes, bilan global actuel et fluctuations au cours des 500 derniers millions d'années. *Science Géologie Bulletin Strasbourg* **94**: 1–161.
- Raymond PA, Bauer JE. 2001. Riverine export of aged terrestrial organic matter to the North Atlantic Ocean. *Nature* **409**: 497–500.
- Raymond PA. 2005. Carbon cycle, the age of the Amazon's breath. *Nature* **436**: 669–470.
- Renard KG, Foster GR, Weesies GA, McCool DK, Yoder DC. 1997. Predicting soil erosion by water: a guide to conservation planning with the revised universal soil loss equation (RUSLE). In *USDA Agriculture Handbook*. USDA: Blacksburg, VA; 703.
- Renard KG, Foster GR, Weesies GA, Porter JP. 1991. RUSLE: revised universal soil loss equation. *Journal of Soil and Water Conservation*: 30–33 (January–February).
- Renard KG, Foster GR, Yoder DC, McCool DK. 1994. RUSLE revisited: status, questions, answers, and the future. *Journal of Soil and Water Conservation*: 213–220 (May–June).

- Revel JC, Guiesse M. 1995. Erosion due to cultivation of calcareous clay soils on the hillsides of south west France. I. Effect of former farming practices. *Soil Tillage Research*. 35(3): 147–155.
- Ribeyeix–Claret C. 2001. Agriculture et Environnement en Gascogne Gersoise. Erosion du sol et pollution diffuse par phosphore. Le cas du bassin versant d’ Audradé (Gers). Ph.D thesis Université Toulouse II.
- Richards K. 1993. Sediment delivery and the drainage network. In *Channel Network Hydrology*, Beven K, Kirkby MJ (eds). John Wiley & Sons: Chichester.
- Richey JE, Salati E, Dos Santos U. 1985. Biochemistry of the Amazon River: an update. In: Degens, E. T., Kempe, S. and Herrera, R. (Eds) *Transport of Carbon and Minerals in Major World Rivers*, Pt. 3. Mitt, Geol.-Paläont. Inst. Univ. Hamburg, SCOPE/UNEP Sonderbd. 58 : 245-58.
- Richey JE, Hedges JI, Devol AH, Quay PD. 1990. Biogeochemistry of carbon in the Amazon River. *Limnology Oceanography* 35: 352–371.
- Risse LM, Nearing MA, Nicks AD, Laflen JM. 1993. Error assessment in the universal soil loss equation. *Soil Science Society of America Journal* 57: 825–833.
- Robertson AI, Boon PI, Bunn SE, Ganf GG, Hergceg AL, Hilman TJ, Walker KF. 1996. A scoping study into the role, importance, source, transportation and cycling of carbon in the riverine environment, Report to the Murray–Darling Basin Commission, Project R6067, MDBC, Canberra.
- Roehl JE. 1962. Sediment sources areas, delivery ratios and influencing morphological factors. *International Association of Hydrological Sciences Publication* 59: 202–213.
- Rosenfeld JS, Roff JC. 1992. Examination of the carbon base in southern Ontario streams using stable isotopes. *Journal of the North American Benthological Society* 11: 1–10.
- Rostamian R, Jalth A, Afyuni M, Mousavi SF, Heidarpour M, Jalalian A, Abbaspour KC. 2008. Application of a SWAT model for estimating runoff and sediment in two mountainous basins in central Iran. *Hydrological Science* 53(5): 977–988.
- Rovey EW, Woolhiser DA, Smith RE. 1977. A distributed kinematic model of upland watersheds. *Hydrology Papers*, vol. 93. Colorado State University, Fort Collins, CO.
- Rovira A, Batalla R. 2006. Temporal distribution of suspended sediment transport in a Mediterranean basin: the Lower Tordera (NE Spain). *Geomorphology* 79: 58–71.
- Sadar M. 2002. Turbidity instrumentation – An overview of today’s available technology. In *Turbidity and Other Sediment Surrogates Workshop*, Reno.
- Salant N, Hassan M, Alonso C. 2008. Suspended sediment dynamics at high and low storm flows in two small watersheds. *Hydrological Processes* 22: 1573–1587.

- Sarin MM, Sudheer AK, Balakrishna K. 2002. Significance of riverine carbon transport: A case study of a large tropical river. Godavari (India). *Science in China, series C* **45**: 97–108.
- Sayer AM, Walsh RPP, Bidin K. 2006. Pipeflow suspended sediment dynamics and their contribution to stream sediment budgets in small rainforest catchment, Sabah, Malaysia. *Forest Ecology and Management* **224**: 119–130.
- Schimel DS, Braswell BH, Holland EA, McKeown R, Ojima DS, Painter TH, Parton WJ, Townsend AR. 1994. Climate, edaphic, and biotic controls over storage and turnover of carbon in soils. *Global Biogeochemical Cycle* **8**(3): 279–293.
- Schmidt KH, Morche D. 2006. Sediment output and effective discharge in two small high mountain catchments in the Bavarian Alps, Germany. *Geomorphology* **80**: 131–145.
- Serrat P. 1999. Present sediment yield from a mediterranean fluvial system: the Agly River (France). *Comptes rendus de l'académie des sciences, Série II Fascicule A : Sciences de la Terre et des Planètes* **329** (3) : 189–196.
- Setegn SG, Srinivasan R, Dargahi B, Melesse AM. 2009. Spatial delineation of soil vulnerability in the Lake Tana Basin, Ethiopia. *Hydrological Processes* **23**: 3738–3750.
- Sharma P, Rai SC. 2004. Streamflow, sediment and carbon transport from a Himalayan watershed. *Journal of Hydrology* **289**: 190–203.
- Shen ZY, Gong YW, Li YH, Hong Q, Xu L, Liu RM. 2009. A comparison of WEPP and SWAT for modelling soil erosion of the Zhangjiachong watershed in the three Gorges Reservoir Area. *Agricultural Water Management* **96**: 1435–1442.
- Shibata R, Mitsunashi H, Miyake Y, Nakano S. 2001. Dissolved and particulate carbon dynamics in a cool-temperate forested basin in northern Japan. *Hydrological Processes* **15**: 1817–1828.
- Shields A. 1936. Anwendung der Ähnlichkeitsmechanik und der Turbulenzforschung auf die Geschiebebewegung. *Mitteilungen der Preussischen Anstalt Wasserbau and Schiffbau* **26**.
- Sickingabula HM. 1998. Factors controlling variations in suspended sediment concentration for single-valued sediment rating curves, Fraser River, British Columbia, Canada. *Hydrological Processes* **12**: 1869–1894.
- Smith HG, Drogovich D. 2008. Sediment budget analysis of slope-channel coupling and in-channel sediment storage in an upland catchment, south-eastern Australia. *Geomorphology* **101**: 643–654.

- Smith HG. 2008. Estimation of suspended sediment loads and delivery in an incised upland headwater catchment, south-eastern Australia. *Hydrological Processes* **22**: 3135–3148.
- Smith RE. 1981. A kinematic model for surface mine sediment yield. *Transactions of the ASAE*: 1508– 1514.
- Smith SV, Renwick WH, Buddenmeier RW, Crossland CJ. 2001. Budgets of soil erosion and deposition for sediment and sedimentary organic carbon across the conterminous United States. *Global Biogeochemical Cycles* **15**: 697–707.
- Steegen A, Govers G, Nachtergaele J, Takken I, Beuselinck L, Poesen J. 2000. Sediment export by water from an agricultural catchment in the Loam Belt in central Belgium. *Geomorphology* **33**: 25–36.
- Steegen A, Govers G. 2001. Correction factors for estimating suspended sediment export from loess catchments. *Earth Surface Processes and Landforms* **26**: 441–449.
- Stutter MI, Langan SJ, Cooper RJ. 2008. Spatial contributions of diffuse inputs and within-channel processes to the form of stream water phosphorus over storm events. *Journal of Hydrology* **350** (3–4): 203–214.
- Sugawara M. 1995. The development of a hydrological model-tank. In *Time and the River*, Kite GW (ed). *Water Resources Publications*, Colorado: 201–258.
- Svoray T, Ben-Said S. 2010. Soil loss, water ponding and sediment deposition variations as a consequence of rainfall intensity and landuse: a multi-criteria analysis. *Earth Surface Processes and Landforms* **35**: 200–216.
- Syvitski JP, Morehead MD, Nicholson M. 1998. HYDROTREND: a climate-driven hydrologic-transport model for predicting discharge and sediment load to lakes or oceans. *Computer and Geosciences* **24** (1): 51–68.
- Tate KR, Scott NA, Parshotam A, Brown L, Wilde RH, Giltrap DJ, Trustrum NA, Gomez B, Ross DJ. 2000. A multi-scale analysis of a terrestrial carbon budget. Is New Zealand a source or sink of carbon? *Agriculture, Ecosystems and Environment* **82**: 229–246.
- Tazioli GS. 1981. 'Nuclear techniques for measuring sediment transport in natural streams-Examples from instrumented basins. *Proc., Erosion and sediment transport measurement*, International Association of Hydrological Sciences, Wallingford, U.K: 63–81.
- Thorne PD, Vincent CE, Hardcastle PJ, Rehman S, Pearson N. 1991. Measuring suspended sediment concentrations using acoustic backscatter devices. *Marine Geology, Amsterdam* **98**: 7–16.
- Thurman EM. 1985. *Organic Geochemistry of Natural Waters*. Martinus Nijhoff / Dr. W. Junk Publishers: Boston.

- Thiessen AH. 1911. Precipitation averages for large areas. *Monthly Weather Review* **39** : 1082– 1084.
- Townsend SA, Boland KT, Wrigley TJ. 1992. Factors contributing to a fish kill in the Australian wet/dry tropics. *Water Research* **26**: 1039–1044.
- Tripathi MP, Raghuwanshi NS, Rao GP. 2006. Effect of watershed subdivision on simulation of water balance components. *Hydrological Processes* **20**(5): 1137–1156.
- Trustrum NA, Gomez B, Page MJ, Reid LM, Hicks DM. 1999. Sediment production, storage and output: The relative role of large magnitude events in steepland catchments. *Z Geomorph. N.F., Suppl.–Bd.* **115**: 71–86.
- USDA Soil Conservation Service. 1972. National Engineering Handbook, Hydrology Section 4 (Chapters 4–10).
- Valero-Garcés BL, Navas A, Machín J, Walling D. 1999. Sediment sources and siltation in mountain reservoirs: a case study from the Central Spanish Pyrenees. *Geomorphology* **28**: 23–41.
- Van Rijn LC. 1984. Sediment transport part II: Suspended load transport. *Journal of Hydraulic Engineering, ASCE* **110** (11): 1613–1641.
- Van Sickle J, Beschta RL. 1983. Supply-based models of suspended sediment transport in streams. *Water Resources Research* **19**(3): 768–778.
- Verstraeten G, Poesen J. 2002. Regional scale variability in sediment and nutrient delivery from small agricultural catchments. *Journal of Environmental Quality* **31**: 870–879.
- Vervier P, Dobson M, Pinay P. 1993. Role of interaction zones between surface and ground waters in DOC transport and processing: considerations for river restoration. *Freshwater Biology* **29**: 275–284.
- Veyssy E, Etcheber H, Lin RG, Buat-Menard P, Maneux E. 1999. Seasonal variation and origin of Particulate Organic Carbon in the lower Garonne River at La Re´ole (Southwestern France). *Hydrobiologia* **391**: 113–126.
- Veyssy E. 1998. Transfers des mati`eres organiques des bassins versants aux estuaires. Ph.D thesis, University of Bordeaux 1.
- Viney NR, Sivapalan M. 1999. A conceptual model of sediment transport: application to the Avon River Basin in Western Australia. *Hydrological Processes* **13**: 727–743.
- Walker KF, Boulton AJ, Thom MC, Sheldom F. 1994. Effects of water-level changes induced by weirs on the distribution of littoral plants along the River Murray, South Australia. *Australian Journal of Marine and Freshwater Research* **45**: 1421–1438.
- Walling DA, Webb BW. 1996. Erosion and sediment yield: a global overview. *IAHS Publication* **236**: 3–19.

- Walling DE, He Q. 1999. Improved models for estimating soil erosion rated from 137Cs measurements. *Journal of Environmental Quality* **28**: 611–622.
- Walling DE, Webb BW. 1982. Sediment availability and the prediction of storm–period sediment yields. Recent development in the explanation and prediction of erosion and sediment yield. *IHAS Publication* **137**: 327–337.
- Walling DE. 1977. Assessing the accuracy of suspended sediment rating curves for a small basin. *Water Resources Research* **13**: 531–538.
- Walling DE. 1978. Suspend sediment and solute response characteristics of river Exe, Devon, England. In: Davidson–Arnott, R., Nickling, W. (Eds.), *Research in Fluvial Systems. Geoabstracts, Norwich*: 167–197.
- Walling DE. 1983. The sediment delivery problem. *Journal of Hydrology* **65**: 209–237.
- Walling DE, Webb BW. 1985. Estimating the discharge of contaminants to coastal waters by rivers: Some cautionary comments. *Marine Pollution Bulletin* **16**: 488–492.
- Walling DE, Webb BW. 1986. Solutes in river systems. In: Trudgill, S.T. (Ed.), *Solute Process*. John Wiley & Sons Ltd., Chichester, 251–320.
- Wallis PM, Hynes HB, Telang SA. 1981. The importance of groundwater in the transportation of allochthonous dissolved organic matter to the stream draining a small mountain basin. *Hydrobiologia* **79**: 77–90.
- Ward GM, Ward AK, Dahm CN, Aumen NG. 1994. Origin and formation of organic and inorganic particles in aquatic systems. In Wotton, R.S. (Ed), *The Biology of Particles in Aquatic Systems*. Lewis Publishers, Boca Raton, Florida.
- WBGU–German Advisory Council on Global Change. 1998. *Word in transition: ways towards sustainable management of freshwater resources*. Annual Report, Berlin, Heidelberg, Springer, New York.
- Welch NH, Allen PB. 1973. Field calibration and evaluation of a nuclear sediment gage. *Water Resources Research* **9**(1): 154–158.
- Williams GP. 1989. Sediment concentration versus water discharge during single hydrologic events in rivers. *Journal of Hydrology* **111**: 89–106.
- Williams JR. 1969. Flood routing with variable travel time or variable storage coefficients. *Transactions of the ASAE* **12**(1): 100–103.
- Williams JR, Berndt HD. 1972. Sediment yield computed with Universal equation. *Journal of the Hydraulics Division, American Society of Civil Engineers* **98**: 2087–2098.

- Williams JR. 1975. Sediment–yield prediction with universal equation using runoff energy factor. Present and Prospective Technology for Predicting Sediment Yield and Sources: Proceedings of the Sediment Yield Workshop 1975, USDA Sedimentation Lab., Oxford, November 28–30, 1972. *ARS–S–40*: 244–252.
- Williams JR. 1977. Sediment delivery ratios determined with sediment and runoff models. *International Association of Hydrological Sciences Publication* **122**: 168–179.
- Williams JR. 1982. Testing the Modified Universal Soil Loss Equation. Iri: Proceedings of the Workshop on Estimating Erosion and Sediment Yield on Rangelands. U.S. Department of Agriculture ARM–W–**26**: 157–161.
- Williams JR. 1995. The EPIC model. In: Singh, V.P. (Ed.), Computer Models of Watershed Hydrology. Water Resources Publications, Highlands Ranch, CO, pp. 909–1000.
- Winchell M, Srinivasan R, Di Luzio M, Arnold J. 2007. ArcSWAT Interface for SWAT User’s Guide. Blackland Research Center, Texas Agricultural Experiment station and USDA Agricul–tural Research Service.
- Wischmeier WH, Johnson CB, Cross BV. 1971. A soil erodibility nomograph for farmland and construction sites. *Journal of Soil and Water Conservation* **26**: 189–193.
- Wischemeier WH, Smith DD. 1978. Predicting rainfall erosion losses – A guide to conservation planning. USDA Agricultural Handbook **537**, 58pp.
- Wood S, Roxburgh SH, Mackey B, Woldendorp G. 2002. Assessing the carbon sequestration potential of managed forest: a case study in temperate Australian forest. Version 5, November 2002, CRC for carbon accounting, ANU, Canberra.
- Worrall F, Burt T. 2005. Predicting the future DOC flux from upland peat catchments. *Journal of Hydrology* **300**: 126–139.
- Worrall F, Reed M, Warburton J, Burt TP. 2003. Carbon budget for a British upland peat catchment. *The Science of Total Environment* **312**: 133–146.
- Wotton RS. 1994. Particulate and dissolved organic matter as food. In Wotton, R.S. (Ed), The biology of particles in aquatic systems. Lewis Publishers, Boca Raton, Florida.
- Wren DG, Barkdoll BD, Kuhnle RA, Derrow RW. 2000. Field techniques for suspended–sediment measurement. *Journal of Hydraulic Engineering–ASCE* **126** (2): 97–104.
- Xu ZX, Pang JP, Liu CM, Li JY. 2009. Assessment of runoff and sediment yield in the Miyun Reservoir catchment by using SWAT model. *Hydrological Processes* **23**: 3619–3630.

- Yalin MS. 1977. Mechanics of sediment transport. Pergamon press, 298p.
- Yang J, Reichert P, Abbaspour KC, Yang H. 2007. Hydrological modelling of the Chaohe basin in China: statistical model formulation and Bayesian inference. *Journal of Hydrology* **340**: 167–182.
- Young RA, Onstad CA, Bosch DD, Anderson WP. 1989. AGNPS: a nonpoint–source pollution model for evaluating agricultural watersheds. *Journal of Soil and Water Conservation*: 168–173.
- Zabaleta A, Martínez M, Uriarte JA, Antigüedad U. 2007. Factors controlling suspended sediment yield during runoff events in small headwater catchments of the Basque Country. *Catena* **71**: 179–190.

Annexe 1

Measured data of suspended sediment concentrations (January 2007-June 2009)
and dissolved and particulate organic carbon concentrations
(January 2008-June 2009) in the Save catchment from

N	Samples	Field date	Real date	Hours	Vol (ml)	Filter (g)	Filter+SSC (g)	SSC (mg l⁻¹)
1	L1	15/02/2007	10/02/2007 19:29	19h29	740	0.0875	0.0957	11
2	L3	15/02/2007	12/02/2007 10:35	10h35	500	0.0782	0.092	28
3	L4	15/02/2007	12/02/2007 14:11	14h11	500	0.0808	0.1478	134
4	L5	15/02/2007	13/02/2007 07:04	7h04	500	0.084	0.1172	66
5	L7	15/02/2007	13/02/2007 14:38	14h38	400	0.0867	0.1313	112
6	L8	15/02/2007	14/02/2007 04:47	4h47	400	0.0819	0.1074	64
7	L1	28/02/2007	26/02/2007 06:37	6h37	500	0.0939	0.0977	8
8	L2	28/02/2007	26/02/2007 09:57	9h57	500	0.0759	0.0942	37
9	L3	28/02/2007	26/02/2007 15:27	15h27	400	0.0807	0.1007	50
10	L7	28/02/2007	26/02/2007 23:57	23h57	215	0.075	0.1145	184
11	L9	28/02/2007	27/02/2007 02:17	2h17	300	0.0764	0.146	232
12	L11	28/02/2007	27/02/2007 04:17	4h17	300	0.0822	0.1514	231
13	L1	07/03/2007	01/03/2007 07:42	7h42	400	0.0798	0.1354	139
14	L2	07/03/2007	02/03/2007 19:36	19h36	540	0.0769	0.1176	75
15	L1	14/03/2007	08/03/2007 19:40	19h40	500	0.0846	0.1169	65
16	L3	14/03/2007	08/03/2007 22:12	22h12	500	0.0874	0.1436	112
17	L6	14/03/2007	09/03/2007 03:10	3h10	400	0.0758	0.1641	221
18	L8	14/03/2007	09/03/2007 05:48	5h48	300	0.0811	0.1801	330
19	L10	14/03/2007	09/03/2007 12:10	12h10	300	0.0746	0.2024	426
20	L12	14/03/2007	09/03/2007 15:23	15h23	400	0.0885	0.2362	369
21	L1	21/03/2007	20/03/2007 16:49	16h49	500	0.079	0.1244	91
22	L1	04/04/2007	24/03/2007 21:28	21h28	500	0.0897	0.1201	61
23	L2	04/04/2007	25/03/2007 00:18	0h18	350	0.0904	0.144	153
24	L4	04/04/2007	25/03/2007 07:08	7h08	350	0.0886	0.1832	270
25	L5	04/04/2007	25/03/2007 14:58	14h58	300	0.0872	0.1986	371
26	L7	04/04/2007	25/03/2007 18:31	18h31	300	0.0896	0.1462	189
27	L8	04/04/2007	28/03/2007 02:38	2h38	500	0.0893	0.132	85
28	L9	04/04/2007	28/03/2007 02:41	2h41	500	0.0885	0.1234	70
29	L10	04/04/2007	02/04/2007 22:38	22h38	500	0.0887	0.1069	36
30	L1	03/05/2007	27/04/2007 12:20	12h20	950	0.0737	0.1634	94
31	L2	03/05/2007	01/05/2007 18:46	18h46	850	0.0758	0.1178	49
32	L8	03/05/2007	02/05/2007 10:32	10h32	275	0.0751	0.2154	510
33	L1	10/05/2007	03/05/2007 17:34	17h34	300	0.0845	0.1735	297
34	L2	10/05/2007	04/05/2007 03:44	3h44	300	0.0755	0.1264	170
35	L3	10/05/2007	06/05/2007 09:44	9h44	400	0.0876	0.1334	115
36	L1	06/12/2007	26/11/2007 22:28	22h28	250	0.091	0.2708	719

37	L2	06/12/2007	27/11/2007 14:28	14h28	500	0.0895	0.1045	30
38	L3	06/12/2007	28/11/2007 17:18	17h18	500	0.0924	0.0986	12
39	L1	12/12/2007	10/12/2007 14:56	14h56	500	0.0757	0.1068	62
40	L2	12/12/2007	11/12/2007 03:16	3h16	500	0.0747	0.1807	212
41	L1	19/12/2007	13/12/2007 12:59	12h59	500	0.0851	0.1526	135
42	L2	19/12/2007	16/12/2007 15:25	15h25	400	0.0806	0.0982	44
43	LARRA	09/01/2007	09/01/2007 09:30	9H30	500	0.0928	0.094	2
44	LARRA	15/01/2007	15/01/2007 13:00	13H00	500	0.0768	0.0813	9
45	LARRA	25/01/2007	25/01/2007 08:45	8H45	500	0.0812	0.0848	7
46	LARRA	01/02/2007	01/02/2007 15:45	15H45	500	0.0794	0.0802	2
47	LARRA	07/02/2007	07/02/2007 12:45	12H45	500	0.0828	0.0839	2
48	LARRA	15/02/2007	15/02/2007 09:00	9h	500	0.0913	0.1144	46
49	LARRA	21/02/2007	21/02/2007 09:40	9H40	500	0.09	0.1053	31
50	LARRA	28/02/2007	28/02/2007 09:40	9h40	400	0.0808	0.1431	156
51	LARRA	07/03/2007	07/03/2007 09:08	9H08	500	0.0765	0.0924	32
52	LARRA	14/03/2007	14/03/2007 16:15	16H15	500	0.0913	0.1132	44
53	LARRA	21/03/2007	21/03/2007 09:05	9H05	500	0.0806	0.1014	42
54	LARRA	04/04/2007	04/04/2007 08:55	8H55	500	0.0843	0.1092	50
55	LARRA	20/04/2007	20/04/2007 14:50	14H50	500	0.0752	0.1228	95
56	LARRA	03/05/2007	03/05/2007 13:30	13H30	500	0.0764	0.2535	354
57	LARRA	10/05/2007	10/05/2007 14:50	14H50	500	0.0902	0.1125	45
58	LARRA	24/05/2007	24/05/2007 15:05	15H05	500	0.0795	0.1027	46
59	LARRA	31/05/2007	31/05/2007 08:50	8H50	500	0.09	0.1721	164
60	LARRA	07/06/2007	07/06/2007 15:30	15H30	500	0.094	0.1495	111
61	LARRA	14/06/2007	14/06/2007 08:55	8h55	800	0.2043	0.2369	41
62	LARRA	21/06/2007	21/06/2007 08:45	8H45	500	0.0789	0.1153	73
63	LARRA	27/06/2007	27/06/2007 08:20	8h20	500	0.086	0.1169	62
64	LARRA	12/07/2007	12/07/2007 08:55	8h55	850	0.098	0.1242	31
65	LARRA	18/07/2007	18/07/2007 12:55	12h55	750	0.0995	0.1132	18
66	LARRA	26/07/2007	26/07/2007 15:00	15h	500	0.0873	0.0986	23
67	LARRA	06/08/2007	06/08/2007 21:55	21h55	700	0.0965	0.125	41
68	LARRA	24/08/2007	24/08/2007 09:28	9h28	750	0.0958	0.1215	34
69	LARRA	29/08/2007	29/08/2007 13:55	13h55	790	0.0992	0.1094	13
70	LARRA	07/09/2007	07/09/2007 09:25	9h25	750	0.0993	0.1168	23
71	LARRA	12/09/2007	12/09/2007 14:20	14H20	500	0.0849	0.0983	27
72	LARRA	19/09/2007	19/09/2007 09:05	9H05	500	0.092	0.1074	31
73	LARRA	26/09/2007	26/09/2007 09:24	9H24	500	0.087	0.1043	35
74	LARRA	02/10/2007	02/10/2007 09:25	9H25	500	0.0912	0.1074	32
75	LARRA	09/10/2007	09/10/2007 09:50	9H50	850	0.0999	0.1135	16
76	LARRA	17/10/2007	17/10/2007 09:50	9H50	500	0.092	0.102	20
77	LARRA	24/10/2007	24/10/2007 14:40	14H40	500	0.0903	0.097	13
78	LARRA	08/11/2007	08/11/2007 09:10	9H10	500	0.0923	0.0953	6
79	LARRA	14/11/2007	14/11/2007 11:35	11H35	500	0.0906	0.0937	6
80	LARRA	21/11/2007	21/11/2007 09:50	9h50	790	0.098	0.1024	6
81	LARRA	06/12/2007	06/12/2007 09:30	9H30	500	0.0906	0.0936	6

82	LARRA	12/12/2007	12/12/2007 09:30	9H30	500	0.0906	0.1255	70
83	LARRA	19/12/2007	19/12/2007 09:50	9H50	500	0.0862	0.0945	17
84	L1	09/01/2008	23/12/2007 18:04		450	0.0905	0.1	21
85	L2	09/01/2008	24/12/2007 00:10		460	0.0906	0.0975	15
86	L3	09/01/2008	25/12/2007 00:12		460	0.0891	0.0965	16
87	L4	09/01/2008	26/12/2007 12:44		460	0.0912	0.0985	16
88	L5	09/01/2008	27/12/2007 21:50		420	0.0901	0.094	9
89	L6	09/01/2008	28/12/2007 02:32		460	0.0895	0.0944	11
90	L7	09/01/2008	28/12/2007 20:15		460	0.0907	0.0952	10
91	L8	09/01/2008	29/12/2007 22:04		440	0.0894	0.1	24
92	L10	09/01/2008	31/12/2007 18:19		500	0.0884	0.094	11
93	L11	09/01/2008	02/01/2008 18:08		455	0.0883	0.0928	10
94	L12	09/01/2008	03/01/2008 14:16		470	0.0904	0.0941	8
95	LARRA	17/01/2008	17/01/2008 09:00	9h	490	0.0885	0.1243	73
96	LARRA	20/01/2008	20/01/2008 09:00		500	0.0931	0.0941	2
97	LARRA	23/01/2008	23/01/2008 09:00		430	0.0889	0.1117	53
98	LARRA	07/02/2008	07/02/2008 09:00	9h	600	0.0882	0.0954	12
99	LARRA	13/02/2008	13/02/2008 09:00		360	0.0899	0.0931	9
100	LARRA	27/02/2008	27/02/2008 09:00	9h	450	0.0888	0.0924	8
101	LARRA	05/03/2008	05/03/2008 09:00	9h15	450	0.0893	0.0927	8
102	LARRA	12/03/2008	12/03/2008 10:00	9h45	480	0.0898	0.0935	8
103	LARRA	19/03/2008	19/03/2008 09:50	9h45	470	0.0903	0.0945	9
104	LARRA	26/03/2008	26/03/2008 09:30	9h27	420	0.0896	0.1476	138
105	L1	26/03/2008	19/03/2008 16:33		450	0.0906	0.0932	6
106	L2	26/03/2008	19/03/2008 21:13		430	0.0885	0.0965	19
107	L3	26/03/2008	21/03/2008 18:13		300	0.0898	0.0938	13
108	L4	26/03/2008	23/03/2008 09:43		426	0.1267	0.1305	9
109	L5	26/03/2008	25/03/2008 23:43		455	0.0883	0.1062	39
110	L6	26/03/2008	26/03/2008 06:03		364	0.0758	0.1093	92
111	L1	02/04/2008	28/03/2008 10:19		240	0.0906	0.369	1160
112	L2	02/04/2008	28/03/2008 11:39		380	0.0895	0.1697	211
113	L3	02/04/2008	28/03/2008 12:39		320	0.0912	0.1975	332
114	L4	02/04/2008	28/03/2008 13:29		300	0.0904	0.1986	361
115	L5	02/04/2008	28/03/2008 14:09		200	0.0897	0.1661	382
116	L6	02/04/2008	28/03/2008 14:49		250	0.0899	0.1797	359
117	L7	02/04/2008	28/03/2008 15:39		234	0.0887	0.261	736
118	L8	02/04/2008	28/03/2008 16:49		300	0.0917	0.3053	712
119	L9	02/04/2008	28/03/2008 18:19		215	0.089	0.2282	647
120	L10	02/04/2008	28/03/2008 19:49		250	0.0894	0.3422	1011
121	LARRA	02/04/2008	02/04/2008 09:50	9h45	480	0.0911	0.1405	103
122	LARRA	03/04/2008	03/04/2008 12:40	12h45	445	0.09	0.14	112
123	LARRA	04/04/2008	04/04/2008 11:00		390	0.0913	0.1227	81
124	LARRA	05/04/2008	05/04/2008 13:30	13h30	480	0.0898	0.1125	47
125	LARRA	09/04/2008	09/04/2008 10:00	10h	470	0.0883	0.0982	21
126	LARRA	12/04/2008	12/04/2008 11:00		315	0.0886	0.1492	192
127	LARRA	14/04/2008	14/04/2008 16:50	16h15	695	0.0904	0.1145	35
128	LARRA	17/04/2008	17/04/2008 13:30	13h30	440	0.089	0.1001	25
129	LARRA	21/04/2008	21/04/2008 16:30	16h30	240	0.0892	0.4578	1536
130	LARRA	22/04/2008	22/04/2008 16:10	16h10	430	0.09	0.1951	244
131	LARRA	23/04/2008	23/04/2008 15:35	15h35	460	0.0923	0.1688	166
132	LARRA	24/04/2008	24/04/2008 15:50	15h50	500	0.0891	0.1366	95
133	LARRA	30/04/2008	30/04/2008 10:00	10h	480	0.0898	0.1051	32

134	LARRA	14/05/2008	14/05/2008 10:00		500	0.0913	0.0972	12
135	LARRA	21/05/2008	21/05/2008 10:00		450	0.0905	0.1482	128
136	LARRA	28/05/2008	28/05/2008 10:00		450	0.0893	0.1486	132
137	L1	21/05/2008	16/05/2008 11:45		400	0.087	0.1918	262
138	L2	21/05/2008	19/05/2008 20:39		447	0.0887	0.222	298
139	L1	05/06/2008	01/06/2008 09:28		214	0.0744	0.1227	226
140	L2	05/06/2008	01/06/2008 11:18		156	0.0741	0.1726	631
141	L4	05/06/2008	01/06/2008 13:48		226	0.074	0.4471	1651
142	L6	05/06/2008	01/06/2008 17:38		96	0.0758	1.5871	15743
143	L7	05/06/2008	01/06/2008 23:38		100	0.076	0.7821	7061
144	L12	05/06/2008	02/06/2008 04:08		112	0.0759	0.471	3528
145	L14	05/06/2008	02/06/2008 10:18		108	0.076	0.3815	2829
146	L15	05/06/2008	02/06/2008 11:28		140	0.0737	0.4817	2914
147	L16	05/06/2008	02/06/2008 23:38					4750
148	LARRA	04/06/2008	04/06/2008 09:30		220	0.077	0.6584	2643
149	LARRA	05/06/2008	05/06/2008 14:30		363	0.0768	0.2845	572
150	LARRA	10/06/2008	10/06/2008 11:00		490	0.0775	0.1244	96
151	LARRA	12/06/2008	12/06/2008 15:15		291	0.0774	0.4622	1322
152	LARRA	13/06/2008	13/06/2008 13:30	13h30	430	0.0768	0.436	835
153	LARRA	14/06/2008	14/06/2008 16:30		350	0.0768	0.1577	231
154	LARRA	15/06/2008	15/06/2008 16:00		353	0.076	0.189	320
155	LARRA	18/06/2008	18/06/2008 10:00		490	0.075	0.1392	131
156	LARRA	26/06/2008	26/06/2008 10:00		500	0.0752	0.1121	74
157	LARRA	03/07/2008	03/07/2008 10:00	10h	450	0.0887	0.1128	54
158	LARRA	09/07/2008	09/07/2008 09:40	9h40	500	0.0764	0.1075	62
159	LARRA	16/07/2008	16/07/2008 09:25	9h25	480	0.0745	0.1073	68
160	LARRA	23/07/2008	23/07/2008 10:00	10h	500	0.076	0.093	34
161	LARRA	08/08/2008	08/08/2008 09:55	9h55	500	0.0751	0.1001	50
162	LARRA	20/08/2008	20/08/2008 13:30	13h30	470	0.0743	0.0939	42
163	LARRA	04/09/2008	04/09/2008 09:40	9h40	470	0.076	0.0943	39
164	LARRA	12/09/2008	12/09/2008 09:45	9h45	490	0.0762	0.0972	43
165	LARRA	17/09/2008	17/09/2008 09:50	9h50	500	0.0749	0.0941	38
166	LARRA	24/09/2008	24/09/2008 09:00	9h	497	0.0763	0.0895	27
167	LARRA	08/10/2008	08/10/2008 11:45	11h45	480	0.075	0.1243	103
168	LARRA	15/10/2008	15/10/2008 09:55	9h55	480	0.0743	0.0833	19
169	LARRA	23/10/2008	23/10/2008 09:40	9h40	480	0.0742	0.084	20
170	LARRA	29/10/2008	29/10/2008 09:40	9h40	500	0.076	0.0879	24
171	LARRA	05/11/2008	05/11/2008 10:00	10h	500	0.0751	0.112	74
172	L1	07/11/2008	07/11/2008 02:54	2h54	240	0.0745	0.5521	1990
173	LARRA	12/11/2008	12/11/2008 09:40	9h40	500	0.0742	0.0903	32
174	LARRA	19/11/2008	19/11/2008 09:45	9h45	740	0.076	0.0878	16
175	L1	26/11/2008	24/11/2008 18:49		250	0.0752	0.1208	182
176	L2	26/11/2008	25/11/2008 01:09		250	0.0757	0.1535	311
177	L3	26/11/2008	25/11/2008 04:29		250	0.0763	0.214	551
178	L4	26/11/2008	25/11/2008 09:19		200	0.0742	0.2818	1038
179	L5	26/11/2008	26/11/2008 01:09		180	0.0749	0.2211	812
180	LARRA	26/11/2008	26/11/2008 09:00	9h40	204	0.0753	0.1427	330
181	LARRA	03/12/2008	03/12/2008 09:00	10h	500	0.0763	0.0843	16
182	LARRA	08/12/2008	08/12/2008 09:00	10h	410	0.075	0.117	102
183	L1	08/12/2008	06/12/2008 00:06		350	0.0765	0.1167	115
184	L2	08/12/2008	06/12/2008 04:48		350	0.0763	0.1419	187
185	L3	08/12/2008	07/12/2008 16:22		250	0.0738	0.1424	274

186	LARRA	10/12/2008	10/12/2008 10:00	10h	450	0.0745	0.1206	102
187	L1	18/12/2008	14/12/2008 18:24		200	0.089	0.1448	279
188	L2	18/12/2008	14/12/2008 21:51		200	0.0907	0.1319	206
189	L3	18/12/2008	15/12/2008 21:02		200	0.0891	0.1738	424
190	L4	18/12/2008	17/12/2008 07:11		200	0.0882	0.1088	103
191	LARRA	18/12/2008	18/12/2008 10:00	10h	480	0.0764	0.1003	50
192	LARRA	07/01/2009	07/01/2009 10:00	10h	500	0.089	0.0957	13
193	LARRA	14/01/2009	14/01/2009 10:00	10h	500	0.091	0.0943	7
194	L1	21/01/2009	20/01/2009 18:01		400	0.0895	0.1141	62
195	LARRA	21/01/2009	21/01/2009 09:00	10h	500	0.0906	0.1153	49
196	L1	27/01/2009	23/01/2009 04:46		200	0.0898	0.2428	765
197	L3	27/01/2009	23/01/2009 07:46		143.5	0.0882	0.2078	833
198	L5	27/01/2009	23/01/2009 09:46		150	0.0905	0.2387	988
199	L7	27/01/2009	23/01/2009 11:16		164	0.088	0.2571	1031
200	L9	27/01/2009	23/01/2009 12:46		144	0.0994	0.2955	1362
201	L11	27/01/2009	23/01/2009 14:56		142	0.1062	0.3004	1368
202	L13	27/01/2009	23/01/2009 20:06		154	0.0964	0.4244	2130
203	L14	27/01/2009	24/01/2009 08:36		175	0.12	0.3537	1335
204	L15	27/01/2009	24/01/2009 21:56		135	0.1003	0.2482	1096
205	L16	27/01/2009	26/01/2009 07:26		156	0.0935	0.2605	1071
206	LARRA	27/01/2009	27/01/2009 12:00	12h	250	0.09	0.1921	408
207	L1	04/02/2009	28/01/2009 05:50		240	0.01211	0.254	1008
208	L2	04/02/2009	28/01/2009 17:52		206	0.0986	0.1567	282
209	L3	04/02/2009	28/01/2009 20:31		250	0.1191	0.1822	252
210	L4	04/02/2009	29/01/2009 01:16		220	0.095	0.1519	259
211	L5	04/02/2009	29/01/2009 07:06		250	0.0997	0.1617	248
212	L6	04/02/2009	29/01/2009 16:05		250	0.0931	0.1598	267
213	L7	04/02/2009	29/01/2009 23:40		250	0.099	0.1577	235
214	L8	04/02/2009	30/01/2009 02:47		250	0.0921	0.1486	226
215	LARRA	04/02/2009	04/02/2009 09:00	9h	500	0.0923	0.1196	55
216	L1	11/02/2009	11/02/2009 07:45		200	0.0991	0.1575	292
217	L2	11/02/2009	11/02/2009 08:45		233	0.0951	0.1363	177
218	LARRA	11/02/2009	11/02/2009 10:00	10h	450	0.1006	0.1497	109
219	L1	18/02/2009	11/02/2009 10:45		220	0.101	0.1464	206
220	L2	18/02/2009	11/02/2009 11:40		250	0.0764	0.133	226
221	L3	18/02/2009	11/02/2009 12:46		213	0.0939	0.2447	708
222	L4	18/02/2009	11/02/2009 14:01		250	0.0757	0.2141	554
223	L5	18/02/2009	11/02/2009 15:35		228	0.095	0.2772	799
224	L6	18/02/2009	11/02/2009 17:39		200	0.0966	0.3017	1026
225	L7	18/02/2009	11/02/2009 20:51		220	0.1	0.3265	1030
226	L8	18/02/2009	12/02/2009 05:17		200	0.1057	0.2318	631
227	L9	18/02/2009	12/02/2009 19:13		250	0.0942	0.2003	424
228	L10	18/02/2009	13/02/2009 16:45		230	0.0764	0.1285	227
229	L11	18/02/2009	13/02/2009 20:53		250	0.0976	0.1501	210
230	L12	18/02/2009	13/02/2009 23:57		250	0.0759	0.1269	204
231	L13	18/02/2009	14/02/2009 02:26		250	0.0762	0.1263	200
232	L14	18/02/2009	14/02/2009 04:26		250	0.0747	0.127	209
233	L15	18/02/2009	14/02/2009 06:21		250	0.0744	0.1301	223
234	L16	18/02/2009	14/02/2009 08:37		250	0.0763	0.1315	221
235	L17	18/02/2009	14/02/2009 11:53		250	0.0739	0.129	220
236	L18	18/02/2009	14/02/2009 18:34		250	0.0761	0.1804	417
237	L19	18/02/2009	15/02/2009 01:34		250	0.0748	0.1252	202

238	L20	18/02/2009	15/02/2009 11:44		250	0.0752	0.1205	181
239	L21	18/02/2009	16/02/2009 05:44		250	0.0741	0.1101	144
240	L22	18/02/2009	18/02/2009 07:26		250	0.0752	0.1483	292
241	LARRA	18/02/2009	18/02/2009 10:00	10h	500	0.0744	0.0984	48
242	LARRA	25/02/2009	25/02/2009 10:00	10h	480	0.1219	0.1364	30
243	LARRA	03/03/02009	03/03/200910:00	10h	490	0.1279	0.1514	48
244	LARRA	12/03/2009	12/03/2009 10:00	10h	500	0.129	0.1409	24
245	LARRA	25/03/2009	25/03/2009 10:00	10h	750	0.1305	0.1408	14
246	LARRA	27/03/2009	27/03/2009 10:00	10h	750	0.1254	0.1342	12
247	L1	15/04/2009	12/04/2009 02:00		400	0.1312	0.2643	333
248	L2	15//04/2009	12/04/2009 05:00		350	0.1273	0.2265	283
249	L3	15//04/2009	12/04/2009 08:00		300	0.1271	0.2025	251
250	L4	15//04/2009	12/04/2009 11:00		300	0.1291	0.2465	391
251	L5	15//04/2009	12/04/2009 22:00		300	0.1257	0.2158	300
252	L6	15//04/2009	14/04/2009 04:00		300	0.1302	0.1954	217
253	L7	15//04/2009	14/04/2009 10:00		300	0.1282	0.183	183
254	L8	15//04/2009	14/04/2009 15:00		300	0.1256	0.1725	156
255	LARRA	15//04/2009	15/04/2009 10:00		300	0.1277	0.1562	95
256	L1	22/04/2009	20/04/2009 23:00		300	0.1254	0.2954	567
257	L2	22/04/2009	21/04/2009 00:00		300	0.1263	0.4428	1055
258	L3	22/04/2009	21/04/2009 01:00		250	0.1242	0.3364	849
259	L4	22/04/2009	21/04/2009 02:00		250	0.1256	0.3279	809
260	L5	22/04/2009	21/04/2009 03:00		200	0.1296	0.2792	748
261	L6	22/04/2009	21/04/2009 06:00		250	0.1276	0.2439	465
262	L7	22/04/2009	21/04/2009 10:00		160	0.1257	0.2218	601
263	L8	22/04/2009	21/04/2009 12:00		180	0.1262	0.259	738
264	L9	22/04/2009	21/04/2009 13:00		170	0.127	0.239	659
265	L10	22/04/2009	21/04/2009 14:00		160	0.1262	0.245	743
266	L11	22/04/2009	21/04/2009 15:00		180	0.1241	0.2689	804
267	L12	22/04/2009	21/04/2009 21:00		160	0.1266	0.2643	861
268	L13	22/04/2009	22/04/2009 08:00		180	0.127	0.2148	488
269	LARRA	22/04/2009	22/04/2009 10:00	10h	250	0.1255	0.213	350
271	LARRA	29/04/2009	29/04/2009	10h	350	0.1332	0.1765	124
272	L1	13/05/2009	29/04/2009 17:48		350	0.1286	0.2578	369
273	L2	13/05/2009	30/04/2009 06:15		300	0.1284	0.3106	607
274	L3	13/05/2009	01/05/2009 20:07		250	0.1251	0.2487	494
275	L4	13/05/2009	01/05/2009 23:21		350	0.1272	0.2354	309
276	L5	13/05/2009	02/05/2009 01:30		450	0.1239	0.21	191
277	L6	13/05/2009	02/05/2009 03:12		400	0.1275	0.2011	184
278	L7	13/05/2009	02/05/2009 04:43		450	0.1283	0.2046	170
279	L8	13/05/2009	02/05/2009 06:24		450	0.1262	0.2437	261
280	L9	13/05/2009	02/05/2009 08:38		250	0.1276	0.2641	546
281	L10	13/05/2009	02/05/2009 15:39		350	0.1252	0.2891	468
282	L11	13/05/2009	02/05/2009 17:04		235	0.1282	0.4094	1197
283	L12	13/05/2009	02/05/2009 18:35		250	0.1252	0.2973	688
284	L13	13/05/2009	02/05/2009 20:27		400	0.1292	0.3067	444
285	L14	13/05/2009	02/05/2009 23:23		250	0.1234	0.2954	688
286	L15	13/05/2009	03/05/2009 04:56		200	0.1269	0.329	1011
287	L16	13/05/2009	03/05/2009 14:29		220	0.1268	0.2561	588
288	L17	13/05/2009	05/05/2009 00:01		250	0.125	0.1995	298
289	L18	13/05/2009	10/05/2009 19:02		250	0.1255	0.1966	284
290	LARRA	13/05/2009	10h		500	0.1343	0.2058	143

291	L1	20/05/2009	15/05/2009 00:00		500	0.1326	0.143	21
292	L2	20/05/2009	15/05/2009 02:17		500	0.1351	0.2264	183
293	L3	20/05/2009	15/05/2009 04:31		500	0.1338	0.2115	155
294	L4	20/05/2009	15/05/2009 21:34		400	0.1341	0.2049	177
295	L5	20/05/2009	16/05/2009 14:23		300	0.1339	0.2238	300
296	LARRA	20/05/2009	20/05/2009 10:00		500	0.1318	0.1508	38
297	LARRA	27/05/2009	27/05/2009	10h	500	0.1334	0.1559	45
298	LARRA	03/06/2009	03/06/2009	10h	500	0.1313	0.1408	19
299	LARRA	10/06/2009	10/06/2009	10h	500	0.1316	0.1499	37
300	LARRA	17/06/2009	17/06/2009	10h	500	0.1327	0.1448	24
301	LARRA	24/06/2009	24/06/2009	10h	500	0.1312	0.1421	22

Measured data of dissolved and particulate organic carbon concentrations from January 2008- June 2009 in the Save catchment

N	Samples	Field date	Real date	DOC (mg l ⁻¹)	POC (%)	POC (mg l ⁻¹)
1	L11	09/01/2008	02/01/2008 18:08	2.00	7.98	0.64
2	L12	09/01/2008	03/01/2008 14:16	1.84	6.26	0.49
3	LARRA	17/01/2008	17/01/2008 09:00	1.89	2.64	1.47
4	LARRA	20/01/2008	20/01/2008 09:00	2.78	3.38	0.27
5	LARRA	23/01/2008	23/01/2008 09:00	3.17	2.39	1.32
6	LARRA	07/02/2008	07/02/2008 09:00	2.02	7.09	0.71
7	LARRA	13/02/2008	13/02/2008 09:00	1.63	4.42	0.46
8	LARRA	27/02/2008	27/02/2008 09:00	1.65	2.84	0.31
9	LARRA	05/03/2008	05/03/2008 09:00	1.70	3.98	0.28
10	LARRA	12/03/2008	12/03/2008 10:00	1.70	3.96	0.32
11	LARRA	19/03/2008	19/03/2008 09:50	1.69	2.38	0.27
12	LARRA	26/03/2008	26/03/2008 09:30	1.92	1.86	3.15
13	L1	26/03/2008	19/03/2008 16:33	2.15	2.04	0.13
14	L2	26/03/2008	19/03/2008 21:13	1.67	3.12	0.61
15	L3	26/03/2008	21/03/2008 18:13	1.66	3.21	0.43
16	L4	26/03/2008	23/03/2008 09:43	1.65	3.59	0.32
17	L5	26/03/2008	25/03/2008 23:43	1.65	3.35	0.89
18	L6	26/03/2008	26/03/2008 06:03	2.03	2.42	3.29
19	L1	02/04/2008	28/03/2008 10:19	3.66	2.08	21.73
20	L2	02/04/2008	28/03/2008 11:39	3.89	2.07	4.37
21	L3	02/04/2008	28/03/2008 12:39	4.22	2.07	6.01
22	L4	02/04/2008	28/03/2008 13:29	4.54	2.10	7.05
23	L5	02/04/2008	28/03/2008 14:09	3.66	2.16	9.51
24	L6	02/04/2008	28/03/2008 14:49	4.38	1.93	8.76
25	L7	02/04/2008	28/03/2008 15:39	3.87	1.87	9.85
26	L8	02/04/2008	28/03/2008 16:49	6.12	1.92	15.99
27	L9	02/04/2008	28/03/2008 18:19	3.21	1.87	17.94
28	L10	02/04/2008	28/03/2008 19:49	3.19	1.99	18.80
29	LARRA	02/04/2008	02/04/2008 09:50	2.53	2.02	2.42

30	LARRA	03/04/2008	03/04/2008 12:40	3.85	7.83	7.63
31	LARRA	04/04/2008	04/04/2008 11:00	3.93	1.54	1.11
32	LARRA	05/04/2008	05/04/2008 13:30	3.72	1.97	1.02
33	LARRA	09/04/2008	09/04/2008 10:00	2.66	2.48	0.62
34	LARRA	12/04/2008	12/04/2008 11:00	2.81	1.72	3.82
35	LARRA	14/04/2008	14/04/2008 16:50	2.87	2.43	0.76
36	LARRA	17/04/2008	17/04/2008 13:30	2.51	3.20	0.96
37	LARRA	21/04/2008	21/04/2008 16:30	2.86	1.55	23.39
38	LARRA	22/04/2008	22/04/2008 16:10	5.08	1.85	4.36
39	LARRA	23/04/2008	23/04/2008 15:35	4.37	3.42	6.45
40	LARRA	24/04/2008	24/04/2008 15:50	4.00	2.37	2.18
41	LARRA	30/04/2008	30/04/2008 10:00	2.68	3.10	1.08
42	LARRA	14/05/2008	14/05/2008 10:00	1.79	3.14	0.52
43	LARRA	21/05/2008	21/05/2008 10:00	3.66	1.47	1.65
44	LARRA	28/05/2008	28/05/2008 10:00	3.18	1.53	4.18
45	L1	21/05/2008	16/05/2008 11:45	1.88	1.96	5.38
46	L2	21/05/2008	19/05/2008 20:39	3.78	1.63	4.75
47	L1	05/06/2008	01/06/2008 09:28	3.20	1.79	5.04
48	L2	05/06/2008	01/06/2008 11:18	3.40	1.50	8.47
49	L4	05/06/2008	01/06/2008 13:48	3.24	1.40	23.12
50	L6	05/06/2008	01/06/2008 17:38	3.37	1.10	173.16
51	L7	05/06/2008	01/06/2008 23:38	4.03	1.22	86.42
52	L12	05/06/2008	02/06/2008 04:08	5.46	1.23	42.07
53	L14	05/06/2008	02/06/2008 10:18	7.87	1.23	31.51
54	L15	05/06/2008	02/06/2008 11:28	5.01	1.11	34.35
55	L16	05/06/2008	02/06/2008 23:38	4.89	1.24	58.89
56	LARRA	04/06/2008	04/06/2008 09:30	4.12	1.16	29.38
57	LARRA	05/06/2008	05/06/2008 14:30	4.91	1.44	8.20
58	LARRA	10/06/2008	10/06/2008 11:00	2.36	1.88	1.54
59	LARRA	12/06/2008	12/06/2008 15:15	6.14	1.33	16.20
60	LARRA	13/06/2008	13/06/2008 13:30	4.55	1.52	13.80
61	LARRA	14/06/2008	14/06/2008 16:30	3.97	1.70	5.53
62	LARRA	15/06/2008	15/06/2008 16:00	3.24	1.60	4.64
63	LARRA	18/06/2008	18/06/2008 10:00	2.92	1.90	2.09
64	LARRA	26/06/2008	26/06/2008 10:00	2.11	1.67	1.34
65	LARRA	03/07/2008	03/07/2008 10:00	1.82	2.59	1.35
66	LARRA	09/07/2008	09/07/2008 09:40	1.50	3.13	1.82
67	LARRA	16/07/2008	16/07/2008 09:25	1.70	1.69	1.29
68	LARRA	23/07/2008	23/07/2008 10:00	1.80	1.92	0.65
69	LARRA	08/08/2008	08/08/2008 09:55	1.97	1.92	1.01
70	LARRA	20/08/2008	20/08/2008 13:30	1.82	1.96	0.86
71	LARRA	04/09/2008	04/09/2008 09:40	2.21	2.09	0.96
72	LARRA	12/09/2008	12/09/2008 09:45	2.05	2.13	0.99
73	LARRA	17/09/2008	17/09/2008 09:50	1.87	2.02	0.67
74	LARRA	24/09/2008	24/09/2008 09:00	1.94	2.08	0.59

75	LARRA	08/10/2008	08/10/2008 11:45	2.54	2.45	2.60
76	LARRA	15/10/2008	15/10/2008 09:55	2.21	2.63	0.49
77	LARRA	23/10/2008	23/10/2008 09:40	2.47	3.24	0.45
78	LARRA	29/10/2008	29/10/2008 09:40	2.35	2.44	0.61
79	LARRA	05/11/2008	05/11/2008 10:00	2.90	3.08	1.84
80	L1	07/11/2008	07/11/2008 02:54	4.84	1.10	22.54
81	LARRA	12/11/2008	12/11/2008 09:40	4.12	2.59	0.84
82	LARRA	19/11/2008	19/11/2008 09:45	2.61	2.46	0.47
83	L1	26/11/2008	24/11/2008 18:49	5.23	2.87	5.62
84	L2	26/11/2008	25/11/2008 01:09	2.95	2.67	10.67
85	L3	26/11/2008	25/11/2008 04:29	3.01	0.90	5.62
86	L4	26/11/2008	25/11/2008 09:19	3.43	0.97	10.47
87	L5	26/11/2008	26/11/2008 01:09	4.03	0.95	8.19
88	LARRA	26/11/2008	26/11/2008 09:00	4.88	1.79	6.72
89	LARRA	03/12/2008	03/12/2008 09:00	3.00	2.71	0.51
90	LARRA	08/12/2008	08/12/2008 09:00	4.20	2.37	2.71
91	L1	08/12/2008	06/12/2008 00:06	3.28	2.55	3.11
92	L2	08/12/2008	06/12/2008 04:48	2.70	2.44	4.34
93	L3	08/12/2008	07/12/2008 16:22	4.30	2.04	5.99
94	LARRA	10/12/2008	10/12/2008 10:00	2.96	2.61	2.58
95	L1	18/12/2008	14/12/2008 18:24	3.56	1.64	5.18
96	L2	18/12/2008	14/12/2008 21:51	2.92	2.26	4.87
97	L3	18/12/2008	15/12/2008 21:02	4.15	1.64	9.15
98	L4	18/12/2008	17/12/2008 07:11	3.96	2.34	2.87
99	LARRA	18/12/2008	18/12/2008 10:00	3.18	2.12	1.46
100	LARRA	07/01/2009	07/01/2009 10:00	1.92	3.26	0.49
101	LARRA	14/01/2009	14/01/2009 10:00	1.87	3.40	0.35
102	L1	21/01/2009	20/01/2009 18:01	2.67	3.14	2.12
103	LARRA	21/01/2009	21/01/2009 09:00	2.00	2.51	1.57
104	L1	27/01/2009	23/01/2009 04:46	3.79	2.70	18.63
105	L3	27/01/2009	23/01/2009 07:46	4.35	2.63	21.31
106	L5	27/01/2009	23/01/2009 09:46	4.30	2.38	21.07
107	L7	27/01/2009	23/01/2009 11:16	4.50	2.16	22.95
108	L9	27/01/2009	23/01/2009 12:46	4.99	2.03	25.82
109	L11	27/01/2009	23/01/2009 14:56	4.42	1.78	24.28
110	L13	27/01/2009	23/01/2009 20:06	5.05	1.70	35.39
111	L14	27/01/2009	24/01/2009 08:36	5.62	1.80	24.09
112	L15	27/01/2009	24/01/2009 21:56	5.69	1.76	19.50
113	L16	27/01/2009	26/01/2009 07:26	5.07	1.71	18.90
114	LARRA	27/01/2009	27/01/2009 12:00	4.52	2.23	8.91
115	L1	04/02/2009	28/01/2009 05:50	4.25	1.90	10.32
116	L2	04/02/2009	28/01/2009 17:52	4.48	2.16	6.04
117	L3	04/02/2009	28/01/2009 20:31	4.00	1.95	5.07
118	L4	04/02/2009	29/01/2009 01:16	4.35	2.11	5.70
119	L5	04/02/2009	29/01/2009 07:06	4.23	2.28	5.49
120	L6	04/02/2009	29/01/2009 16:05	3.64	2.15	6.01
121	L7	04/02/2009	29/01/2009 23:40	4.14	1.99	4.96
122	L8	04/02/2009	30/01/2009 02:47	4.01	2.13	4.92
123	LARRA	04/02/2009	04/02/2009 09:00	2.63	2.02	1.29
124	L1	11/02/2009	11/02/2009 07:45	4.24	2.51	6.52
125	L2	11/02/2009	11/02/2009 08:45	2.88	1.89	4.15

126	LARRA	11/02/2009	11/02/2009 10:00	2.94	2.64	3.29
127	L1	18/02/2009	11/02/2009 10:45	2.77	2.04	4.24
128	L3	18/02/2009	11/02/2009 12:46	2.51	1.37	10.45
129	L5	18/02/2009	11/02/2009 15:35	2.86	1.49	12.66
130	L7	18/02/2009	11/02/2009 20:51	4.19	1.71	16.77
131	L8	18/02/2009	12/02/2009 05:17	4.29	1.77	12.06
132	L9	18/02/2009	12/02/2009 19:13	4.78	1.89	8.27
133	L11	18/02/2009	13/02/2009 20:53	3.89	1.97	4.54
134	L13	18/02/2009	14/02/2009 02:26	4.00	2.11	4.44
135	L15	18/02/2009	14/02/2009 06:21	3.92	2.10	4.48
136	L16	18/02/2009	14/02/2009 08:37	3.84	2.14	4.77
137	L18	18/02/2009	14/02/2009 18:34	3.78	1.88	8.66
138	L20	18/02/2009	15/02/2009 11:44	3.07	2.02	3.66
139	L21	18/02/2009	16/02/2009 05:44	2.84	1.92	3.01
140	L22	18/02/2009	18/02/2009 07:26	2.79	1.88	6.36
141	LARRA	18/02/2009	18/02/2009 10:00	2.62	2.66	1.39
142	LARRA	25/02/2009	25/02/2009 10:00	2.04	2.50	0.75
143	LARRA	03/03/02009	03/03/02009 10:00	2.04	3.47	1.66
144	LARRA	12/03/2009	12/03/2009 10:00	2.30	3.14	0.75
145	LARRA	25/03/2009	25/03/2009 10:00	2.07	4.36	0.60
146	LARRA	27/03/2009	27/03/2009 10:00	2.16	0.31	0.04
147	L1	15/04/2009	12/04/2009 02:00	2.78	2.49	8.28
148	L2	15/04/2009	12/04/2009 05:00	3.87	1.30	3.67
149	L3	15/04/2009	12/04/2009 08:00	3.86	1.96	4.92
150	L4	15/04/2009	12/04/2009 11:00	4.27	2.20	8.60
151	L5	15/04/2009	12/04/2009 22:00	6.67	2.22	6.66
152	L6	15/04/2009	14/04/2009 04:00	4.53	2.07	4.49
153	L7	15/04/2009	14/04/2009 10:00	4.38	2.36	4.32
154	L8	15/04/2009	14/04/2009 15:00	4.71	2.57	4.02
155	LARRA	15/04/2009	15/04/2009 10:00	4.26	2.99	2.84
156	L1	22/04/2009	20/04/2009 23:00	3.65	2.06	11.66
157	L2	22/04/2009	21/04/2009 00:00	3.69	2.35	24.78
158	L3	22/04/2009	21/04/2009 01:00	4.04	2.22	18.83
159	L4	22/04/2009	21/04/2009 02:00	5.25	0.25	2.04
160	L5	22/04/2009	21/04/2009 03:00	5.46	2.23	16.67
161	L6	22/04/2009	21/04/2009 06:00	5.83	2.19	10.18
162	L7	22/04/2009	21/04/2009 10:00	5.20	1.95	11.70
163	L8	22/04/2009	21/04/2009 12:00	4.95	1.78	13.12
164	L9	22/04/2009	21/04/2009 13:00	4.49	1.81	11.91
165	L10	22/04/2009	21/04/2009 14:00	4.76	1.88	13.95
166	L11	22/04/2009	21/04/2009 15:00	5.12	1.87	15.03
167	L12	22/04/2009	21/04/2009 21:00	5.83	1.77	15.22
168	L13	22/04/2009	22/04/2009 08:00	6.32	2.12	10.33
169	LARRA	22/04/2009	22/04/2009 10:00	5.99	2.00	6.99
170	LARRA	29/04/2009	29/04/2009 10:00	3.54	1.08	1.34
171	L1	13/05/2009	29/04/2009 17:48	4.40	1.76	6.49
172	L2	13/05/2009	30/04/2009 06:15	3.83	1.55	9.40
173	L3	13/05/2009	01/05/2009 20:07	2.93	1.89	9.33
174	L4	13/05/2009	01/05/2009 23:21	3.09	1.69	5.21
175	L5	13/05/2009	02/05/2009 01:30	2.68	1.72	3.30
176	L6	13/05/2009	02/05/2009 03:12	2.65	1.55	2.86
177	L7	13/05/2009	02/05/2009 04:43	2.65	1.62	2.75

178	L8	13/05/2009	02/05/2009 06:24	2.50	1.57	4.09
179	L9	13/05/2009	02/05/2009 08:38	2.46	1.65	9.00
180	L10	13/05/2009	02/05/2009 15:39	4.92	2.15	10.06
181	L11	13/05/2009	02/05/2009 17:04	5.19	2.02	24.16
182	L12	13/05/2009	02/05/2009 18:35	5.03	1.99	13.69
183	L13	13/05/2009	02/05/2009 20:27	5.18	NA	NA
184	L14	13/05/2009	02/05/2009 23:23	5.28	2.17	14.92
185	L15	13/05/2009	03/05/2009 04:56	5.24	2.08	21.01
186	L16	13/05/2009	03/05/2009 14:29	5.20	2.01	11.80
187	L17	13/05/2009	05/05/2009 00:01	3.42	1.98	5.89
188	L18	13/05/2009	10/05/2009 19:02	2.74	2.23	6.33
189	LARRA	13/05/2009	13/05/2009 10:00	2.05	0.43	0.61
190	L1	20/05/2009	15/05/2009 00:00	2.81	15.25	3.17
191	L2	20/05/2009	15/05/2009 02:17	2.50	2.03	3.72
192	L3	20/05/2009	15/05/2009 04:31	2.30	2.08	3.24
193	L4	20/05/2009	15/05/2009 21:34	2.83	2.07	3.67
194	L5	20/05/2009	16/05/2009 14:23	4.56	2.03	6.07
195	LARRA	20/05/2009	20/05/2009 10:00	3.08	2.76	1.05
196	LARRA	27/05/2009	27/05/2009 10:00	2.07	2.37	1.07
197	LARRA	03/06/2009	03/06/2009 10:00	1.91	2.83	0.54
198	LARRA	10/06/2009	10/06/2009 10:00	2.21	2.43	0.89
199	LARRA	17/06/2009	17/06/2009 10:00	1.77	3.55	0.86
200	LARRA	24/06/2009	24/06/2009 10:00	1.78	3.11	0.68

Annexe 2

Agricultural management practices in the Save catchment

Pasture

Year	Month	Days	Mgt Operation	Machine / Product	Quantity (kg/ha)
1	April	10	Tillage	Generic Spring Ploughing Operation	
1	April	20	Fertilizer	0-25-25	300
1	April	25	Tillage	Roller Harrow 15 Ft	
1	April	25	<i>Plant/Begin</i>	<i>Corn Silage</i>	
1	April	25	Fertilizer	Ammonitrates	60
1	May	20	Fertilizer	Urea	195
1	June	10	Fertilizer	Urea	220
1	July	10	Irrigation		30 mm
1	July	31	Irrigation		30 mm
1	August	10	Irrigation		30 mm
1	August	31	Irrigation		30 mm
1	September	10	Irrigation		30 mm
1	September	25	Harvest and kill		
2	January	15	Tillage	Generic Spring Ploughing Operation	
2	February	5	Fertilizer	15-15-15	400
2	February	5	Tillage	Roller Harrow 15 Ft	
2	February	10	<i>Plant/Begin</i>	<i>Tall Fescue</i>	
2	February	10	Tillage	Roller Groover	
2	July	1	Grazing		60 days
2	October	31	Kill/End		
3	March	1	<i>Plant/Begin/Begin</i>	<i>Tall Fescue</i>	
3	July	1	Grazing		60 days
3	October	31	Kill/End		
4	March	1	<i>Plant/Begin/Begin</i>	<i>Tall Fescue</i>	
4	July	1	Grazing		60 days
4	October	31	Kill/End		
5	March	1	<i>Plant/Begin/Begin</i>	<i>Tall Fescue</i>	
5	July	1	Grazing		60 days
5	October	31	Kill/End		

Sunflower

Year	Month	Days	Mgt operation	Machine / Product	Quantity (kg/ha)
1	April	1	Tillage	Fldcdscr	
1	April	5	Fertilizer	15-15-15	193,3
1	April	10	<i>Plant/Begin Sunflower</i>		
1	May	16	Fertilizer	15-15-15	193,3
1	Oct	1	Harvest and kill		
1	Oct	9	<i>Plant/Begin WWHT</i>		
2	Jan	12	Fertilizer	15-15-15	306.6
2	Feb	17	Fertilizer	15-15-15	306.6

2	Mars	20	Fertilizer	15-15-15	306.6
2	July	10	Harvest and kill		
2	Sept	8	Tillage	subchpw	

Winter Wheat

Year	Month	Days	Mgt operation	Machine / Product	Quantity (kg/ha)
1	Oct	9	<i>Plant/Begin WPTH</i>		
2	January	12	Fertilizer	15-15-15	306.6
2	February	17	Fertilizer	15-15-15	306.6
2	March	20	Fertilizer	15-15-15	306.6
2	July	10	Harvest and kill		
2	September	8	Tillage	Subchpw	
3	April	1	Tillage	Fldcdscr	
3	April	5	Fertilizer	15-15-15	193.3
3	April	10	<i>Plant/Begin Sunflower</i>		
3	May	16	Fertilizer	15-15-15	193.3
3	Oct	1	Harvest and kill		

Annexe 3

Association de la légende de la carte pédologique du BV de la Save au 1/80000 (cartes papiers CACG) avec la légende détaillée du guide des sols de la région Midi Pyrénées restituée sur le site de la CRAMP avec les profils pédo.

Tableau de synthèse de la correspondance entre les codes de la légende de la carte pédo du BV de la Save (CACG) et les profils de la légende de la carte morpho pédo Midi pyrénées de la CRAMP

SAVE CACG	Type de sol	Unité	
131	1		2
132	1		1
322	2		4
321	2		3 ou T 3 U 2b
325	3		1
353	3		5
331	4		1
335	4		5
332	4		2
351	4	3 ou 4	
212	5		3
213	5		2
221	5		6
520	7		1
518	9	1 ou 2	
327	15		2
328	15		3
326	15		1
127	16		1
129	16		2
9999	13	Bati	
620	NR	Zone boisée lors des relevés (1960)	

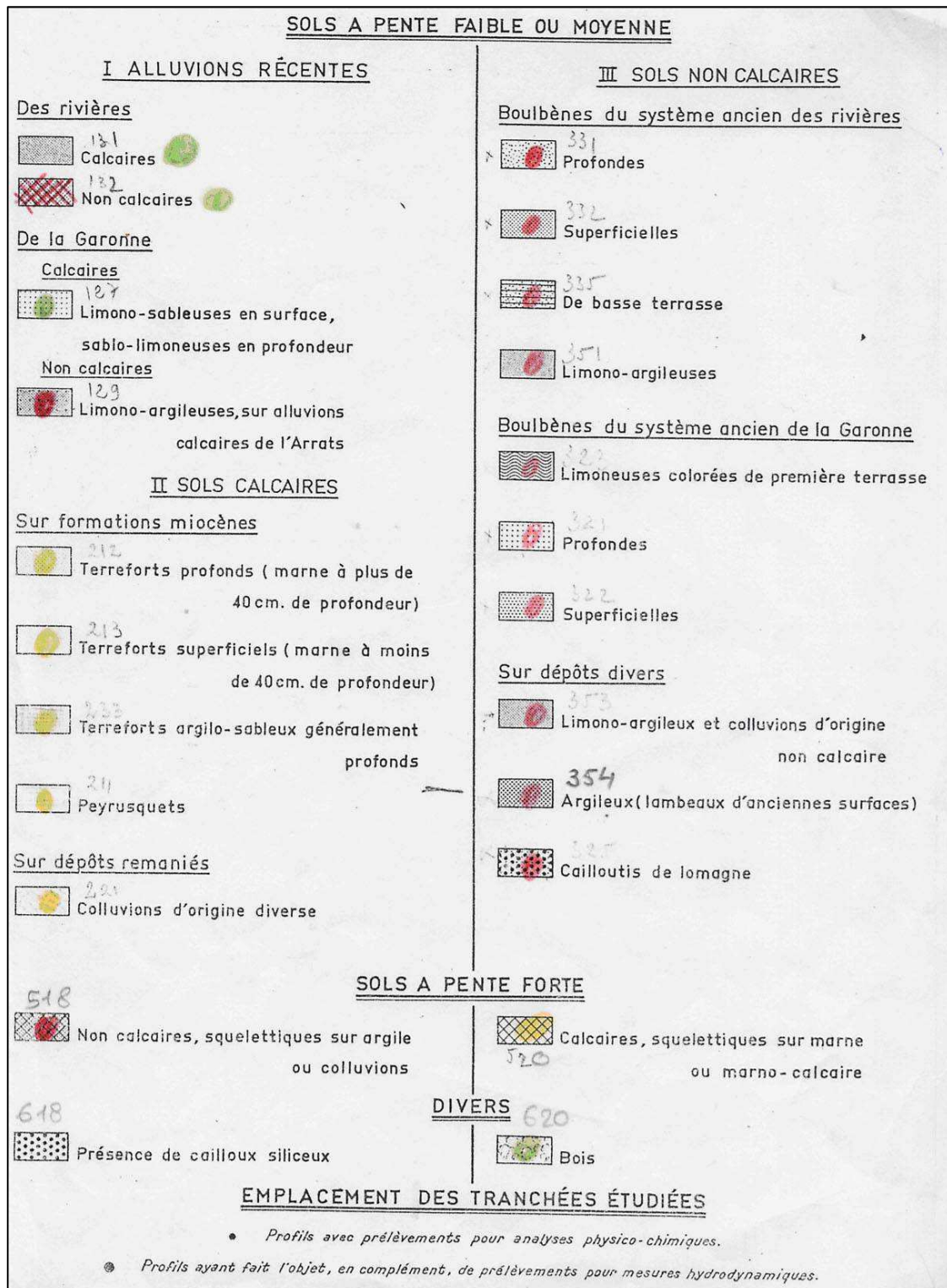


Tableau Excel de la légende de la carte pédologique du BV de la Save au 1/80000 (CACG)
avec codification des thèmes

CODE_SOL	TOPOGRAPHIE	NATURE	DESCRIPTION	CARACTERISTIQUES
131	Pente faible ou moyenne (<15%)	Alluvions recentes	Alluvions des rivieres	Calcaires
132	Pente faible ou moyenne (<15%)	Alluvions recentes	Alluvions des rivieres	Non calcaires
127	Pente faible ou moyenne (<15%)	Alluvions recentes	Alluvions de la Garonne Calcaires	Limono-sableuses en surface, sablo- limoneuses en profondeur
129	Pente faible ou moyenne (<15%)	Alluvions recentes	Alluvions de la Garonne non Calcaires	Limono-argileuses, sur alluvions calcaires de l Arrats
212	Pente faible ou moyenne (<15%)	Calcaires	Sur formations miocenes	Terreforts profonds (marnes a plus de 40 cm de profondeur)
213	Pente faible ou moyenne (<15%)	Calcaires	Sur formations miocenes	Terreforts superficiels (marnes a moins de 40 cm de profondeur)
221	Pente faible ou moyenne (<15%)	Calcaires	Sur depots remanies	Colluvions d origine diverse
331	Pente faible ou moyenne (<15%)	Non calcaires	Boulbenes du systeme ancien des rivieres	Profondes
332	Pente faible ou moyenne (<15%)	Non calcaires	Boulbenes du systeme ancien des rivieres	Superficielles
335	Pente faible ou moyenne (<15%)	Non calcaires	Boulbenes du systeme ancien des rivieres	De basse terrasse
351	Pente faible ou moyenne (<15%)	Non calcaires	Boulbenes du systeme ancien des rivieres	Limono-argileuses
321	Pente faible ou moyenne (<15%)	Non calcaires	Boulbenes du systeme ancien de la Garonne	Profondes
322	Pente faible ou moyenne (<15%)	Non calcaires	Boulbenes du systeme ancien de la Garonne	Superficielles
327	Pente faible ou moyenne (<15%)	Non calcaires	Sol du Plateau de Lannemezan	Sols noirs sur limons
328	Pente faible ou moyenne (<15%)	Non calcaires	Sol du Plateau de Lannemezan	Sols bruns sur limons
353	Pente faible ou moyenne (<15%)	Non calcaires	Sur depots divers	Limono-argileux et colluvions d origine non calcaire
325	Pente faible ou moyenne (<15%)	Non calcaires	Sur depots divers	Cailloutis de lomagne
326	Pente faible ou moyenne (<15%)	Non calcaires	Sur argile rouge	
518	Pente forte (<15%)	Non calcaires	Sur argile ou colluvions	squelettiques
520	Pente forte (<15%)	Calcaires	Sur marne ou marno- calcaire	Squelettiques
620	Pente forte (<15%)	NR	NR	Bois

Codification des grands thèmes morpho-pedo dont les profils détaillés ont pu être extraits du guide des sols consultable depuis le site de la CRAMP.

Code_corr	Types de sol (carte morpho-pedoCRAMP)
1	Basses plaines d'alluvions récentes Vallées secondaires de Gascogne
2	Terrasses planes d'alluvions anciennes mal drainées à boubènes - Garonne (en aval de Toulouse)
3	Hautes terrasses anciennes découpées
4	Terrasses d'alluvions anciennes - Vallées secondaires Terrasses d'alluvions anciennes (et glacis de limons soliflues) Sud de la Gascogne
5	Coteaux peu à moyennement accidentés - Coteaux argilo-calcaires peu à moyennement accidentés Gascogne
16	Basse plaine d'alluvions récentes Garonne (en aval de Toulouse)
7	Coteaux argilo-calcaires accidentés avec bancs de calcaire Gascogne
9	Coteaux accidenté sur molasse acide argileuse ou argilo-caillouteuse - Sud Gascogne et Piémont Pyrénéen
15	Hauts niveaux bien conservés - Plateaux de Lannemezan et de Gers

Type	Unité	Description
1	2	Sols alluviaux argileux et calcaires
1	1	Sols alluviaux non calcaires des zones amont des rivières gascognes
16	1	Sols peu évolués d'apport alluvial de texture sableuse à limoneuse en surface souvent sableuse à sablo-graveleuse à moyenne profondeur.
16	2	Sols bruns calcaires ou bruns eutrophes, de texture limoneuse à argilo-limoneuse.
5	3	Sols argilo-calcaires profonds sur marne à 60-80 cm (terreforts profonds)
5	2	Sols argilo-calcaires superficiels au-dessus de marne (30-35 % de la surface)
5	6	Sols argilo-calcaires de colluvionnement (10 % de la surface)
4	1	Boulbènes profondes des terrasses
4	2	Boulbènes superficielles des terrasses
4	5	Sols limoneux hydromorphes (boulbènes de basse terrasse)
4	3	boulbènes colorées profondes
4	4	boulbènes colorées superficielles qui sont souvent caillouteuses
2	3	Boulbènes moyennes
3	2b	Les boulbènes profondes (épaisseur de l'horizon limoneux > 50 cm)
2	4	Boulbènes superficielles
3	5	Colluvions profondes hydromorphes
3	1	Sols caillouteux des hauts niveaux ou cailloutis de Lomagne
15	2	Terres noires à Touyas sur limons jaunes
15	3	Sols bruns profonds sur limons ou argile jaune
15	1	Sol noir profond hydromorphe sur argile rouge (unité 1)
9	1	Sols bruns caillouteux superficiels sur argiles à galets du Pliocène.
9	2	Sols bruns limono-argileux ou argilo-limoneux superficiels sur argile à faible profondeur
7	1	Sols argilo-calcaires superficiels sur marnes ou marno-calcaires

Correspondance entre les codes de la légende de la carte pédo du BV de la Save (CACG) et les profils de la légende de la carte morpho pédo Midi pyrénées de la CRAMP

Sols à pente à faible ou moyenne <15% = Coteaux peu à moyennement accidentés

I Alluvions récentes

- Des rivières

= Type 1 Basses plaines d'alluvions récentes Vallées secondaires de Gascogne

131 Calcaires

1 Unité 2 = Sols alluviaux argileux et calcaires

132 Non calcaires

1 Unité 1 = Sols alluviaux non calcaires des zones amont des rivières gascognes

- De la Garonne

= Type 16 Basse plaine d'alluvions récentes Garonne (en aval de Toulouse)

127 Calcaires Limono-sableuses en surface, sablo-limoneuses en profondeur

16 Unité 1 (??) = Sols peu évolués d'apport alluvial de texture sableuse à limoneuse en surface souvent sableuse à sablo-graveleuse à moyenne profondeur.

129 Non Calcaires Limono-argileuses, sur alluvions calcaires de l Arrats

16 Unité 2 (??) Sols bruns calcaires ou bruns eutrophes, de texture limoneuse à argilo-limoneuse.

II Sols calcaires

= Type 5 Coteaux peu à moyennement accidentés - Coteaux argilo-calcaires peu à moyennement accidentés Gascogne

- Sur formations miocènes (dépôts molassiques)

212 Terreforts profonds (marnes a plus de 40 cm de profondeur)

5 Unité 3 : Sols argilo-calcaires profonds sur marne à 60-80 cm (terreforts profonds)

213 Terreforts superficiels (marnes a moins de 40 cm de profondeur)

5 Unité 2 : Sols argilo-calcaires superficiels au-dessus de marne (30-35 % de la surface).

- Sur dépôts remaniés

221 Pente faible ou moyenne Sols Calcaires Sur dépôts remaniés Colluvions d origine diverse

5 Unité 6 : Sols argilo-calcaires de colluvionnement (10 % de la surface).

III Sols non calcaires

- Boulbènes du système ancien des rivières

= Type 4 Terrasses d'alluvions anciennes - Vallées secondaires Terrasses d'alluvions anciennes (et glacis de limons soliflues) Sud de la Gascogne

331 Profondes

4 Unité 1 : Boulbènes profondes des terrasses

332 Superficielles

4 Unité 2 : Boulbènes superficielles des terrasses

335 De basse terrasse

4 Unité 5 : Sols limoneux hydromorphes (boulbènes de basse terrasse)

351 Limono-argileuses (ou colorées)

4 Unité 3 boulbènes colorées profondes

4 Unité 4 boulbènes colorées superficielles qui sont souvent caillouteuses

- Boulbènes du système ancien de la Garonne

Type 2 = Terrasses planes d'alluvions anciennes mal drainées à boulbènes - Garonne (en aval de Toulouse)

321 Profondes

7.1.1. 2 Unité 3 : Boulbènes moyennes

ou

Type 3 = Hautes terrasses anciennes découpées

3 Unité 2b - Les boulbènes profondes (épaisseur de l'horizon limoneux > 50 cm)

322 Superficielles

2 Unité 4 : Boulbènes superficielles

- Sur dépôts divers

Type 3 = Hautes terrasses anciennes découpées

353 Limono-argileux et colluvions d'origine non calcaire

3 Unité 5 : Colluvions profondes hydromorphes

325 Cailloutis de Lomagne

3 Unité 1 : Sols caillouteux des hauts niveaux ou cailloutis de Lomagne

- Sols du plateau de Lannemezan

Type 15 = Hauts niveaux bien conservés - Plateaux de Lannemezan et de Gers

327 Sol noirs sur limons

15 Unité 2 : Terres noires à Touyas sur limons jaunes

328 Sol bruns sur limons

15 Unité 3 : Sols bruns profonds sur limons ou argile jaune

326 Sols sur argile rouge

15 Unité 1 : Sol noir profond hydromorphe sur argile rouge (unité 1)

Sols à pentes fortes (>15%) = Coteaux accidentés
--

518 Non calcaire squelettiques sur argile ou colluvions

Type 9 = Coteaux accidenté sur molasse acide argileuse ou argilo-caillouteuse - Sud Gascogne et Piémont Pyrénéen

9 Unité 1 : Sols bruns caillouteux superficiels sur argiles à galets du Pliocène.
ou

9 Unité 2 : Sols bruns limono-argileux ou argilo-limoneux superficiels sur argile à faible profondeur

520 Calcaire squelettiques sur marne ou marno-calcaire

Type 7 = Coteaux argilo-calcaires accidentés avec bancs de calcaire Gascogne

7 Unité 1 : Sols argilo-calcaires superficiels sur marnes ou marno-calcaires

RESUME

L'étude du transport fluvial des matières en suspension (MES) et du carbone organique dans les rivières du monde informe sur le taux d'érosion des continents, le cycle du carbone et la contribution du carbone terrestre à l'océan. Les objectifs du travail sont, d'une part, de décrire, analyser et quantifier la dynamique des MES et du carbone organique, particulaire (COP) et dissous (COD), lors des périodes de crue, d'évaluer la contribution des événements de crue sur les flux annuels et, d'autre part, de quantifier ces flux sur le long terme par une approche de modélisation agro-hydrologique. L'étude expérimentale est basée sur l'échantillonnage à l'exutoire des données par un prélèvement manuel et automatique dans un bassin versant agricole de 1 110 km² du Sud-ouest de la France, la Save, un affluent de la Garonne, de Janvier 2007 à Juin 2009. Concernant l'approche de modélisation, le modèle SWAT 2005 (Soil and Water Assessment Tool) est utilisé pour décrire le transport et quantifier le flux des MES et du COP sur du long terme (1999-2008) intégrant les données hydro-climatiques, l'occupation du sol et les itinéraires techniques des pratiques agricoles dans ce bassin.

Les résultats montrent la forte variabilité temporelle de la dynamique de transport des MES, COP et COD durant les différentes crues saisonnières. Ces flux sont notamment transportés au printemps grâce aux fréquences importantes des crues et à la durée des crues. La quantification de flux (MES, COP et COD) pendant les crues contribuant aux flux annuel à été estimée. Le flux annuel des MES en 2007 est de 16 614 tonnes, représentant 15 t km⁻² (85% du flux annuel transporté en crue pour 16% de la durée annuelle) et il est de 77 960 tonnes représentant 70 t km⁻² en 2008 (95% du flux annuel transporté en crue pour 20% de la durée annuelle). Le transport du COP et COD durant les crues est respectivement de 76% et 62% du flux total pour 22% de la durée totale (Janvier 2008 à Juin 2009). Les flux de COP et COD exportés de la Save sont de 3091 tonnes et 1238 tonnes, représentant respectivement, 1,8 t km⁻² an⁻¹ et 0,7 t km⁻² an⁻¹. En utilisant des analyses statistiques, les facteurs hydro-climatiques qui conditionnent la dynamique du transport montrent de bonnes corrélations entre la précipitation totale, le débit de crue, le flux d'eau et les flux de MES, COP et COD. De plus, la dynamique des MES, COP et COD pour les différents crues a été examinée, en utilisant l'analyse des hystérésis.

Les résultats du modèle agro-hydrologique SWAT montrent la forte variabilité temporelle des flux annuels de MES et COP (1999-2008). Le flux annuel de MES varie de 4 766 tonnes à 123 000 tonnes, représentant un flux spécifique de 48 t km⁻² an⁻¹ et le flux annuel de POC varie de 120 tonnes à 3 100 tonnes, représentant un flux spécifique de 1,2 t km⁻² an⁻¹. La régression entre le flux d'eau annuel et le flux de MES simulé a été établie et les zones potentielles d'érosion sont également identifiées par modélisation pour le bassin versant de la Save.

ABSTRACT

The study of the fluvial suspended sediment and organic carbon transport through the world's streams and rivers provides information on the erosion rate of continents, the cycling of carbon on earth, and the contribution of terrestrial carbon to the oceans. The objectives of the research are, on the one hand, to describe and analyse the transport dynamics of suspended sediment (SS), and dissolved and particulate organic carbon (DOC and POC) during flood events with assessment of flood load contribution and, on the other hand, to quantify the long term fluxes by agro-hydrological modelling approach. The experimental study is based on the field experiment for extensive data collection at the catchment outlet from both manual and automatic sampling within the Save agricultural catchment, 1110 km², a tributary of the Garonne River in Southwest France from January 2007 through June 2009. For modelling approach, the SWAT model (Soil and Water Assessment Tool) was applied to study long term trend of sediment transport processes, sediment and particulate organic carbon yield taking into account hydrolo-climatic data (1999-2008), landuse, and agricultural management practices within the catchment.

Our results revealed high temporal variability in transport dynamics during different seasonal flood events. SS, DOC and POC load were strongly transported during spring resulting from frequent flood events of high magnitude and timing of flood. The quantification of flood loads of SS, DOC and POC contributing to annual load was estimated. Annual sediment transport in 2007 yielded 16 614 tonnes, representing 15 t km⁻² (85% of annual load transport during floods for 16% of annual duration), while the 2008 sediment yield was 77 960 tonnes, representing 70 t km⁻² (95% of annual load transport during floods for 20% of annual duration). The transport of POC and DOC during flood events exhibited 76% and 62% of their total loads within 22% of the whole duration (January 2008 to June 2009). POC and DOC export from the Save catchment amounted to 3091 t and 1238 t, representing 1.8 t km⁻² y⁻¹ and 0.7 t km⁻² y⁻¹, respectively. The hydro-climatic factors conditioning the transport dynamics using statistical analyses revealed strong correlations between total precipitation, flood discharge, total water yield with SS, POC, DOC load transport. Moreover, SS, POC and DOC dynamics using concentration-discharge relationship (hysteresis patterns) at different flood events during rising and falling flow were also examined.

SWAT agro-hydrological model results show strong temporal variability of annual sediment and POC yield from the Save catchment (1999-2008). Annual sediment yield ranged from 4766 t to 123000 t, representing a mean specific sediment yield of 48 t km⁻² y⁻¹ and annual POC yield ranged from 120 t to 3100 t, representing a mean specific POC yield of 1.2 t km⁻² y⁻¹. A regression between annual water yield and simulated annual sediment yield was established and potential source areas of erosion were also identified by modelling for the Save agricultural catchment.